Kinetic Studies of the Hydrolyses and Aminolyses of Phosphorus (V) Chlorides And Proton Transfer at Carbon

RICHARD JOSEPH DELLEY

Kinetic Studies of the Hydrolyses and Aminolyses of Phosphorus (V) Chlorides

And

Proton Transfer at Carbon

By

Richard J. Delley

M.Chem. (Hons), Chemistry (2008)

Submitted to the Department of Chemistry

In Partial Fulfilment of the Requirements for the

Degree of Doctor of Philosophy

at

Durham University

2012

Gratia Gratiam Parit

Acknowledgements

I would like to express my thanks to Drs. David R W Hodgson and AnnMarie O'Donoghue for their invaluable support, guidance and expertise throughout the course of my PhD. In addition, I am also grateful to the ESPRC for funding this research project.

The work presented in this thesis would not have been possible without the help of the department's technical staff, namely: Dr. Alan Kenwright, Mr Ian McKeag and Mrs Catherine Heffernan (NMR); Dr. Mike Jones and Dr. Jackie Mosely (mass spectrometry); Mr Tony Baxter, Mrs Elizbeth Wood and Mr Philip Rochester in stores and glassblowing by Malcolm Richardson.

I would like express gratitude to Casey, Gem, Louis and Richard for all the great times together, discussions and general distractions.

Finally, I would like to thank my family and friends for support and patience over the course of my PhD.

Memorandum

The work presented within this thesis was carried out at Durham University between October 2008 and December 2011. The thesis is the work of the author, except where acknowledged by reference, and has not been submitted for any other degree. The copyright of this thesis lies solely with the author and no quotation from it should be published without written consent and information derived from it should be acknowledged.

Parts of this work have been published in:

- Kwan, I. C. M.; Delley, R. J.; Hodgson, D. R. W.; Wu, G. *Chem. Commun*. **2011**, *47*, 3882-3884.
- Delley, R. J.; Bandyopadhyay, S.; Fox, M. A.; Schliehe, C.; Hodgson, D. R. W.; Hollfelder, F.; Kirby, A. J.; O'Donoghue, A. C. *Org. Biomol. Chem*. **2012**, *10*, 590-596.
- Delley, R. J.; O'Donoghue, A. C.; Hodgson, D. R. W. *J. Org. Chem.* **2012**, *77*, 5829-5831.

This work has been presented at:

- RSC Organic Reaction Mechanisms Group, SymPoc 2009, Glasgow University, Glasgow, UK – *poster*
- RSC Bioorganic Forum, June 2009, Liverpool University, Liverpool, UK – *poster*
- RSC Faraday Discussion 145: Frontiers in Physical Organic Chemistry, September 2009, Cardiff University, Cardiff, UK – *poster*
- 3rd EuCheMS Chemistry Congress, August 2010, Nürnberg, Germany – *poster*
- RSC Organic Reaction Mechanisms Group, 'Younger' Physical Organic Chemists' residential Meeting, September 2010, Gregynog, UK –*oral presentation*
- 1st NORSC Network Seminar Day, October 2010, University of York, York, UK – *oral presentation*
- RSC Carbohydrate and Bioorganic Interest Groups Joint Meeting, April 2011, King's College London, London, UK – *poster*

- 1st Durham Chemistry Postgraduate Research Symposium, June 2011, University of Durham, Durham, UK – *oral presentation*
- RSC 21st IUPAC International Conference on Physical Organic Chemistry, September 2012, Durham, UK – *poster*

Statement of Copyright

Table of Contents

Abstract

Phosphorus oxychloride ($POCl_3$) and thiophosphoryl chloride ($PSCl_3$) are useful phosphorylating reagents. However, they are usually used under dry conditions as their reactivity toward water has been perceived as a problem.

As part of an on-going program to develop aqueous aminophosphorylation procedures, we have investigated the reactivities of phosphodichloridate and thiophosphodichloridate ions in aqueous solutions as more selective water-soluble alternatives to $POCl_3$ and $PSCl_3$.

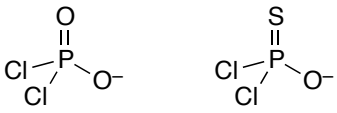

We report the pH-k_{obs} profiles for the hydrolyses of phosphodichloridate and thiophosphodichloridate ions in aqueous solutions. Both species show broad pH-k_{obs} plateaus that extend to high pHs. The aminolyses of phosphodichloridate and thiophosphodichloridate ions in aqueous amine solutions have also been followed. Good selectivity towards aminolysis over hydrolysis processes has been observed.

We have applied our kinetic data towards the optimisation of aqueous aminophosphorylation procedures, which has led to near-quantitative conversion of amino-nucleosides to thiophosphoramidate products.

Finally, an additional research project focused upon *peri*-dimethylamino substituent effects on proton transfer at carbon in α-naphthylacetate esters. Rate constants for the exchange of hydrogen for deuterium at the α-CH_2 positions of naphthalen-1-yl-acetic acid *tert*-butyl ester and 8-(*N*,*N*-dimethylamino-naphthalen-1-yl)-acetic acid *tert*-butyl ester have been determined in potassium deuteroxide solutions.

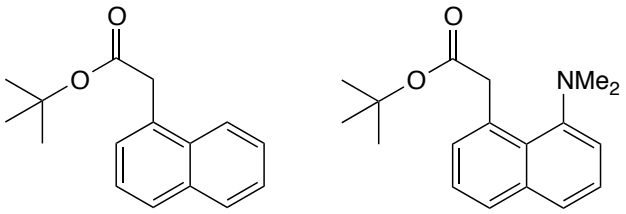

Abbreviations

Å	angstrom(s)
Abs	absorbance
Ac	acetyl
Ar	aryl
A_{max}	absorbance maximum
A_{min}	absorbance minimum
aq.	aqueous
br.	broad (spectral)
Bu	butyl
^{o}C	degree celsius
cm^{-1}	wavenumbers
^{13}C NMR	carbon 13 nuclear magnetic resonance
δ	chemical shift
d	doublet
DMSO	dimethyl sulfoxide
D_2O	deuterium oxide
Dvd	digital versatile disk
Et	ethyl
EtOAc	ethyl acetate
equiv	equivalent
FB	free base
g	gram(s)
HCl	hydrochloric acid
^{1}H NMR	proton nuclear magnetic resonance
hr	hour(s)
Hz	hertz
I	ionic strength
IR	infra red
J	coupling constant
k	rate constant
K	equilibrium constant
K_a	acidity constant
kcal	kilocalorie(s)
λ	wavelength
L	litre(s)
LFER	linear free energy relationship

lit.	literature
ln	natural logarithm
log	logarithm
M	moles/litre (Molar)
m-	*meta*
m	multiplet (spectral)
Me	methyl
MeCN	acetonitrile
MeO	methoxy
µL	microlitre(s)
min	minute(s)
mL	millilitre(s)
mm	millimetre(s)
mmol	millimole(s)
mol	mole(s)
ms	millisecond(s)
m/z	mass per unit charge
NaOH	sodium hydroxide
o-	*ortho*
p-	*para*
Ph	phenyl
ppm	parts per million
ps	picoseconds
R	alkyl substituents
Rf	retention factor
RNA	ribonucleic acid
r.t.	room temperature
ρ	reaction constant
σ	substituent constant
sec, s	second(s)
s	singlet (spectral)
t	triplet (spectral)
tert-	tertiary
THF	tetrahydrofuran
TLC	thin layer chromatography
TS	transition state
UV	ultraviolet
Vis	visible
wt.	Weight

Chapter 1
Introduction

1.0 Foreword

In this thesis the reactivities of various phosphorus (V) chlorides in aqueous solution will be investigated. These reagents are traditionally used under dry conditions, for example in the preparation of nucleoside phosphates, as their reactivities towards water have been perceived as a problem. In order to contextualise the main work of the project, some literature examples towards the synthesis of phosphates and phosphate analogues in anhydrous and aqueous solution will be presented in this chapter and their associated advantages and disadvantages will be discussed.

The Hodgson group is interested in the development of aqueous phosphorylation chemistry as part of research into the synthesis and biological application of phosphate mimics. Once synthesised, these mimics may be studied in biological systems, for example in the bioconjugation of RNA. The development of aqueous methods of phosphorylation using phosphorus (V) chlorides as phosphorylating agents in the literature and from the Hodgson group in Durham will therefore be discussed. In particular, the reactivities of phosphorus (V) chlorides towards amines in aqueous solution are investigated.

Currently there is a lack of kinetic data on the reactivities of phosphorus (V) chlorides in aqueous solution, which hampers the optimisation of the use of these reagents in water. Kinetic data are essential in determining the reaction conditions required for clean phosphorylation of amines (and other nucleophiles) in aqueous solution, where hydrolysis of the phosphorylating species is minimized. In order to demonstrate how differences in reactivity between competing hydrolysis and aminolysis processes may be exploited, we discuss a strategy developed by King *et al.* in which product yields from reactions of reactive electrophiles with nucleophiles in aqueous solutions are maximised through prediction of optimal reaction pH. This strategy is discussed at the end of this chapter and related ideas are applied to the development of aqueous methods of phosphorylation using phosphorus (V) chlorides.

1.1 Phosphates

In this section the importance of phosphates **1** in nature is briefly overviewed. Literature studies of the reactions of phosphorus (V) and chlorides with nucleoside sugars to generate nucleoside phosphates are presented and discussed. The relative merits of each method are presented and discussed as part of developing more effective methods towards phosphorylation.

Phosphates are essential to life and are usually present in nature as mono, di and tri esters. For example, ribonucleic and deoxyribonucleic acids are composed of phosphate diester backbones in which a third ionisable group ensures this material is charged, thus preventing unwanted transfer across cell membranes. The main sources of energy within the body, for example adenosine triphosphate and creatine phosphate, also utilise phosphates.

In 1969, Yoshikawa *et al.* developed a simple and convenient method for the phosphorylation at the 5′ position of unprotected nucleosides **1** using phosphorus oxychloride ($POCl_3$) in a trialkyl phosphate solvent system (Scheme 1.1).[1, 2]

Scheme 1.1 Synthesis of nucleoside phosphate monoesters *via* the Yoshikawa method.[1, 2]

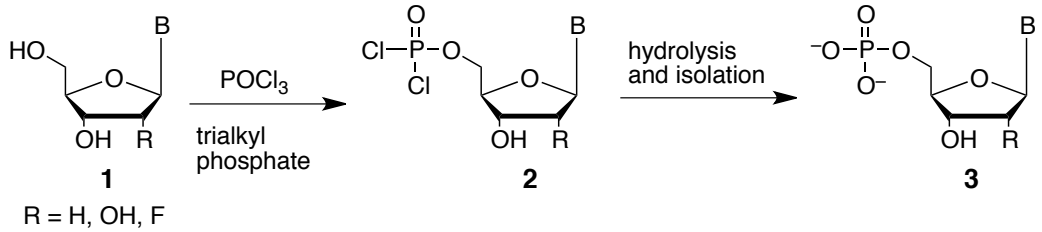

Yoshikawa *et al.* postulated that the reaction of phosphorus oxychloride **4** with trialkyl phosphate **5** led to the formation of ionised structure **6** (Scheme 1.2), which resulted in a decrease in the reactivity of the phosphorylating agent

Scheme 1.2 Yoshikawa's postulated reaction of $POCl_3$ with trialkyl phosphate to generate the active phosphorylating agent 6.

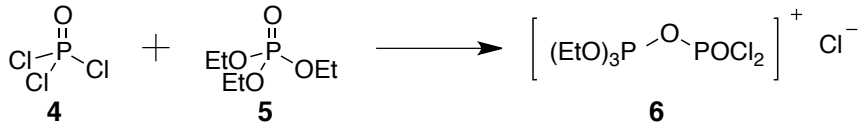

The resulting decrease in electrophilicity of the phosphorylating agent is suggested to impart improved selectivity towards the 5′-OH over other nucleophilic centres within nucleosides. Consequently, protection of the base or sugar was not required. Subsequent hydrolysis of the reactive phosphodichloridate intermediate **2** in aqueous solution led to the formation of nucleoside monophosphate **3**.

Given its simplicity and convenience, the Yoshikawa method has been used extensively in the literature and is held in high regard in many review articles and books.[3] Even so, the postulated mechanism has not been confirmed.

The Yoshikawa method was augmented by Ludwig in the synthesis of adenosine 5′-triphosphate and 2′-deoxyadenosine 5′-triphosphate from adenosine **7** and 2′-deoxyadenosine **8**, respectively.[4] Phosphorylation of **7** and **8** in trialkyl phosphate generated adenosine 5′-phosphodichloridate **9** and 2′-deoxyadenosine 5′-phosphodichloridate **10**. These were subsequently treated with tri-n-butylammonium pyrophosphate in anhydrous DMF followed by aqueous triethylammonium bicarbonate buffer (pH 7.5) to give adenosine 5′-triphosphate **11** and 2′-deoxyadenosine 5′-triphosphate **12**, respectively (Scheme 1.3).

Scheme 1.3 Synthesis of adenosine 5′-triphosphate and 2′-deoxyadenosine 5′-triphosphate.

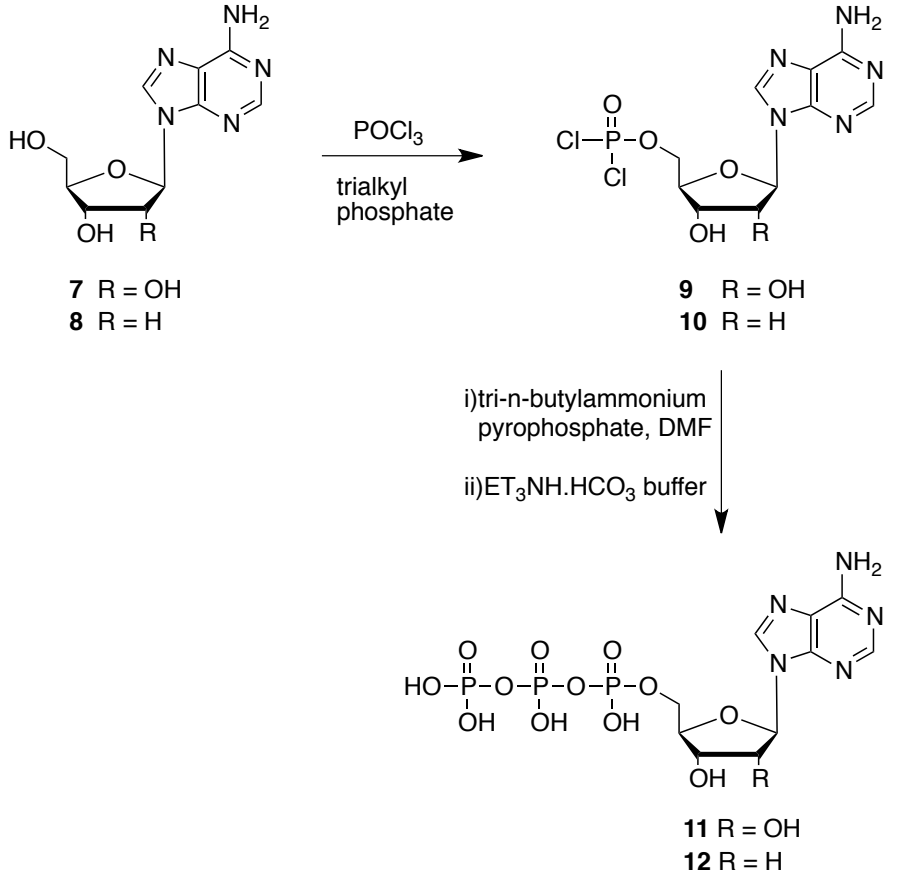

7 R = OH
8 R = H

9 R = OH
10 R = H

11 R = OH
12 R = H

Adenosine 5′-triphosphate **11** and 2′-deoxyadenosine 5′-triphosphate **12** were purified by ion exchange chromatography and isolated yields of 86 and 78% were obtained, respectively.

Although the Yoshikawa method has been successfully used throughout the literature to form nucleoside phosphates, the preparation of reagents for adapted methods, very time consuming purification hinder the synthesis of desired products, which are often formed in lower yields that the two examples cited above.

To address these issues, the Hodgson group has applied the idea of click chemistry to the preparation of alkylated thiophosphoramidates in aqueous solution (Scheme 1.4). Alkylated thiophosphoramidates represent simple phosphate diester mimics and the wide range of alkylating agents and primary amines available provides an opportunity to introduce diversity into their structures.

Scheme 1.4 Application of click chemistry to preparation of alkylated thiophosphoramidate analogues.

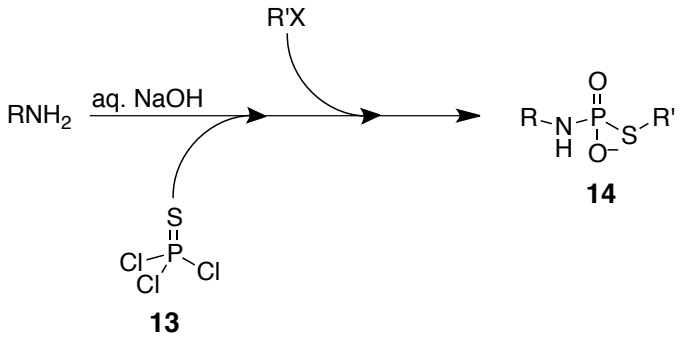

As presented in Scheme 1.4, the click chemistry procedure simply involves the addition of thiophosphoryl chloride **13** to an amine (RNH_2) in aqueous solution, followed by addition of an alkylating agent (R`X). In favourable cases, alkylated thiophosphoramidate products **14** were formed in essentially quantitative yields which avoided the need for tricky purification steps. The reactions were performed in single reaction vessels where reaction times were on the order of hours. Given that thiophosphoryl chloride **13** and a large range of amines and alkylating agents are commercially available, the preparation of starting materials is not required when using common amines. However, amines which are commercially unavailable, for example 5'-amino-5'-deoxynucleosides, need to be prepared prior to thiophosphorylation. The "click" concept developed by Trmčić and Hodgson is discussed in further detail in Section 1.2.1.2.

1.2 Phosphoramidates and thiophosphoramidates

As part of developing phosphoramidates and thiophosphoramidates as potential mimics to phosphate esters, we hope to develop and optimize aqueous thiophosphorylation strategies for amines. To understand the reactivities of phosphoramidate analogues in aqueous solution, literature studies pertaining to their hydrolysis in aqueous solution are presented and discussed. Synthetic procedures towards (thio)phosphoramidates from the literature are then described. The complexities of these methods demonstrate the potential benefits of aqueous (thio)phosphorylation strategies for amines and highlight the need for optimisation if near quantitative conversions of (thio)phosphorylating agent to (thio)phosphoramidate product are to be observed.

Phosphoramidates and thiophosphoramidates are analogues of phosphates and thiophosphates respectively, where a hydroxyl group is replaced by an amino group (Figure 1.1).

Figure 1.1 The structure of a phosphoramidate 15 and thiophosphoramidate 16.

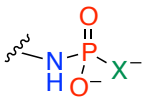

X = O 15
X = S 16

Kinetic studies have shown that phosphoramidates **15** and thiophosphoramidates **16** are unstable with respect to hydrolysis in aqueous solutions of pH<10. Although structurally similar, *S*-alkylated and non-*S*-alkylated thiophosphoramidates **16** have shown greater stability towards hydrolysis than their phosphoramidate analogues **15** in acidic solution.[5] At pHs above 10, the stability of (thio)phosphoramidates increases considerably. These studies are discussed in greater detail in Section 1.2.2.

Owing to the nucleophilicity of S^-, it is possible for non-*S*-alkylated thiophosphoramidates **16** to react with a wide range of electrophiles to generate a large array of *S*-alkylated thiophosphoramidates which may act as phosphate diester mimics.

We now present literature methods towards the synthesis of (thio)phosphoramidates and discuss mechanistic studies regarding their hydrolysis in aqueous solution.

1.2.1 Synthetic procedures towards (thio)phosphoramidates

In order to illustrate the problems associated with tricky syntheses and purification of (thio)phosphoramidates, the following sections will discuss a variety of different literature synthetic methods towards the preparation of oxy and thiophosphoramidates. These will begin with early research and lead to the development of aqueous phosphorylation methods. The chapter will conclude with the optimisation of (thio)phosphoramidate synthetic methods through the use of aqueous click chemistry.

1.2.1.1 Oxyphosphoramidates

The reaction of 5'-amino-5'-deoxynucleosides **17** and **18** with phosphochloridates **19** ($p$$NO_2$BnO)$_2$POCl or ($CH_2CCl_3O$)$_2$POCl) in solutions of dioxane/ tetrahydrofuran was observed by Jastorff and Hettler to generate phosphorylated 5'-amino-5'-deoxynucleosides **22** (Scheme 1.5).[6, 7]

Scheme 1.5 Preparation of phosphorylated 5'-amino-5'-deoxynucleosides 22 through reaction of 5'-amino-5'-deoxynucleosides 17 and 18 with protected phosphochloridates 19. [6, 7]

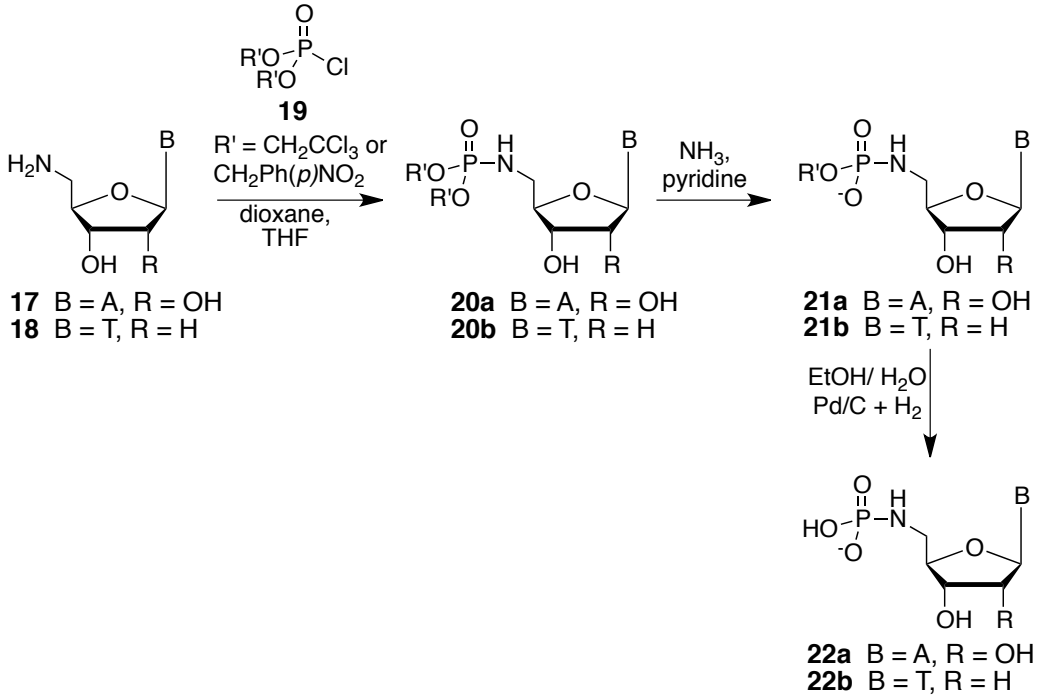

Phosphorylation of 5'-amino-5'-deoxynucleosides **17** and **18** using phosphochloridate species **19** led to the preparation of *O*,*S*'-dialkyl-*N*-alkyl phosphoramidates **20** in yields of 50 to 85%. Addition of **20** to a solution of pyridine and ammonia (1:1) resulted in the quantitative cleavage of one P-OR' bond, leading to diester mimics **21**. The remaining P-OR' bond of ester **21** was not susceptible to further alkaline hydrolysis and so no further reaction was observed in this solution. Cleavage was, however, achieved through catalytic hydrogenation using palladium over carbon in aqueous ethanol at high pH (~10), where the rate of phosphoramidate hydrolysis was minimal. This generated the desired phosphorylated 5'-amino-5'-deoxynucleosides **22**. Purified yields of 5' nucleoside phosphoramidate **22** were not given, however, they may be expected to be low due to the multiple step approach. This method is further

complicated as the phosphorylating agent is not commercially available, and so would need to be prepared prior to phosphorylation.

An alternative synthetic method towards oxyphosphoramidates was developed by Hampton *et al.* and involved reaction of 5'-amino-5'-deoxyinosine **23** with phosphorus oxychloride in dry acetonitrile to give 5'-amino-5'-deoxyinosine 5'-*N*-phosphate **24** (Scheme 1.6).[8, 9]

Scheme 1.6 Phosphorylation of 5'-amino-5'-deoxyinosine 23 using $POCl_3$ to give 5'-amino-5'-deoxyinosine 5'-*N*-phosphate 24.[8, 9]

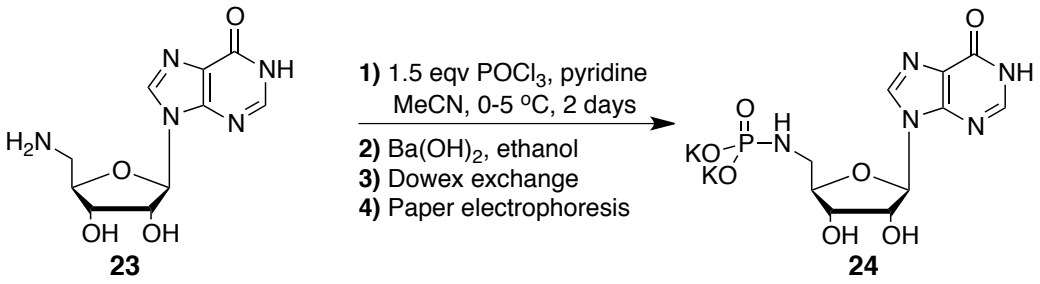

The procedure involved addition of 5'-amino-5'-deoxyinosine **23** to a dry acetonitrile solution containing $POCl_3$ and pyridine at 0 °C. Long reaction times (~2 days) were necessary to ensure quantitative phosphorylation of the amine. Laborious precipitation plus ion-exchange with $Ba(OH)_2$ and Dowex (K^+) ion-exchange resin gave the crude phosphoramidate as a potassium salt. Time-consuming paper electrophoresis in ammonium formate ($pK_a \sim 4.5$) buffer at pH 8 was then necessary to yield 5'-amino-5'-deoxyinosine 5'-*N*-phosphate **24** as a white solid. Although this procedure did not require the use of protecting groups, time-consuming purification was necessary to isolate 5'-amino-5'-deoxyinosine 5'-*N*-phosphate **24** as a pure potassium salt.

The stability of 5'-amino-5'-deoxyinosine 5'-*N*-phosphate in the ammonium formate buffer (pH = 8) used in paper electrophoresis was not discussed by Hampton *et al*. However, as part of studies described later in this section, Williamson determined the half-life of 5'-amino-5'-deoxyguanosine in aqueous solution of pH 8 as 2.5 h.[10, 11] Given the similarity in structure of these amino nucleosides, it is likely that 5'-amino-5'-deoxyinosine 5'-*N*-phosphate **24** was observed to undergo hydrolysis to 5'-amino-5'-deoxyinosine **23** and inorganic phosphate during purification by paper electrophoresis.

In addition, the isolated yield of 5'-amino-5'-deoxyinosine 5'-*N*-phosphate **24** was not reported.

As part of an investigation into the enzymatic synthesis of a series of nitrogen and sulphur analogues of dihydroxyacetone phosphate (DHAP), phosphoramidate **26** was synthesised by Duncan and Drueckhammer from the addition of $POCl_3$ to aqueous solution of aminoalcohol **25** (Scheme 1.7).[12]

Scheme 1.7 Synthesis of the phosphoramide analogue of DHAP.[12]

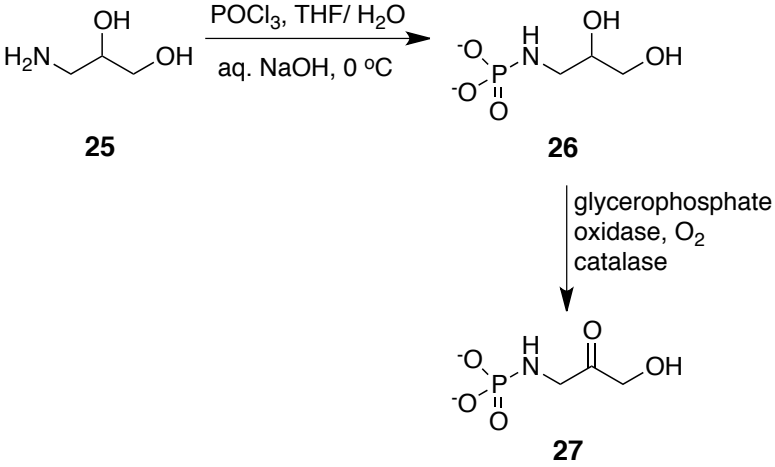

The synthesis of phosphoramidate **26** involved the addition of $POCl_3$ in THF (5 mL) to an aqueous solution of aminoalcohol **25** (10 mL, 0 °C) over a period of 30 min. Co-addition of 6 M sodium hydroxide solution was necessary to ensure the reaction pH was maintained between 9 and 11, where the amine functionality of aminoalcohol **25** lies in its neutral form and any contribution from a hydroxide catalysed hydrolysis term is minimised as much as possible.

Scheme 1.Scheme 1.8 shows the possible reaction pathways and products from the addition of $POCl_3$ to an aqueous solution of aminoalcohol **25**.

Scheme 1.8

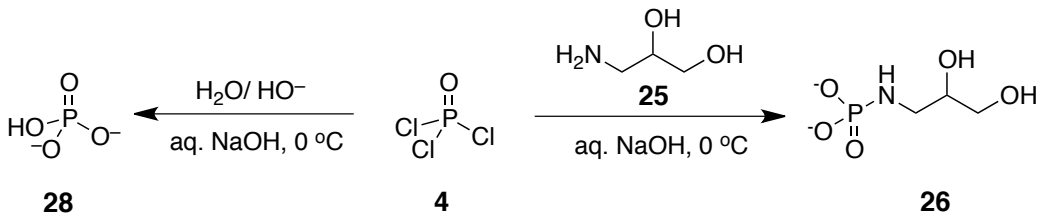

Due to the greater nucleophilicity of the amino functionality of **25**, phosphorus oxychloride reacted predominantly with the amino group to generate phosphoramidate **26**, rather than with competing water and hydroxide nucleophiles to give inorganic phosphate **28**. Following phosphorylation, the resulting phosphoramidate **26** was treated with glycerophosphate oxidase and subsequently oxidised to generate DHAP analogue **27**.

Kers and Stawinski have reported a synthetic route towards the 5'-*N*-bridging phosphoroamidate, O-dimethoxytritylthymidin-3'-yl *N*(3'-tert-butyldimethyisilyl-thymidin-5'-yl) phosphoramidate **33**.[13, 14] The procedure involves coupling of nucleosides **30** and **31** to form dithymidine H-phosphonamidate **32**, which is followed by oxidation to give phosphoramidate **33** (Scheme 1.9).

Scheme 1.9

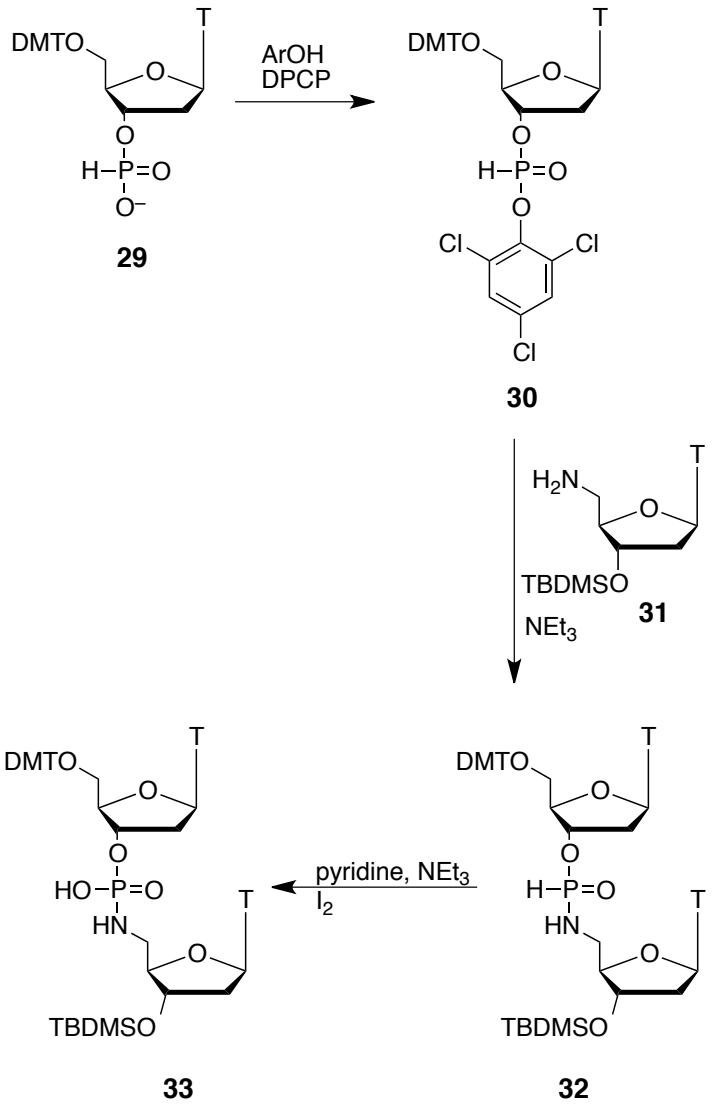

Scheme 1.9 illustrates the *in* situ reaction of 5'-O-dimethoxytritylthymidine 3'-H-phosphonate **29** with 2,4,6-trichlorophenol to form the corresponding nucleoside aryl H-phosphonate diester **30**. Once formed, **30** was reacted with protected amino nucleoside **31** to generate the *N*-alkyl-H-phosphonamidate **32**. Finally, stirring in an aqueous solution of pyridine, triethylamine and iodine gave the dithymidine phosphoramidate analogue **33** in a yield of 86% (calculated over 2 steps from **30**).

As part of kinetic studies of the hydrolysis of 3'-*N*-bridging phosphoramidates, Ora *et al.* have developed synthetic methods towards phosphoramidate analogues 3'-amino-3'-

deoxythymidylyl-3',5'-thymidine (TnpT, **36**) and 3'-amino-3'-deoxyuridylyl-3',5'-uridine (UnpU, **37**) (Scheme 1.10).[5,15]

Scheme 1.10

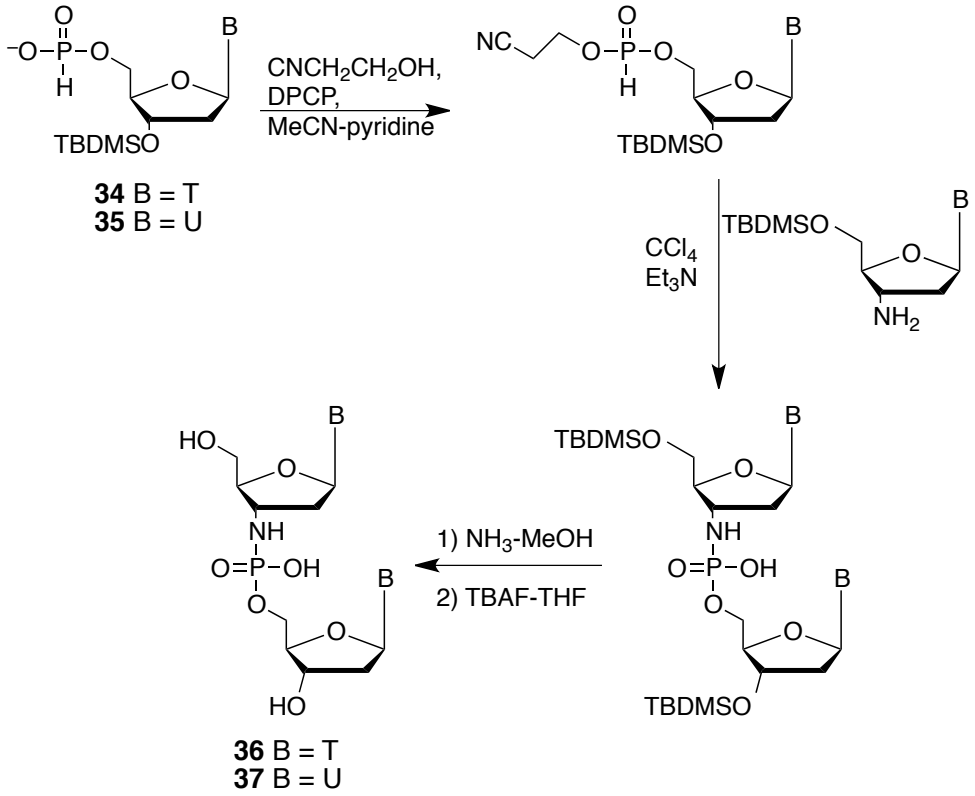

3'-amino-3'-deoxythymidylyl-3',5'-thymidine **36** and 3'-amino-3'-deoxyuridylyl-3',5'-uridine **37** were purified by Dowex® (50W × 2) cation exchange chromatography. One of the major obstacles towards the synthesis of phosphoramidates **36** and **37** is the large number of time-consuming steps required, which includes the preparation of 5'-O-(tert-butyldimethylsilyl)thymidine 5'-hydrogenphosphonate **34** and 5'-O-(tert-butyldimethylsilyl)uridine 5'-hydrogenphosphonate **35** starting materials.

As part of investigations into general acid catalysis by the hepatitis delta virus ribozyme, Das and Piccirilli synthesised cytosine and guanosine phosphoramidites **38** and **39** and linked them together by solid-phase synthesis to give oligonucleotides **40** bearing a 5' sulphur bridging unit (Scheme 1.11).[16, 17]

Scheme 1.11

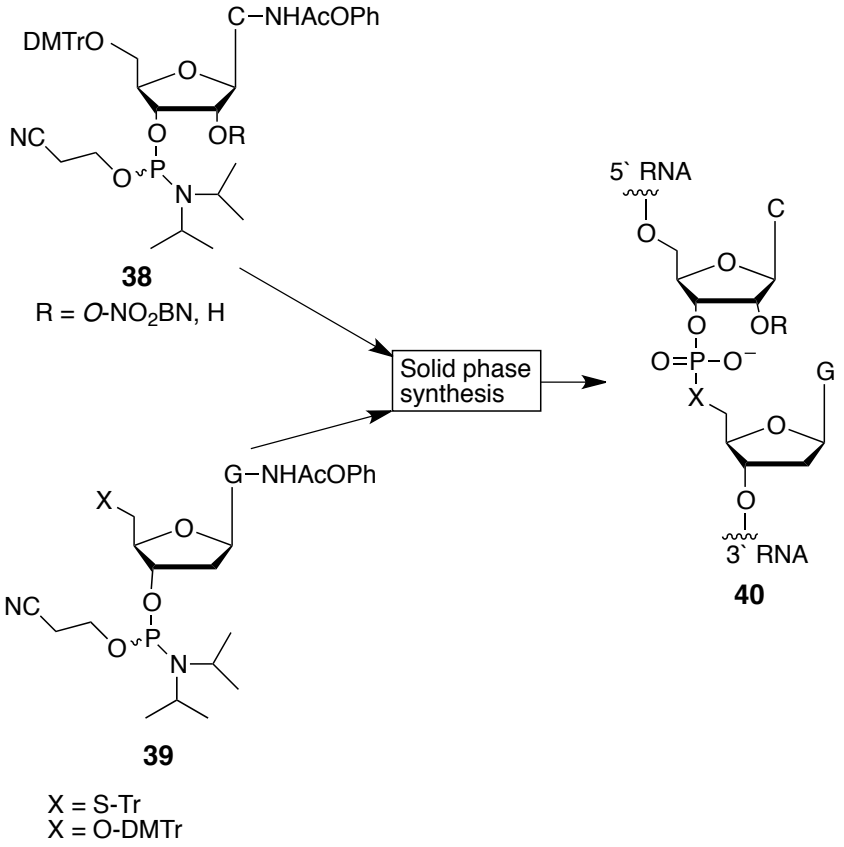

Nucleoside phosphoramidites **38** and **39** were prepared through phosphitylation with *N*-methylimidazole triflate. Global protection was required for each phosphoramidate precursor to prevent unwanted side reactions at reactive functional groups. The efficiency of coupling in solid-state synthesis was not reported.

In a study of RNA bioconjugates, Hodgson and Williamson studied the incorporation of novel initiators into RNA. The initiator 5'-amino-5'-deoxyguanosine-5'-*N*-phosphoramidate **44** was synthesised using an aqueous phosphorylation methodology, where time-consuming chromatography steps were avoided.

After achieving poor results from the application of Yoshikawa and Hampton methods to the phosphorylation of of 5'-amino-5'-deoxyguanosine **41**, Williamson and Hodgson adapted Drueckhammer's[12] aqueous-based phosphorylation strategy towards the synthesis of 5'-amino-5'-deoxyguanosine-5'-*N*-phosphoramidate **44** (Scheme 1.12).[11,10]

Scheme 1.12 Phosphorylation of 5'-deoxy-5'-aminoguanosine 44 under aqueous conditions.[11,10]

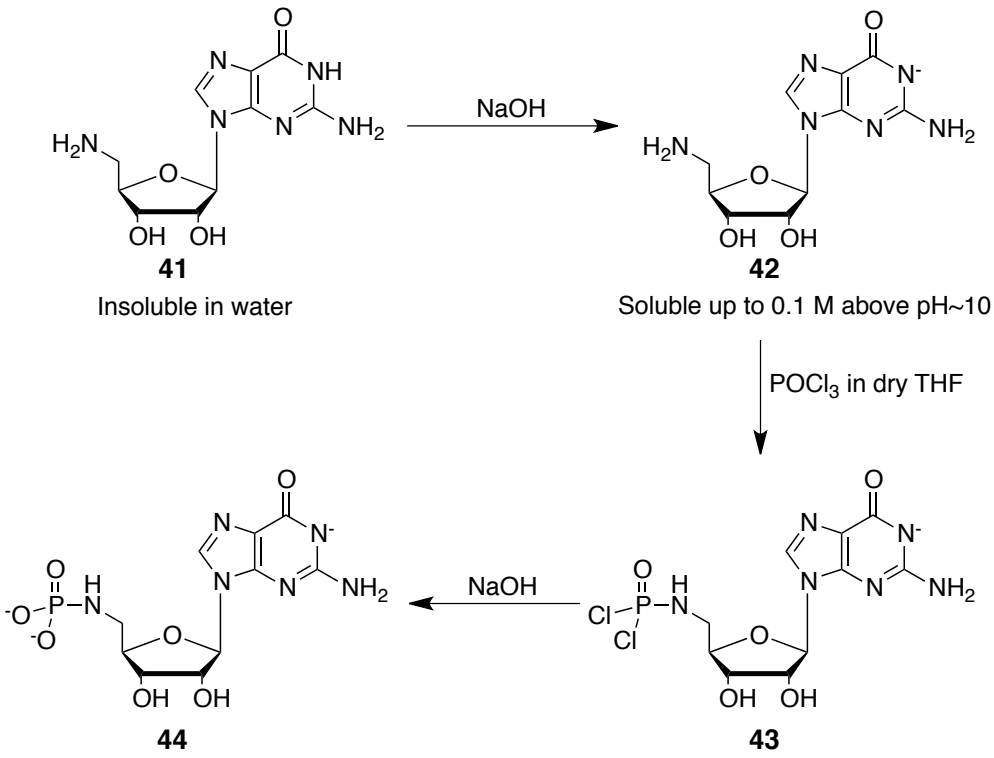

Owing to the insolubility of 5'-deoxy-5'-aminoguanosine **41** in many solvents, including water of low or neutral pH, addition of one equivalent of NaOH was necessary to deprotonate the *N*-1 position of the guanyl group and thus solubilise 5'-deoxy-5'-aminoguanosine **42**. A solution of $POCl_3$ in dry THF was subsequently added dropwise to a rapidly stirred aqueous solution of deprotonated 5'-deoxy-5'-aminoguanosine **42**. This resulted in phosphorylation of the 5'-amine functionality leading to the formation of the aminophosphodichloridate **43**. Subsequent hydrolysis of dichloridate **43** gave 5'-amino-5'-deoxyguanosine-5'-*N*-phosphoramidate **44**. In addition to the formation of **44**, small amounts of 2' and 3' phosphate esters of **42** were observed.

Selective phosphorylation at the 5'-amino position of **42** was observed due to the greater nucleophilicity of the amine *vs* water. The effect of the number of added equivalents of sodium hydroxide upon the conversion of $POCl_3$ to phosphoramidate **44** was investigated by ^{31}P NMR spectroscopic analyses of reaction products containing between 4 and 6.5 equivalents of NaOH (Figure 1.2).

Figure 1.2 **The effect of a change in concentration of NaOH upon the conversion of $POCl_3$ to phosphoramidate 44, determined by ^{31}P NMR spectroscopy. [11]**

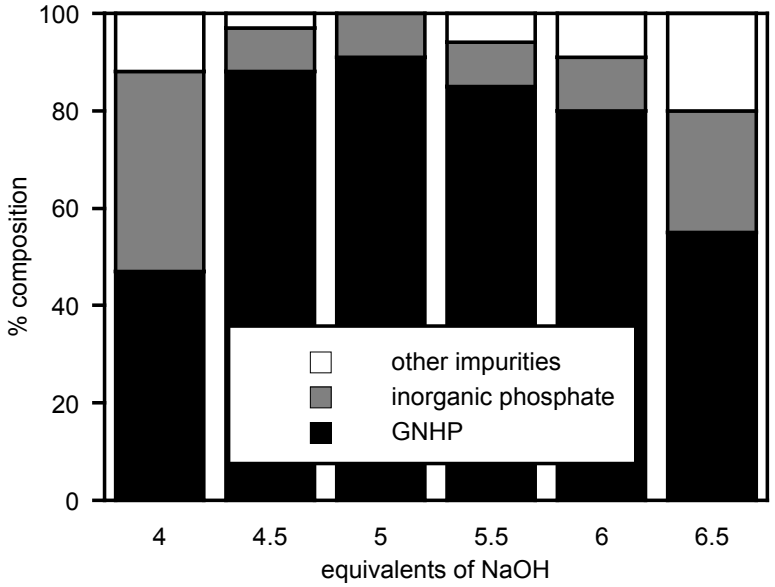

(*Reproduced by permission of The Royal Society of Chemistry)*

Scheme 1.13 shows some of the competing processes that are thought to lead to the observed reaction products.

Scheme 1.13

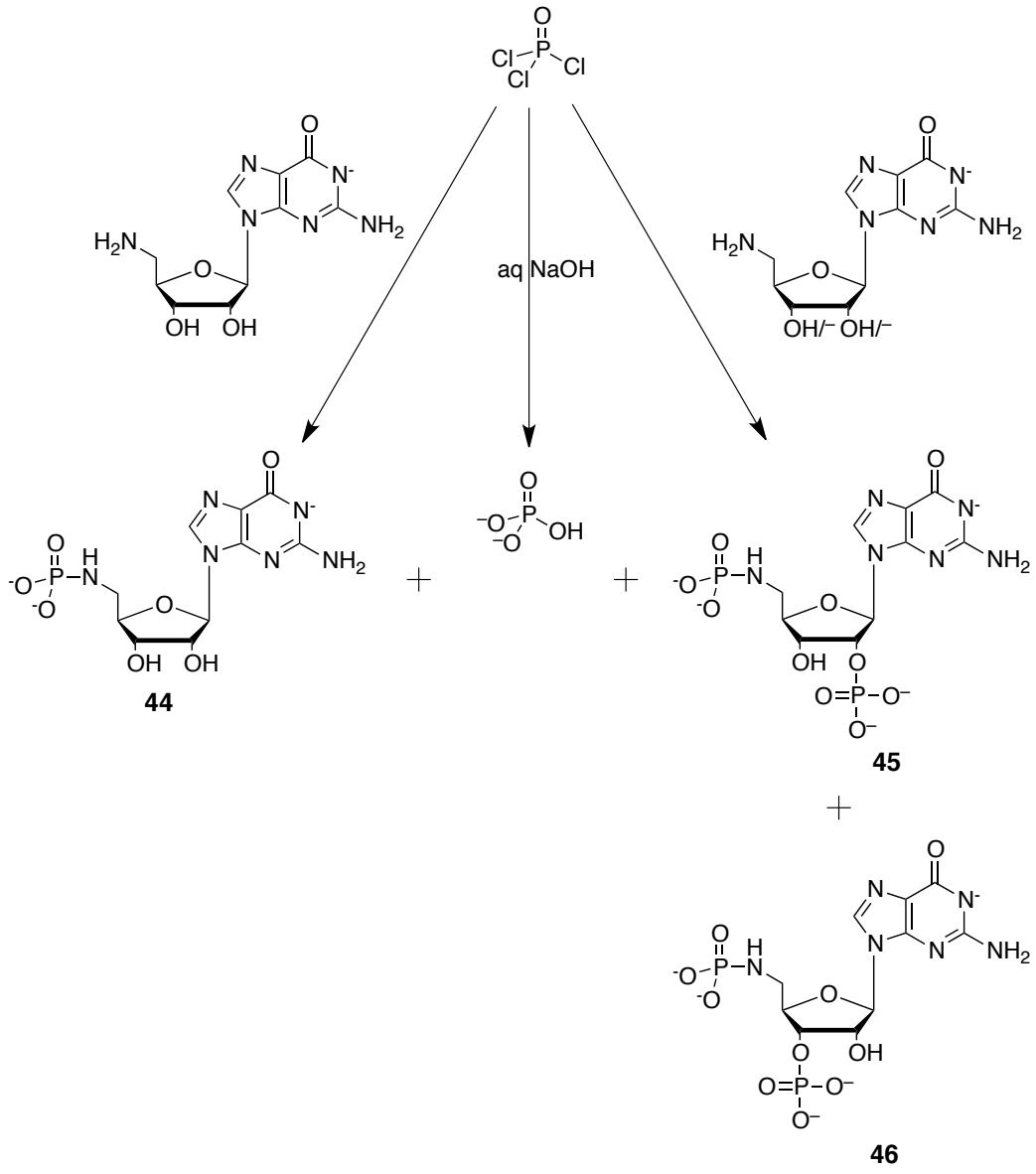

Competing reactions of phosphorus oxychloride in aqueous 5'-deoxy-5'-aminoguanosine solutions are shown in a simplified form in Scheme 1.13. From Figure 1.2, it can be seen that phosphorylation of 5'-deoxy-5'-aminoguanosine **41** to give 5'-amino-5'-deoxyguanosine-5'-*N*-phosphoramidate (GNHP) **44** is selective over hydrolysis of phosphorus oxychloride and nucleophilic attack by the 2' and 3' hydroxyl groups of **42** at $POCl_3$ in aqueous solutions containing five equivalents of NaOH. Protonation of 5'-amino-5'-deoxyguanosine at lower NaOH concentrations led to its precipitation out of solution. At reduced amine concentrations, the conversion of $POCl_3$ to inorganic phosphate was increased. In addition, a decrease in pH over the

course of the reaction may be accompanied by the precipitation of 5'-amino-5'-deoxyguanosine in these solutions. The amount of inorganic phosphate formed during phosphorylation was also observed to rise as the concentration of NaOH was increased above 5 equivalents; this may be a consequence of an increase in the rate of hydrolysis at higher hydroxide concentrations, thus competing with the phosphorylation of 5'-deoxy-5'-aminoguanosine **42**. In addition, deprotonation of the 2' and 3' hydroxyl groups of 5'-deoxy-5'-aminoguanosine (pK$_a$ ~ 12.4) at high pH likely leads to nucleophilic attack by either hydroxyl group at $POCl_3$ to give 2' and 3' phosphoesters (defined as 'other impurities') **45** and **46**, respectively.[11]

Following the reaction of $POCl_3$ and 5'-deoxy-5'-aminoguanosine **41** in an aqueous solution containing five equivalents of sodium hydroxide, THF was removed and the product mixture was analysed by ^{31}P NMR spectroscopy. A 90% conversion from $POCl_3$ to the desired 5'-amino-5'-deoxyguanosine-5'-*N*-phosphoramidate **44** was observed using five equivalents of sodium hydroxide. As part of developing simple aqueous phosphorylation chemistry with no time-consuming chromatography steps required, crude 5'-amino-5'-deoxyguanosine-5'-*N*-phosphoramidate initiator was incorporated into RNA *via* transcription.[10, 11]

1.2.1.2 Thiophosphoramidates

Following the successful aqueous phosphorylation of 5'-amine-5'-deoxyguanosine in our research group,[10, 11] attempts were made to develop and optimize aqueous thiophosphorylation strategies for amines. This section focuses on literature methods of thiophosphorylation using phosphorus (V) chlorides that lead up to the development of an aqueous-based strategy by the DRWH research group. Several literature examples of thiophosphorylation are now presented.

As part of an investigation into the activity of potential antimalarial agents, Mara *et al.* synthesised a series of substituted thiophosphoramidate analogues of amiprophos ethyl **49** (Scheme 1.14).[18]

Scheme 1.14 Preparation of thiophosphoramidate analogues of amiprophos ethyl 49.[18]

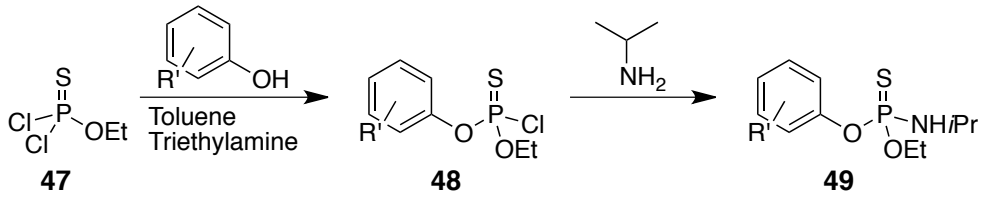

Reactions were performed under anhydrous conditions and involved the addition of ethyl dichlorophosphate **47** to a solution of toluene containing the given substituted phenol and triethylamine. Monochloridates **48** was formed following stirring for 7 h under nitrogen, and isopropylamine was subsequently added to the reaction solution and stirred for an additional 8 h. Products were purified *via* column chromatography to give thiophosphoramidates **49** in yields of 35 to 80%.

As part of research into the development of more effective anti-retroviral agents, Venkatachalam *et al.* studied the hydrolysis pathways of substituted aryl thiophosphoramidates of stavudine **52**.[19] Thiophosphoramidate derivatives of stavudine were synthesised according to Scheme 1.15.

Scheme 1.15 Venkatachalam's synthetic route to thiophosphoramidate derivatives of stavudine.[19]

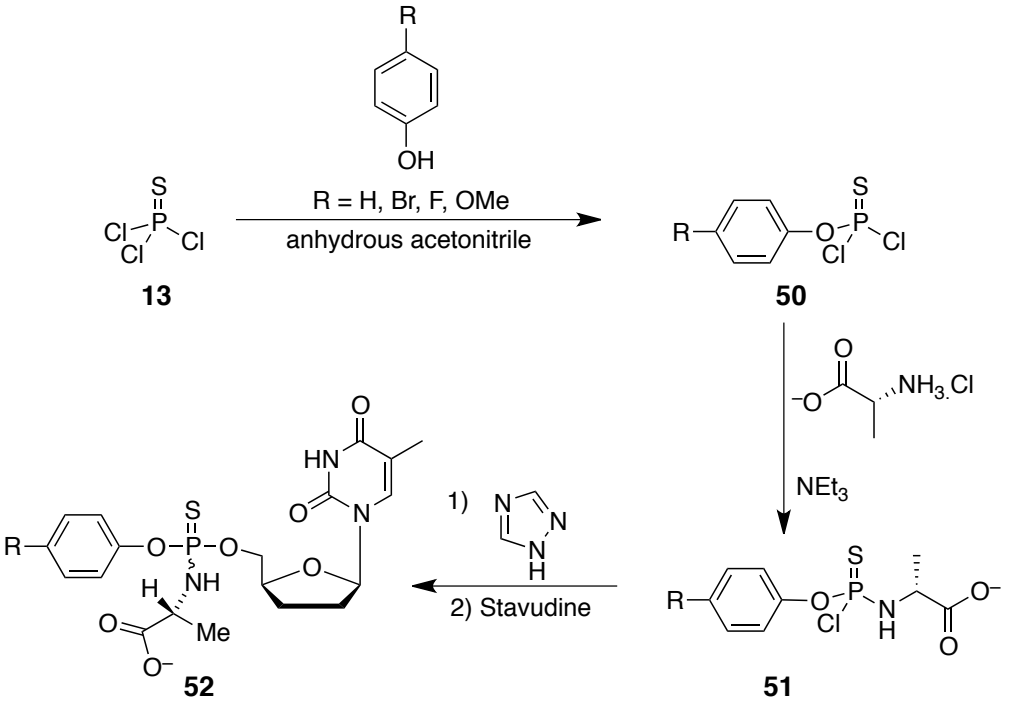

Reaction of thiophosphoryl chloride **13** with various 4-substituted phenols (R = H, Br, F and OMe) was performed in an anhydrous acetonitrile solution containing triethylamine. Following the addition of 4-substituted phenol, the reaction solution was stirred at room temperature for 5 h and then refluxed for an addition 2 h. The crude mixture was filtered, evaporated to dryness and purified by vacuum distillation to give purified thiophosphorodichloridates **50** in yields of ~50%. Reaction of dichloridates **50** with L-alanine methylester hydrochloride and triethylamine in anhydrous acetonitrile solution led to the formation of the corresponding thiophosphorochloridate **51**. 1,2,4 Triazole and stavudine were subsequently added to the reaction solution and the mixture was stirred at 50 °C for 2 weeks. Following this time, solvents were removed under reduced pressure and **52** was purified by column chromatography and preparative TLC. Thiophosphoramidates **52** were isolated in yields of ~12%. Although successful, this method involves long reaction times, several chromatography steps and results in a very low yield.

In an attempt to thiophosphorylate proteins such as thymidylate synthase, Ruman *et al.* prepared an array of thiophosphorylated amino acids derivatives **54-56** from diammonium thiophosphoramidate **53** in aqueous ammonium carbonate buffer (Scheme 1.16).[20]

Scheme 1.16 Reaction of diammonium thiophosphoramidate with an array of amino acids.[20]

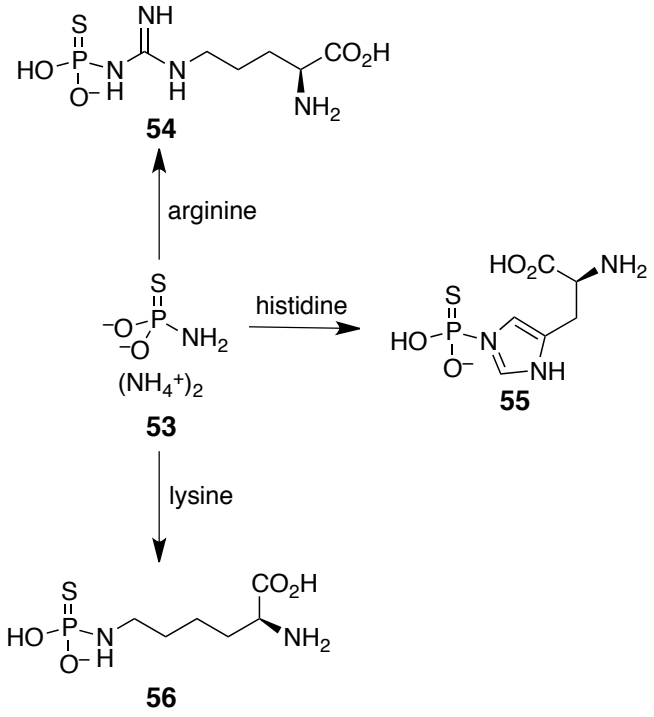

Diammonium thiophosphoramidate **53** was prepared from the reaction of thiophosphoryl chloride **13** with ammonium hydroxide, according to a published method by Pirrung *et al.* (Scheme 1.17).[21]

Scheme 1.17 Pirrung's synthesis of diammonium thiophosphoramidate 53 and potassium thiophosphoramidate 57.[21]

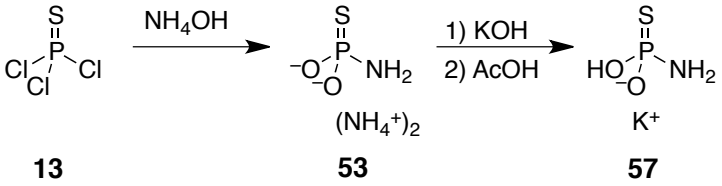

As shown in Scheme 1.17, thiophosphoryl chloride was added dropwise to a stirred solution of 10% ammonium hydroxide at 0 °C. This resulted in a homogeneous solution and acetone was subsequently added to precipitate pure diammonium thiophosphoramidate **53**. Following filtration and washing in ether, diammonium thiophosphoramidate was heated in KOH solution for 30 min. Addition of acetic acid decreased the reaction pH to pH 6, where protonation of a hydroxyl group led to the

formation of the potassium thiophosphoramidate **57** which was precipitated in ethanol and filtered to give a white solid in a yield of 78%.[21]

The benefits of this aqueous phosphorylation method towards thiophosphoramidates **53** and **57** are clear; the reaction procedure was simple, short (~minutes) and did not require protection of starting materials, thiophosphoramidate products were formed in high yields where time-consuming chromatography was not required.

Addition of diammonium thiophosphoramidate to an ammonium carbonate solution containing arginine, histidine or lysine led to the formation of thiophosphoramidates **54**, **55** and **56**, respectively. Ammonium carbonate buffers were necessary for maintaining a high reaction pH; this ensured that the amine functionality of the amino acid remained in its reactive form throughout the reaction. Reactions were followed by ^{31}P NMR spectroscopy and were shown to be complete following stirring for 72 h. No indication was given of the isolated yields in each case.

S-non-bridging thiophosphoramidate based dinucleotides **62** bearing a nitrogen linkage were prepared by Kers and Stawinksi in organic solution using H-phosphonate methodology, according to Scheme 1.18.[13]

Scheme 1.18 Preparation of oligo thiophosphoramidates analogues 62.[13]

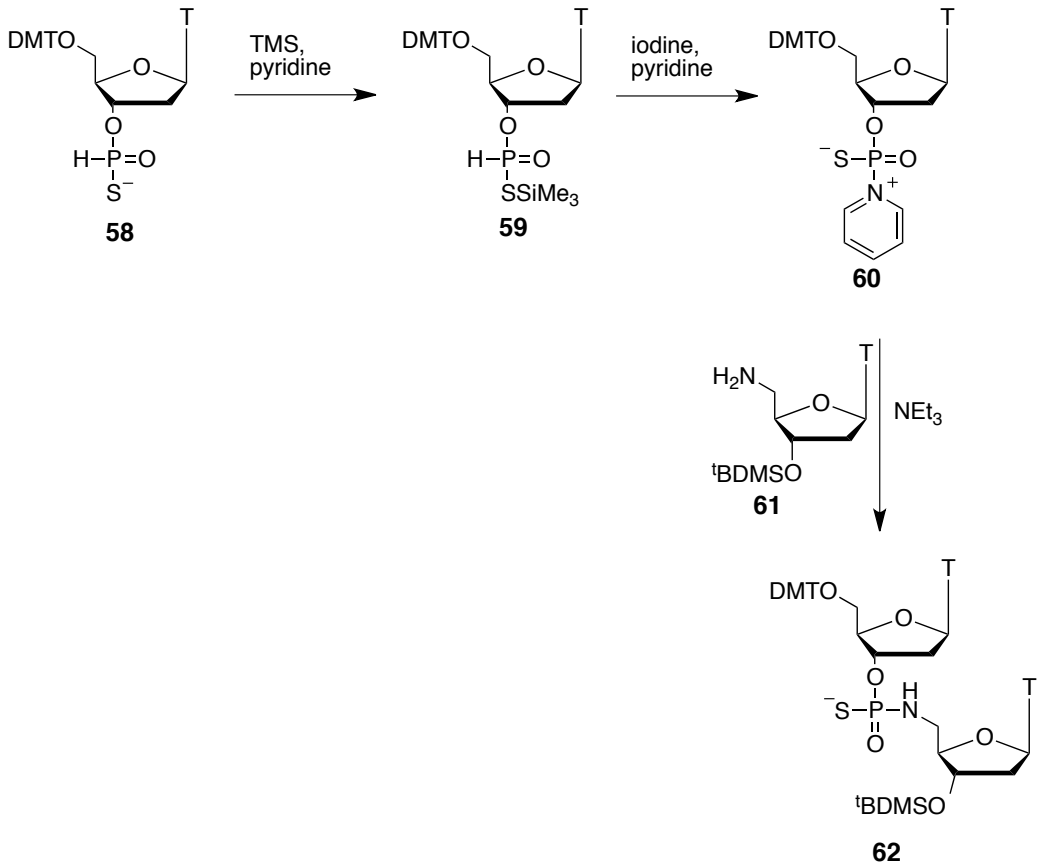

As shown in Scheme 1.18, oligothymidine H-phosphonothioate **58** was silylated with trimethylsilyl chloride (TMS) in the presence of pyridine to give **59**. Addition of iodine subsequently led to the pyridine adduct of **60**. Subsequent nucleophilic attack by the 5'-amino functionality of the protected thymidine **61** gave rise to oligothymidine *S*-non-bridging thiophosphoramidate **62**. A 70% yield was obtained following purification by reverse-phase chromatography.

In a continuation of aqueous phosphorylation studies of 5'-deoxy-5'-aminoguanosine, Trmčić and Hodgson developed effective methods towards thiophosphorylation of commercially available amines in aqueous reaction media using thiophosphoryl chloride (Scheme 1.19).[22]

Scheme 1.19 Thiophosphorylation of commercially available amines 63 in aqueous solution.[22]

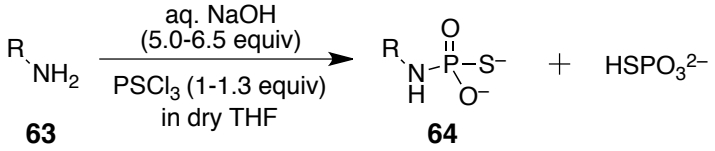

Thiophosphoryl chloride was added in THF to stirred aqueous mixtures containing NaOH and a commercially available amine **63**. It was necessary to employ THF as a co-solvent given the poor solubility of $PSCl_3$ in aqueous solution. Reaction solutions were stirred for 1 h following addition of $PSCl_3$ to ensure complete reaction. In general, thiophosphoramidate products **64** were synthesised in conversion levels of 91 to 98%, according to Scheme 1.19. Inorganic thiophosphate was generated as a minor impurity, which is likely due to a competing reaction of sodium hydroxide with $PSCl_3$.

Following the successful thiophosphorylation of one equivalent of amine using 1.0 to 1.2 equivalents of $PSCl_3$, Trmčić and Hodgson applied a "click" chemistry approach towards the alkylation of thiophosphoramidates in a one-pot method (Scheme 1.20).

Scheme 1.20 Application of "click" chemistry to one-pot thiophosphorylation and alkylation of amines in aqueous solution

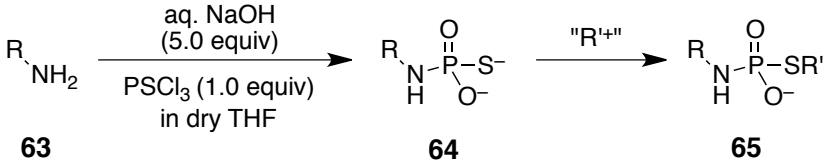

Preliminary studies focused upon alkylation of thiophosphoramidates **64** using an excess of methyl iodide. Following alkylation, product mixtures were washed with diethyl ether to remove excess alkylating agent and were subsequently analysed by ^{31}P and ^{1}H NMR spectroscopy after lyophilisation. High conversions of thiophosphoramidate to *S*-methylthiophosphoramidate **65** were observed (Table 1.1).

Table 1.1

Substrate	Conversion to *N*-alkyl *S*-methylthiophosphoramidate (%)
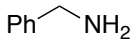	98[a], 94[b]
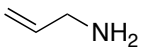	97[a], 96[b]
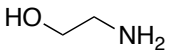	93[a], 80[b]
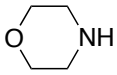	97[a], 91[b]

[a]Determined by ^{31}P NMR spectroscopy. [b] Determined by ^{1}H NMR spectroscopy.

The results in Table 1.1 show that high conversions to *S*-methylthiophosphoramidate were observed, with small amounts of impurities due to unreacted starting materials and *S*-methylated thiophosphate. The need for time-consuming ion exchange chromatography was therefore significantly reduced.

After obtaining these promising results, Trmčić and Hodgson expanded this study to cover a range of amine substrates and alkylating agents, which included conjugate acceptors, epoxides, and halides. In most cases, high conversions (> 90%) were observed. However, the alkylation of benzylamine **66** using 5'-deoxy-5'-iodoguanosine **68** (Scheme 1.21) was an exception to this.

Scheme 1.21

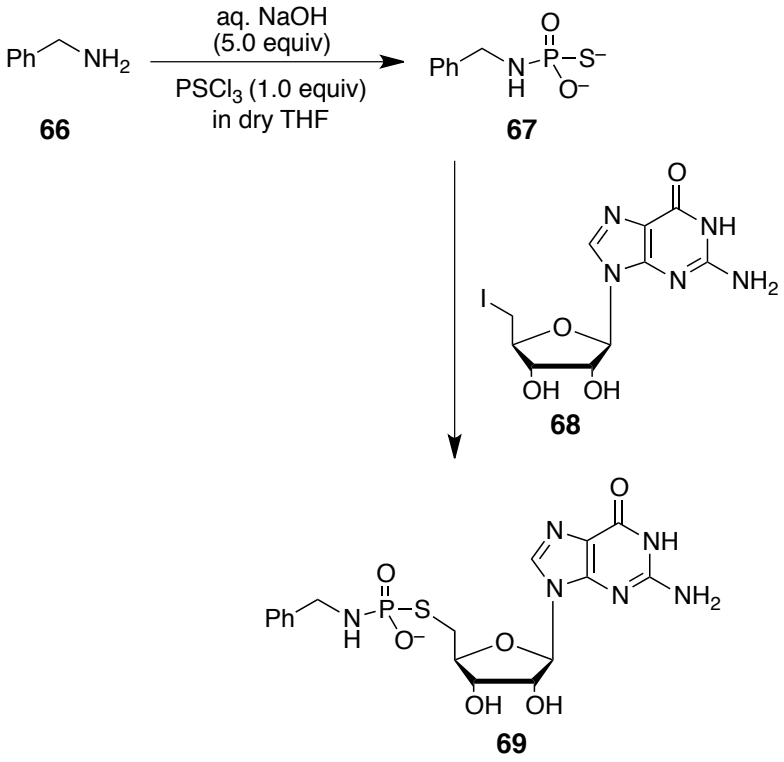

Benzylamine **66** was thiophosphorylated using the same aqueous phosphorylation method. 5'-Deoxy-5'-iodoguanosine **68** was subsequently added to an excess of thiophosphoramidate **67**. Due to the solubility, steric and electronic factors which reduce the reactivity of 5'-deoxy-5'-iodoguanosine, it was necessary to heat the reaction solution at 50 °C for 32 h for appreciable levels of *S*-alkylation to occur. Following the reaction, only a moderate level of conversion to **69** (73%) was observed.

Given the success of the "click" chemistry approach to the synthesis of alkylated thiophosphoramidates, Trmčić applied the method to the formation of alkylated 5'-5'-amino-5'-deoxyadenosine and 5'-amino-5'-deoxyguanosine thiophosphoramidates (Scheme 1.22).

Scheme 1.22 Preparation of *S*-alkylated 5'-adenosine and guanosine thiophosphoramidates in a "one-pot" reaction.

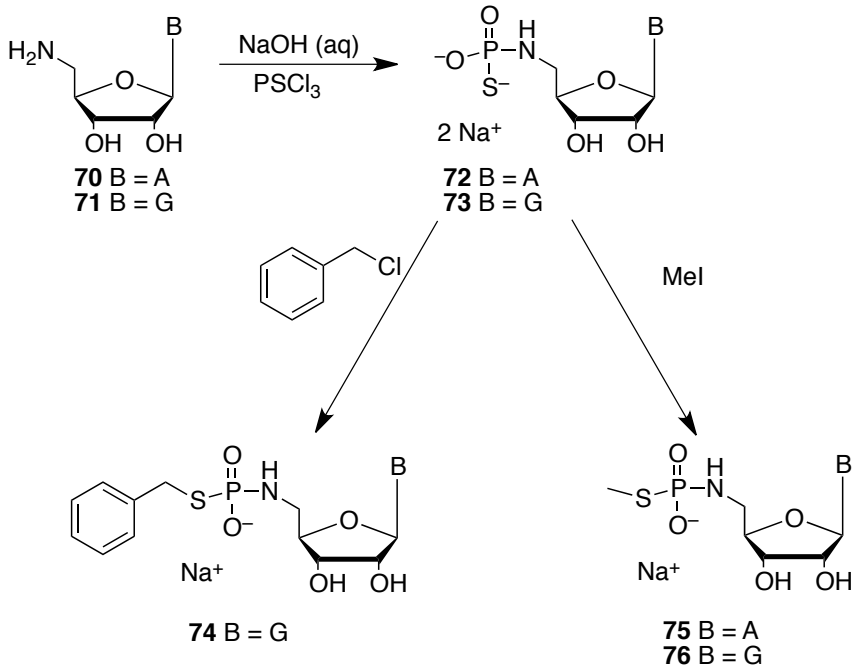

A solution of thiophosphoryl chloride in dry THF was added to one equivalent of 5'-amino-5'-deoxyadenosine **70** or 5'-amino-5'-deoxyguanosine **71** in aqueous sodium hydroxide solution and was stirred for 1 h. Thiophosphoramidates **72** and **73** were then alkylated upon addition of an excess of methyl iodide or benzyl chloride to the reaction solutions to give *S*-alkylated thiophosphoramidates **74**-**76**.

5'-Amino-5'-deoxyadenosine **70** and 5'-amino-5'-deoxyguanosine **71** showed moderate conversions (71 to 78% by ^{31}P NMR spectroscopy) when transformed into an *S*-alkylated thiophosphoramidates. Typical by-products observed were *S*-alkylated inorganic thiophosphate, inorganic phosphate, 5'-amino-5'-nucleoside and some additional unknown phosphorus containing compounds.

In summary, Trmčić and Hodgson have developed an aqueous "click" chemistry procedure towards the synthesis of *S*-alkylated thiophosphoramidates in a one-pot procedure. High conversions (> 90%) were observed for transformations using simple amines, which avoid the need for purification by HPLC or chromatography. Moderate conversions (~70 to 80%) were observed for more complicated amines such as 5'-aminonucleosides.

1.2.1.3 Conclusions

The literature examples discussed in Sections 1.2.1.1 and 1.2.1.2 show the variety of different methods available in generating phosphoramidates and thiophosphoramidates. Although successful, (thio)phosphorylation in organic media generally generates products in only moderate yields, following tricky reaction procedures and time-consuming purification methods.

Procedures which utilise a (thio)phosphoramidate salt as (thio)phosphorylating agent in aqueous solution involve simpler purification methods, however, these require time consuming reactant preparation steps and slow reactions, primarily due to the absence of a good leaving group in the (thio)phosphorylating agent.

In contrast, Hodgson's method of (thio)phosphorylation employs a reactive thiophosphorylating agent in an aqueous environment where laborious chromatography may not be necessary, leading to high product yields, significantly shorter reaction times than alternative synthetic methods (hours *vs* days).

In order to avoid unwanted chromatography steps, near-quantitative aqueous (thio)phosphorylation of amines to (thio)phosphoramidates must be developed across a range of amine nucleophiles. For new methods to be developed, the reactivity of (thio)phosphorylating agents towards water needs to be understood. The optimal reaction conditions for the phosphorylation of 5'-deoxy-5'-aminoguanosine **41** to 5'-amino-5'-deoxyguanosine-5'-*N*-phosphoramidate **44** were simply determined by a trial and error method. The reaction pH was not maintained throughout the reaction and so decreased upon the reaction of phosphorus oxychloride with 5'-deoxy-5'-aminoguanosine **42** and with water. Reaction of $POCl_3$ and sodium hydroxide was an issue in these studies as no kinetic data relating to the hydroxide-catalysed hydrolysis of $POCl_3$ is available in the literature. In addition, reaction pH was not maintained during phosphorylation and so competing hydrolysis and aminolysis terms may differ during the course of the reaction.

An understanding of reactivity of (thio)phosphorylating agents towards water would enable optimal reaction conditions to be predicted for any given (thio)phosphorylation

reaction without the need for any time consuming trial and error methods required for the determination of optimal reaction pH. This in turn will substantially improve synthetic methods towards (thio)phosphoramidates. A simple technique that may be used for the determination of optimal pH for aqueous based reactions is discussed in Section 1.3.

1.2.2 Hydrolysis of phosphoramidates and thiophosphoramidates

Although limited, literature studies pertaining to the hydrolysis of phosphoramidates and thiophosphoramidates in aqueous solution provide an insight into their reactivities and mechanisms of hydrolysis as a function of pH. As a large focus of this thesis concerns maximising the conversion of (thio)phosphorylating agent to (thio)phosphoramidate product in aqueous solution, the hydrolysis of (thio)phosphoramidates to inorganic (thio)phosphate by-product must be considered. To gain an understanding of the stability of (thio)phosphoramidates across a broad pH range, this section will briefly overview the kinetic and mechanistic literature for the hydrolysis of phosphoramidates and thiophosphoramidates.

1.2.2.1 Phosphoramidate hydrolysis

In a detailed mechanistic study of the hydrolyses of aryl phosphoramidates, Chanley and Feageson determined rates of phosphoramidate hydrolysis in water and 1:1 water:dioxane solutions between pH ~1-9. This research established that phosphoramidates are stable in their dianion form at high pH, hydrolyse within hours in a pH-independent manner at neutral pH, and are more susceptible to hydrolysis at lower pHs. The mechanism of phosphoramidate monoanion hydrolysis at neutral pH was not fully understood and so two possible mechanisms for hydrolysis were postulated; reaction *via* a reactive metaphosphate species or *via* a bimolecular pathway. These are presented in Scheme 1.23.[23]

Scheme 1.23 Proposed mechanisms for the hydrolysis of the phosphoramidate monoanion.[23]

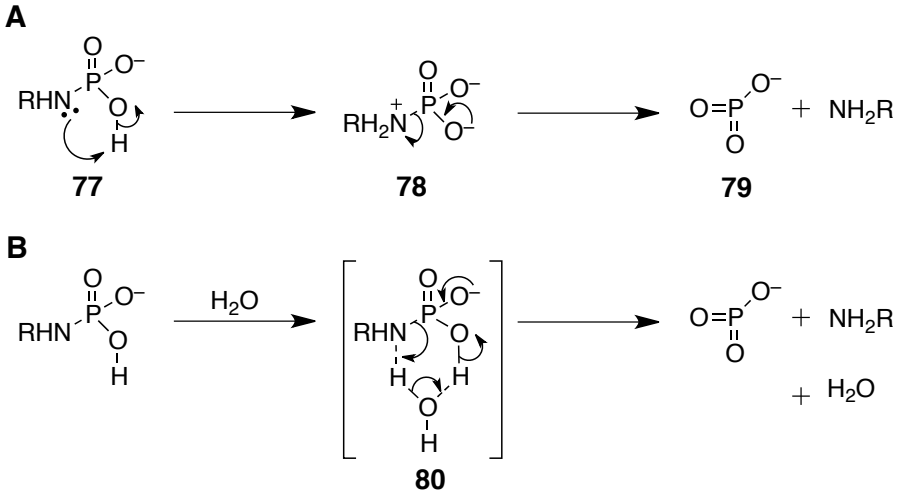

In Scheme 1.23, both mechanisms of hydrolysis involve proton transfer to the amino functionality leading to the formation of metaphosphate species **79**. Hydrolysis of the phosphoramidate monoanion may proceed by mechanism **A** which involves internal proton transfer from the alcohol to amine functionalities of **77** to generate the zwitterion intermediate **78**. Subsequent departure of the amine leads to the formation of a metaphosphate species and free amine. A hydrolysis mechanism that proceeds *via* pathway **A** would be expected to show a decrease in k_{obs} upon a decrease in the water content of the reaction solution, due to the unfavourable formation of a zwitterion species in a less polar solvent.

Alternatively, hydrolysis may proceed through cyclic intermediate **80**, formed from co-ordination of water with the amino and hydroxyl functionalities of the phosphoramidate (mechanism **B**). This cyclic arrangement may facilitate proton transfer from the hydroxyl to amine functionality, thus leading to the departure of the amine and generation of metaphosphate species.

Chanley and Feageson determined that differences in the rate of hydrolysis in water and 1:1 dioxane water were too small to account for the unfavourable formation of a zwitterion in less polar solvent. The hydrolysis of phosphoramidate monoanions *via* mechanism **B** was deemed most likely and was in agreement with a cyclic mechanism postulated by Westheimer for phosphoric acid esters hydrolysis.[24] However, without

direct evidence towards the existence of metaphosphate species **79**, the mechanism of phosphoramidate hydrolysis could not be conclusively identified.

In an extension of these mechanistic studies, Benkovic and Sampson studied the structure-reactivity correlations for the hydrolysis of a series of aryl and alkyl phosphoramidates in a range of solvent systems.[25]

For example, Figure 1.3 shows a plot of pH against log k_{obs} for the hydrolysis of *N*-(n-butyl)phosphoramidate.

Figure 1.3 **pH–log k_{obs} plot for the hydrolysis of *N*-(n-butyl)phosphoramidate at 55 °C, constructed from data reported by Benkovic.[25]**

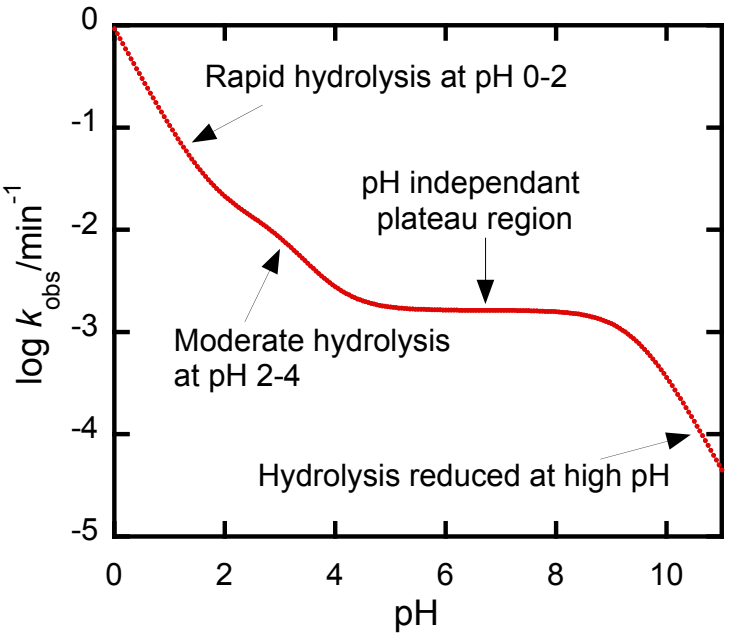

Scheme 1.24 shows the ionisation states of *N*-(n-butyl)phosphoramidate within the pH region (0-11) shown in Figure 1.3.

Scheme 1.24 **Ionisation states of *N*-(n-butyl)phosphoramidate within the pH region 0-11.[25]**

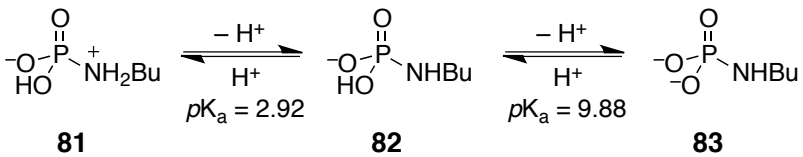

81 **82** **83**

The pH-rate profile for the hydrolysis of *N*-(n-butyl)phosphoramidate (Figure 1.3) can be broken down into four main regions. *N*-(n-butyl)phosphoramidate is present as **81** between pH 0-2, where it is most susceptible to hydrolysis with a half-life on the order of minutes. Upon an increase in pH from 2 to 5, the amino group of **81** is deprotonated and its susceptibility to cleavage upon nucleophilic attack is significantly reduced. Thus, phosphoramidate stability increases significantly within this pH region, where **81** is converted to **82**, such that moderate rates of hydrolysis ($t_{1/2}$ ~ 4 h) are observed at pH 5. Between pH 4 and 9 lies a pH independent region corresponding to the hydrolysis of the *N*-(n-butyl)phosphoramidate monoanion **82**. At higher pHs (pH>9) **82** is deprotonated to give *N*-(n-butyl)phosphoramidate dianion **83**. Upon deprotonation the rate of hydrolysis decreases rapidly such that phosphoramidate hydrolysis is minimal in very basic solution.

In a continuation of these mechanistic studies, Benkovic and Sampson proposed unimolecular and bimolecular mechanisms of hydrolysis (Scheme 1.25). [25]

Scheme 1.25 Phosphoramidate hydrolysis by unimolecular (A) and bimolecular (B) mechanisms.[25]

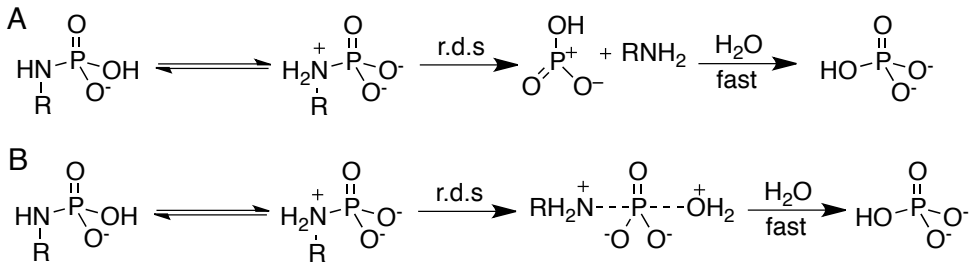

Mechanism A involves rapid pre-equilibrium formation of zwitterionic and non-zwitterionic forms, which is followed by rate-determining loss of the amine functionality (Scheme 1.25A). Alternatively, hydrolysis may proceed by a bimolecular rate-determining step involving loss of the amine functionality for a molecule of solvent (Scheme 1.25B).

If mechanism A were in operation, the highly reactive metaphosphate species should show no selectivity towards solvent molecules of greater nucleophilicity. However, Sampson and Benkovic observed a clear dependence of the selectivity of phosphate

ester products towards the nucleophilicities of incoming solvent molecules, which suggests that bimolecular reaction mechanism B must be in operation.

1.2.2.1 Thiophosphoramidate hydrolysis

Only a handful of kinetic studies of the hydrolysis of thiophosphoramidates have been reported in the literature.[5, 15, 19] The most thorough of these was undertaken by Ora *et al.*, which followed the hydrolysis of 3'-5'-thiophosphoramidate oligonucleosides.

Ora proposed that the mechanism of thiophosphoramidate hydrolysis in acidic solution (pH < 5) involves protonation of the nitrogen atom within **84** to generate **85**, which is susceptible to nucleophilic attack by incoming water molecules (Scheme 1.26).

Scheme 1.26 Ora's proposed mechanism of hydrolysis of 3'-5'-thiophosphoramidate oligonucleosides.[5]

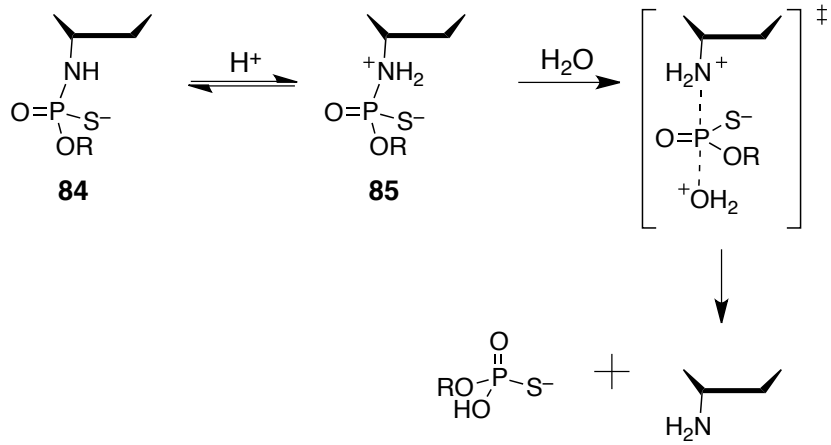

Comparative kinetic studies of the hydrolysis of 3'-5'-thiophosphoramidate oligonucleosides by Ora showed that thiophosphoramidates are more stable with respect to hydrolysis than their oxy- analogues (k_{PO}/k_{PS} = 12) between pH 2-6. Oxy-phosphoramidates were expected to be more susceptible towards hydrolysis than their thio equivalents at low pH due to a lower pK_{aH} of the nitrogen substituent of the thiophosphoramidate group. Thus, at low pH a greater proportion of oxyphosphoramidate would be present in its reactive form than with the equivalent thiophosphoramidate, and as such the oxyphosphoramidate would be more susceptible to hydrolysis *via* Scheme 1.26.

1.2.2.3 Conclusions

The kinetic studies of hydrolysis of oxy and thiophosphoramidates discussed in this section have provided an understanding of the stabilities of these compounds in aqueous solution across a broad pH range. As part of the aim of maximising conversions of (thio)phosphorylating agent to (thio)phosphoramidate product, these studies highlight the importance of storing (thio)phosphoramidate products at high pH following their synthesis.

1.3 Optimisation of reactions in aqueous solution

The usefulness of water as a solvent has been demonstrated by Duncan and Drueckhammer, and Hodgson, Williamson and Trmčić.[10-12, 22] It is extremely useful as a solvent in chemical reactions given its advantageous physical properties:

- Its abundance across the planet makes it the cheapest solvent available
- Due to its high boiling point and low melting point, it is liquid across a large temperature range
- Safe and easy to handle

The determination of observed rate constants for the hydrolysis of phosphorus (V) chlorides in aqueous solution across a broad pH range will provide a kinetic insight into the rate constants that contribute to hydrolysis. An understanding of these terms will enable reactions in aqueous solution to be optimised, such that conversions of (thio)phosphorylating agent to (thio)phosphoramidate may be maximised and the formation of unwanted hydrolysis products may be minimised.

This section concerns the study of a strategy developed by King and Rathore pertaining to competing reactions of nucleophiles with hydrolysable electrophiles in aqueous solution. By studying this strategy we hope to understand how the phosphorylation of amines in aqueous solution may be exploited, such that we can develop near-quantitative aqueous phosphorylation methods using phosphorus (V) chlorides. Application of this strategy towards aqueous phosphorylation chemistry is therefore discussed at the end of the chapter.

Reaction of electrophiles with nucleophiles in water have been investigated by King and Rathore as part of a strategy of using kinetic data as a simple means of predicting and maximising product yields. This strategy has successfully been employed in optimising the sulfonylation and acylation of amines as representative electrophile-nucleophile systems and C-alkylation of acidic ketones. In each case, competing reaction of electrophile with desired nucleophile and water/ hydroxide were considered (Scheme 1.27).

Scheme 1.27 Competing reactions of electrophile with nucleophile, water and hydroxide in aqueous solution.

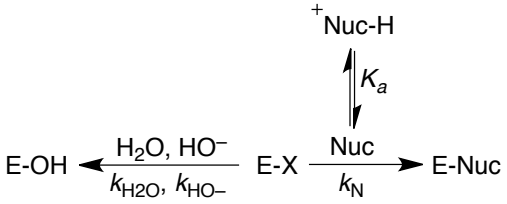

The contribution of hydrolysis of an electrophile is given by the pseudo first-order rate constant, k_0, (Equation 1.1).

$$k_0 = k_w + k_{OH}[HO^-] = k_w + k_{OH}K_w / [H^+] \qquad \textbf{Equation 1.1}$$

k_{hyd} comprises a pH independent k_w term and a hydroxide catalysed k_{OH}[OH] term which are determined from the kinetics of electrophile hydrolysis at neutral and basic pHs, respectively. At high pH, the relative contribution of the $k_{OH}[^-OH]$ term is expected to be considerably greater than the pH independent k_w term in the overall rate equation, due to the greater nucleophilicity of hydroxide *vs* water.

The pseudo first order rate constant, k_N, corresponds to the reaction between electrophile with a given nucleophile (Equation 1.2).

$$k_N = k_{nuc}[Nuc] = k_{nuc}Nu_T K_a / ([H^+] + K_a) \qquad \textbf{Equation 1.2}$$

The total concentration of nucleophile in the reaction, Nu_T, is dependent on its pK_a and is given by in Equation 1.3.

$$Nu_T = [Nu] + [^+NuH] \qquad \textbf{Equation 1.3}$$

With the nucleophile pK_a and kinetic data (k_w, k_{OH} and k_{nuc} rate constants) in hand, k_0 and k_N observed rate constants (Equation 1.1 and 1.2) may be plotted against reaction pH to show the relative contributions of each electrophile-consuming reaction as a function of pH. A typical pH-rate plot using k_0 and k_N observed rate constants determined from Equation 1.1 and 1.2 is given in Figure 1.4.

Figure 1.4 **A typical pH–log k_{obs} profile for the reaction of a nucleophile with hydrolsable electrophile in aqueous solution.** [26]

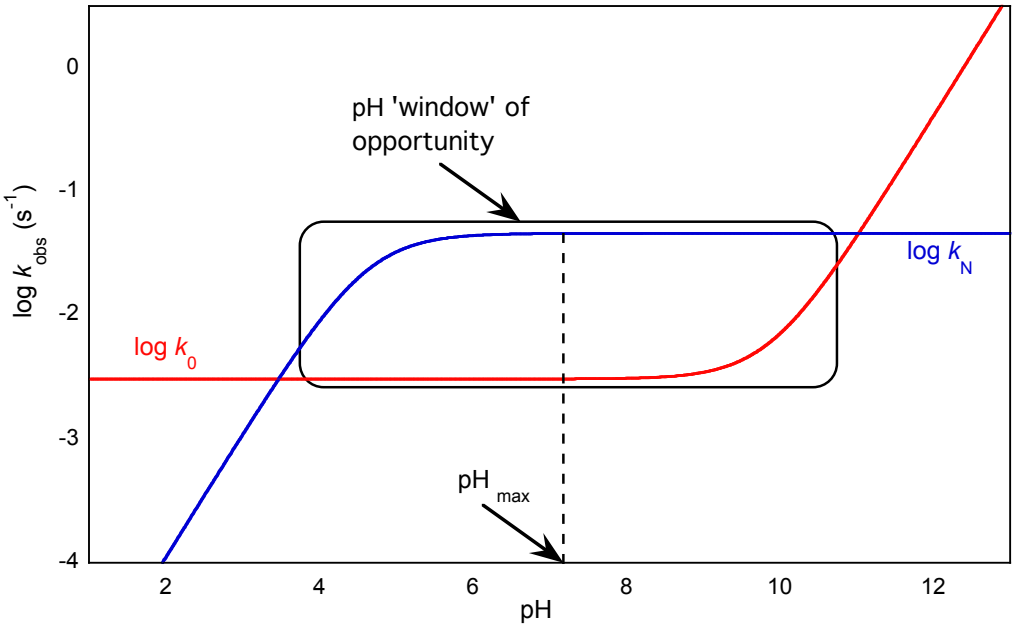

Figure 1.4 provides a qualitative means of determining the 'pH window of opportunity', which is defined as the pH region in which the greatest product yield due to reaction of a given nucleophile and electrophile is observed. It can be mathematically calculated from Equation 1.4.

$$\text{pH 'window' of opportunity} = \text{pH}_{max} \pm \frac{1}{2}[\log (k_w/k_{OH}) + \text{p}K_w - \text{p}K_a] \qquad \textbf{Equation 1.4}$$

In Equation 1.4, pH_{max} is defined as the reaction pH necessary to form the greatest product yield for the reaction of a given nucleophile and hydrolysable electrophile in water (Equation 1.5).

$$\text{pH}_{max} = \frac{1}{2}[\log (k_w / k_{OH}) + \text{p}K_w + \text{p}K_a] \qquad \textbf{Equation 1.5}$$

From Equation 1.5 we can see that the magnitude of pH_{max} depends only on the kinetic rate constants k_w and k_{OH} for electrophile hydrolysis and the pK_a of the conjugate acid of the nucleophile. Thus the magnitude of pH_{max} can be calculated independently of the rate constant for the reaction between nucleophile and electrophile, k_{nuc}, and the overall nucleophile concentration. However, pH_{max} gives no indication to the relative contributions of nucleophile and water based reactions.

The width of the pH 'window' of opportunity is defined as the pH region over which the nucleophile-electrophile product is formed at high yield (Equation 1.6).

$$\text{Width of pH 'window' of opportunity} = [\log (k_w/k_{OH}) + pK_w - pK_a] \quad \textbf{Equation 1.6}$$

It is determined by the two pH values at which the rate constant k_0 is equal to k_N. A larger pH 'window' corresponds to a greater pH range in which the desired product is formed in maximum yield. This allows adequate variation in reaction pH without any decrease in product yield. Conversely, a smaller pH 'window' corresponds to a narrower pH region over which the desired product is formed in maximum yield. In this case little variation in experimental pH can be tolerated if the product is to be formed in the greatest possible yield.

1.3.1 Determination of the pH 'window' of opportunity for the aminolysis of benzenesulfonyl chloride in water

King *et al.* applied experimentally determined kinetic data to Equations 1.1 and 1.5 to predict the pH_{max} and pH window of opportunity for the aminolysis of benzenesulfonyl chloride **86** in aqueous solutions of aniline (pK_a = 4.60) and benzylamine (pK_a = 9.34) (Scheme 1.28).[26]

Scheme 1.28 Aminolysis of benzenesulfonyl chloride in aqueous solutions of aniline and benzylamine.

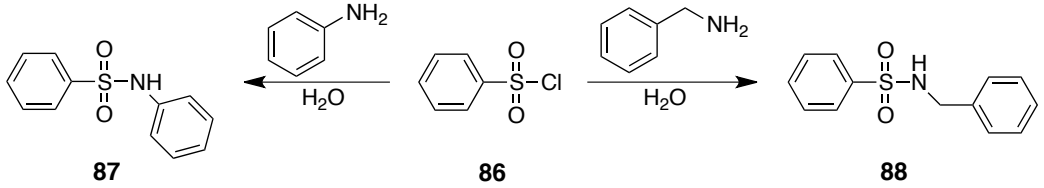

87 **86** **88**

pH–log k_{obs} profiles for the hydrolysis and aminolysis of benzenesulfonyl chloride in aqueous solutions of aniline and benzylamine were determined through application of kinetic data ($k_w = 3.06 \times 10^{-3}\ s^{-1}$, $k_{OH} = 40.4\ mol^{-1}\ dm^{-3}\ s^{-1}$, $k_N = 4.6\ M^{-1}s^{-1}$ (aniline) and $19.0\ M^{-1}s^{-1}$ (benzylamine)) to Equations 1.1-1.6.[26, 27, 28] These are shown in Figure 1.5.

Figure 1.5 **Calculated pH–log k_{obs} profiles for the aminolysis of benzenesulfonyl chloride 86 in aqueous solutions of aniline and benzylamine, in competition with hydrolysis.[26, 27, 28]**

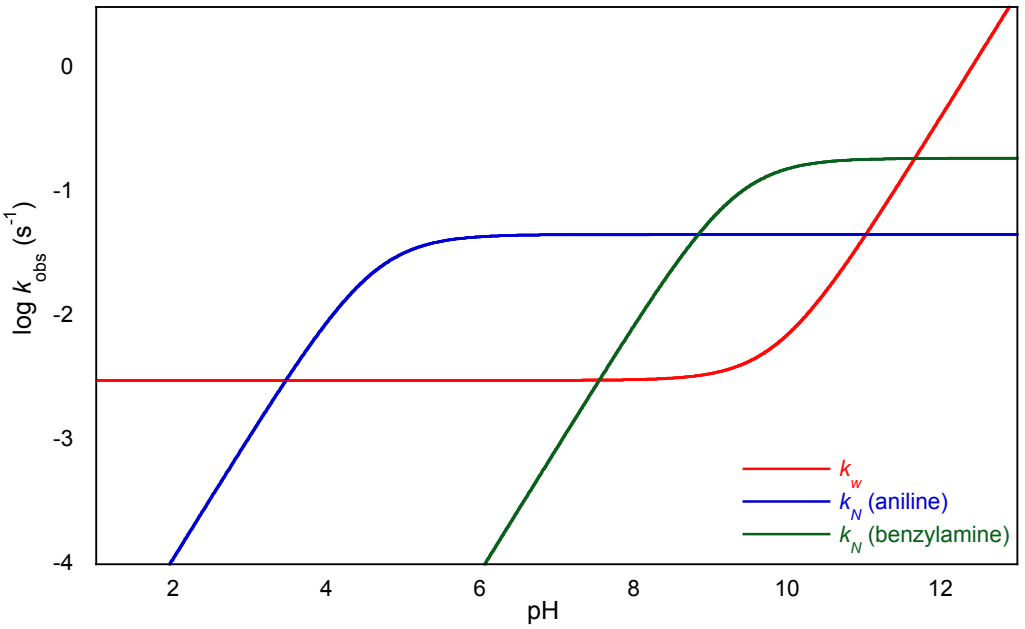

The calculated pH–log k_{obs} profiles for the hydrolysis and aminolysis of benzenesulfonyl chloride in Figure 1.5 clearly show pH 'windows' of opportunity for reaction of aniline (pH 4.6 to 9.8) and benzylamine (pH 9.3 to 9.9) in aqueous solution. A large pH 'window' is observed for reaction with aniline as a result of its low conjugate acid pK_a. Consequently, highest-possible product yields of aminolysis product **87** and **88** may therefore be formed over a large variation in reaction pH. The pH 'window' of opportunity is much narrower for the aminolysis of benzylamine, owing to the higher pK_a of its conjugate acid. As a result, deprotonation of the conjugate acid of benzylamine occurs over a pH range where the $k_{OH}[^{-}OH]$ term significantly increases such that when benzylamine is in its fully neutral form, k_N is of a similar magnitude to k_0. Thus, the kinetic advantage due to high amine concentrations in forming product at high yields is lost by the increase in reactivity of hydrolysis. Outside these pH 'windows' of opportunity, hydrolysis of benzenesulfonyl chloride is expected to dominate over aminolysis, leading to the formation of benzene sulfonate as the major reaction product.

1.3.2 Limitations and assumptions

Although the method developed by King is a simple means of predicting product yields from aqueous-based reactions, the validity of Equations 1.1-1.6 depends on three main assumptions.

For predicted yields to be observed, effective pH control is necessary to ensure reaction pH remains constant over the course of the reaction. Product yields for reactions with a large pH 'window' of opportunity are less susceptible to small changes in reaction pH. In contrast, product yields for reactions with a narrow 'window' are highly susceptible to pH changes. For example, if the reaction pH changes by ± 2 pH units from the calculated optimum (pH 9.6) during the reaction of benzenesulfonyl chloride and benzylamine, product yields will be reduced from 97 to 46% aminolysis product. Thus, effective pH control is essential if predicted yields are to be observed. This can be achieved through the use of a pH-stat meter or by using strong non-nucleophilic buffers of appropriate pK_a.

Secondly, in order for Equations 1.1 and 1.5 to be valid the observed rate constant for any given reaction must be due only to the reaction of electrophile with water and nucleophile (Equation 1.7).

$$k_{obs} = k_0 + k_N[\text{Nuc}] \qquad \textbf{Equation 1.7}$$

Equation 1.7 considers the total consumption of the electrophile by hydrolysis and reaction with the nucleophile. If the given electrophile reacts by an additional pathway, the observed yield at a pH within the 'window' of opportunity may differ from that predicted by Equations 1.1 and 1.5. Mechanistic studies for the reaction to be studied are therefore essential in determining whether other reactions occur in addition to those between the electrophile and nucleophile in aqueous solution.

The final limitation is that the kinetics of reactant mixing must be faster than the rate of reaction.[29] When the kinetics of reactant mixing are significantly faster than that of a reaction, the observed rate constant for the reaction of water or nucleophile with a hydrolysable electrophile in water is simply given by Equation 1.7.[30] However, when the kinetics of mixing are slower than for the reaction of water or nucleophile with a

hydrolysable electrophile in water, the observed rate constant for the reaction will depend upon the kinetics of mixing. As a result of mixing, the observed product yield will be affected by the mixing efficiency. It is therefore essential to ensure that the rate of mixing is faster than that of the reaction if predicted product yields are to be observed. Efficient mixing can be achieved through the use of stopped-flow apparatus for kinetic studies.

In summary, King *et al.* have shown that pH-yield profiles for simple reactions between nucleophiles and hydrolysable electrophiles in aqueous solution can be predicted and maximised through the application of kinetic data to Equations 1.1-1.7. Through the determination of kinetic parameters and applying methods analogous to the pH optimisation method developed by King et al., we hope to predict pH 'windows' of opportunity for the aminolysis of phosphorus (V) chlorides in aqueous amine solutions. Thus, determination of kinetic data relating to the hydrolysis and aminolysis of phosphorus (V) chlorides in aqueous solution is essential.

1.4 Project overview

As part of an on-going strategy to develop simple and effective aqueous-based methods towards phosphoramidates and thiophosphoramidates, this thesis is concerned with gaining an understanding towards the reactivity of phosphorylating agents towards water, hydroxide, and a range of structurally different amines in an attempt to optimise methods of phosphorylation.

The hydrolyses of several phosphorus (V) chlorides have been followed in aqueous solutions, using ^{31}P NMR spectroscopy and conventional and stopped-flow UV-Visible spectrophotometry, in an attempt to understand their reactivity towards water and hydroxide nucleophiles (Chapter 2).

The reaction of a wide range of structurally different amines towards two promising (thio)phosphorylating agents, oxy and thiophosphodichloridate, in aqueous solution are explored and discussed in Chapter 3, as part of an investigation into reaction times and the dependence on amine concentration on (thio)phosphoramidate yield.

In Chapter 4, we have applied our understanding of the reactivities of phosphorus (V) chlorides towards the synthesis of 5'-nucleoside (thio)phosphoramidates in aqueous solution.

Chapter 2

Kinetic studies of the hydrolyses of phosphorus (V) chlorides

2.0 Foreword

This chapter describes investigations of the hydrolyses of phosphorus (V) chlorides in aqueous solution. In Section 2.1 a brief review of relevant literature pertaining to kinetic studies of hydrolyses of phosphorus (V) chlorides and methods of determination of rate constants is presented. Section 2.2 describes the results obtained from kinetic studies of hydrolyses of phosphorus (V) chlorides. This includes the synthesis of oxy and thiophosphodichloridate ions (Section 2.21), determination of pseudo first-order rate constants for the hydrolysis of oxy and thiophosphodichloridates (Section 2.23) and preliminary efforts towards the determination of pseudo first-order rate constants for the hydrolysis of phosphorus oxychloride and thiophosphoryl chloride (Section 2.24). These results are discussed in Section 2.3.

2.1 Introduction

As part of the overall project aim of using phosphorus (V) chlorides as reagents for the phosphorylation of amines in aqueous solutions, kinetic data on the competing hydrolysis processes of phosphorylating agents is essential. Typically, phosphorylation reactions are undertaken at high pH (>10) where the substrate amine is in its neutral, nucleophilic form. Therefore, kinetic studies of hydrolyses at high pH are essential where there is potential for reaction with hydroxide ions which may compete against amine attack on the (thio)phosphorylating agent.

2.1.1 Historical background

Qualitative studies of the hydrolysis of phosphorus (V) chlorides were first reported at the start of the 20th century when Meerwein and Bodendorf observed that only two equivalents of base were required to neutralise the acid formed following immediate addition of phosphorus oxychloride **4** to cold water.[31] Meerwein proposed that these observations were indirect proof of the formation of phosphorodichloridate **89** as an intermediate formed upon initial hydrolysis of phosphorus oxychloride (Scheme 2.1).

Scheme 2.1

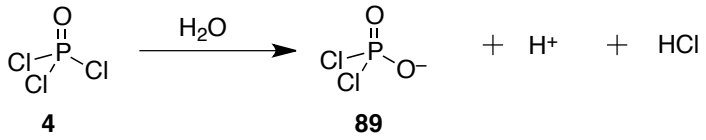

4 **89**

Several decades later, Askitopoulos and Goubeau were able to precipitate salts of phosphorodichloridic acid using nitrogen containing bases under conditions of limiting water content. Although, salts of phosphorodichloridate **89** could not be purified, its presence confirmed that it was the initial hydrolysis product of $POCl_3$.[32, 33]

As part of identifying additional hydrolysis intermediates, Grunze studied the complete hydrolysis of $POCl_3$ in water and postulated a pathway for hydrolysis of phosphorodichloridic acid to inorganic phosphate (Scheme 2.2).[34-36]

Scheme 2.2 Grunze's postulated hydrolysis pathway of phosphorodichloridate ion. [34-36]

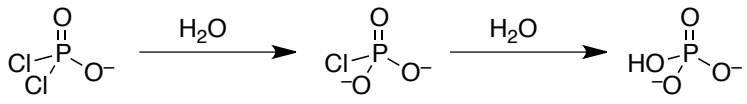

89 **90** **28**

Phosphorodichloridate ion **89** was added to an excess of water and the resulting products were analysed by paper chromatography. It was observed that hydrolysis of phosphorodichloridate led only to the formation of inorganic phosphate and the postulated phosphomonochloridate intermediate **90** was not observed. From these observations, Grunze concluded that the rate of hydrolysis of the phosphoromonochloridate ion **90** must be significantly faster than the rate of its formation.

2.1.2 Kinetic and mechanistic studies of hydrolysis of phosphoryl (V) chlorides

2.1.2.1 Hydrolysis of phosphorus oxychloride

In 1962, kinetic studies of the hydrolysis of phosphorus oxychloride by Hudson and Moss continued the interest in the field.[37] The hydrolysis of phosphorus oxychloride to oxyphosphodichloridate ion was followed in aqueous dioxane solutions (33:67 v/v water/ dioxane) at pH 7 using stopped flow-ion sensitive electrode apparatus.[38] Upon hydrolysis of $POCl_3$, two equivalents of hydronium ion and one of chloride ion were generated (Scheme 2.3).

Scheme 2.3 Partial-hydrolysis of phosphorus oxychloride to phosphodichloridate ion, generating two equivalents of hydronium ion and one of chloride ion.[37]

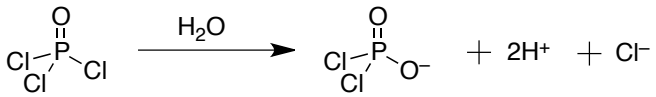

4 **89**

The formation of chloride ions was followed potentiometrically using a silver/ silver chloride electrode.[38] This allowed for the determination of observed rate constants for hydrolysis, k_{obs}, (Table 2.1). The accuracy of these results was confirmed by

potentiometric determination of the concentration of chloride ions as a function of time using a silver/silver chloride electrode system in a balancing-cell method.[39]

Table 2.1 **Observed rate constants for the hydrolysis of phosphorus oxychloride to oxyphosphodichloridate ion in aqueous dioxane solutions (33:67 v/v water/ dioxane) at pH 7.[37]**

$[POCl_3] \times 10^3$ (mol dm^{-3})	Temperature (°C)	k_{obs} (s^{-1})[a]
1.90	26.4	65.5
0.97	25.0	62.4

[a]Determined from stopped flow potentiometric experiments using a silver/ silver chloride electrode

The experimentally observed rate constants, k_{obs}, presented in Table 2.1 are defined by Equation 2.1; k_0 and k_{HO} rate constants are introduced in Scheme 2.4.

$$k_{obs} = k_0 + k_{OH}[HO^-] \qquad \textbf{Equation 2.1}$$

Scheme 2.4

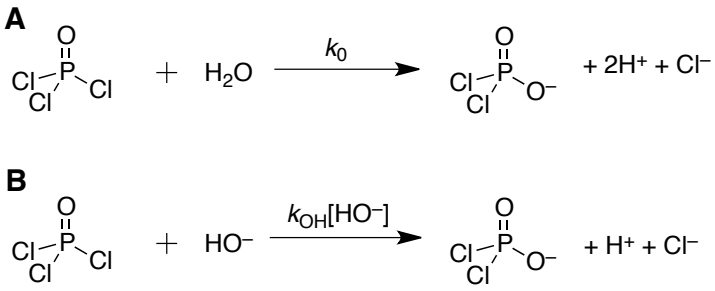

As shown in Scheme 2.4, the pseudo first-order rate constant k_0 relates to the uncatalysed reaction of phosphorus oxychloride and water (Scheme 2.4A), whilst the second-order rate constant k_{OH} corresponds to the hydroxide catalysed reaction of phosphorus oxychloride and hydroxide ion (Scheme 2.4B).

Hydrolysis was only studied at pH 7 and therefore no indication was given of the contribution of the uncatalysed (k_0) and catalysed (k_{OH}) rate constants to the observed rate constant for reaction. The observed rate constant for hydrolysis is likely to be dominated by the pseudo first-order rate constant k_0 at pH 7, where hydroxide is present at a low concentration. Therefore, the uncatalysed rate constant for hydrolysis

may be estimated as 62 s^{-1}. Hydrolysis was not followed in reaction solutions of high pH and thus no data are provided relating to the magnitude of the second-order hydroxide term, k_{OH}.

Mechanistic studies by Hudson *et al.* have shown P-Cl bond cleavage for the hydrolysis of $POCl_3$ to phosphodichloridate ion to proceed by an $S_N2(P)$ mechanism *via* a pentacoordinate transition state (**91**), as shown in Scheme 2.5.[40]

Scheme 2.5 Mechanism of hydrolysis of phosphorus oxychloride to phosphodichloridate ion.[40]

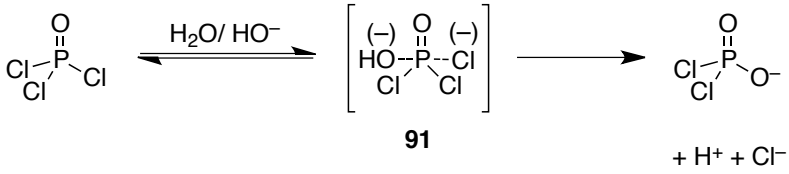

In an attempt to understand the mechanism of hydrolysis of diethyl phosphochloridate, Dostrovsky and Halmann studied the hydrolysis of $(EtO)_2P^{18}OCl$ in aqueous solution.[41, 42] Following hydrolysis, the ^{18}O content of the solution was determined, however, ^{18}O isotopes were not observed. Thus, hydrolysis was suggested to proceed *via* a pathway in which exchange of oxygen between water and the phosphoryl group does not occur. [41, 42] On the basis of these kinetic studies, it was suggested that the mechanism of hydrolysis cannot proceed through a reversible intermediate. Instead, these studies are in agreement with the bimolecular 'S_N2-like' mechanism shown in Scheme 2.5.

2.1.2.2 Hydrolysis of oxyphosphodichloridate ions

Following these studies, Hudson and Moss followed the subsequent hydrolysis of the oxyphosphodichloridate ion using a previously developed automated titrator technique.[43] Owing to the slower hydrolysis and insolubility of oxyphosphodichloridate ions in 67% dioxane solutions, reactions were followed in fully aqueous solution. A known quantity of oxyphosphodichloric acid was added to a reaction vessel containing an equivalent of base, which was thermostated at 25 °C. The reaction pH was monitored throughout hydrolysis using a pH electrode fitted to an

automatic titrator containing base. The volumes of base titrated during the course of hydrolysis were then correlated to determine the rate of acid production as a function of time. This led to the accurate determination of k_{obs} for the reaction.

Observed rate constants for hydrolysis, k_{obs}, were determined in aqueous solutions at pH 4 (I=0) and 7 (I=0 and I=1.5) at 25 °C, and are given in Table 2.2.[37] The accuracy of these results was confirmed from determination of the concentration of chloride ion throughout hydrolysis using the same potentiometric method employed in following the hydrolysis of phosphorus oxychloride.

Table 2.2 Observed rate constants, k_{obs}, for the hydrolysis of oxyphosphodichloridate ion in aqueous solution of varying composition at 25 °C.[37]

Composition	$k_{obs} \times 10^3$ (s^{-1})[a]
pH 4.0 (I=0)	3.11
pH 7.0 (I=0)	3.21
pH 7.0 (I=1.5 (KCl))	6.26

[a]Determined from the rate of acid production using an automated titrator technique.[43]

The results in Table 2.2 suggest that the observed rate constants for hydrolysis are almost identical at pH 4 and 7 where ionic strength is uncontrolled. Thus, within this pH region the observed rate constant can be concluded to be due only to the pH-independent hydrolysis reaction (Equation 2.2)

$$k_{obs} = k_0 \qquad \textbf{Equation 2.2}$$

The pseudo first-order rate constant, k_0, was estimated as 6.26×10^{-3} s^{-1} for the hydrolysis of oxyphosphodichloridate under aqueous conditions at I=1.5 (KCl) and 25 °C. Comparison of observed rate constants for the hydrolysis of phosphorus oxychloride in aqueous dioxane solution (Table 2.1) with those of oxyphosphodichloridate in fully aqueous solution (Table 2.2) shows that the initial reaction of $POCl_3$ is around 10^4 fold faster than that of oxyphosphodichloridate to oxyphosphomonochloridate. Hudson and Moss did not observe the formation of oxyphosphomonochloridate and reported that its hydrolysis may be significantly faster than the hydrolysis of oxyphosphodichloridate. These results therefore suggest that

rapid hydrolysis of phosphorus oxychloride to oxyphosphodichloridate ion is followed by rate determining hydrolysis to inorganic phosphate.

Scheme 2.6 shows the potential pathways for the hydrolysis of oxyphosphodichloridate ion to inorganic phosphate in aqueous solution at pH 7 (pathways **A**-**F**).

Scheme 2.6 Hudson's suggested pathways for the hydrolysis of oxyphosphodichloridate ion to inorganic phosphate in aqueous solution at pH 7.[37]

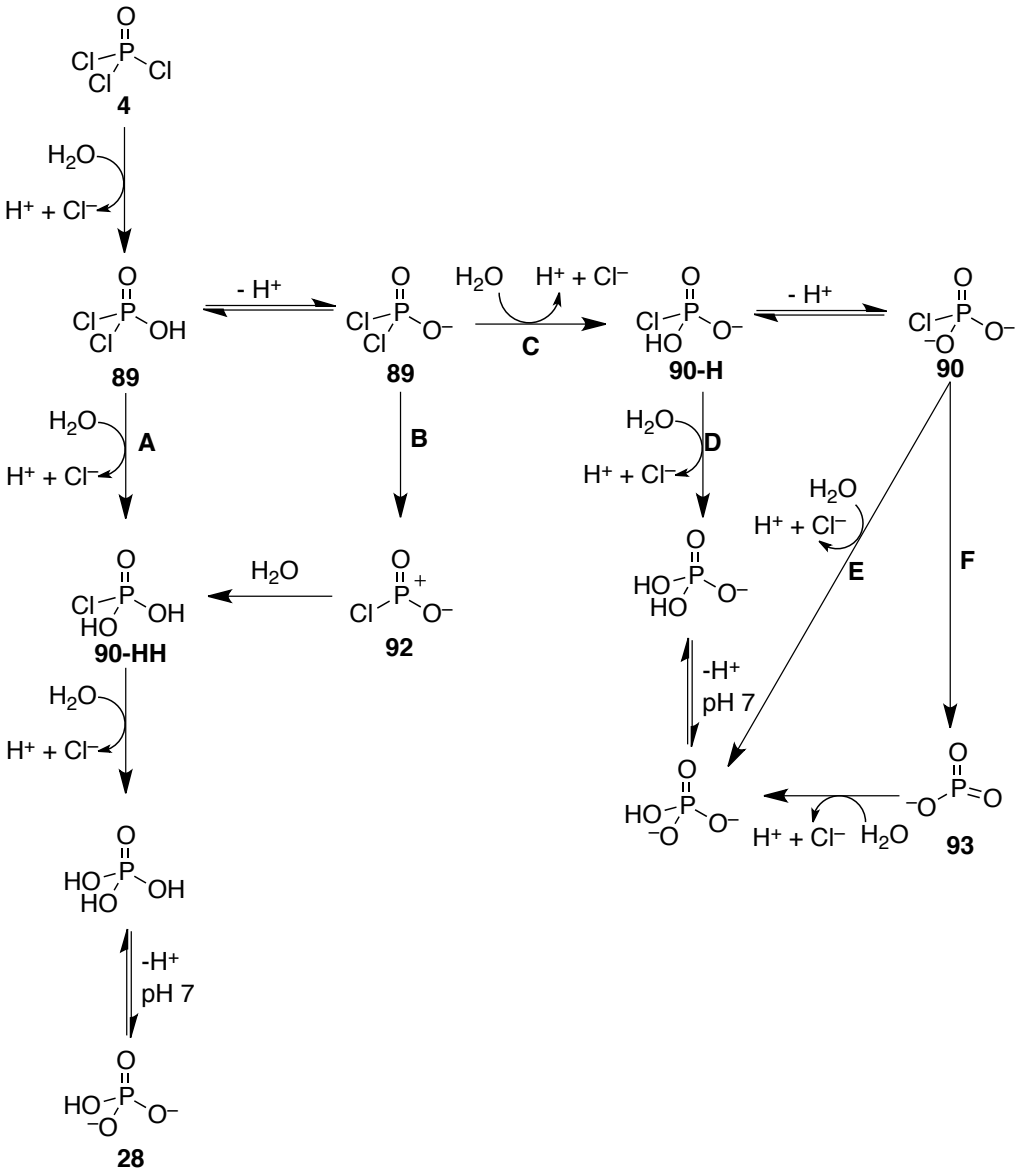

Hudson and Moss's conclusions of the pathway of hydrolysis are summarised in the following four paragraphs:

Hydrolysis *via* pathway **A** involves nucleophilic attack on phosphodichloridic acid **89-H** by water; displacement of one chloride group by a hydroxyl group leads to phosphochloridic acid **90** in its fully protonated form. Subsequent reaction with water generates phosphate **28**, which is present in a mixture of mono- and di-anionic forms at pH 7.

Hydrolysis pathways **B**-**F** proceed *via* deprotonation of phosphodichloridic acid to phosphodichloridate ion **89**. Expulsion of a Cl^- ion from **89** generates metaphosphate intermediate **92** *via* an S_N1-like rate-limiting ionisation mechanism (pathway **B**). Nucleophilic displacement of the final chloride functionality with water gives phosphochloridic acid **90**, which is followed by nucleophilic attack by water to give inorganic phosphate **28**.

Alternatively, phosphodichloridate **89** ion may react with water to form phosphochloridate monoanion **90-H** (pathway **C**). Nucleophilic attack by water on **90-H** results in the cleavage of the remaining P-Cl bond leading to the formation of inorganic phosphate monoanion (pathway **D**), which is deprotonated to give a mixture of mono and dianion forms at pH 7. Pathway **E** involves deprotonation of phosphochloridate monoanion **90-H** to phosphochloridate dianion **90**, which is followed by reaction with water to generate inorganic phosphate. However, expulsion of Cl^- from phosphochloridate dianion **90** may occur to generate the metaphosphate intermediate **93** (Pathway **F**). Following its formation, nucleophilic attack by water will result in its transformation to inorganic phosphate.

The fact that there is no change in rate constant from pH 4 to 7 suggests that the hydrolysis of $KOPOCl_2$ must proceed by the same mechanism under these conditions. Given the pK_a of $HOPOCl_2$ is expected to be < 1, the mechanism of hydrolysis between pH 4 and 7 must proceed *via* $KOPOCl_2$ by either pathway **B** or **C**, rather than by pathway **A**.

To identify the mechanism in operation, Hudson and Moss studied the reaction of the oxyphosphodichloridate ion in aqueous solutions of varying concentration of pyridine and pyridine-4-aldehyde.[37] The results are shown in Table 2.3.

Table 2.3 Observed rate constants, k_{obs}, and second order rate constants, k_{amine}, for the aminolysis of $KOPOCl_2$ in aqueous solutions containing pyridine and pyridine-4-aldehyde at 25 °C. [37]

Amine	[Amine] $\times 10^2$ (mol dm^{-3})	$k_{obs} \times 10^3$ (s^{-1})	$k_{amine} \times 10^1$ (M^{-1} s^{-1})
Pyridine (28 ºC)	2.5	12.8	2.62
Pyridine-4-aldehyde (25 ºC)	1.9	7.22	1.52

The bimolecular rate constants for the aminolysis of $HOPOCl_2$ by pyridine and pyridine-4-aldehyde shown in Table 2.3 are approximately 2.5×10^3 times greater than the bimolecular rate constant for the hydrolysis of phosphodichloridate ion in water (5.8×10^{-5} M^{-1} s^{-1}). If hydrolysis were to occur by an ionisation mechanism (pathway **B**), second-order rate constants for the hydrolysis and aminolysis of $HOPOCl_2$ would be expected to be similar given that ionisation would be rate-limiting rather than reaction with nucleophiles. In contrast, if hydrolysis were to proceed by the bimolecular pathway **C**, selectivity towards the nucleophile should be observed due to the greater stability of the phosphorylating intermediate. Since a large increase in k_{obs} is observed upon the addition of pyridine, we can see that the phosphodichloridate ion is in fact sensitive to the nature of the nucleophile present. Therefore pathway **B** can be eliminated as a possible pathway in the mechanism for the hydrolysis of $HOPOCl_2$. The observed results due to hydrolysis or aminolysis are therefore consistent with results expected for hydrolysis *via* pathway **C**.

As indicated earlier, a strong kinetic salt effect was observed for the hydrolysis of the oxyphosphodichloridate ion, in which the rate constant for hydrolysis was shown to increase 2-fold upon an increase in ionic strength from 0 to 1.5 (KCl).[37] The dependence of k_{obs} on ionic strength was interpreted by Hudson *et al.* as showing an increase in polarity from the ground to the transition state during hydrolysis, which is

favoured at higher ionic strength. The result is the formation of a transition state similar in structure to that of intermediate **94** (Scheme 2.7).

Scheme 2.7 Proposed transition state for hydrolysis of $KOPOCl_2$.[37]

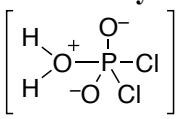

94

Hudson *et al.* attributed an increase in polarity during hydrolysis as evidence that the hydrolysis of $KOPOCl_2$ proceeds *via* bimolecular pathway **C** rather than ionisation pathway **B**.

In 2010, Achmatowicz *et al.* determined kinetic parameters for the hydrolysis of oxyphosphodichloridic acid at low pH, in an attempt to quantify an unwanted latent exothermic event associated with reaction between phosphorus oxychloride and dimethylformamide in an industrial context.[44]

Kinetic investigations were undertaken in aqueous acetonitrile solutions (45:55 v/v water/acetonitrile) of varying sodium hydroxide concentration (0 – 2.44 M) at 25 °C. Phosphorus oxychloride (in dry acetonitrile) was added to each reaction solution to generate oxyphosphodichloridic acid substrate and hydrogen chloride at a concentration of 1.22 M. Neutralisation of sodium hydroxide with hydrogen chloride significantly reduced the pH of each reaction solution such that kinetic studies were followed under acidic conditions. However, the pH of each reaction solution was not recorded before or after hydrolysis and there was no obvious attempt to maintain a constant pH. Two additional equivalents of HCl, corresponding to a 2.44 M increase in [HCl], were produced during the hydrolysis of oxyphosphodichloridic acid to inorganic phosphate. Therefore, hydrolysis in solutions at higher initial concentrations of NaOH will occur at higher pH values than those with lower initial NaOH concentrations. Reaction progress was followed by ^{31}P NMR spectroscopy, by monitoring the decrease in the signal at –2 ppm due to oxyphosphodichloridic acid and the increase in the signal at 0 ppm due to inorganic phosphate. The decay of the signal due to oxyphosphodichloridic acid was followed over time and plots of $\ln(\text{concentration}_0 - \text{concentration}_t)$ *vs* time gave first-order rate constants for hydrolysis.

These are given in Table 2.4. Although hydrolysis has been previously shown to be highly dependant on ionic strength,[37] reactions were not undertaken at a constant ionic strength.

Table 2.4 Observed rate constants, k_{obs}, for the hydrolysis of oxyphosphodichloridic acid, determined from addition of phosphorus oxychloride (affording a concentration of 1.22 M in reaction solution) to aqueous acetonitrile solutions (45:55 v/v water/acetonitrile) of varying sodium hydroxide concentration at 25 °C.[44]

Initial [NaOH] (mol dm^{-3})	$k_{obs} \times 10^4$ (s^{-1})	Final [HCl] (mol dm^{-3})[a]
0	1.1	3.66
1.22	1.5	2.44
2.44	6.8	1.22

[a]Estimated through calculation of HCl generated upon hydrolysis, following neutralisation of NaOH.

Achmatowicz *et al.* attempted to correlate the results in Table 2.4 with those obtained by Hudson and Moss.[37] Observed rate constants for hydrolysis in reaction solutions of varying water content were extrapolated to pure water at low pH and correlated through Equation 2.3.

$$\text{Difference in } k_{obs} = (k_{obs} \times [H_2O])_{45\%\ H2O} / (k_{obs} \times [H_2O])_{100\%\ H2O} \qquad \textbf{Equation 2.3}$$

An 18-fold difference in observed rate constants was determined using Equation 2.3. However, the effect of water content on the observed rate constant is likely over simplified by this approach. Application of the Grunwald-Winstein equation is more likely to provide a more accurate comparison of these data sets.[45]

Achmatowicz *et al*. concluded from the data in Table 2.4 that the observed rate constants for hydrolysis are very much dependent on the acidity of the reaction solution. This is likely to be due to a change in mechanism upon protonation of oxyphosphodichloridate ions to the corresponding oxyphosphodichloric acid (Scheme 2.8).

Scheme 2.8 Competing mechanisms of hydrolysis of oxyphosphodichloridic acid/ oxyphosphodichloridate ions at very low pH.

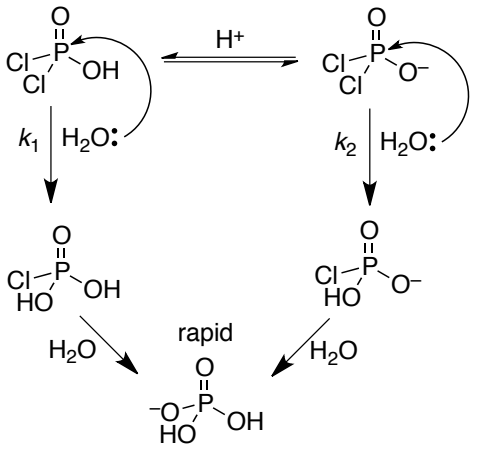

Scheme 2.8 shows the parallel pseudo first-order pathways for the hydrolysis of dichloridate and its corresponding acid. Studies by Achmatowicz *et al.* suggested the hydrolysis of phosphodichloridic acid is slower than that of the dissociated oxyphosphodichloridate ion, although the difference is small.[44] However, as pH was not monitored and ionic strength was not constant, this may not be the case. A larger proportion of reactant is in its acidic form in solutions with no added sodium hydroxide compared to those with added NaOH. In the most acidic solutions, hydrolysis predominantly occurs through the slower mechanism k_1, leading to a smaller observed rate constant. In addition, hydrochloric acid generated during the reaction will further decrease the reaction pH and therefore increase the amount of oxyphosphodichloridic acid present. Thus, the equilibrium between these species is shifted toward the acidic form as the reaction proceeds.

These results suggest a possible pH dependent region for the hydrolysis of $KOPOCl_2$ at very low pH, where a decrease in the observed rate constant is expected upon a decrease in pH of strongly acidic reaction solutions, corresponding to the protonation of phosphodichloridate to its acid form. We will use some of these results and ideas in the discussing the hydrolysis of phosphodichloridic acid in fully aqueous solution (Section 2.3).

2.1.2.3 Stability of oxyphosphomonochloridate ion

The phosphomonochloridate ion was never observed in kinetic studies undertaken in aqueous solution by Hudson and Moss, and Grunze.[34, 35, 37] In addition, it was deemed too reactive to be synthesised or isolated. Hudson and Moss suggested, based on kinetic studies of the hydrolysis of tetra-alkyl pyrophosphates by Brown and Hamer, that the rapid hydrolysis of KO_2POCl *vs* $KOPOCl_2$ indicates that hydrolysis of the former proceeds by an S_N1 process (pathway **F**, Scheme 2.6).[46]

In an attempt to further understand the reactivity of the oxyphosphochloridate ion in aqueous solution, Mitchell employed a simple mass spectrometry technique to determine relative amounts of partial hydrolysis products from the reaction of phosphorus pentachloride with limiting amounts of [^{18}O] enriched water.[47, 48]

Limiting amounts of 95 % atom [^{18}O] enriched water were added, under an inert atmosphere, to neat solutions of phosphorus pentachloride. Ratios of PCl_5 : $^{18}OH_2$ were varied from 1:0.28 to 1:3.72. Each reaction mixture was left to stand for 10 minutes to generate partial hydrolysis products $POCl_3$, $HOPOCl_2$, and $HOPO_2Cl$; the amount of each formed depended entirely on the amount of $^{18}OH_2$ added. An excess of non-enriched water was subsequently added to each solution, resulting in complete hydrolysis of each intermediate to give a mixture of inorganic phosphate containing 0 – 4 ^{18}O atoms derived from labelled $^{18}OH_2$ (Scheme 2.9).

Scheme 2.9 Partial hydrolysis of PCl_5 in [^{18}O] enriched water to give inorganic phosphate of varying mass.

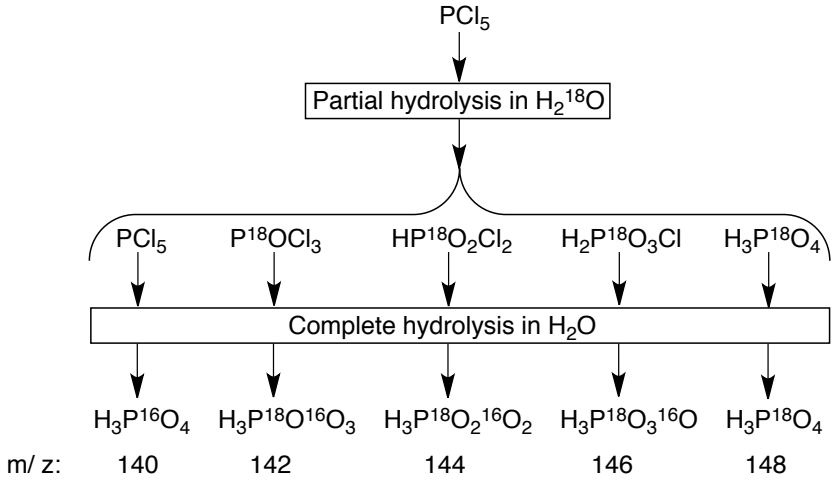

Following hydrolysis, isotopomers of inorganic phosphate were converted into their trimethyl phosphate esters and analysed by electron impact ionization mass spectrometry. Relative molecular masses of each trimethyl phosphate ester were calculated from potential incorporation of ^{18}O atoms during the partial-hydrolysis step. Linear regression analysis of the mass spectrum for each reaction mixture gave estimates of the molecular proportions of each intermediate present following partial hydrolysis. The resulting fractional composition of partial PCl_5 hydrolysis mixtures is given in Figure 2.1.

Figure 2.1 Yields of $POCl_3$ (□), $KOPOCl_2$ (Δ), $KOPO_2Cl$ (♦) and H_3PO_4 (◊) formed by partial hydrolysis of PCl_5.

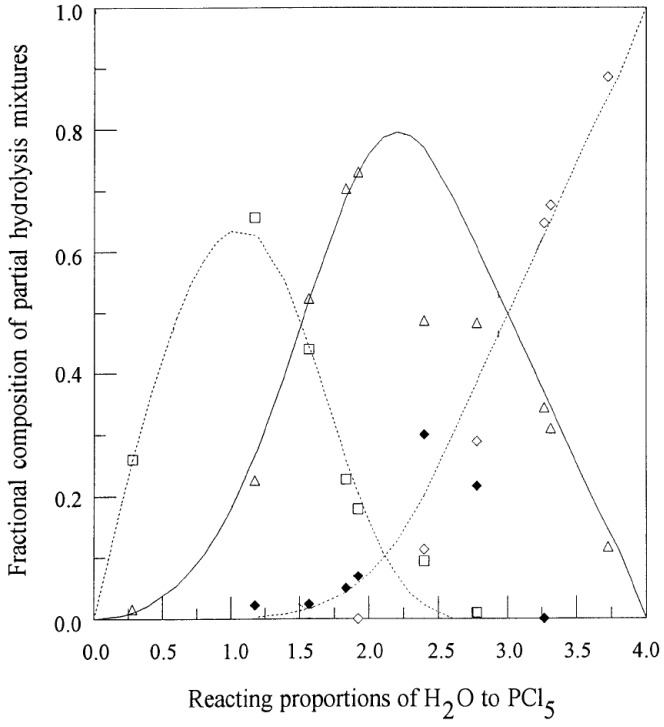

(Reproduced with permission from Royal Society of Chemistry)

The results in Figure 2.1 show that oxyphosphochloridate ion **90** was observed in solution of molecular proportions of H_2O:PCl_5 from 1.181 to 3.26:1. The build up of monochloridate ion **90** clearly demonstrates its relative stability in solutions of limited water content compared with aqueous solution, where hydrolysis is rapid with no detection of the monochloridate species. The amount of H_2O is clearly crucial in maximising yields of monophosphochloridate ion. The amount of water should be

sufficient to ensure partial hydrolysis of the oxyphosphodichloridate ion, but limited to avoid a sufficiently aqueous solution that would favour the mechanism of rapid hydrolysis. In solutions of greater water content than 3.3:1 H_2O:PCl_5 oxyphosphodichloridate was observed to hydrolyse to inorganic phosphate with no observable build up of oxyphosphochloridate **90**.

Initial reacting proportions at H_2O:PCl_5 = 2.40:1 in Figure 2.1 correspond to $POCl_3$: $HOPOCl_2$: H_2PO_2Cl: H_3PO_4: H_2O = 0.1: 0.49: 0.3: 0.11: 0.33. These indicate that there is only enough water to solvate about half of the protons of the mono, di, and tribasic acids formed during hydrolysis. Thus under these conditions, undissociated forms of each intermediate were favoured in preference to their anionic forms. Hence, the accumulation of the monochloridate species indicates a change in mechanism as the water-content becomes (rate) limiting, which forces hydrolysis to occur by pathway **A** (Scheme 2.6).

2.1.2.4 Kinetic studies of hydrolysis of thiophosphoryl (V) chlorides

Although kinetic studies of the hydrolysis of phosphorus oxychloride **4** have been made,[49] there are no corresponding kinetic studies of the hydrolysis of thiophosphoryl chloride **13** to date. One major obstacle to the study of the aqueous chemistry of thiophosphoryl chloride is its insolubility in water. For example, studies by Segall *et al.* estimated the half-life of thiophosphoryl chloride in aqueous solution (pH 7.4) as ~ 13 min by ^{31}P NMR spectroscopy.[49] From comparison of literature values for the half-lives for hydrolysis of $POCl_3$ and $PSCl_3$ (1×10^{-2} *vs* 8×10^2 s),[43,49] a large 10^4 fold difference in reactivity suggests that the kinetic data determined for $PSCl_3$ by Segall may in fact correspond to the hydrolysis of a later reaction intermediate (e.g. thiophosphodichloridic acid). Thus potential issues related to mass transfer between phases have not been taken into account.

Thiophosphodichloridate ion ($KOPSCl_2$) **95** is fully water soluble and so it should be possible to study the kinetics of hydrolysis in aqueous solution. An estimate of its half-life in aqueous solution has been reported as ~ 2 min by ^{31}P NMR spectroscopy studies.[49] This data, however, was presented as only a crude measure of reactivity and

was limited to pH 7. It is also unclear if ionic strength and a constant temperature was maintained.

2.1.3 Synthesis of oxy and thiophosphodichloridate ions

Hydrolytic synthetic methods towards the phosphodichloridate ions involved quantitative addition of water to mixtures of $POCl_3$ in dry organic solvents.[50] Although successful, these methods involved multiple side reactions that led to the formation of by-products such as inorganic phosphate, pyrophosphates and combined pyrophosphate-phosphites.

Initial attempts to synthesise the phosphodichloridate ions using aprotic synthetic methods suppressed the hydrolysis of dichloridates to inorganic (thio)phosphate through the formation of these ions as formamidine and quaternary ammonium salts. [51, 52] More recently, Segall *et al.* developed an aprotic method for the synthesis of oxy and thiophosphodichloridate ions as potassium salts. $POCl_3$ or $PSCl_3$ was added to dry potassium hydrogen carbonate in dry acetone, under an inert atmosphere.[49] The proposed mechanism for the synthesis of oxy and thiophosphodichloridate ions is given in Scheme 2.10.

Scheme 2.10 Mechanism for the synthesis of oxy and thiophosphodichloridate ions.[49]

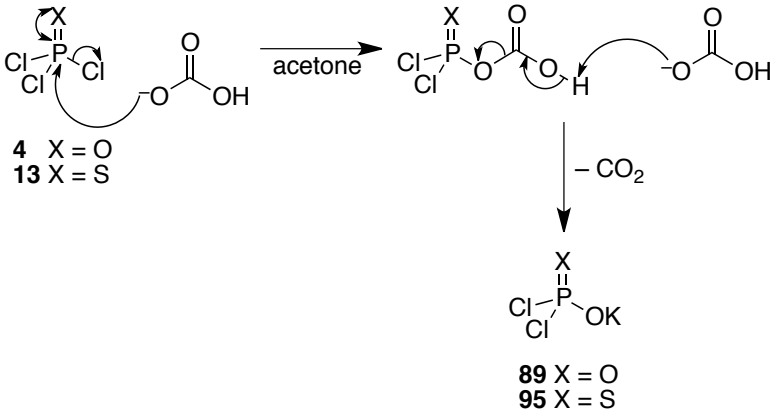

4 X = O
13 X = S

89 X = O
95 X = S

This method was used to synthesize both phosphodichloridic acids and their dichloridate ions, depending on the amount of $KHCO_3$ added to the reaction mixture. Following reaction, Segall filtered potassium chloride from the reaction solution and

demonstrated that solvent could be removed in *vacuo* to give the desired product as a white solid. Reaction was shown to occur at only one P–Cl bond, even in a large excess of $KHCO_3$. This ensured that a mixture of hydrolysis products could not be formed and thus established a method of synthesising pure phosphodichloridic acid or phosphodichloridate ions.

2.1.4 Determination of rate constants in aqueous solution

Given that the rate constant for the reaction of $POCl_3$ to the phosphodichloridate ion in aqueous dioxane solution was 62 s^{-1}, it is clear that reaction of $POCl_3$, and likely $PSCl_3$, in fully aqueous solution could only be followed by an analytical technique which ensured rapid mixing of phosphorylating agent with aqueous solution. The subsequent hydrolysis of phosphodichloridate ion to inorganic phosphate occurs with an estimated half-life on the order of minutes and so may be followed by conventional analytical techniques such as ^{31}P NMR spectroscopy and UV-Vis spectrophotometry, where rapid mixing is not required.

For those reactions which contain no chromophore, such as the hydrolysis of phosphorus (V) chlorides, it is not possible to directly follow the progress of reaction by UV-Vis spectrophotometry. Khalifah studied the catalysis of carbon dioxide hydration by carbonic anhydrases B and C in attempt to quantify the effect of pH on enzyme activity.[53] Neither reagent or product possessed a chromophore and thus there was no associated absorbance change that could be followed upon hydration. However, an equivalent of acid was generated upon hydration. Reaction of this proton with an added indicator **96** led to an absorbance change upon the formation of **96-H** that allowed reaction progress to be followed indirectly by stopped-flow UV-Vis spectrophotometry (Scheme 2.11)

Scheme 2.11 Protonation of indicator upon hydrolysis of carbon dioxide.

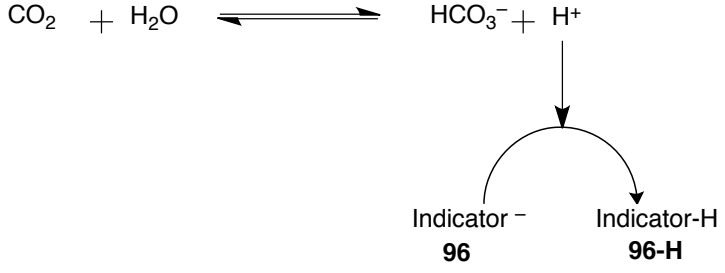

Reaction of carbon dioxide was followed in aqueous solutions containing buffer and phenolate species, across a pH range of 5.83 to 8.75. Rate constants for hydration, $k_{hydration}$, were estimated to be very much slower than protonation of buffer and indicator.[54] Thus the change in absorbance of phenolate during hydrolysis could therefore be directly related to the process of hydration.

The pK_a values of both buffer and indicator should be near-identical to ensure they are protonated to the same extent throughout each reaction. If the pK_a of the buffer and indicator differ by more than ~1 pK_a units, they will be protonated to significantly different extents during the reaction. As a consequence, a linear relationship between the observed absorbance change and amount of protons generated during the reaction under study will not be observed.

For example, if the indicator has a pK_a value one unit higher than that of the buffer, a large absorbance change per proton generated will be observed for the initial reaction, corresponding to a decrease in the concentration of the ionized form of the indicator. Consumption of the indicator over time would lead to protonation of the buffer, and a significant decrease in the absorbance change per proton generated. Conversely, if the indicator has a pK_a value one unit lower than that of the buffer a smaller absorbance change per proton generated will be observed for the initial reaction, corresponding to a decrease in the ionisation state of the buffer. Under these conditions the overall rate of absorbance change cannot directly correspond to the rate of hydration of carbon dioxide.

It was therefore necessary to use buffers and indicators of similar pK_a in following hydrolyses in the pH region 5.83 to 8.75. The buffers and accompanying indicators that were used are detailed in Table 2.5.

Table 2.5 Buffer and indicator combinations used in following the hydration of carbon dioxide in aqueous solution, showing differences in their pK_as and the corresponding pH of each solution.

Buffer (pK_a)	Indicator (pK_a)	Δ pK_a	pH
3, 5-Lutidine (6.21)	*p*-Nitrosophenol (6.20)	0.01	5.83
Bis-tris (6.60)	Chlorophenol red (6.3)	0.30	6.21
Imidazole (7.14)	*p*-Nitrophenol (7.15)	0.01	7.66
1,2-dimethylimidazole (8.22)	Metacresol purple (8.3)	0.08	8.75

To confirm that a linear relationship between absorbance change and proton generating reaction would be observed, volumetric amounts of hydrogen carbonate were added to each reaction solution (Table 2.5) and resulting changes in absorbance were measured. These were plotted against [HCO^-_3] (mM) for each reaction solution (Figure 2.2).

Figure 2.2 **Titration plots for buffer indicator systems 3,5-lutidine (0.05 M) with 4-nitrophenol (3.0 x 10^{-5} M) (A), bis-tris (0.05 M) with 3-chlorophenol red (2.7 x 10^{-5} M) (B), *N*-methyl-imidazole (0.10 M) with 4-nitrophenol (4.0 x 10^{-5} M) (C), and 1,2-dimethyl imidazole (0.10 M) with metacresol purple (3.0 x 10^{-5} M) (D).**

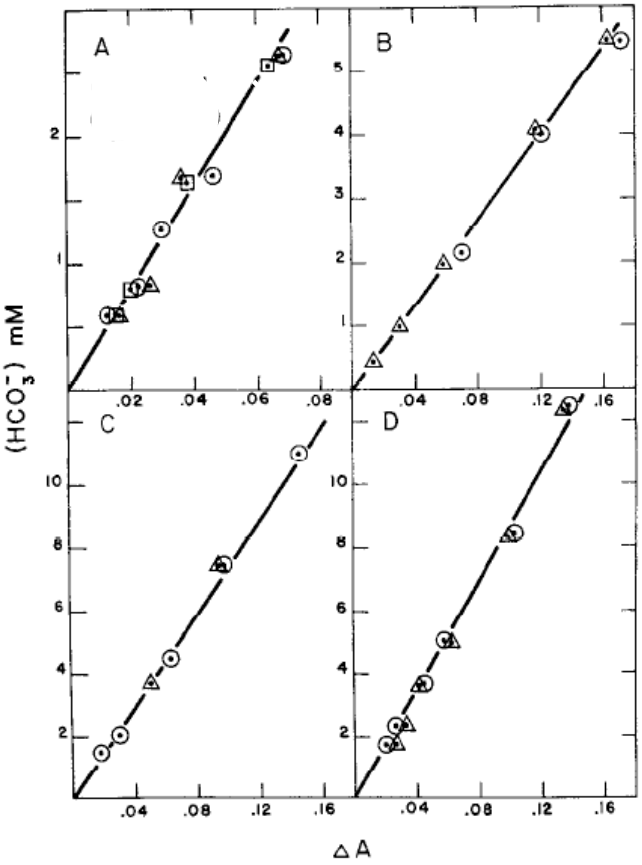

(Reproduced with permission from The Journal of Biological Chemistry)

Figure 2.2 shows that linear correlations were observed between absorbance changes and the amount of HCO^-_3 added to each reaction solution. This example demonstrates that it is possible for acid and base generating reactions to be indirectly followed by UV-Vis spectrophotometry in the presence of an ionisable indicating species.[53]

2.2 Results

2.2.1 Kinetic studies on the hydrolysis of oxy and thiophosphodichloridate ions

In order to assess the feasibility of using phosphodichloridate and thiodichloridate ions as reagents for the (thio)phosphorylation of amines in water, kinetic studies of the hydrolyses of these ions were performed over a broad range of pH values.

2.2.1.1 Synthesis

A rigorous kinetic study of the hydrolyses of phosphorus (V) chlorides in aqueous solution requires the syntheses of oxy and thiophosphodichloridate ions **89** and **95**. These were achieved using an adapted established literature method.[49, 50] Reaction of freshly distilled phosphorus oxychloride and thiophosphoryl chloride with oven-dried potassium hydrogen carbonate in dry acetonitrile under an inert atmosphere yielded oxy and thiophosphodichloridate ions respectively (Scheme 2.12).

Scheme 2.12

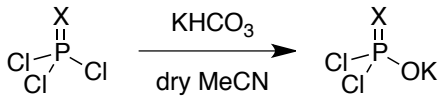

4 X = O
13 X = S

89 X = O
95 X = S

Oxy and thiophosphodichloridate ions were synthesised in acetonitrile rather than acetone, owing to its higher boiling point facilitating more accurate handling of volumetric solutions, and to facilitate our longer term goal of performing aminolysis studies on dichloridates **89** and **95** where acetone would react with the amines.

Reaction times for the synthesis of oxy and thiophosphodichloridate ions were 10 min and 12 h, respectively. These were the same reaction times as used by Segall *et al.* and we were able to prepare both dichloridate salts **89** and **95** in homogeneous forms without needing to perform further optimizations. Given that solid forms of **89** and **95** could not be redissolved in anhydrous solvents, each dichloridate was synthesised in a volumetric amount of dry acetonitrile at known concentrations. These solutions were used directly in kinetic studies. The purities of dichloridates **89** and **95** were confirmed

by ^{31}P NMR spectroscopy in consultation with literature data.[49] It was found that stock solutions of phosphodichloridate **89** were stable for a few days when stored at –18 °C, whereas solutions of thiophosphodichloridate **95** solutions were much more stable with no detectable decomposition after more than one month of storage at –18 °C. In both cases, similar stabilities were found by Segall *et al.* when using acetone as the solvent.[49] Therefore, fresh solutions of **89** were prepared immediately prior to each kinetic run to minimise hydrolysis prior to addition to each reaction solution. Solutions of **95** were prepared and either immediately used in kinetic studies or stored at –18 °C for study at a later date.

2.2.1.2 Preliminary ^{31}P NMR spectroscopic studies

The hydrolyses of oxy and thiophosphodichloridate to inorganic (thio)phosphate were initially followed by ^{31}P NMR spectroscopy to confirm the reactivity of each dichloridate species and estimate the rate constants for their hydrolysis in aqueous solution (Scheme 2.13).

Scheme 2.13

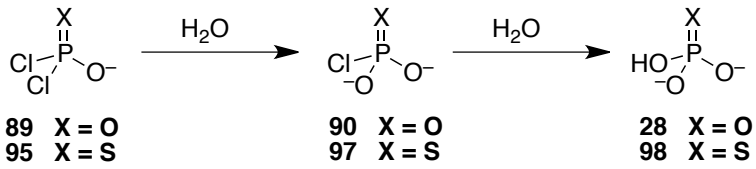

89 X = O, **95** X = S **90** X = O, **97** X = S **28** X = O, **98** X = S

^{31}P NMR spectroscopy experiments were performed on short timescales (~ 1 min) and spectra were continuously acquired over the course of the reaction. Each reaction contained a high concentration of phosphorylating agent to ensure that each phosphorus-containing species could be resolved and quantified. Aqueous solutions were buffered with mono- and dibasic potassium carbonate to minimize any significant pH changes and thus ensure that the chemical shifts of each phosphorus-containing species did not change as the reactions progressed.

Solutions of carbonate buffer in D_2O (0.5 M, 800 μL, pD ≈ 11) were locked and shimmed in the NMR spectrometer (162 MHz) prior to the start of each reaction. This minimized any time delay between the start of each reaction and acquisition of NMR

data. Reactions were initiated by the addition of a concentrated solution of dichloridate to the locked sample, followed by mixing by inversion and immediate analysis.

^{31}P NMR experiments comprising 16 transients were collected for the hydrolysis of each dichloridate species. The resulting ^{31}P NMR spectra for the hydrolyses of oxy and thiophosphodichloridate to inorganic (thio)phosphate are shown in Figure 2.3.

Figure 2.3 **^{31}P NMR spectroscopic studies on the hydrolyses of (A) phosphodichloridate 89 and (B) thiophosphodichloridate 95 at pH ~11. The reaction time and relative amounts of reactant and product are indicated above each spectrum.**

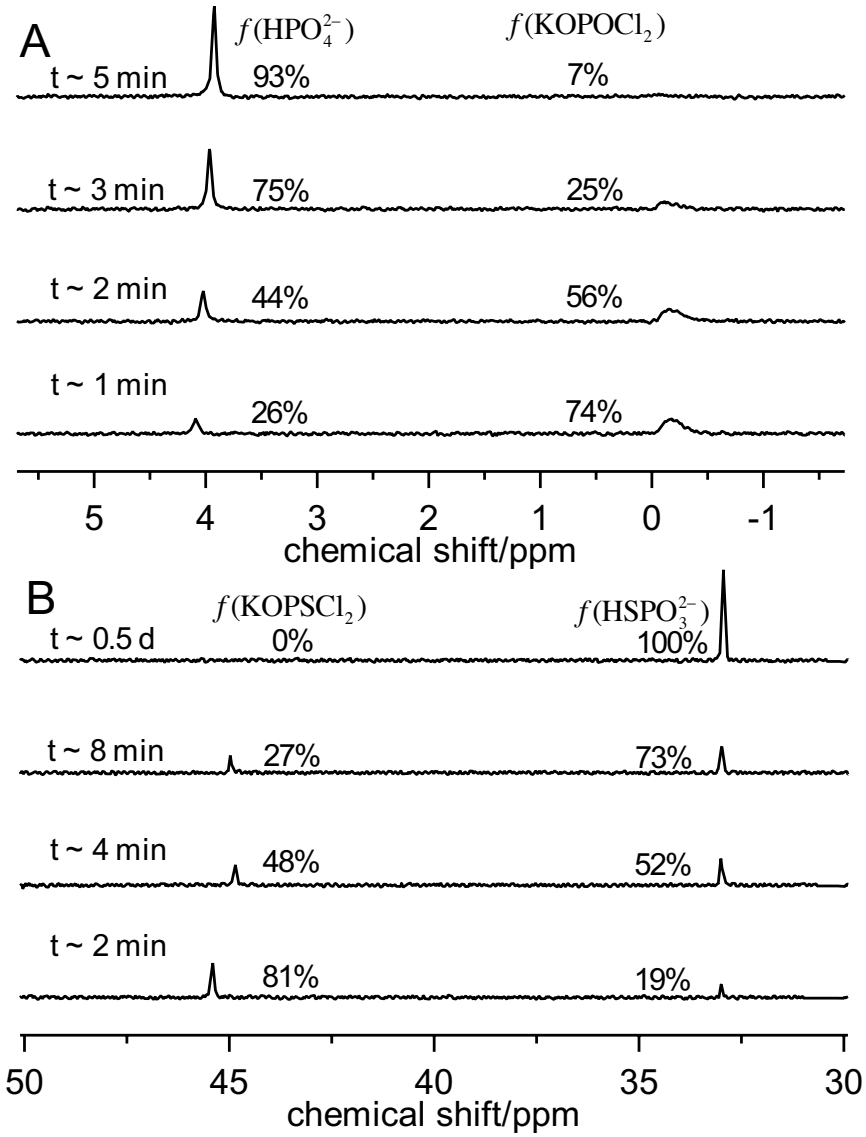

Upon addition of **89** to a 90% FB × 0.5 M carbonate buffer (pH ~11), the signal at ~ 0 ppm disappeared with the concomitant appearance of a signal at ~4 ppm (Figure 2.3A). Upon addition of **95** to a 90% FB × 0.5 M carbonate buffer (pH ~11), the signal at ~46 ppm was shown to convert into the signal at ~33 ppm (Figure 2.3B). The signals at 4 and 33 ppm were assigned as inorganic phosphate and inorganic thiophosphate, respectively, by spiking experiments. The chemical shifts of the signals at 0 and 46 ppm were similar to those obtained for oxy and thiophosphodichloridic acid in mixed water-acetonitrile solvents (-2 and 40 ppm, respectively).[49]

Half-lives for the hydrolyses of oxy and thiophosphodichloridate were estimated as two and four min, respectively, from changes in the intensity of signals due to oxy and thiophosphodichloridate ions (Figure 2.3).

2.2.1.3 UV-Vis spectrophotometric studies

The hydrolyses of oxy and thiophosphodichloridate to inorganic (thio)phosphate were followed by UV-Vis spectrophotometry, across a broad pH-range, using an adapted indicator-based method.

During the hydrolyses of $KOPOCl_2$ **89** and $KOPSCl_2$ **95**, two equivalents of hydronium ion are generated upon initial hydrolysis to monochloridate salts **90** and **97** in the rate-determining step (Scheme 2.14).

Scheme 2.14

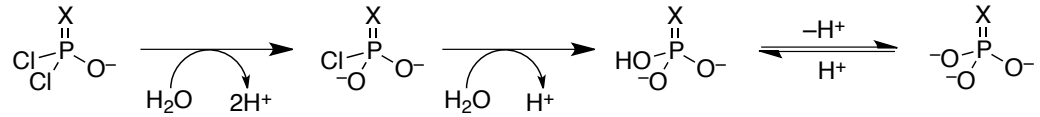

89 X = O
95 X = S

90 X = O
97 X = S

28 X = O
98 X = S

One or two equivalents of protons are subsequently generated upon hydrolysis to inorganic phosphate **28** and thiophosphate **98**, depending on the final reaction pH and thus its ionisation state. Given the monochloridate species **90** and **97** are hydrolysed rapidly upon their formation, changes in the absorbance due to the indicator only contain kinetic information about the initial rate-determining hydrolysis step.

Aqueous reaction solutions were buffered to control reaction pH and were supplemented by indicators of similar pK_a. A decrease in the reaction pH during hydrolysis was necessary to ensure a detectable change in absorbance was observed. The pK_a of buffer and indicator differed by no more than 0.5 units; this ensured that these species were protonated to similar extents upon hydrolysis. To ensure linear responses between absorbance change and addition of protons was observed for each buffer and indicator combination, absorbance changes were monitored upon addition of volumetric amounts of hydrogen chloride over the pH range of the reaction. For example, the absorbance of the phosphate buffer (90% FB, I=1) containing 4-nitrophenol indicator (90% FB) was monitored at 25 °C upon addition of volumetric hydrochloric acid solution (Figure 2.4).

Figure 2.4 Absorbance change upon addition of volumetric HCl solution to phosphate buffer (90% FB) containing the indicator 4-nitrophenol (90% FB) at I=1 (KCl) and 25 °C.

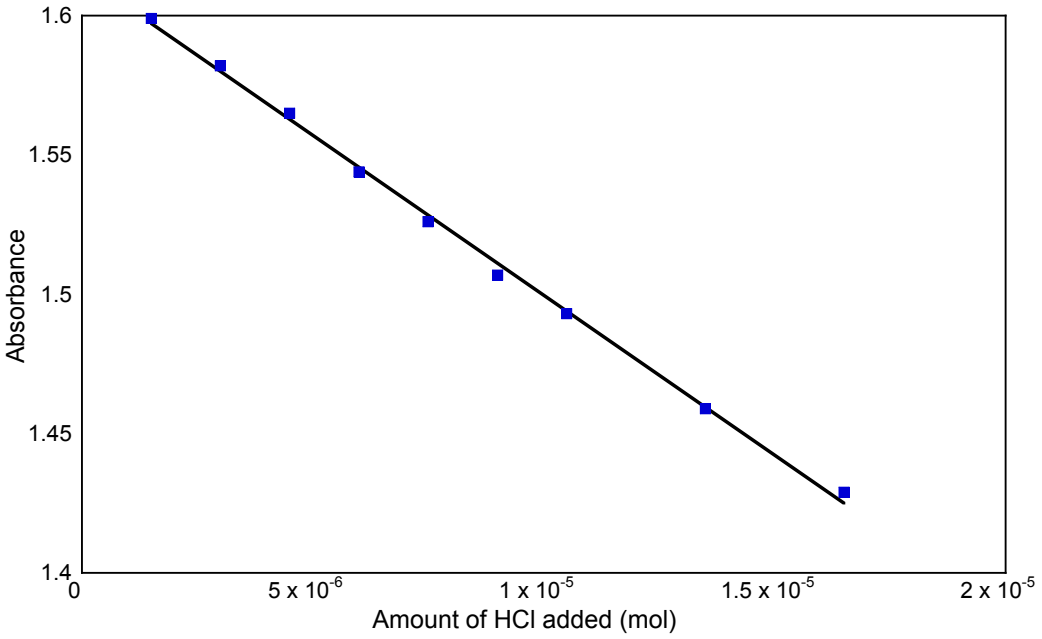

Figure 2.4 shows a linear correlation of absorbance *vs* amount of HCl added which indicates that a linear correlation between absorbance and generation of protons upon the hydrolysis of oxy and thiophosphodichloridate ions should be observed.

The hydrolyses of $KOPOCl_2$ and $KOPSCl_2$ were followed in solutions containing phosphate buffer with 4-nitrophenol (pH 1.99, 2.86, 6.49 and 7.50), formate buffer with 2,4-dinitrophenol (pH 3.53 and 4.53) and carbonate buffers with 2,5-dimethylphenol (pH 9.74 and 10.63). Hydrolyses were also followed in potassium hydroxide solutions of pH 11.88 – 13.23 with the indicator 1,3,5 trinitrobenzene.

During hydrolysis, it is conceivable that the indicating phenolates **99** may react with the oxy and thiophosphodichloridate ions to generate phosphate ester **100**, which may contribute to k_{obs} (Scheme 2.15).

Scheme 2.15

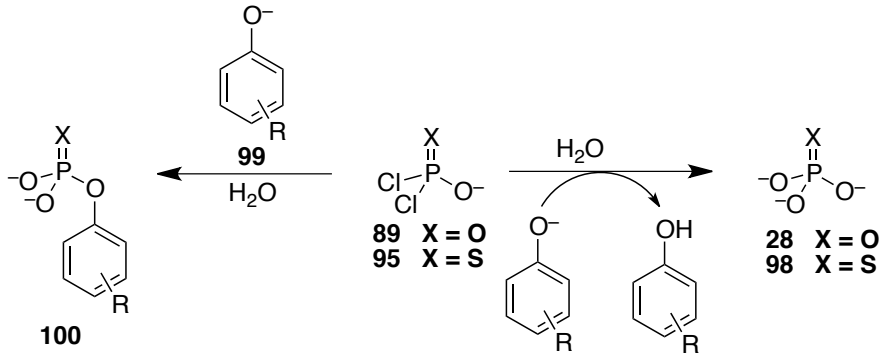

To ensure that oxy and thiophosphodichloridate ions did not react with phenolate indicators **99** under the reaction conditions used in these UV-Vis spectroscopy studies, oxy and thiophosphodichloridate ions were added to aqueous solutions of varying high concentrations of 2,5-dimethyl phenolate, the most nucleophilic phenolate used, and the reaction products were immediately analysed by ^{31}P NMR spectroscopy (Figure 2.5).

Figure 2.5 **^{31}P NMR spectroscopic studies of the hydrolyses of (A) phosphodichloridate and (B) thiophosphodichloridate in aqueous solution of varying concentration of 2,5 dimethylphenolate. The concentrations of 2,5 dimethylphenolate are indicated above each spectrum.**

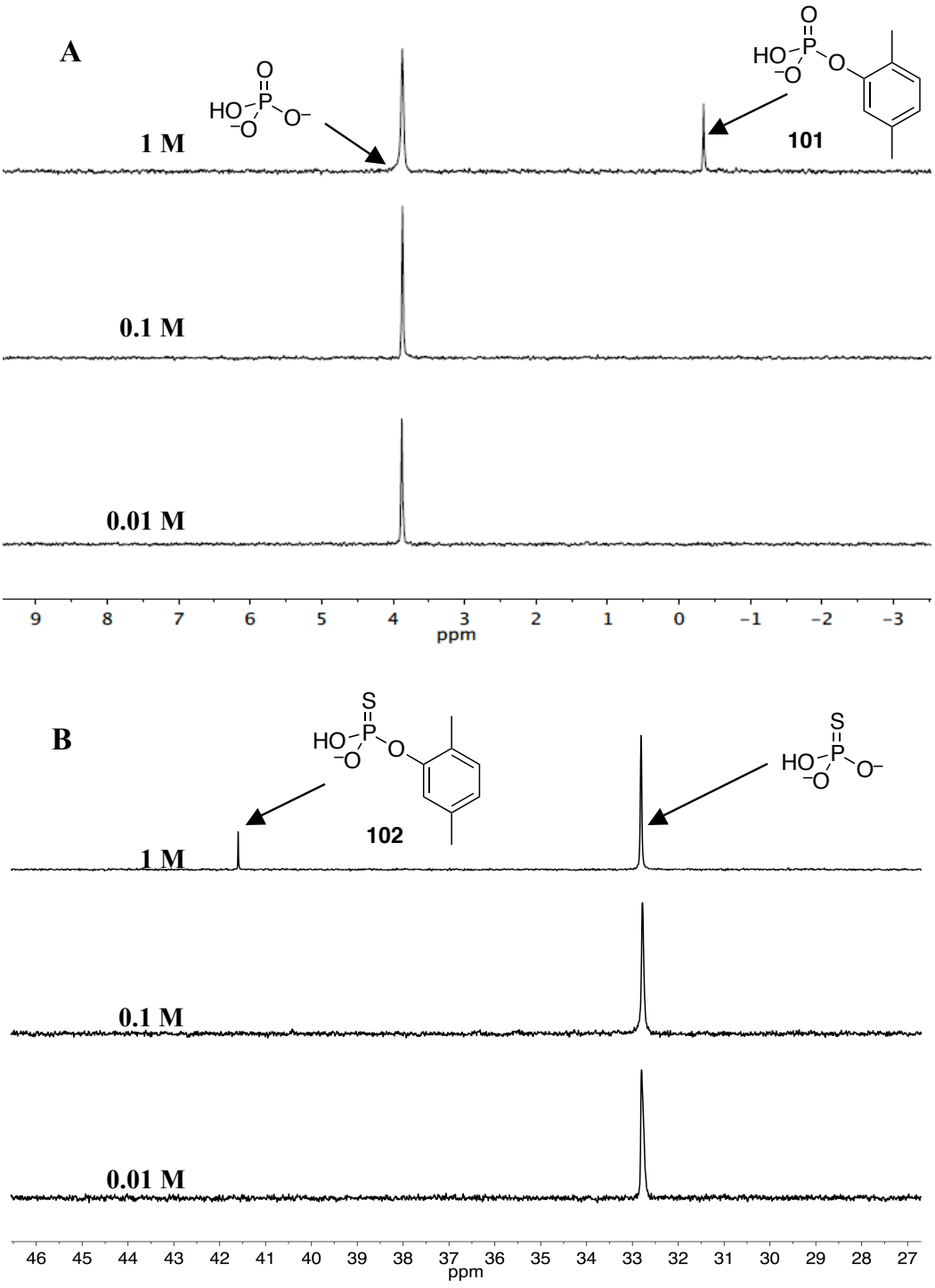

The signals due to the hydrolysis products of oxy and thiophosphodichloridate ions were identified ~ 4 and 33 ppm by spiking with inorganic phosphate and inorganic thiophosphate, respectively. Additional signals at –0.5 and 42.2 ppm were observed in 1 M solutions of 2,5 dimethylphenolate, which are likely to correspond to phosphate monoester **101** and thiophosphate monoester **102**, respectively. These studies clearly show that any reaction between oxy or thiophosphodichloridate and 2,5 dimethylphenolate occurs only at very high phenolate concentrations (~1 M). Reaction between oxy and thiophosphodichloridate ions and each phenolate indicator should therefore not occur under the experimental conditions of hydrolysis, where phenolate indicators are present at concentrations of 0.18 to 0.80 mM.

For reactions at high pH (>10.63), a suitable combination of buffer and ionisable indicator, of similar pK_a, could not be found. Therefore, these reactions were undertaken in solutions of potassium hydroxide and 1,3,5 trinitrobenzene. Reaction between hydroxide ions and 1,3,5 trinitrobenzene **103** generates the Meisenheimer σ complex **104** (Scheme 2.16).[55]

Scheme 2.16 Reaction of hydroxide ion with 1,3,5 trinitrobenzene to generate the Meisenheimer complex 25.[55]

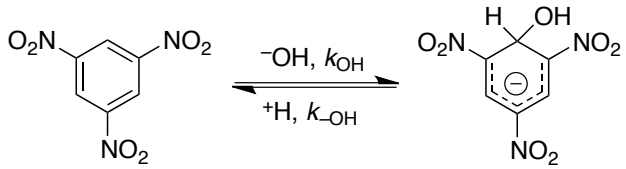

103 **104**

A pH-dependant equilibrium exists between **103** and **104**. Upon the hydrolysis of oxy or thiophosphodichloridate, the equilibrium is shifted toward the formation of 1,3,5 trinitrobenzene **104**. Bernasconi determined the rate constants for hydroxide addition (k_{OH}) and removal (k_{-OH}) of 1,3,5 trinitrobenzene in water to be 37.5 mol^{-1} dm^3 s^{-1} and 9.8 s^{-1} at 25 °C, respectively.[56] Given that the reaction of **104** with hydrochloric acid, k_{-OH}, is likely to be very much faster (~2000 fold) than the hydrolysis of either phosphodichloridate ion, even at very high pH, the resulting decrease in absorbance due to **104** may then be followed and used to determine rate constants for hydrolysis.

Typically, stock solutions of oxy and thiophosphodichloridate in acetonitrile were prepared at concentrations of 0.33 M and reactions were initiated by addition of these stock solutions to the relevant reaction solution, which had been thermostated at 25 °C for 10 minutes. The resulting decreases in absorbance of indicators were subsequently followed. In general, absorbance decreases of ~0.1 units were observed which correspond to decreases in pH of ~0.15. For reactions at high pH (≥ 11.88) the observed pseudo first-order rate constants, k_{obs}, were determined from kinetic data for the first 25% of the reaction, corresponding to pH decreases of ~0.05.

The observed experimental first-order rate constant can potentially be the sum of rate constants for several parallel hydrolysis processes, including a pH independent (k_0) and hydroxide catalysed (k_{HO}) reaction. The rate constant for hydrolysis, k_{obs}, is defined as in Equation 2.4.

$$k_{obs} = k_0 + k_{OH}[HO^-] + k_B[B] \qquad \textbf{Equation 2.4}$$

Buffer catalysis ($k_B[B]$) may be a contributing term where there is general base catalysis of hydrolysis. To assess the contribution of the term for general base catalysis in each buffer used in hydrolysis, experiments were performed at several different concentrations of the buffer base (using a constant ratio of buffer acid/base forms) in order to maintain the same pH. If there was general base catalysis of hydrolysis then the observed pseudo-first-order rate constant for hydrolysis (k_{obs}) would increase with the increasing concentration of buffer.

Values for experimental first-order rate constants for hydrolysis of oxy and thiophosphodichloridates (k_{obs}, s^{-1}) were obtained from least-squares analysis of absorbance versus time data in solutions of varying buffer concentrations. Figure 2.6 shows a plot of the observed rate constants, k_{obs}, against varying concentrations of carbonate buffer for the hydrolyses of $KOPOCl_2$ (■) and $KOPSCl_2$ (•) in aqueous solutions.

Figure 2.6 Plot of the observed rate constants, k_{obs}, against concentrations of phosphate buffer for the hydrolyses of $KOPOCl_2$ (■) and $KOPSCl_2$ (•) in aqueous solution.

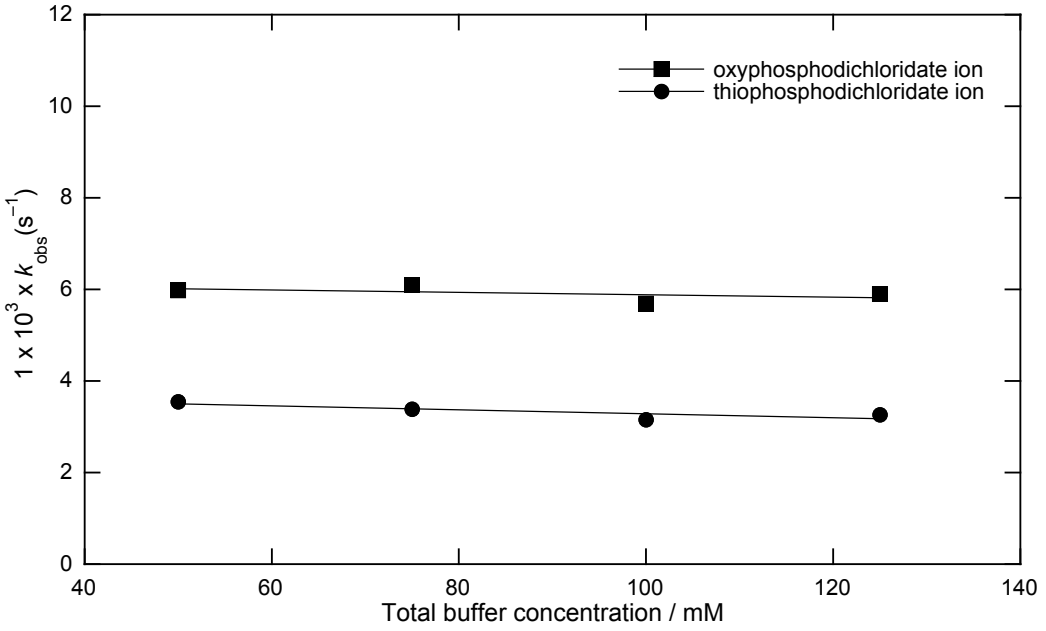

Shown in Figure 2.6 are plots of k_{obs} values against the concentration of phosphate buffer for oxy and thiophosphodichloridate ions. The slopes of these plots are essentially zero with increases in buffer concentrations. The slopes indicate that general base catalysis is not observed for the hydrolysis of oxy and thiophosphodichloridate ions. This has also been shown to be the case for the hydrolysis of $KOPOCl_2$ and $KOPSCl_2$ in all other buffers used in these kinetic studies (Appendix A). Therefore, the observed rate equation for hydrolysis (Equation 2.4) may be simplified to give Equation 2.5.

$$k_{obs} = k_0 + k_{OH}[HO^-] \qquad \textbf{Equation 2.5}$$

Figure 2.7 shows a typical kinetic trace of absorbance versus time with a first-order exponential fit to the data, obtained at 291 nm for hydrolysis of $KOPOCl_2$ in an aqueous solution containing 50% FB carbonate buffer (0.1 M, pH = 9.74) and 2,5 dimethylphenol (0.80 mM) at 25 °C and I=1 (KCl).

Figure 2.7 **Hydrolysis of oxyphosphodichloridate ion in carbonate buffer (50% FB × 100 mM, pH 9.74) with the indicator 2,5 dimethylphenol (50% FB × 0.80 mM) at 25 °C and *I*=1 (KCl); (A) plot of absorbance against time, (B) plot of ln (A_t-A_∞) against time.**

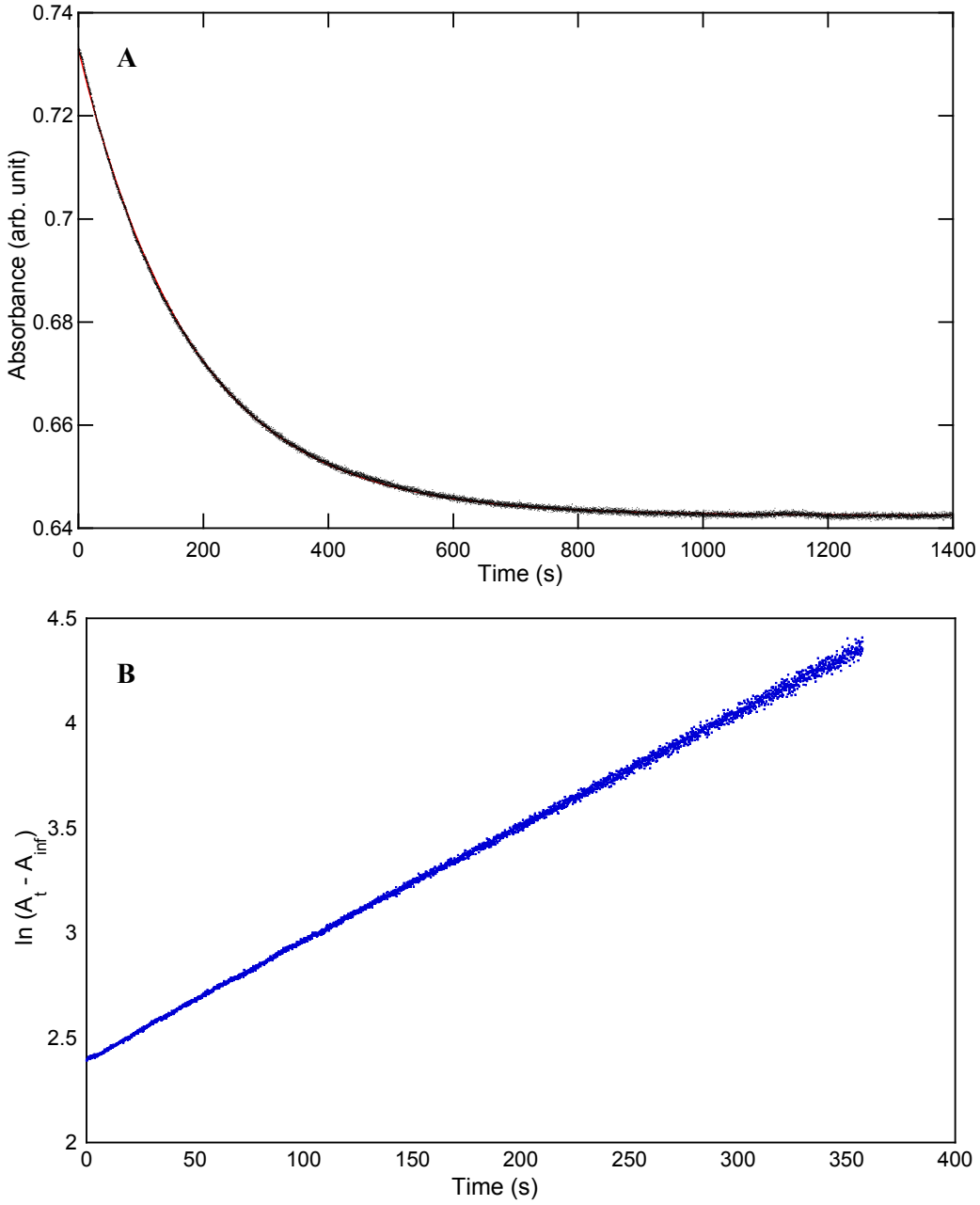

Experimental pseudo first-order rate constants for hydrolysis at this pH and different buffer concentrations, k_{obs} (s^{-1}), were obtained by non-linear least squares analysis of absorbance versus time data.

2.2.1.3.1 Hydrolysis of the oxyphosphodichloridate ion

The hydrolysis reaction of oxyphosphodichloridate ion was investigated in a range of aqueous buffers and KOH solutions using the indicator-based UV-Vis spectrophotometric method (Scheme 2.17).

Scheme 2.17 Hydrolysis reaction of oxyphosphodichloridate ion in aqueous solution.

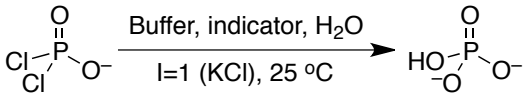

89 **28**

Upon hydrolysis of the oxyphosphodichloridate ion, the decrease in absorbance of indicating phenolates/ Meisenheimer intermediate **102** was followed. The resulting pseudo first-order absorbance decay plots correspond to the hydrolysis of oxyphosphodichloridate ion **89**.

Table 2.6 summarises the reaction data for the hydrolysis of oxyphosphodichloridate in aqueous solution. All remaining first-order plots for the hydrolysis of $KOPOCl_2$ are available on the supplementary information dvd.

Table 2.6 Rate constants for the hydrolysis of oxyphosphodichloridate 89 in buffer and KOH solution at the given wavelength (nm) of indicator used, at 25 °C and *I*=1 (KCl).[a]

Buffer	Indicator ([Indicator] × 10^3/M)	λ (nm)	[$KOPOCl_2$] × 10^3 (M)	k_{obs}[a] × 10^3 (s^{-1})	Start pH	End pH
0.100 M × 50% FB H_3PO_4 /KH_2PO_4	2-aminobenzoic acid (0.50)	328	2.00	6.03	1.99	1.83
0.100 M × 90% FB H_3PO_4 /KH_2PO_4	2-aminobenzoic acid (0.50)	328	2.00	5.92	2.86	2.68
0.100 M × 90% FB HCO_2H/ HCO_2K	2,4-dinitrophenol (0.18)	401	2.70	6.10	4.53	4.32
0.100 M × 50% FB KH_2PO_4 /K_2HPO_4	4-nitrophenol (0.27)	400	1.10	5.82	6.49	6.39
0.100 M × 90% FB KH_2PO_4 /K_2HPO_4	4-nitrophenol (0.27)	400	1.10	5.79	7.50	7.40
0.100 M × 50% FB $KHCO_3$ /K_2CO_3	2,5-dimethylphenol (0.80)	291	1.10	5.81	9.74	9.64
0.100 M × 90% FB $KHCO_3$ /K_2CO_3	2,5-dimethylphenol (0.80)	291	1.10	6.00	10.63	10.52
0.010 M KOH	1,3,5-trinitrobenzene (0.30)	439	0.28	5.37	11.88	11.71
0.025 M KOH	1,3,5-trinitrobenzene (0.30)	439	0.69	6.54	12.31	12.18
0.050 M KOH	1,3,5-trinitrobenzene (0.30)	439	1.39	8.06	12.62	12.43
0.075 M KOH	1,3,5-trinitrobenzene (0.30)	439	2.06	8.60	12.78	12.58
0.100 M KOH	1,3,5-trinitrobenzene (0.30)	439	2.75	9.90	12.92	12.72
0.150 M KOH	1,3,5-trinitrobenzene (0.23)	439	4.13	12.6	13.10	12.96
0.200 M KOH	1,3,5-trinitrobenzene (0.15)	439	5.50	15.1	13.23	12.99

(a) The value of the first-order rate constant, k_{obs} (s^{-1}), was obtained directly from least squares analysis of absorbance versus time data available on the supplementary information dvd.

Shown on the following page is the pH-k_{obs} profile obtained for the hydrolysis of oxyphosphodichloridate ion in aqueous solution (Figure 2.8).

Figure 2.8 pH-k_{obs} profile for the hydrolysis of $KOPOCl_2$ at 25 °C and I=1 (KCl).

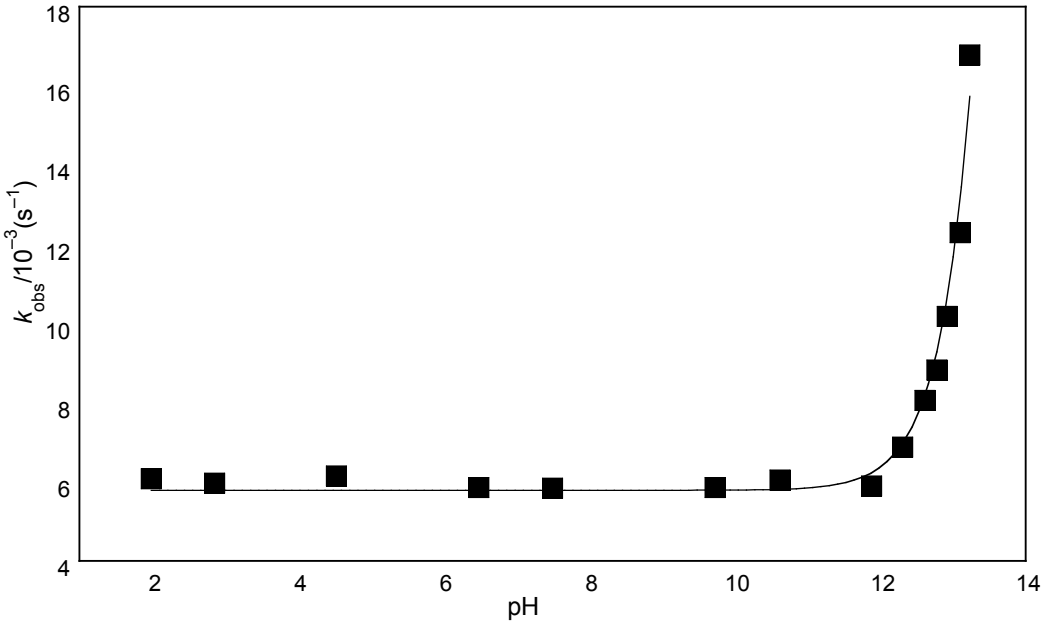

Estimates of the second-order rate constant for hydroxide-catalysed hydrolysis, k_{HO^-} ($M^{-1}s^{-1}$), and the first-order rate constant for buffer-independent hydrolysis, k_0 (s^{-1}), were obtained by non-linear least squares analysis. Equation 2.6 was fitted to the experimental data, shown as (■), where x = pH.

$$k_{obs} = k_{HO^-}10^{-x} + k_0 \qquad \textbf{Equation 2.6}$$

For the hydrolysis of oxyphosphodichloridate **89**, values of $k_0 = 5.8 \times 10^{-3}$ s^{-1} and $k_{OH} = 5.3 \times 10^{-2}$ M^{-1} s^{-1} were obtained. The error associated with k_0 may be estimated as ± 0.3 from comparison of k_0 (5.8×10^{-3} s^{-1}) with the k_{obs} values determined in solutions of pH 1.99 – 10.63. This corresponds to an error of 5% within the data presented in Table 2.6.

2.2.1.3.2 Hydrolysis of the thiophosphodichloridate ion

The hydrolysis of the thiophosphodichloridate ion **95** was investigated in a range of aqueous buffers and KOH solutions using the indicator-based UV-Vis spectrophotometric method (Scheme 2.18).

Scheme 2.18 Hydrolysis reaction of thiophosphodichloridate 95 in aqueous solution.

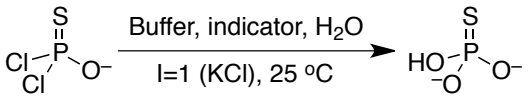

95 **98**

Upon hydrolysis of the thiophosphodichloridate ion, the decrease in absorbance of indicating phenolates/ Meisenheimer intermediate **102** was followed. The resulting pseudo first-order absorbance decay plot corresponded to the hydrolysis of thiophosphodichloridate **95**.

Table 2.7 summarises the reaction data for the hydrolysis of thiophosphodichloridate **95**. All remaining first-order plots for the hydrolysis of $KOPSCl_2$ are available on the supplementary information dvd.

Table 2.7 Rate constants for the hydrolysis of thiophosphodichloridate 95 in buffer and KOH solution at the given wavelength (nm) of indicator used, at 25 °C and *I*=1 (KCl).[a]

Buffer	Indicator ([Indicator] × 10^3/M)	λ (nm)	[$KOPSCl_2$] × 10^3 (M)	k_{obs}[a] × 10^3 (s^{-1})	Start pH	End pH
0.100 M × 50% FB H_3PO_4 /KH_2PO_4	2-aminobenzoic acid (0.50)	328	2.00	3.77	1.99	1.81
0.100 M × 90% FB H_3PO_4 /KH_2PO_4	2-aminobenzoic acid (0.50)	328	2.00	3.20	2.86	2.69
0.100 M × 50% FB HCO_2H/ HCO_2K	2,4-dinitrophenol (0.18)	401	2.00	3.83	3.53	3.33
0.100 M × 90% FB HCO_2H/ HCO_2K	2,4-dinitrophenol (0.18)	401	2.70	3.80	4.53	4.32
0.100 M × 50% FB KH_2PO_4 /K_2HPO_4	4-nitrophenol (0.27)	400	1.10	3.68	6.49	6.40
0.100 M × 90% FB KH_2PO_4 /K_2HPO_4	4-nitrophenol (0.27)	400	1.10	3.60	7.50	7.41
0.100 M × 50% FB $KHCO_3$ /K_2CO_3	2,5-dimethylphenol (0.80)	291	1.10	3.33	9.74	9.64
0.100 M × 90% FB $KHCO_3$ /K_2CO_3	2,5-dimethylphenol (0.80)	291	1.10	3.32	10.63	10.54
0.010 M KOH	1,3,5-trinitrobenzene (0.30)	439	0.28	3.14	11.88	11.72
0.025 M KOH	1,3,5-trinitrobenzene (0.30)	439	0.69	3.50	12.31	12.17
0.050 M KOH	1,3,5-trinitrobenzene (0.30)	439	1.39	3.56	12.62	12.45
0.100 M KOH	1,3,5-trinitrobenzene (0.30)	439	2.75	3.83	12.92	12.84
0.200 M KOH	1,3,5-trinitrobenzene (0.15)	439	5.50	4.03	13.23	13.01

(a) The value of the first-order rate constant, k_{obs} (s^{-1}), was obtained directly from least squares analysis of absorbance versus time data available on the supplementary information dvd.

Shown on the following page is the pH-k_{obs} profile obtained for the hydrolysis of thiophosphodichloridate ion **95** (Figure 2.9).

Figure 2.9 pH-k_{obs} profile for the hydrolysis of $KOPSCl_2$ 95 at 25 °C and I=1 (KCl).

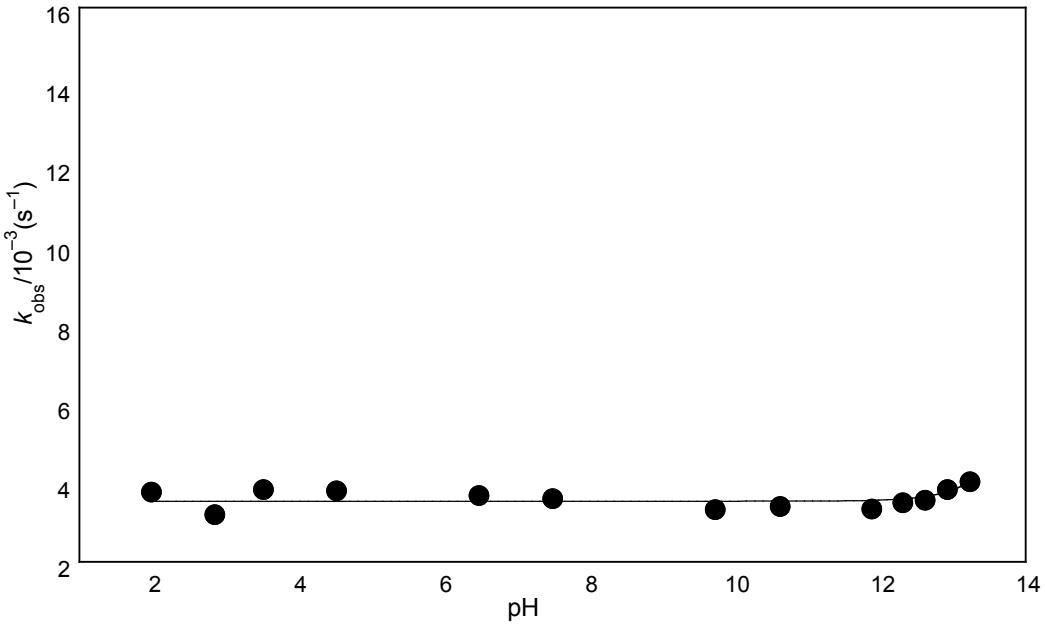

Estimates of the first-order rate constant for buffer-independent hydrolysis of $KOPSCl_2$, k_0 (s^{-1}), were obtained by non-linear least squares analysis.

A value of $k_0 = 3.6 \pm 0.4 \times 10^{-3}$ s^{-1} was obtained for the hydrolysis of thiophosphodichloridate **95** in aqueous solution.

2.2.1.4 Kinetic studies on the hydrolysis of phosphorus oxychloride and thiophosphoryl chloride

The hydrolysis of phosphorus oxychloride **4** and thiophosphoryl chloride **13** to their respective (thio)phosphodichloridate ions was investigated by UV-visible stopped-flow spectrophotometry using the indicator-based approach employed in the hydrolysis study of oxy and thiophosphodichloridate ions.

The UV-visible stopped-flow spectrophotometer was equipped with two glass syringes of volumes 250 μL and 2.5 mL which contained solutions of (thio)phosphorylating agent in anhydrous acetonitrile and buffer in aqueous acetonitrile solution at I=1 (KCl), respectively. In each kinetic run, (thio)phosphorylating agent (25 μL) and phosphate buffer in aqueous acetonitrile (250 μL) were mixed into the reaction

chamber at a ratio of 1:10. No attempt was made to maintain or control the temperature of each reaction followed by UV-visible stopped-flow spectrophotometry.

2.2.1.4.1 Hydrolysis of Phosphorus Oxychloride

The hydrolysis of phosphorus oxychloride to oxyphosphodichloridate ion was investigated in buffered aqueous acetonitrile solutions (35 % H_2O, 65% MeCN) at *I*=1 (KCl) using the indicator-based UV-Vis stopped-flow spectrophotometric method (Scheme 2.19).

Scheme 2.19 Hydrolysis reaction of phosphorus oxychloride in buffered aqueous acetonitrile solutions (35 % H_2O, 65% MeCN) at *I*=1 (KCl).

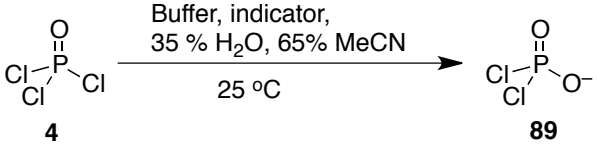

4 **89**

Upon the hydrolysis of $POCl_3$, the decrease in absorbance of the indicating phenolate was followed. The observed rate constant for reaction was determined from the resulting pseudo first-order absorbance decay plot.

Table 2.8 summarises the kinetic data for the hydrolysis of $POCl_3$ to oxyphosphodichloridate ion in aqueous acetonitrile solutions (35 % H_2O, 65% MeCN) at *I*=1 (KCl) containing potassium phosphate and potassium carbonate buffers.

Table 2.8 Rate constants for the hydrolysis of phosphorus oxychloride 4 to oxyphosphodichloridate ion 89 in buffered aqueous acetonitrile solutions (35 % H_2O, 65% MeCN) at the given wavelength (nm) of indicator used, at *I*=1 (KCl).

Buffer	Indicator ([Indicator] × 10^3/M)	λ (nm)	[$POCl_3$] × 10^3 (M)	k_{obs}[a] (s^{-1})
10 mM × 90% FB KH_2PO_4 /K_2HPO_4	4-nitrophenol (0.35)	400	1.8	14.4
5 mM × 90% FB $KHCO_3$ /K_2CO_3	2,5-dimethylphenol (0.64)	291	0.4	14.4

The observed rate constants for the hydrolysis of $POCl_3$ to oxyphosphodichloridate were determined as 14.4 s^{-1} at pH 6.5 and 10.6 (Table 2.8). To determine whether these values were due to the hydrolysis of $POCl_3$ or the result of a mixing effect, the hydrolysis of $POCl_3$ to oxyphosphodichloridate ion was followed in buffered aqueous acetonitrile solutions of varying water content (35-80% water content). From the application of the Grunwald-Winstein theory to the hydrolysis of phosphorus oxychloride in aqueous solution, k_{obs} was expected to increase as the water content of the reaction solution was increased.[45] The results of these experiments are summarised in Table 2.9

Table 2.9 Rate constants for the reaction of phosphorus oxychloride in aqueous acetonitrile solutions of varying water content, containing potassium phosphate (10 mM × 90% FB KH_2PO_4 /K_2HPO_4) and 4-nitrophenol (0.35 mM) at 400 nm.

Water content (%)	$[POCl_3] \times 10^3$ (M)	k_{obs}[a] (s^{-1})
35	1.8	14.4
45	1.8	14.9
45	1.8	14.2
65	1.8	14.5
80	1.8	14.5

As shown in Table 2.9, the observed rate constants for the hydrolysis of $POCl_3$ to oxyphosphodichloridate ion did not change as a function of water content in the reaction mixture. These results are discussed in Section 2.3.2.

2.2.1.4.2 Hydrolysis of Thiophosphoryl Chloride

The hydrolysis of thiophosphoryl chloride to thiophosphodichloridate was investigated in buffered aqueous acetonitrile solutions (35 % H_2O, 65% MeCN) at I=1 (KCl) using the indicator-based UV-Vis stopped-flow spectrophotometric method (Scheme 2.20).

Scheme 2.20 Hydrolysis reaction of thiophosphoryl chloride in buffered aqueous acetonitrile solutions (35 % H_2O, 65% MeCN) at I=1 (KCl).

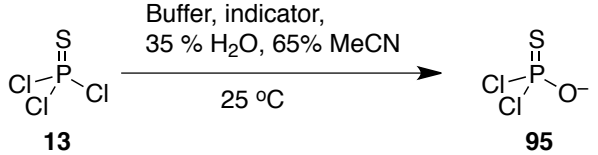

13 **95**

Upon hydrolysis of $PSCl_3$ **13**, the decrease in absorbance of the indicating phenolate was followed. The resulting absorbance decay plots were not zero, first or second-order, and it was therefore not possible to determine first-order rate constants for the hydrolysis of $PSCl_3$ to thiophosphodichloridate in aqueous acetonitrile solutions by stopped-flow UV-Visible spectrophotometry.

2.3 Discussion

2.3.1 Hydrolysis of oxy and thiophosphodichloridate ions

To date there has been no reported assessment of the hydrolysis of oxy and thiophosphodichloridate in aqueous solution across a broad pH range. Our studies have investigated the hydrolyses of both species, across a broad pH range, in fully aqueous solution.

2.3.1.1 ^{31}P NMR spectroscopy studies

^{31}P NMR spectra for the hydrolysis of oxy and thiophosphodichloridate ions are shown in Figure 2.3 and were obtained at pD ~11 in fully aqueous solution as detailed in Section 2.1. Clean conversions of oxy and thiophosphodichloridate ions to inorganic phosphate and thiophosphate were observed at pH ~10 with half lives of two and four minutes, respectively (Figure 2.3 A and B).

The accumulation of oxy and thiophosphomonochloridate ions was not observed by ^{31}P NMR spectroscopy during the hydrolysis of oxy and thiophosphodichloridate in aqueous solution, respectively. This result is in full agreement with research studies by Grunze, and Hudson and Moss, which suggests that the mechanism of hydrolysis of the monochloridate ion is rapid in fully aqueous solution. The absence of the thiophosphomonochloridate species in these studies suggests the mechanism of hydrolysis of thiochloridate ions is similar to that of the more studied oxychloridate ion. These results suggest that the hydrolysis of these species would be too fast to follow using stopped-flow spectrophotometric techniques. In contrast, kinetic studies undertaken by Mitchell identified the build-up of the oxyphosphomonochloridate ion **90** in solutions of PCl_5 containing limited amounts of water.[48] The enhanced stability of **90** in non-aqueous solution was attributed to a change in mechanism as discussed in Section 2.1.2.3.

Although these ^{31}P NMR spectroscopy studies have been successful in estimating observed rate constants for the hydrolysis of oxy and thiophosphodichloridates ions in aqueous solution, the uncatalysed pseudo first-order rate constant, k_0, and potential

second-order hydroxide catalysed rate constant, k_{OH}, could not be accurately determined for hydrolysis across a broad pH range.

Short acquisition times (~1 min) and high concentrations of phosphodichloridate ion (0.16 M) were necessary to ensure that signals could be accurately resolved and integrated. These reaction conditions led to the formation of substantial amounts of hydrochloric acid, resulting in the generation of 0.5 M HCl, upon hydrolysis to inorganic (thio)phosphate. Throughout these kinetic studies, high concentrations of carbonate buffer (0.5 M) were employed in an effort to maintain a constant reaction pH. Under these reaction conditions, hydrolysis was calculated to protonate all of the carbonate buffer present in solution, corresponding to a 2 unit decrease in pH. It was therefore not possible to maintain reaction pH under these experimental conditions.

In addition, k_{obs} was expected to increase significantly at higher pH, where a hydroxide catalysed hydrolysis is expected to dominate. This in turn was expected to lead to faster reaction times, which will likely be too fast to follow by ^{31}P NMR spectroscopy. For reactions that may still be followed, higher concentrations of oxy and thiophosphodichloridate ions would be required to ensure signals could be resolved and integrated. It would therefore be very difficult to accurately determine the second-order rate constant k_{OH} due to large pH changes occurring upon hydrolysis. An alternative technique for monitoring the hydrolysis processes was therefore sought.

2.3.1.2 UV-Vis spectrophotometric studies

Reactions of oxy and thiophosphodichloridate ions **89** and **95** were followed by UV-visible spectrophotometry in aqueous solution at 25 ºC and ionic strength I=1 (KCl), as detailed in Section 2.2.

Khalifah developed an indicator-based UV-visible spectrophotometric method for following acid or base generating reactions that involve no direct change in absorbance. Unfortunately, the method was developed to follow reactions over a very narrow pH range (5.83 to 8.75). We have developed new combinations of buffer and indicator in order to expand this method to follow reactions over a much broader pH range (1.99 to 13.23).

Hydroxide-catalysed observed rate constants were successfully determined in potassium hydroxide solutions between pH 11.88 and 13.23 using the indicator 1,3,5 trinitrobenzene; first order traces with constant end-points were observed. However, it was not possible to study hydrolysis in potassium hydroxide solutions of 1,3,5 trinitrobenzene at higher pH. This was primarily because the Meisenheimer intermediate **104** was observed to degrade at very high pH (pH>~13.5), which led to a small continual decrease in absorbance. This occurred in parallel with any change in absorbance due to the hydrolysis of the thiophosphodichloridate ion. Resulting absorbance plots corresponded to several different processes and so were not first-order. In addition, a constant absorbance value, A_{inf}, was not observed following complete hydrolysis of the thiophosphodichloridate ion. Alternative combinations of buffers and indicators were sought, however none were found that were suitable for following hydrolysis above pH 13.

2.3.1.2.1 Hydrolysis of $KOPOCl_2$

The pH-k_{obs} profile for the hydrolysis of oxyphosphodichloridate **89** in aqueous solution (Figure 2.8) can be broken down into two main sections. Between pH 2 and 12 lies a pH independent plateau, where the observed rate constant, k_{obs}, depends only on the pseudo first-order rate constant, k_0. We have determined the magnitude of k_0 as ~ 5.5×10^{-3} s^{-1} for reaction in fully aqueous solution. This is in close agreement with the pseudo first-order rate constant determined potentiometrically by Hudson and Moss (6.3×10^{-3} s^{-1}; obtained in water at pH 7 and at an ionic strength of I=1.5 (KCl).[37]

Between pH 12 and 13 lies a pH-dependent region, where the observed rate constant for hydrolysis, k_{obs}, increases as the reaction pH is increased, which corresponds to an increase in the magnitude of the hydroxide catalysed hydrolysis term, $k_{OH}[HO^-]$. Given the greater reactivity of hydroxide *vs* water toward $KOPOCl_2$, the hydroxide catalysed term $k_{OH}[HO^-]$ dominates and contributes most to the observed rate constant for hydrolysis at high pH. Given that the magnitude of the k_{obs} rate constant was shown to depend on $[^-OH]$ between pH 12 and 13, it appears from Figure 2.8 that the $k_{OH}[^-OH]$ term will contribute very little to the observed rate constant for typical phosphorylation of amines in aqueous solution of pH ~less than 12.

Although the aim of these studies was to understand the reactivity of the oxyphosphodichloridate ion under reaction conditions used in aminolysis reactions, i.e. reaction at high pH, we also studied hydrolysis at low pH to determine if any acid-catalysed processes operate in acid solution. A change in mechanism is expected upon the protonation of the oxyphosphodichloridate ion, resulting in a change in the observed rate constant for reaction. Given there is no change in k_{obs} between pH 1.99 and 10.63, the pK_a of the oxyphosphodichloridate ion must be less than ~1. Attempts were made to study the hydrolysis of $KOPOCl_2$ at lower pHs (<1.99) using the indicator-based UV-Vis spectrophotometry approach. However, no suitable combination of indicator and buffer, of sufficiently low pK_a (~1) could be found to cover this pH region.

Kinetic studies by Achmatowicz *et al.* measured a decrease in the observed rate constant for the hydrolysis of $KOPOCl_2$ **89** in very acidic organic-aqueous solutions of ~ 1.2 to 3.7 M HCl. A change in the mechanism of hydrolysis was observed upon the protonation of oxyphosphodichloridate ion to form phosphodichloridic acid, resulting in a slower hydrolysis, where hydrolysis of the acid form was significantly slower than the monoanionic form. These studies suggest that a substantial decrease in k_{obs} for hydrolysis of $KOPOCl_2$ may be observed in fully aqueous solution of pH values below pH 1.99. Therefore, the pH-k_{obs} profile may contain three different pH regions; a pH-dependent region at very low pH, a pH-independent plateau between pH 1.99 and 12, and a pH-dependent region in alkaline solutions above pH 12.

2.3.1.2.2 Hydrolysis of $KOPSCl_2$

The pH-k_{obs} profile for the hydrolysis of thiophosphodichloridate **95** in aqueous solution (Figure 2.9) shows a pH independent plateau between pH 1.99 and ~13. The only contributing term to the observed rate constant in this pH region is the uncatalysed hydrolysis term, k_0, which was determined as ~ 4×10^{-3} s^{-1} for reaction in fully aqueous solution. The effect of substituting oxygen with sulfur on the k_0 values for the attack of water as the nucleophile on species 1 and 2 is a 1.6-fold reduction in its magnitude.

An increase in the observed rate constant for hydrolysis was not detected upon an

increase in [KOH] at higher pHs. Thus the magnitude of the second-order rate constant for hydroxide-catalysed hydrolysis, k_{OH}, could not be estimated under the experimental conditions of these investigations.

The results in Figure 2.9 demonstrate that thiophosphodichloridate ions do not show significant reactivity toward hydroxide ions over and above reactivity with water in aqueous solution of [$^{-}$OH] < ~0.2 M. The k_{OH}[$^{-}$OH] term may become significant at pHs much higher than those studied in these reactions, however our studies provide no evidence towards the existence of a k_{OH}[$^{-}$OH] catalysed pH region for the hydrolysis of thiophosphodichloridate ion.

An upper limit on the value of k_{OH} for the hydrolysis of the thiophosphodichloridate ion may be estimated as ~ 1.77×10^{-3} M^{-1} s^{-1} on the basis of the assumption that an upward trend in the pH− k_{obs} profile for **95** must occur at least at 1.5 pH units higher than was observed for **89**.

2.3.1.3 "Thio-effect"

The observed "thio-effect" on the k_0 values for the attack of water as the nucleophile on oxy and thiophosphodichloridate ions **89** and **95** species was determined as a 1.6-fold reduction on substituting oxygen with sulfur. In contrast, the observed "thio-effect" on the k_{OH} values for the attack of hydroxide ions on **89** and **95** was determined as at least $10^{1.5}$ (~31 fold) upon substitution of oxygen for sulfur (Figure 2.10).

Figure 2.10 The observed "thio-effect" on the k_0 and k_{OH} values for the attack of water and hydroxide on oxy and thiophosphodichloridate ions.

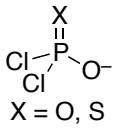

X = O, S

k_0: $k_{O/S}$ = 1.6

k_{HO}: $k_{O/S}$ = ~31

"Thio-effects" of 0.1-0.3 have been observed for the hydrolysis of phosphate monoesters, where dissociative mechanisms dominate. In contrast, the hydrolysis of phosphodiesters, where concerted S_N2(P) mechanisms are expected, generally result in

higher effects of 4-11. Thus, a 1.6-fold "thio-effect" on k_0 values for the hydrolysis of oxy and thiophosphodichloridate ions suggests that nucleophilic attack by water proceeds *via* an $S_N2(P)$-like mechanism, as suggested by Hudson and Moss.[37] However, due to the good leaving group ability of chloride, its cleavage may result in a transition state being more dissociative in nature than for oxy-leaving groups seen in phosphoesters.

Larger "thio-effects" of 10-160 have been observed for the hydrolysis of phosphate triesters, where associative mechanisms are generally encountered due to a lack of charge at the phosphorus centre.[57] A 31-fold "thio-effect" on k_{OH} values for the hydrolysis of oxy and thiophosphodichloridate ions may therefore be due to differing amounts of negative charge stabilization by oxygen and sulfur in the transition state. Thus, the increased nucleophilicity of hydroxide ions over water could result in a move toward a more associative mechanism in the case of phosphodichloridate **89**, with the greater anionic change at the transition state being accommodated by the more electronegative oxygen substituent (and chlorine atoms). With thiophosphodichloridate **95**, on the other hand, the less electronegative sulfur substituent, is less able to accommodate this build up of negative charge and a lower k_{OH} is therefore observed.

2.3.2 Hydrolysis of phosphorus oxychloride and thiophosphoryl chloride

Attempts were made towards the determination of rate constants for the hydrolysis of phosphorus oxychloride and thiophosphoryl chloride in aqueous solution by stopped-flow UV-Vis spectrophotometry. However, these studies were unsuccessful.

The hydrolysis of phosphorus oxychloride was initially studied in aqueous potassium phosphate and carbonate buffers, which were made up in 65% acetonitrile and 35% water at I=1 (KCl). First-order traces were observed for each reaction with constant end-points and observed rate constants were determined as 14.4 s^{-1} at pH 7.5 and 10.6.

The determined observed rate constant (k_{obs} = 14.4 s^{-1}) for hydrolysis at pH 7.5 in aqueous acetonitrile solution (35 % H_2O, 65% MeCN) differed in magnitude from the k_{obs} value reported by Hudson and Moss for hydrolysis in aqueous dioxane solution (35

% H_2O, 65% dioxane) at pH 7.5 (k_{obs} = 62.4 s^{-1} at 25 °C). The poor agreement between these k_{obs} values may simply be due to experimental differences in reaction conditions such as reaction temperature (uncontrolled *vs* 25 °C) and co-solvent used (acetonitrile *vs* dioxane).

The lack of change in the observed rate constant as a function of pH (between 7.5 to 10.6) may indicate that k_{obs} for hydrolysis simply depends on the uncatalysed hydrolysis term k_0 within this pH region. Alternatively, identical observed rate constants may be observed at pHs 7.5 and 10.6 as a result of a phase-mixing process. If a rate-limiting mixing process was in operation, k_{obs} would relate only to the transfer of $POCl_3$ into aqueous solution and thus provide no kinetic information regarding the rate of hydrolysis of $POCl_3$.

To determine whether the calculated k_{obs} values were due to the hydrolysis of $POCl_3$ or the result of a mass-transfer mixing process, the reaction of $POCl_3$ was followed in aqueous acetonitrile solutions of varying water content (35-80%). If the determined k_{obs} values correspond only to the hydrolysis of $POCl_3$, it would be expected that an increase in water content of the reaction solution would lead to an increase in k_{obs}.[45] However, the observed rate constant values remained effectively constant upon an increase in water content (35-80% water).

The absence of any change in the observed rate constant upon an increase in pH or water content and poor agreement with available literature data suggests that the kinetics followed may not correspond to the process of hydrolysis and aminolysis of phosphorus oxychloride. Observed rate constants determined upon the addition of $POCl_3$ to aqueous reaction solutions may in fact depend on the rate of mass transfer of $POCl_3$ into aqueous solution, rather than the rate of $POCl_3$ hydrolysis.

2.3.2.1 Thiophosphoryl chloride

There are no available literature studies pertaining to the solubility of thiophosphoryl chloride in aqueous solution. The hydrolysis of thiophosphoryl chloride was studied in aqueous acetonitrile solutions of 35 – 80% acetonitrile composition. First-order traces

were not observed for reaction in any of the solvent mixtures studied. Instead, small absorbance changes were observed over a period of several minutes.

2.4 Summary

As part of an ongoing program to develop aqueous aminophosphorylation procedures, pH-k_{obs} profiles have been determined for the hydrolyses of phosphodichloridate and thiophosphodichloridate ions in aqueous solutions by UV-Vis spectrophotometry.

For the hydrolysis of oxyphosphodichloridate ion **89**, a plateau in reactivity was observed up to pH ~ 12 with $k_0 = 5.7 \times 10^{-3}$ s^{-1}. At higher pH values, the observed rates of hydrolysis increased with hydroxide ion concentration, giving a second-order rate constant $k_{OH} = 5.6 \times 10^{-2}$ M^{-1} s^{-1}.

The hydrolysis of thiophosphodichloridate ion **95** in aqueous solution showed essentially constant reactivity across the pH range from **~** 2 to 13, with $k_0 = 3.6 \times 10^{-3}$ s^{-1}. This demonstrates that thiophosphodichloridate ions **95** do not show significant reactivity toward hydroxide ions over and above reactivity with water, in aqueous solution where [OH−] < **~** 0.2 M.

The observed "thio-effect" on the k_0 values for the attack of water as the nucleophile on oxy and thiophosphodichloridate ions **89** and **95** species was determined as a 1.6-fold reduction on substituting oxygen with sulfur. This suggests that nucleophilic attack by water on **89** and **95** proceeds *via* an $S_N2(P)$-like mechanism, as suggested by Hudson and Moss.[37] In contrast, a larger "thio-effect" (~31 fold) was determined for the k_{OH} values for the attack of hydroxide ions on **89** and **95** upon substitution of oxygen for sulfur. This may be attributed to differing amounts of negative charge stabilization by oxygen and sulfur in the transition state for hydroxide-catalysed hydrolysis, where sulfur is less able to accommodate a build up of negative charge compared to the more electronegative oxygen substituent.

This kinetic data demonstrates that both oxy and thiophosphodichloridate ions are potentially useful phosphorylating agents across a broad range of pHs in aqueous solutions. In respect of the use of amine nucleophiles, we expect to see good selectivity towards aminolysis over hydrolysis processes in aqueous reaction mixtures, given the intrinsic nucleophilicity of *N*-nucleophiles. Kinetic studies of the aminolyses of (thio)phosphodichloridate ions are presented in Chapter 3.

Chapter 3

Kinetic studies of the aminolyses of phosphorus (V) chlorides

3.0 Foreword

This chapter describes investigations of the aminolyses of oxy and thiophosphodichloridate ions in aqueous solution. In Section 3.1 a brief review of relevant literature pertaining to aminolysis studies is presented. Section 3.2 describes the results obtained from kinetic studies of aminolyses. This includes the measurement of pK_as of the conjugate acid forms of relevant amines (Section 3.2.1), determination of second-order rate constants for aminolyses by UV-Vis spectrophotometry (Section 3.2.2), and product analysis studies of aminolysis reactions (Section 3.2.3). These results are discussed in Section 3.3.

3.1 Introduction

The study of the hydrolyses of oxy and thiophosphodichloridate ions **89** and **95** (Chapter 2) has shown that the (thio)phosphorylation of amines in aqueous solution to give phosphoramidates **105** and thiophosphoramidates **106** should be possible at high pHs (up to ~13 for $KOPOCl_2$), where competing reactions between the phosphodichloridate ions and hydroxide ion are minimised (Scheme 3.1).

Scheme 3.1

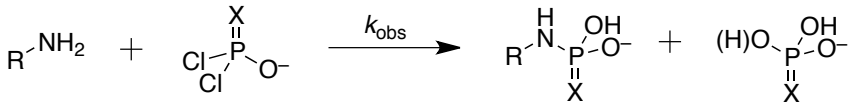

89 X = O
95 X = S

105 X = O
106 X = S

Under these conditions, oxy and thiophosphodichloridate ions may react with even the most basic alkyl amines (pK_{aH} ~ 10), present in their nucleophilic forms, without reacting with hydroxide ions to give inorganic (thio)phosphate.

The following kinetic study of the aminolyses of oxy and thiophosphodichloridate ions in aqueous solution will result in the determination of second order rate constants, k_N, for the reactions of oxy and thiophosphodichloridate ions with a large array of different amine nucleophiles. As part of these kinetic studies, reaction data (k_N) may be correlated with amine pK_a values using Brønsted plots. The Brønsted equation is a linear-free energy relationship that has typically been used to correlate rate constants for reactions catalysed by a series of general acids or bases with their conjugate acid pK_a values. However, the Brønsted equation for proton transfer reactions may be extended to correlate nucleophilicity with base strength, as described by Equation 3.1.

$$\delta(\log k_N) = \beta_{nuc}\,\delta(pK_a) \qquad \textbf{Equation 3.1}$$

In Equation 3.1, k_N corresponds to the rate constant for the reaction under study, K_a is the acidity constant of the conjugate acid of the nucleophile used. β_{nuc} is the sensitivity factor of the reaction and is determined from the gradient of the logarithmic plot of rate constants k_N against the pK_a values of the conjugate acid of the nucleophile used. When the magnitude of β_{nuc} is equal to 1, any change in amine basicity is fully

reflected in the corresponding change in its nucleophilicity. However, when the magnitude of β_{nuc} is less than 1, changes in the basicity of the amine under study are not fully observed in corresponding changes in its nucleophilicity.

As an example, Bunting *et al.* applied the Brønsted equation (Equation 3.1) to the nucleophilic attack of amines at the vinylic carbon centre of 1-methyl-4-vinylpyridinium cation **107** in aqueous solution (Figure 3.1).[58]

Figure 3.1

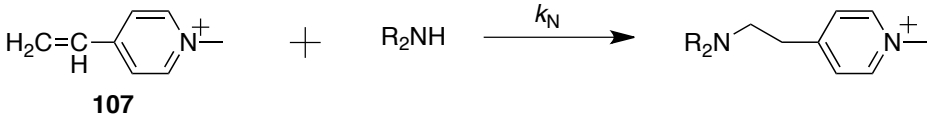

107

Second order rate constants, k_N, were determined for the reactions of 1-methyl-4-vinylpyridinium cation **107** with an extensive range of primary and secondary amines. Logarithmic plots of rate constants k_N against the pK_a values of the conjugate acids of amines used were constructed and β_{nuc} parameters were calculated from the gradient of each slope. β_{nuc} parameters for each class of amine are presented in Table 3.1.

Table 3. 1 **β_{nuc} parameters for Brønsted-type correlations for addition of primary and secondary amines to 1-methyl-4-vinylpyridinium cation 107 in aqueous solution.[58]**

Amine type	β_{nuc}
$RCH_2CH_2NH_2$	0.40
$(RCH_2)_2CHNH_2$	0.45
$(RCH_2)_3CNH_2$	0.38
$RCH_2CH_2NHCH_3$	0.34
$(RCH_2CH_2)_2NH$	0.23
$R(CH_2CH_2)_2NH$	0.29

As shown in Table 3.1, Brønsted correlations of log(k_N) *vs* pK_a led to the determination of β_{nuc} parameters for three structural classes of primary amine as 0.38-0.45 and for three structural classes of secondary amine as 0.23-0.34.

The construction of Brønsted plots for the aminolyses of oxy and thiophosphodichloridate ions in aqueous solution for several different amine classes will provide an opportunity to understand and predict rate constants, k_N, for the reaction of any given amine with oxy and thiophosphodichloridate ions in aqueous solution. Application of predicted k_N rate constants to Equation 3.2 will allow for the calculation and optimisation of selectivities toward aminolysis over hydrolysis processes for (thio)phosphorylation of amines using $KOPOCl_2$ and $KOPSCl_2$.

$$\% \text{ conversion} = \frac{k_N[\text{amine}]}{(k_N[\text{amine}] + (k_0 + k_{HO}[HO^-]))} \qquad \textbf{Equation 3.2}$$

Equation 3.2 may be simplified to Equation 3.3 if (thio)phosphorylation reactions are undertaken at pHs where the hydroxide-catalysed hydrolysis term becomes negligible.

$$\% \text{ conversion} = \frac{k_N[\text{amine}]}{k_N[\text{amine}] + k_0} \qquad \textbf{Equation 3.3}$$

Several assumptions have been made in Equation 3.3 and these are discussed in Section 3.3. However, the application of experimentally-determined hydrolysis data and aminolysis data predicted from Brønsted plots to Equation 3.3 should allow for the determination of expected coversion levels of oxy and thiophosphodichloridate ions to oxy and thiophosphoramidates for a given amine in aqueous solution.

3.2 Results

3.2.1 Determination of aqueous pK_a values of amines

As part of constructing Brønsted plots from reaction data for aminolyses of oxy and thiophosphodichloridate ions **89** and **95**, accurate pK_a values of conjugate acids of each amine were determined under conditions of 25 °C and I=1 (KCl) in fully aqueous solution (Scheme 3.2). The conjugate acid pK_a values of the amines studied are available in the literature, however, differ slightly (~0.3 pK_a values unit difference) from those measured under conditions of 25 °C and I=1 (KCl).

Scheme 3.2

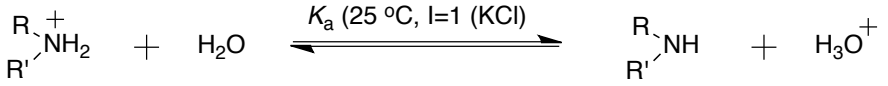

Conjugate acid pK_a values of amines to be used in aminolysis studies were determined by a pH-titration method. Potassium hydroxide solution (0.1 M, I=1 (KCl)) was added to an aqueous solution of the amine in its conjugate acid form ([amine]$_{initial}$ = 0.1 M, I=1 (KCl)), and the pH at 25 °C was recorded after each addition. As an example, the pH-titration for aniline in aqueous solution is presented in Figure 3.1A. First derivatives, d(volume) and d(pH), were then calculated from the pH-titration and dV/dpH was plotted against pH (Figure 3.1B).

Figure 3.2 **A) pH-titration of potassium hydroxide solution (0.1 M) to an aqueous solution of aniline (20 mL × 0.1 M) at 25 °C and *I*=1 (KCl). B) Plot of pH against *d*volume/*d*pH.**

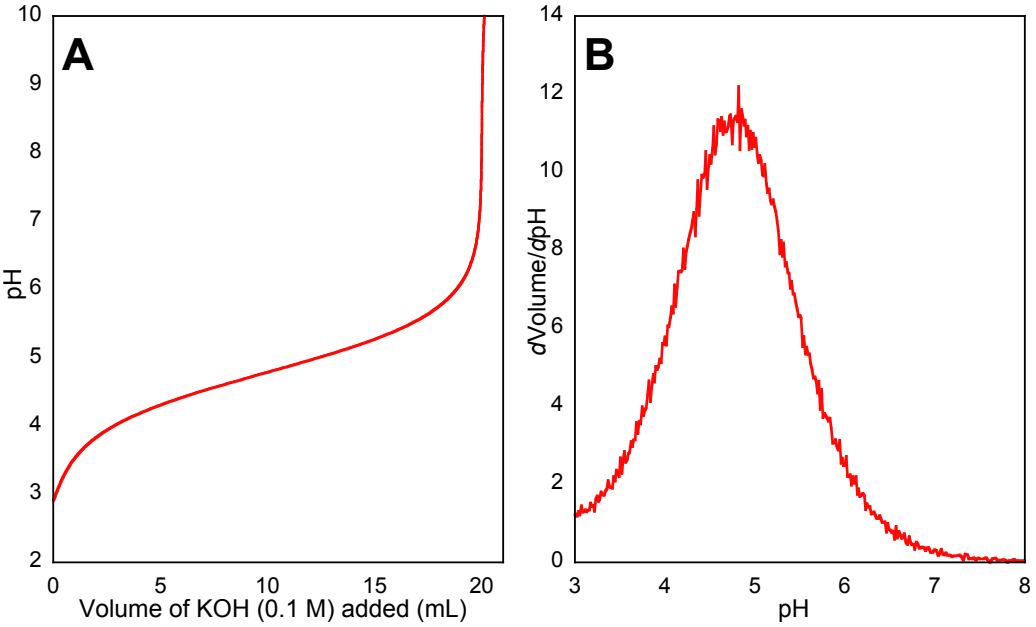

The conjugate acid pK_a value of aniline is equal to the pH at the point of the maximum of the curve in Figure 3.2 B. For aniline, the maximum lies at a pH of 4.73 and so the conjugate acid pK_a value of aniline was determined as 4.73 in water at 25 °C and *I*=1 (KCl).

The pK_a values for the conjugate acids of all other amines studied are presented in Table 3.2.

Table 3.2 pK_a values of conjugate acids of amines in water at 25 °C with ionic strength maintained at 1.0 with potassium chloride.

Amine	pK_a
Aniline	4.73
4-Fluoroaniline	4.83
3-Aminoaniline	5.05
4-Ethoxyaniline	5.54
4-Aminophenol	5.74
2,2,2 Trifluoroethylamine	5.60
Glycine methylester	7.90
2-Methoxyethylamine	9.56
Glycine	9.80
γ-Aminobutyric acid	10.56
1-Methyl piperazine	5.22
Piperazine.HCl	5.98
1-Acetyl piperazine	8.28
Morpholine	8.76
Piperazine	10.14
Methoxylamine	4.71
Hydroxylamine	6.10

With amine pK_a values in hand, Brønsted plots could be constructed for the aminolyses of oxy and thiophosphodichloridate ions in aqueous solution under conditions of 25 °C and I=1 (KCl). This is discussed in greater detail in Section 3.2.2.

3.2.2 Aminolyses of $KOPOCl_2$ and $KOPSCl_2$

Second-order rate constants for the aminolyses of $KOPOCl_2$ and $KOPSCl_2$ (k_N, $M^{-1}s^{-1}$) were determined using an adapted indicator-based UV-Vis spectrometric method developed to follow the hydrolyses of these phosphorylating agents (Section 2.2).

Four different classes of amines (anilines, primary and secondary alkyl amines and hypernucleophilic amines) were chosen for study. Within each class, amines of varying pK_a were studied, allowing for the construction of Brønsted plots. These plots could then potentially be used to predict the reactivities of amines of varying conjugate acid pK_a.

The observed experimental pseudo-first-order rate constant for parallel aminolysis and hydrolysis (k_{obs}) brings together contributions of all potential reactions in aqueous solution, including contributions by solvent (k_{H2O}), hydroxide ($k_{HO}[HO^-]$), and amine (k_N[amine]) (Equation 3.4).

$$k_{obs} = k_0 + k_{OH}[HO^-] + k_N[\text{amine}] + k'_N[\text{amine}]^x \qquad \textbf{Equation 3.4}$$

The pH-rate profile for the hydrolysis of $KOPOCl_2$ (Figure 2.8, Section 2.2.1.3) indicates that the $k_{OH}[^-OH]$ term only becomes significant above pH 12. The pH-rate profile for the hydrolysis of $KOPSCl_2$ (Figure 2.9, Section 2.2.1.3) shows no contribution from the $k_{OH}[^-OH]$ term to the observed rate constant up to pH 13.

Reactions of $KOPOCl_2$ and $KOPSCl_2$ with amines were performed in aqueous solutions at pHs less than 12. Under these reaction conditions, the $k_{OH}[^-OH]$ term for hydrolysis will be negligible and so the observed rate constant for parallel hydrolysis and aminolysis of $KOPOCl_2$ and $KOPSCl_2$ may be simplified to Equation 3.5.

$$k_{obs} = k_0 + k_N[\text{amine}] + k'_N[\text{amine}]^x \qquad \textbf{Equation 3.5}$$

In all cases, plots of k_{obs} values versus amine concentration were linear thus indicating no higher order dependencies on amine concentration. These linear plots show that general base catalysis of hydrolysis and aminolysis processes is not in operation. Therefore, Equation 3.5 may be simplified to Equation 3.6.

$$k_{obs} = k_0 + k_N[\text{amine}] \qquad \textbf{Equation 3.6}$$

We initially planned to follow the parallel hydrolysis and aminolysis reactions of oxy and thiophosphodichloridate ions in aqueous carbonate buffers of pH ~10.5, as under these conditions the majority of amines under study would be in their nucleophilic form. We aimed to follow the change in absorbance due to the indicator 2,5 dimethyl phenolate (λ = 291 nm) upon the addition of phosphodichloridate ions to an aqueous amine solution containing carbonate buffer. Unfortunately, for two reasons, it was not possible to follow parallel hydrolysis and aminolysis reactions of oxy and thiophosphodichloridate ions by this method.

Firstly, the absorbance of aromatic amines such as aniline lies at ~290 nm and therefore overlaps with the absorbance due to the indicator 2,5-dimethylphenolate. Thus, it was not possible to follow any change in absorbance due to 2,5-dimethylphenolate upon addition of (thio)phosphorylating agent to aqueous solution containing aromatic amines. Secondly, a small decrease in the absorbance due to 2,5-dimethylphenolate was observed in aqueous solutions containing amine and carbonate buffer. In contrast, a steady absorbance due to 2,5-dimethyl phenolate was observed in aqueous solutions containing only carbonate buffer. These observations suggested that a potential reaction between amine and buffer resulted in an unwanted decrease in absorbance due to 2,5-dimethylphenolate. For these reasons, it was not possible to follow parallel hydrolysis and aminolysis reactions of (thio)phosphodichloridate ions in aqueous carbonate buffers by UV-Vis spectrophotometry.

However, it was possible to follow the reaction progress of aminolysis of $KOPOCl_2$ **89** and $KOPSCl_2$ **95** in aqueous phosphate buffers (KH_2PO_4/ K_2HPO_4) by monitoring the decrease in absorbance of 4-nitrophenolate (λ = 416 nm) during the course of the reaction. Amines that have conjugate acid pK_as less than 6.2 (at least one pK_a unit lower than that of K_2HPO_4) could be added to the buffer solution in essentially their free forms with no change in the buffer ratio. These amines could therefore be studied by this method. Each amine solution was buffered using mono and dibasic potassium phosphate and the absorbance due to 4-nitrophenolate was followed during the reaction. The absorbance of the 4-nitrophenolate anion was at 416 nm and so overlap with the absorbances due to aromatic amines (anilines) around 300 nm were no longer an issue. Thus a decrease in the indicator absorbance could be followed throughout

each reaction. Prior to addition of $KOPOCl_2$/ $KOPSCl_2$, a steady absorbance due to 4-nitrophenolate was observed in the presence of both amine and phosphate buffer. Observed rate constants for the parallel hydrolysis and aminolysis of $KOPOCl_2$ / $KOPSCl_2$ at several different amine concentrations were successfully determined using this phosphate buffer method for amines of conjugate acid pK_a less than 6.2.

The phosphate buffer method described above could not be used for studying aminolysis with amines of conjugate acid pK_a greater than 6.2 because significant amounts of protonation of the amine are likely to occur. As an alternative, each amine was used as both the nucleophile and to buffer the system with its conjugate acid, where the amine was present in its 90% FB form. The overall concentration of amine was generally varied from 10 to 200 mM in order to allow k_N values to be determined from k_{obs} *vs* [amine] plots. Indicating phenolates were matched with amines of similar conjugate acid pK_a, in a manner similar to that employed in the hydrolysis of oxy and thiophosphodichloridate ions (Section 2.2.1.3). Measurement of the observed rate constants for the reactions of oxy and thiophosphodichloridate ions in several different aqueous amine solutions of varying concentrations allowed for the determination of k_N ($M^{-1}s^{-1}$) values from the gradients of plots of k_{obs} (s^{-1}) values against the concentration of each amine (M). All first-order plots for the aminolyses of $KOPOCl_2$ and $KOPSCl_2$ are available on the supplementary information dvd. k_{obs} (s^{-1}) values for all first-order plots are presented in Appendix B; Tables A1-8.

3.2.2.1 Kinetic data

First order rate constants for aminolyses of oxy and thiophosphodichloridate ions, k_{obs} (s^{-1}), were determined in aqueous solution (Scheme 3.3).

Scheme 3.3 Aminolysis reactions of oxy or thiophosphodichloridate ion in aqueous solution at *I*=1 (KCl) and 25 °C.

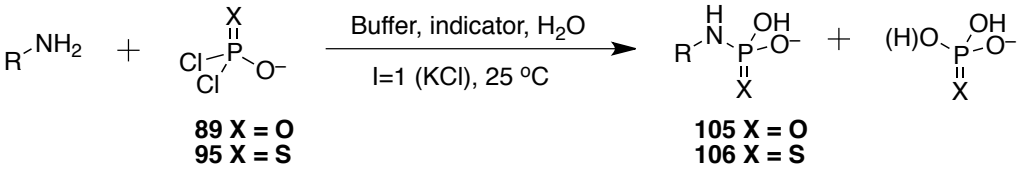

The gradients of plots of k_{obs} (s^{-1}) values against the concentration of each amine (M) allowed for the determination of second order rate constants for aminolyses, k_N ($M^{-1}s^{-1}$) (Figures 3.3 and 3.4).

Figure 3.3 Plots of pseudo first order rate constants k_{obs} (s^{-1}) against [amine] (M) for parallel hydrolysis and aminolysis of $KOPOCl_2$ in aqueous solution of the following amine classes of varying concentration: A) substituted anilines, B) primary alkyl amines, C) secondary alkyl amines and D) hypernucleophilic amines. All reactions were undertaken at 25 °C and *I*=1 (KCl).

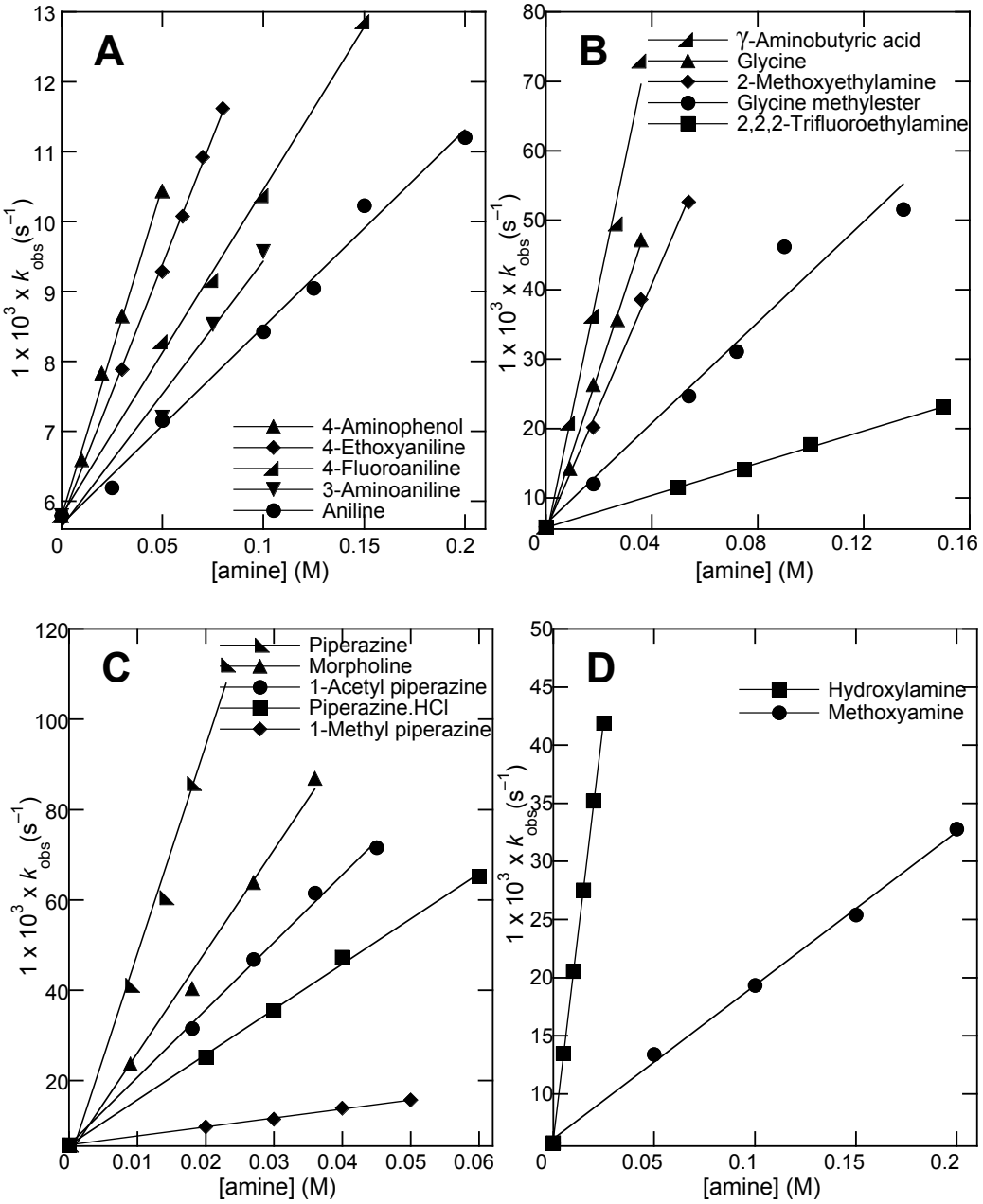

Figure 3.4 **Plots of pseudo first order rate constants k_{obs} (s^{-1}) against [amine] (M) for parallel hydrolysis and aminolysis of $KOPSCl_2$ in aqueous solution of the following amine classes of varying concentration: A) substituted anilines, B) primary alkyl amines, C) secondary alkyl amines and D) hypernucleophilic amines. All reactions were undertaken at 25 °C and *I*=1 (KCl).**

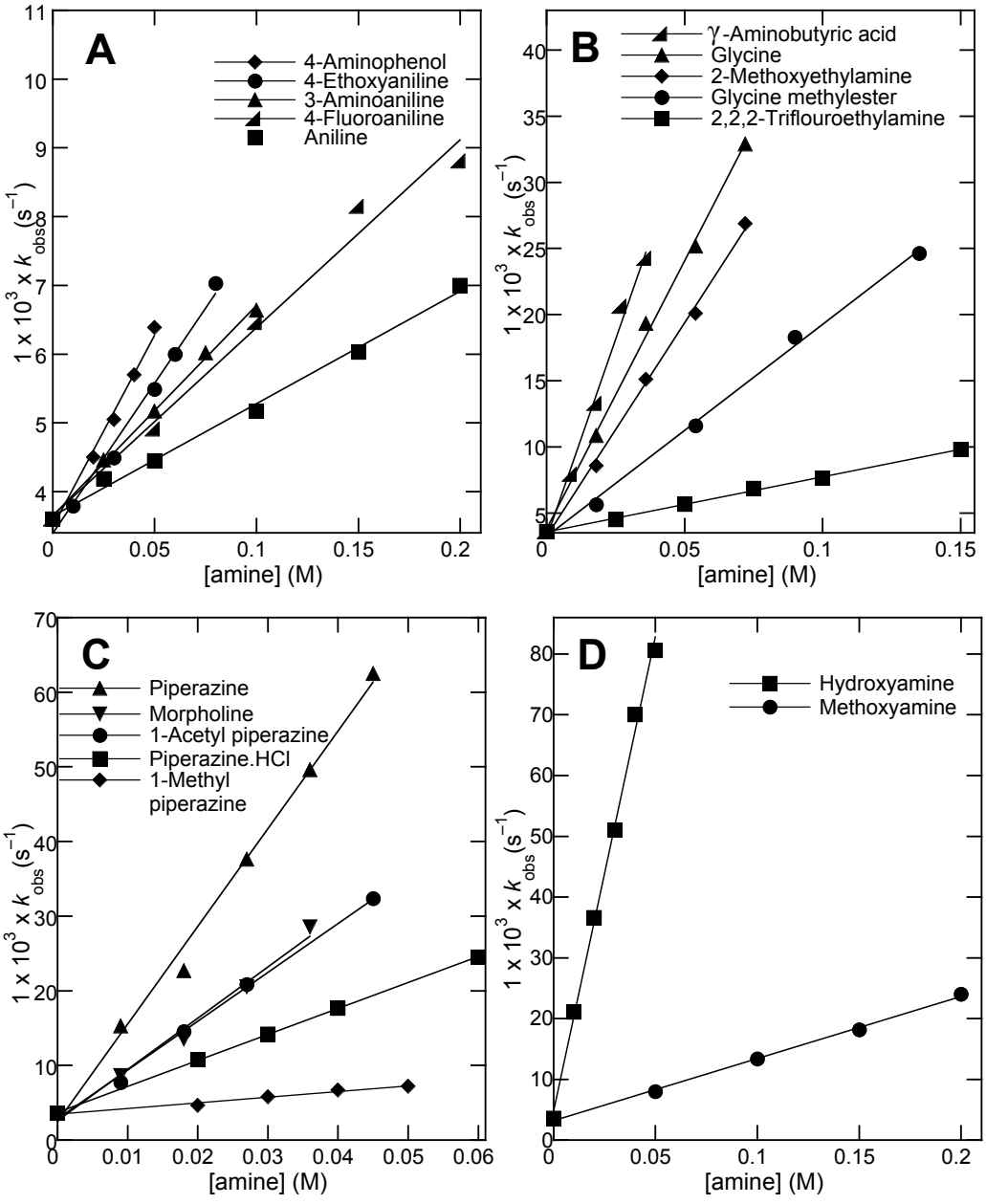

k_N values were determined from the gradients of plots of k_{obs} against [amine] in Figures 3.3 and 3.4 and are summarised in Table 3.3.

Table 3.3 Second order rate constants, k_N ($M^{-1}s^{-1}$), determined from the aminolyses of oxy and thiophosphodichloridate ions in aqueous solution at 25 °C and *I*=1 (KCl).

Amine	pK_a	k_N ($M^{-1}s^{-1}$) ($KOPOCl_2$)	k_N ($M^{-1}s^{-1}$) ($KOPSCl_2$)
Aniline	4.73	0.027	0.016
3-Aminoaniline	4.83	0.039	0.030
4-Fluoroaniline	5.05	0.047	0.027
4-Ethoxyaniline	5.54	0.073	0.044
4-Aminophenol	5.74	0.095	0.055
2,2,2-Trifluoroethylamine	5.60	0.116	0.042
Glycine methyl ester	7.90	0.362	0.156
2-Methoxyethylamine	9.56	0.883	0.327
Glycine	9.80	1.157	0.400
γ -Aminobutyric acid	10.56	1.810	0.680
1-Methyl piperazine	5.22	0.199	0.076
Piperazine.HCl	5.98	1.002	0.348
1-Acetyl piperazine	8.28	1.496	0.654
Morpholine	8.76	2.249	0.686
Piperazine	10.14	4.634	1.310
Methoxylamine	4.71	0.130	0.102
Hydroxylamine	6.10	1.432	1.572

3.2.2.2 Brønsted plots for the aminolyses of oxy and thiophosphodichloridate ions

The pK_a range for each class of amines was as follows: anilines (4.73 to 6.38), primary alkyl amines (5.60 to 10.56), secondary alkyl amines (5.22 to 10.22) and hypernucleophilic amines (4.71 to 6.10). Due to the reactive nature of the hypernucleophilic amines, it was only possible to construct a Brønsted plot over a relatively small conjugate acid pK_a range which was fitted to only two data points.

The log of second order rate constants for aminolyses of oxy and thiophosphodichloridate ions, k_N (Table 3.2), were plotted against the pK_a of the conjugate acid of each amine studied. The resulting Brønsted plots are shown in Figure 3.5.

Figure 3.5 **Plot of log k_N values against the pK_a of the conjugate acid of corresponding amine for the aminolyses of A) $KOPOCl_2$ and B) $KOPSCl_2$ in aqueous solution of anilines (▲), primary alkyl amines (●), secondary alkyl amines (■), and hypernucleophilic amines (◢), determined at 25 ºC and I=0.1 (KCl).**

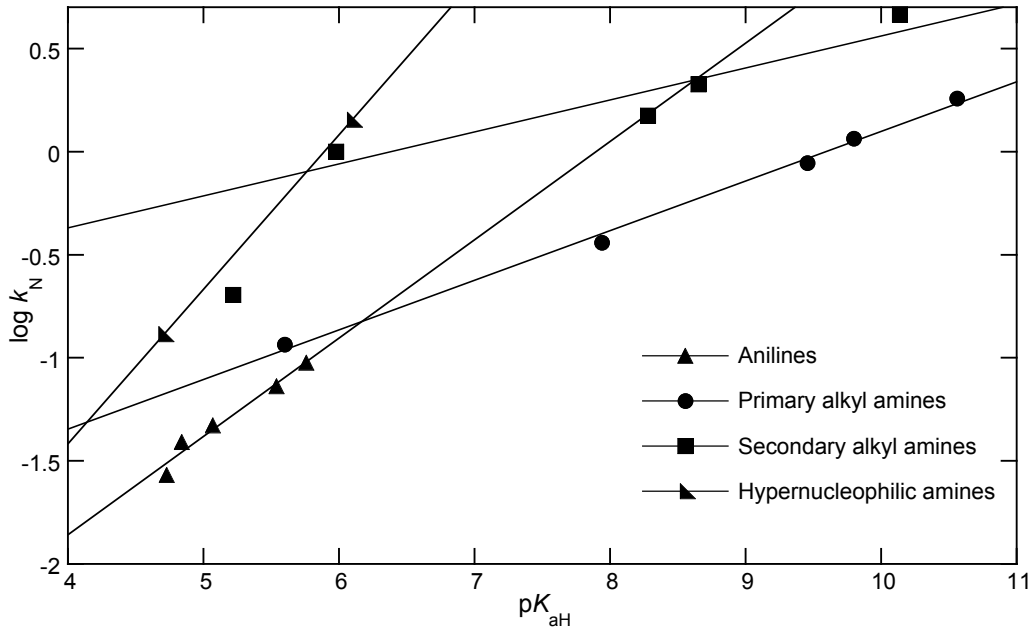

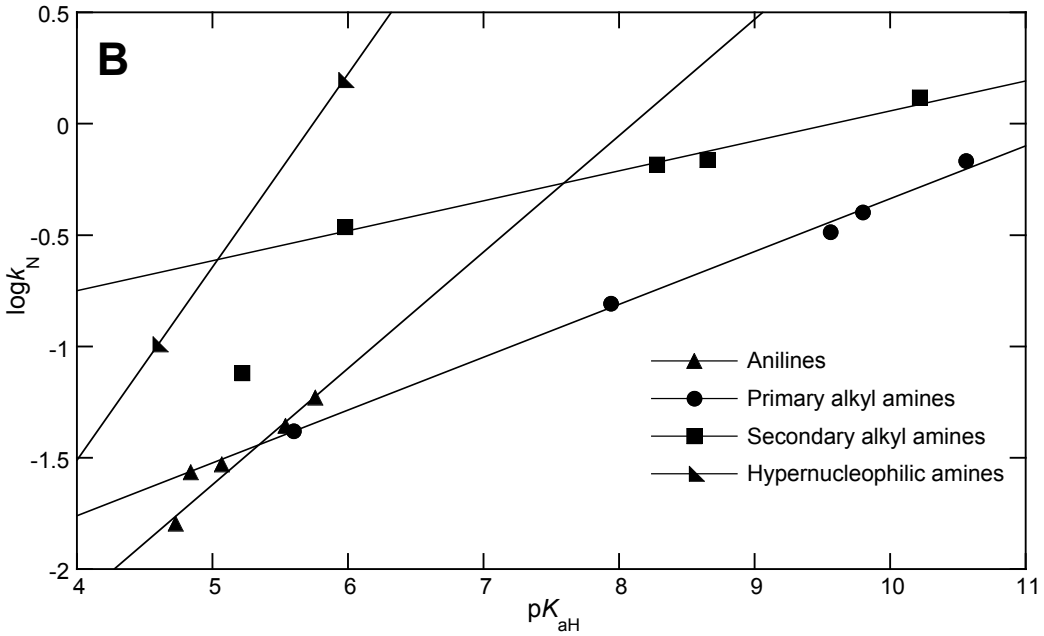

The gradients of plots of log k_N values against the pK_a of each amine conjugate acid allowed for the determination of β_{nuc} values for aminolyses; these are presented in Table 3.4.

Table 3.4

Amine class	β_{nuc} (X=O)	β_{nuc} (X=S)
Substituted anilines	0.48	0.52
Primary alkyl amines	0.24	0.24
Secondary alkyl amine	0.16	0.15
Hypernucleophilic amines	0.75	0.87

3.2.2.3 Hammett plots for the aminolyses of oxy and thiophosphodichloridate ions

From the kinetic data presented in Table 3.2, it was possible to construct Hammett plots of the log of second order rate constants, k_N, for reactions of substituted anilines with $KOPOCl_2$ (A) and $KOPSCl_2$ (B) against σ. These plots are presented in Figure 3.6.

Figure 3.6 Hammett plots of the log of second order rate constants, k_N, for reaction of substituted anilines with A) $KOPOCl_2$ and B) $KOPSCl_2$ against σ.[a]

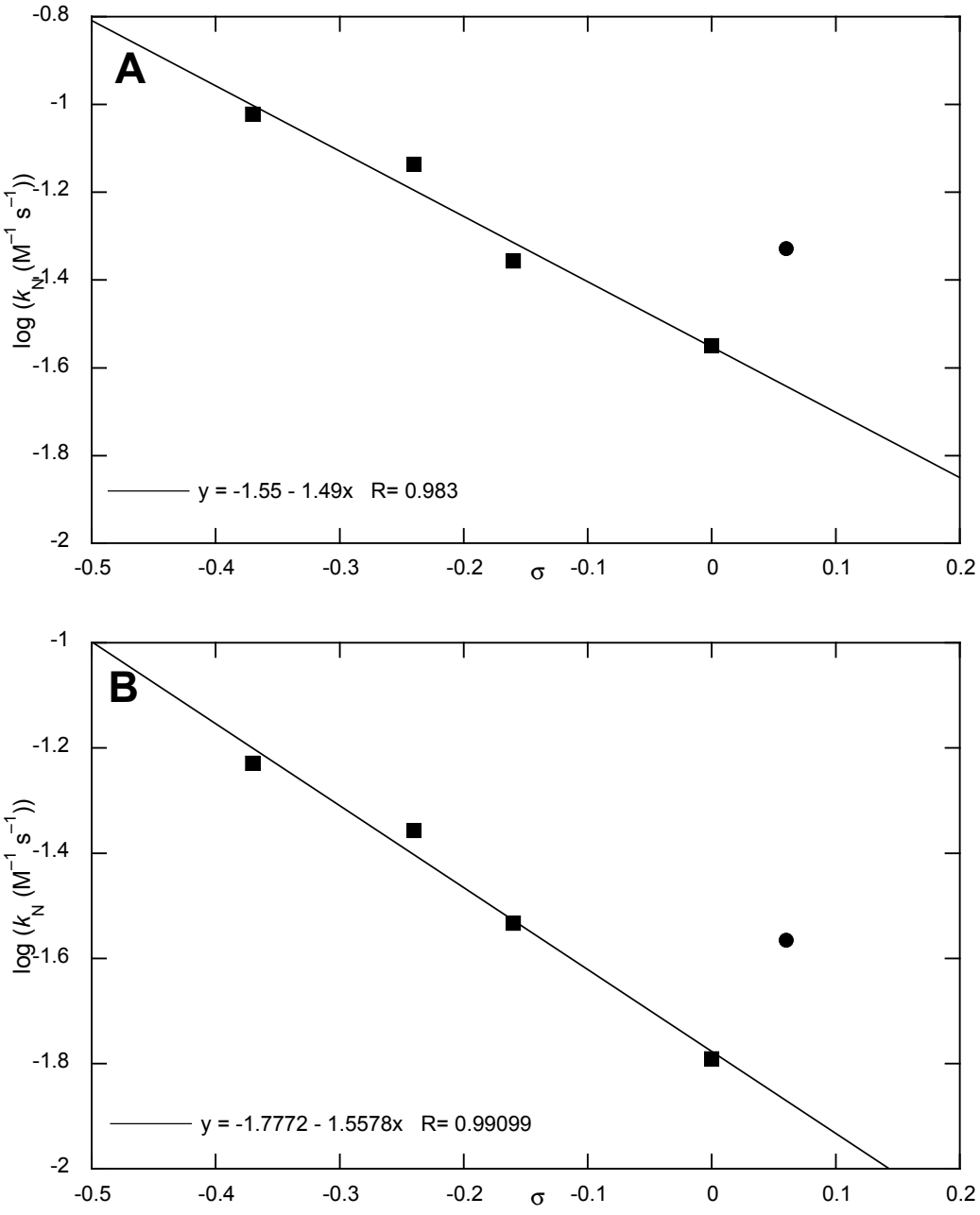

(a) 4-Fluoroaniline data point (●) was omitted from the fitting of substituted aniline data (■) in each Hammett plot.

ρ values were determined from the gradients of plots of log (k_N) against σ in Figure 3.6 and these are presented in Table 3.5.

Table 3.5

ρ (X=O)	ρ (X=S)
–1.45	–1.45

3.2.4 Product analysis studies for aminolyses of oxy and thiophospho-dichloridate ions in aqueous solution

For each amine employed in the UV-Vis studies of aminolyses of oxy and thiophosphodichloridate ions, product analysis studies by ^{31}P NMR spectroscopy were undertaken to determine whether experimental ratios of (thio)phosphoramidate to inorganic (thio)phosphate were similar to those ratios predicted from the application of kinetically determined k_N rate constants (Table 3.3) to Equation 3.3, under conditions where hydrolysis is due only to water.

Due to the low concentration of phosphorylating agent used in the UV-Vis spectrophotometry studies, it was not possible to directly quantify phosphoramidate to inorganic phosphate product ratios by ^{31}P NMR analysis of the UV-Vis product samples. Pseudo first-order (thio)phosphorylation of each amine was therefore undertaken in aqueous solutions of fixed pHs, through the use of strong buffers or by the control of pH using a pH stat instrument.

For amines of conjugate acid pK_a less than ~9.7, reactions were undertaken in aqueous amine solutions of pH ~10.7, which were maintained by a 0.5 M x 90% FB carbonate buffer. This ensured that each amine was present in its nucleophilic form throughout aminolysis. These reactions were undertaken immediately following the preparation of each aqueous amine solution, where any potential reaction between amine and buffer was minimised. For amines of higher conjugate acid pK_a, reactions were undertaken in aqueous solutions where the reaction pH was maintained by a pH stat instrument to ensure that each amine was present in its nucleophilic form throughout aminolysis. Each reaction sample was thermostated at 25 °C for 30 min and then either immediately analysed or stored at –18 °C for analysis at a later time.

3.2.4.1 Product analysis studies for aminolyses of oxyphosphodichloridate ion in aqueous solution

Relative amounts of phosphoramidate, inorganic phosphate and any additional signals (if observed) of each reaction sample were quantified and the results are shown in Table 3.6. The product ratios predicted from the manipulation of kinetically determined k_N rate constants (Table 3.3) using Equation 3.3 are also shown for comparison.

Table 3.6 Product analysis studies for aminolysis of $KOPOCl_2$ in aqueous solution

Amine	[Amine] (M)	Predicted % of phosphoramidate[a]	Observed Signals[b]		
			Phosphoramidate/ % (ppm, multiplicity)	Inorganic phosphate/ %	Other/% (ppm, multiplicity)
Aniline	0.200	50	48 (1.43, s)	53	-
3-Aminoaniline	0.130	50	48 (1.28, s)	52	-
4-Fluoroaniline	0.128	50	54 (1.59, s)	47	-
4-Ethoxyaniline	0.080	50	48 (2.13, s)	52	-
4-Aminophenol	0.050	45	43 (2.28, s)	57	-
2,2,2-Trifluoroethylamine	0.150	74	76 (8.54, t)	24	-
Glycine methylester	0.250	94	85 (9.00, t)	12	4 (9.24, n.d.)
2-Methoxyethylamine	0.090	93	100 (9.97, t)	-	-
Glycine	0.005	50	44 (8.8-9.0, m)	56	-
γ-Aminobutyric acid	0.040	92	87 (7.55, t)	11	2 (7.53, n.d.)
1-Methyl piperazine	0.060	45	97 (9.68-9.72, m)	3	-
1-Acetyl piperazine	0.050	93	93 (9.27-9.30, m)	7	-
Morpholine	0.050	95	94 (9.46, qn)	2	4 (0.5, n.d.)
Piperazine	0.0058	50.0	43 (9.52, s)	41	6 (10.0, t), 11 (9.2-9.4, m)
Methoxylamine	0.020	82	88 (7.80, s)	12	-
Hydroxylamine	0.040	91	29 (8.67, s)	18	4.3 (17.11, s), 16 (14.38, s), 19 (9.05, s), 14 (8.95, s).

(a) Calculated by application of determined k_N rate constants (Table 3.3) to Equation 3.3, under conditions where hydrolysis is due only to k_0. (b) Determined by ^{31}P NMR spectroscopy.

3.2.4.2 Product analysis studies for aminolysis of thiophosphodichloridate ion in aqueous solution

Relative amounts of thiophosphoramidate, inorganic thiophosphate and any additional signals (if observed) of each reaction sample were quantified and the results are shown in Table 3.7. The product ratios predicted from the manipulation of kinetically determined k_N rate constants (Table 3.3) using Equation 3.3 are also shown for comparison.

Table 3.7 Product analysis studies for aminolysis of $KOPSCl_2$ 95 in aqueous solution

Amine	[Amine] (M)	Predicted % of thiophosphoramidate[a]	Observed Signals[b]		
			Thiophosphoramidate/% (ppm, multiplicity)	Inorganic thiophosphate/%	Other/% (ppm, multiplicity)
Aniline	0.200	47	53 (34.9, s)	45	2 (15.6, s)
3-Aminoaniline	0.130	52	62 (33.5, s)	38	-
4-Fluoroaniline	0.128	50	57 (37.3, s)	43	-
4-Ethoxyaniline	0.080	50	52 (36.3, s)	48	-
4-Aminophenol	0.050	45	60 (37.7, s)	17	14 (16.6, s), 10 (3.73, s)
2,2,2-Trifluoroethylamine	0.150	64	72 (41.9, t)	29	1 (15.49, n.d.)
Glycine methylester	0.250	92	100 (43.8, s)		
2-Methoxyethylamine	0.005	30	23 (43.5, t)	76	1 (16.11, n.d)
Glycine	0.010	53	46 (43.0, t)	48	3 (54.7, n.d.)
γ-Aminobutyric acid	0.040	87	79 (43.2, t)	21	-
1-Methyl piperazine	0.060	57	100 (44.1-44.4, m)	0	-
1-Acetyl piperazine	0.050	90	93 (44.0, qn)	7	-
Morpholine	0.050	91	96 (44.3, qn)	4	-
Piperazine	0.0058	68	45 (45.0-44.8, m)	35	7 (44.8, t), 14 (44.0-44.3, m),
Methoxylamine	0.035	50	59 (45.4, s)	41	-
Hydroxylamine	0.100	98	49 (47.8, s)	14	3 (52.4, s), 8 (52.0, s), 8 (16.6, s), 12 (9.03, s), 5 (3.83, s).

(a) Calculated by application of determined k_N rate constants (Table 3.3) to Equation 3.3, under conditions where hydrolysis is due only to k_0. (b) Determined by ^{31}P NMR spectroscopy.

3.3 Discussion

In general, for the amines studied the conversions (%) of oxy and thiophosphodichloridate ions to phosphoramidate and thiophosphoramidate products at a given amine concentration observed by ^{31}P NMR spectroscopy (Tables 3.6 and 3.7) were in agreement with predicted conversions (%) determined from the application of UV-Vis kinetic data (Table 3.3) to Equation 3.3. However, for those amines where predicted conversions were not observed, potential reasons for differences in these values will be discussed below.

Second-order rate constants were determined by UV-Vis spectrophotometry for the reaction of oxy and thiophosphodichloridate ions with 1-methyl piperazine **108** as k_N = 0.201 and 0.078 $M^{-1}s^{-1}$, respectively. These rate constants were lower than expected for a secondary amine of pK_a ~5.2, where k_N was predicted as 0.707 and 0.213 $M^{-1}s^{-1}$ from the Brønsted slopes (Figure 3.5) for reaction of secondary amines with oxy and thiophosphodichloridate ions, respectively. In addition, the percentage conversion of (thio)phosphorylating agent to (thio)phosphoramidate (97 (O) and 100 (S)) observed by ^{31}P NMR spectroscopy was significantly higher than expected (48 (O) and 57 (S)) from application of observed k_N rate constants to Equation 3.3.

1-methyl piperazine **108** has two pK_a values at 5.2 and ~10, however, it was initially unclear which pK_a corresponds to the removal of a proton from the secondary amine group and from the methylated tertiary amine. Khalili *et al.* have suggested that due to a steric effect at the tertiary amine, it is likely that the lower pK_a value corresponds to the removal of a proton from the methylated nitrogen position.[59] In addition, the lower than expected k_N values from the UV-Vis studies suggest that the pK_a value of 5.2 corresponds to the removal of a proton from the tertiary amine group, such that the k_N values of 0.201 and 0.078 $M^{-1}s^{-1}$ are due to nucleophilic attack of the tertiary amino group with oxy and thiophosphodichloridate ions, respectively (Figure 3.7). Following the formation of (thio)phosphoramidate **109**, subsequent hydrolysis is likely to generate inorganic (thio)phosphate.

Figure 3.7

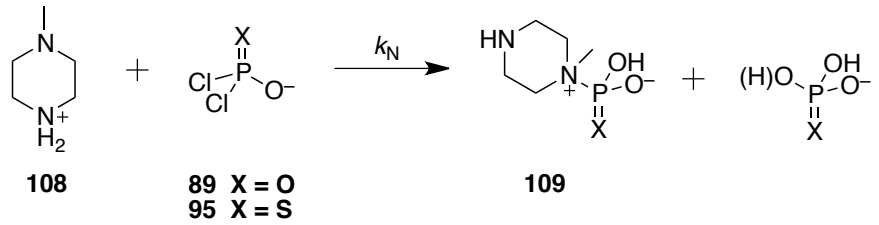

108 **89 X = O** **95 X = S** **109**

^{31}P product analysis experiments were undertaken at a pH of ~10.5, where it is likely that ~25% of the secondary amino group of 1-methylpiperazine **108** is in its nucleophilic form. We can predict k_N values for the reaction of the secondary amino group of 1-methyl piperazine (pK_a~10) with $KOPOCl_2$ and $KOPSCl_2$ from Figure 3.5 as of ~ 4.4 and 1.3 $M^{-1}s^{-1}$, respectively. Even at low amine concentrations of 15 mM, we would expect a ~90 and 80% conversion of (thio)phosphorylating agent to (thio)phosphoramidate product.

The reaction of thiophosphodichloridate ion with 4-aminophenol led to a higher than expected conversion (61 *vs* 45%) of thiophosphorylating agent to thiophosphoramidate product. This may be due to partial deprotonation of the phenol substituent (pK_a = 10.3) of 4-aminophenol in aqueous solutions of pH~10.5, resulting in the formation of small amounts of 4-aminophenolate. The nucleophilicity of the *para*-substituted amino group is likely to be enhanced upon the deprotonation of the phenol group, which may lead to higher than expected conversions of thiophosphodichloridate ion to thiophosphoramidate product.

3.3.1 Mechanistic conclusions

The kinetic data obtained for the aminolyses of oxy and thiophosphodichloridate ions in aqueous solution (Figures 3.3 and 3.4) indicate that the reaction rate depends upon the concentration of amine nucleophile present in the reaction solution. This is in full agreement with kinetic data reported by Hudson and Moss for the pyridinolysis of oxyphosphodichloridate ion in aqueous solution, where the reaction rate was shown to depend on the concentration of pyridine present in solution (Section 2.1.2.2).[37] An S_N1-type mechanism *via* **110** for the reaction of amines with oxy and thiophosphodichloridate ions (Scheme 3.4) is therefore unlikely under the reaction conditions of these experiments.

Scheme 3.4 Elimination of S_N1-type mechanism for the reaction of amines with oxy and thiophosphodichloridate ions 89 and 95 under experimental conditions.

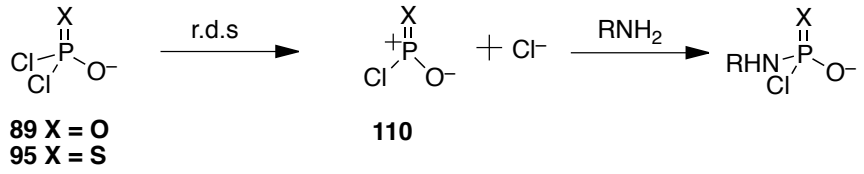

89 X = O
95 X = S

110

The reaction of oxy and thiophosphodichloridate ions **89** and **95** with amines may therefore proceed by either an addition-elimination or a $S_N2(P)$ mechanism. These are presented in Scheme 3.5.

Scheme 3.5 Reaction of amines with (thio)phosphodichloridate ions by A) addition-elimination and B) $S_N2(P)$ mechanisms.

A

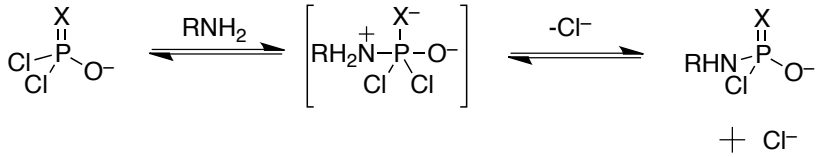

B

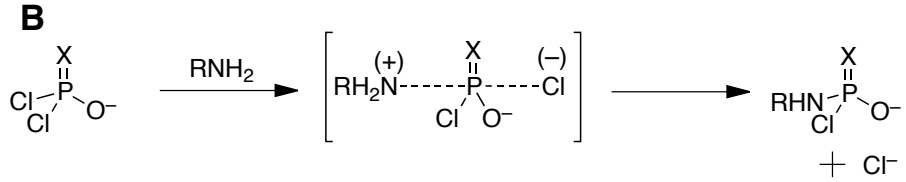

Hammett plots were constructed from appropriate σ values and log (k_N) rate constants determined from the reaction of oxy and thiophosphodichloridate ions with the family of anilines studied (Figure 3.6). A ρ value of –1.45 was determined from the slope of each plot for reaction with oxy and thiophosphodichloridate ions. In both plots the 4-fluoroaniline data point was omitted given its poor correlation with the other data points. These ρ values are consistent with the nucleophilic attack of a substituted aniline at the phosphorus centre of the (thio)phosphorylating agent as there is an decrease in electron density near the substituted benzene ring in the transition state of the rate determining step.

Similar β_{nuc} values have been determined for the aminolysis of oxy and

thiophosphodichloridate ions between each class of amine studied, which suggest that aminolyses proceeds *via* similar mechanisms for these phosphorylating agents.

β_{nuc} values were determined as 0.75 ($KOPOCl_2$) and 0.87 ($KOPSCl_2$) for reaction with the hypernucleophilic amines studied. It was not possible to determine k_N values for hypernucleophilic amines of $pK_a > 6.10$, for example hydrazine ($pK_a = 8.1$), as aminolysis reactions were too fast to follow by UV-Vis spectrophotometry. Therefore, β_{nuc} values were determined from the slopes of plots of k_N against pK_a which were constructed from only two amine data points. Under the assumption that these β_{nuc} values do not significantly change when fitted to additional data points, the hypernucleophilic amines have the largest Brønsted slope of any of the amine classes identified in this study. This suggests that any change in basicity of a hypernucleophilic amine is largely reflected in the corresponding change in its nucleophilicity. In comparison, the nucleophilicity of substituted anilines (β_{nuc} = 0.48 ($KOPOCl_2$) and 0.52 ($KOPSCl_2$)), primary amines (β_{nuc} = 0.24 ($KOPOCl_2$) and 0.24 ($KOPSCl_2$)) and secondary amines (β_{nuc} = 0.16 ($KOPOCl_2$) and 0.15 ($KOPSCl_2$)) appears to be less sensitive towards changes in their basicity.

Second order rate constants, k_N ($M^{-1}s^{-1}$), may be estimated for the (thio)phosphorylation of aromatic, primary and secondary alkyl, and hypernucleophilic amines through application of amine pK_a to the Brønsted plots presented in Figure 3.5. k_0 and predicted k_N rate constants may then be applied to Equation 3.3 to give an estimate of the percentage conversion of (thio)phosphodichloridate ion to (thio)phosphoramidate product at a given amine concentration. There are several assumptions to this method of prediction and these will now be discussed.

Equation 3.3 assumes that oxy and thiophosphodichloridate ions **89** and **95** react only with a molecule of amine or water to generate amino(thio)phosphomonochloridate **111/112** or (thio)phosphochloridate **90/113**, respectively. Following their formation, it is assumed that both species are rapidly hydrolysed to give (thio)phosphoramidate **105/106** and (thio)phosphate products **28/98**, where displacement of the final chlorine by an amine molecule is not observed, i.e. *via* an unselective process (Figure 3.8).

Figure 3.8 Assumed pathways towards (thio)phosphoramidates and inorganic (thio)phosphate

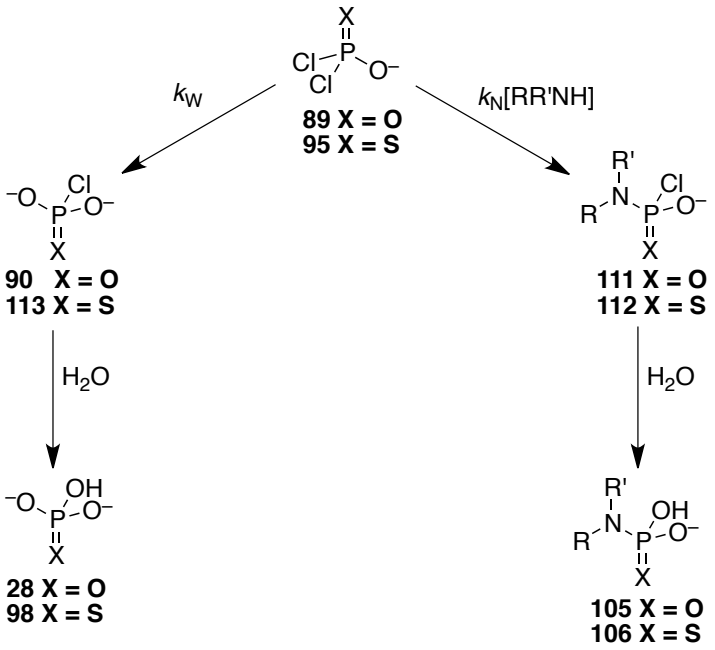

Product analysis studies show that for some amines with multiple reactive centres, for example hydroxylamine and piperazine, multiple signals are observed in addition to those due to (thio)phosphoramidate **105/106** and (thio)phosphate products **28/98**. This suggests that Equation 3.3 fails to provide an accurate prediction for the (thio)phosphorylation of complicated amines such as piperazine. However, for the (thio)phosphorylation of simple amines, such as primary alkyl amines, the conversion of (thio)phosphorylating agent to additional reaction products is essentially zero. Thus, these results suggest that conversions of oxy and thiophosphodichloridate ions to (thio)phosphoramidate products for reactions with simple amine nucleophiles may be accurately predicted from Equation 3.3.

The latter assumption is supported by literature information published by Grunze, Hudson and Moss, and Mitchell,[34, 35, 37, 47, 48] where the oxyphosphomonochloridate ion was expected to immediately hydrolyse to inorganic phosphate upon its formation in aqueous solution. It is also supported by the product analysis data, in which the formation of bis(thio)phosphoramidate product was not identified for any amine studied. If reaction of the aminophosphomonochloridate species with a second amine group were to occur it would be expected that signals due to bisphoshoramidate

product would be observed. However, the product analysis studies cannot distinguish whether (thio)phosphoramidate products were formed *via* reaction of phosphodichloridate ion with an amine and then with water, or alternatively *via* reaction of the phosphodichloridate ion to give the monochloridate ion which then reacts with an amine to give the phosphoramidate product. Therefore, these product analysis studies cannot eliminate the possibility of a reaction between the monochloridate ion and an amine, such that it cannot be proven that the loss of the final chlorine molecule is rapid and non-selective.

A third assumption is that (thio)phosphorylation reactions are undertaken under pseudo-first order reaction conditions with respect to the amine under study. This is a valid assumption for the kinetic studies presented within this chapter. However, as part of developing a "click"-strategy towards the synthesis of thiophosphoramidates in aqueous solution, Trmčić and Hodgson previously added thiophosphoryl chloride to aqueous amine solutions at a 1:1 concentration of amine to thiophosphorylating agent.[22] Under these conditions, as the amine is consumed, the ratio of k_N[amine] : k_0 should decrease such that hydrolysis of oxy and thiophosphodichloridate ions will dominate over the competing aminolysis process toward the end of the reaction. This in turn may lead to lower conversions of (thio)phosphodichloridate ion to (thio)phosphoramidate product. The extent of the difference between observed and predicted conversions of (thio)phosphodichloridate to (thio)phosphoramidate product will depend on the initial amine concentration and the nucleophilicity of the amine under study. For the (thio)phosphorylation of nucleophilic amines, the k_0 term will likely dominate over k_N[amine] towards the end of a reaction where the amine concentration is diminished.

With the Brønsted plots for the aminolyses of oxy and thiophosphodichloridate ions in hand, it is now possible to predict levels of conversion of (thio)phosphorylating agent to (thio)phosphoramidate product for the (thio)phosphorylation of amines of known pK_a (at a given concentration), where k_N rate constants have not been experimentally determined.

For example, as part of an on-going project of (thio)phosphorylating 5'-amino nucleosides in aqueous solution with the need for little or no chromatography, we can

predict the k_N rate constant for the thiophosphorylation of 5'-amino-5'-deoxyguanosine **41** in aqueous solution (Scheme 3.6).

Scheme 3.6 Thiophosphorylation of 5'-amino-5'-deoxyguanosine 41 in aqueous solution.

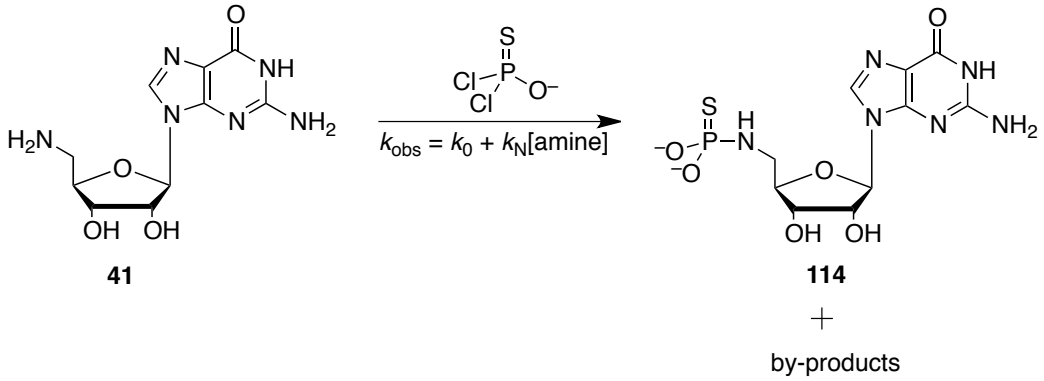

Although the pK_a of the 5'-amino group has not been determined, it is expected to be similar to that of 2-methoxyethylamine (pK_a = 9.56), given the similarity in their structure adjacent to the amino group. We may therefore estimate a k_N rate constant of ~0.35 from the Brønsted plot for the thiophosphorylation of primary alkyl amines (Figure 3.5B).

From the application of the predicted k_N rate constant (~0.35 $M^{-1}s^{-1}$) to k_{obs}, we can expect a 91% conversion of thiophosphodichloridate ion to thiophosphoramidate **114**, under conditions where the amine is in its nucleophilic form at a concentration of 0.1 M and the $k_{HO}[HO^-]$ term is negligible. In addition, the deprotonation at the *N*-1 position of the guanyl group and of the 2' and 3' hydroxyl groups may enhance the nucleophilicity of the 5'-amino group, in a similar way that the phenolate group of 4-aminophenol enhanced the nucleophilicity of the *para* substituted amino group, such that higher than expected conversions may be observed. This concept is discussed in greater detail in Chapter 4, where predicted conversions of oxy and thiophosphodichloridate ions to their (thio)phosphoramidate products are compared with experimentally determined values.

3.4 Summary

As part of understanding the (thio)phosphorylation of amines to give (thio)phosphoramidate products, kinetic investigations have been made into the aminolyses of oxy and thiophosphodichloridate ions in aqueous solution.

Second order rate constants were determined by UV-Vis spectrophotometry for the reaction of oxy and thiophosphodichloridate ions **89** and **95** with the following types of amine in aqueous solution (25 °C and I=1 (KCl)): anilines, primary alkyl amines, secondary alkyl amines and hypernucleophilic amines.

Brønsted plots were constructed from the determined log (k_N) values and measured amine pK_a values for both phosphorylating agents. Similar β_{nuc} values were determined for the (thio)phosphorylation of each class of amine, which suggests that identical mechanisms are in operation for the aminolysis of oxy and thiophosphodichloridate ions.

The constructed Brønsted plots (Figure 3.5) may be used to estimate k_N values for amines that have not been kinetically studied. These rate constants may in turn be used to predict conversions (%) of (thio)phosphodichloridate ions to (thio)phosphoramidate products in aqueous amine solution by application of kinetic data to Equation 3.3.

In Chapter 4 we apply and test our understanding of the kinetics of hydrolyses and aminolyses of oxy and thiophosphodichloridates towards the development of aqueous (thio)phosphorylation synthetic procedures.

Chapter 4

Optimisation of aqueous methods of (thio)phosphorylation

4.0 Foreword

In chapters two and three, kinetic studies of the hydrolyses and aminolyses of oxy and thiophosphodichloridate ions **89** and **95** gave an insight into the reactivities of these phosphorylating agents towards amines, water and hydroxide.

In this chapter we have applied our kinetic understanding to the (thio)phosphorylation of amines in aqueous solution. As part of these investigations we have:

- Determined and compared conversions of phosphorus oxychloride *vs* oxyphosphodichloridate ion to phosphoramidate from reactions with 2-methoxyethylamine in aqueous solution.
- Determined and compared conversions of thiophosphoryl chloride *vs* thiophosphodichloridate ion to thiophosphoramidate from reactions with 2-methoxyethylamine in aqueous solution.
- Determined and compared conversions of thiophosphoryl chloride *vs* thiophosphodichloridate ion to thiophosphoramidate from reactions with 5'-amino-5'-deoxyguanosine in aqueous solution.
- Optimised the alkylation of thiophosphorylated 5'-amino-5'-deoxyguanosine using benzyl chloride, bromoethanol and methyl iodide alkylating agents.

The chapter will end with conclusions about the potential application of oxy and thiophosphodichloridate ions as effective (thio)phosphorylating agents in aqueous solution.

4.1 Introduction

As part of ongoing research into the developments of aqueous methods of (thio)phosphorylation, this introduction describes how the kinetic studies presented in chapters two and three are essential for optimising conversions of oxy and thiophosphodichloridate ions to (thio)phosphoramidate products in aqueous solution. The chapter starts with an introduction of the potential benefits of oxy and thiophosphodichloridate ions as phosphorylating agents in aqueous methods of phosphorylation. We then discuss how phosphorylation may be optimised using the kinetic outcomes discussed previously and describe how aqueous methods developed by Hodgson, Williamson and Trmčić have been adapted to form (thio)phosphoramidates at greater purity level, where chromatography is not required.

The oxy and thiophosphodichloridate ions are attractive phosphorylating agents for use in aqueous phosphorylation because:

- Oxy- and thio- phosphodichloridate ions are fully water soluble in aqueous solution, which ensures efficient and effective mixing upon addition to aqueous amine solutions.
- Oxy- and thio- phosphodichloridate ions may also be prepared as potassium salts, where their stability has been reported by Segall *et al.* to be significantly increased over that observed in anhydrous acetone solution.[49]
- They have potentially altered selectivity towards nucleophiles.

Mixing of dichloridate ions **89** and **95** in aqueous solution avoids problems associated with $POCl_3$ and $PSCl_3$, which are relatively insoluble in water, even when diluted in anhydrous THF or acetonitrile co-solvents. More effective mixing may lead to an increase in the selectivity towards aminolysis rather than hydrolysis.

The ability to synthesise stable potassium salts of the dichloridate ions is of real benefit to the development of a simple and effective (thio)phosphorylation methods, where salts could be used "off the shelf" when required. This avoids the need to prepare acetonitrile solutions of these ions each time they are required for phosphorylation, which in turn simplifies the method of phosphorylation of amines in aqueous solution.

On the other hand, one advantage of using phosphorus oxychloride or thiophosphoryl chloride as phosphorylating agents is that there are at least two possible chances of phosphorylation to occur. If $POCl_3$ or $PSCl_3$ fails to react with the amine present in aqueous solution it is hydrolysed to oxy and thiophosphodichloridates, respectively. In turn, these can react with any remaining amine present in solution to give phosphoramidate product. The reaction of phosphomonochloridate ions in aqueous solution is so fast that it is expected to show little selectivity towards amine nucleophiles. Thus, there are two opportunities for the (thio)phosphorylation of a given amine to occur.

In simplistic terms, the relative amounts of (thio)phosphoramidate and inorganic (thio)phosphate products formed upon addition of (thio)phosphorylating agents to aqueous amine solutions depends on the ratios of kinetic terms due to aminolysis and hydrolysis, according to Scheme 4.1.

Scheme 4.1

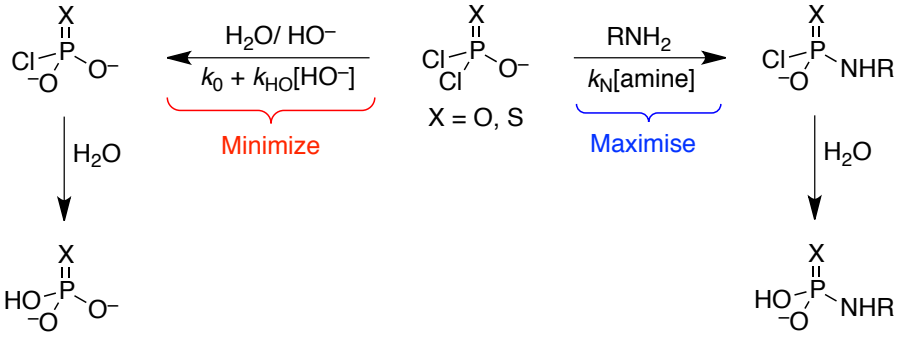

In order to maximise the conversion of oxy and thiophosphodichloridates to oxy and thiophosphoramidates respectively, the hydrolysis terms $k_0 + k_{HO}[HO^-]$ must be minimised relative to the aminolysis term k_N[amine].

The k_{obs}-pH profile for the hydrolysis of the oxyphosphodichloridate ion in aqueous solution shows that a pH-independent region lies between pH 2 and 12, where k_{obs} depends entirely on the uncatalysed hydrolysis term, $k_0 = 5.7 \times 10^{-3} s^{-1}$. Above pH 12, a hydroxide-catalysed hydrolysis term, $k_{HO}[HO^-]$, also contributes towards k_{obs}. As the reaction pH is increased above pH 12, the conversion of $KOPOCl_2$ to phosphoramidate

product will be reduced as a function of pH. In order to minimise the amount of $KOPOCl_2$ that is hydrolysed upon its addition to an aqueous amine solution, the reaction pH should ideally be maintained at a pH no greater than 12, i.e. at a pH where the hydroxide catalysed term for hydrolysis is not in operation. However, very basic amines (conjugate acid $pK_a > 12$) may be present at as a mixture of nucleophilic and protonated at this pH, and so under these circumstances an optimum reaction pH may be determined through the application of the work by King *et al*.[26]

The k_{obs}-pH profile for the hydrolysis of $KOPSCl_2$ in aqueous solution shows no hydroxide catalysed term is in operation between pH 2 and 13, where k_{obs} depends entirely on the uncatalysed hydrolysis term, $k_0 \sim 10^{-3}\ s^{-1}$. Therefore, reaction of amines and $KOPSCl_2$ in aqueous solution may be undertaken at very high pH without any increase in the rate of formation of inorganic thiophosphate. This is particularly useful for the thiophosphorylation of very basic amines, where a high pH is necessary to ensure the reacting amine is in its nucleophilic form.

With the aim of trying to maximise the conversion of oxyphosphodichloridate to phosphoramidate product, performing the phosphorylation reaction below pH 12 should ensure that hydrolysis on $KOPOCl_2$ may only proceed *via* the uncatalysed pathway from reaction with H_2O. In maximising the conversion of thiophosphodichloridate to thiophosphoramidate product, thiophosphorylation may be performed at higher pHs before any decrease in the ratio of thiophosphoramidate to inorganic thiophosphate products, due to a potential hydroxide catalysed reaction, may be observed. However, the phosphorylation of complex amines containing several nucleophilic groups, for instance hydrazine, may lead to complicated product mixtures being formed at high pHs.

In Chapter 3, Brønsted plots were constructed for the aminolysis of oxy and thiophosphodichloridate ions, using four different classes of amine, in aqueous solution. With the conjugate acid pK_a of a given amine in hand, these plots may be used to predict k_N rate constants for the (thio)phosphorylation of that amine using oxy and thiophosphodichloridate ions. The conversion of oxy and thiophosphodichloridate ions to (thio)phosphoramidate product for the amine under study may then be predicted from Equation 4.1.

$$\% \text{ conversion} = \frac{k_N[\text{amine}]}{(k_N[\text{amine}] + (k_0 + k_{HO}[HO^-]))} \qquad \textbf{Equation 4.1}$$

Manipulation of amine and hydroxide concentrations in Equation 4.1 should maximise and minimize the contribution of k_N[amine] and (k_0 + k_{HO}[HO^-]) to k_{obs}, respectively. This in turn should lead to higher conversions of (thio)phosphodichloridate ions to (thio)phosphoramidate products.

4.2 Phosphorylation and thiophosphorylation of 2-methoxy ethylamine

For these initial optimisation experiments we studied the phosphorylation and thiophosphorylation of 2-methoxyethylamine in aqueous solution for the following reasons:

- The conjugate acid pK$_a$ of 2-methoxyethylamine (~ 9.6) is of a similar magnitude to that expected for the 5`-amino group of 5'-amino-5'-deoxyguanosine and so a good model, based on amine basicity, for optimising the phosphorylation of similar amines in aqueous solution.
- With k_N rate constants for the aminolyses of oxy and thiophosphodichloridate ions in aqueous 2-methoxyethylamine solution in hand (k_N = 0.88 and 0.33 $M^{-1}s^{-1}$, respectively), we can accurately predict ratios of (thio)phosphoramidate product to inorganic (thio)phosphate expected for each optimisation experiment for the (thio)phosphorylation of 2-methoxytheylamine.
- 2-methoxyethylamine is soluble in aqueous solution and so presents no issues with mixing.
- The commercial availability of 2-methoxyethylamine avoids the need for time-consuming synthesis of amine starting materials and so can be used extensively in a large number of phosphorylation experiments.

As part of investigations into the conversion of phosphorylating agent to phosphoramidate product across a broad pH range, phosphorylation was studied at the following pHs:

- pH 8.2 and 9.2, where the 2-methoxyethylamine is present as a mixture of protonated and nucleophilic forms
- pH 10.2 and 11.2, where 2-methoxyethylamine is present in its nucleophilic form and hydrolysis should depend only on k_0
- pH 12.7, where hydroxide-catalysed hydrolysis of oxyphosphodichloridate ions is expected to be in operation.

One equivalent of phosphorylating agent in anhydrous acetonitrile was added to a rapidly stirred aqueous solution of 2-methoxyethylamine (0.1 M) at 25 °C. To ensure that the reaction pH was maintained during phosphorylation, 1 M potassium hydroxide solution was added *via* burette to the stirred reaction flask through the use of a Radiometer Titralab TIM 856 pH stat instrument. Following the addition of phosphorylating agent, the reaction solution was stirred until a decrease in pH was no longer observed, corresponding to the consumption of phosphorylating agent. For those reactions undertaken at pHs below pH 11, potassium hydroxide solution was added to increase the pH to ~11, where phosphoramidate products are most stable with respect to hydrolysis. Acetonitrile was removed in *vacuo* and the aqueous solution was lyophilised overnight. The resulting white solids were re-dissolved in D_2O and analysed by ^{31}P NMR spectroscopy immediately.

4.2.1 Phosphorylation of 2-methoxyethylamine

The pH-stat method described in Section 4.2 was applied to the phosphorylation of 2-methoxyethylamine **115** in aqueous solution using either phosphorus oxychloride **4** or oxyphosphodichloridate ion **89** as the phosphorylating agent (Scheme 4.2).

Scheme 4.2 Phosphorylation of 2-methoxyethylamine in aqueous solution using phosphorus oxychloride or oxyphosphodichloridate ion. Reaction pH was maintained by a pH-stat.

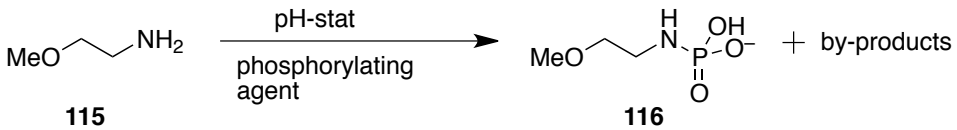

115 **116**

The conversion of phosphorus oxychloride **4** to phosphoramidate **116** and by-products in aqueous amine solution of pH 8.2 to 12.7 is presented in Figure 4.1.

Figure 4.1 **Percentage conversion to phosphorylation products *vs* pH by ^{31}P NMR spectroscopy for the reaction of phosphorus oxychloride with 2-methoxyethylamine in aqueous solution.**

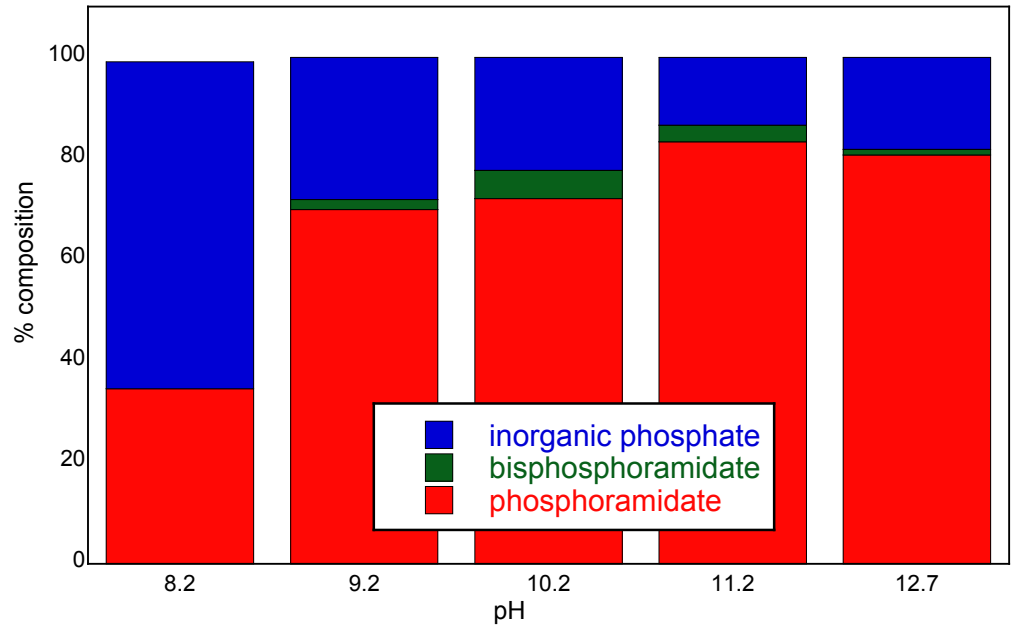

In the competing experiments performed at pH 8.2 *vs* 9.2, the conjugate acid of 2-methoxyethylamine **115** (pK_a = 9.56) was deprotonated to give its nucleophilic form, such that 2-methoxyethylamine was present in ~ 30% of its nucleophilic form at pH 9.2. The conversion of phosphorus oxychloride to phosphoramidate **116** was shown to increase significantly (35 to 70 %) within this pH range as a consequence of the increase in amine concentration present in solution. The optimal pH for conversion was 11.2, where 83% phosphoramidate was formed with bisphosphoramidate (3 %) and phosphate by-products (13 %). Phosphorylation at pH 12.7 resulted in a greater conversion to inorganic phosphate, which may be due to hydroxide catalysed hydrolysis of $POCl_3$. In addition, hydrolysis of oxyphosphodichloridate ion may also have been catalysed by hydroxide at this pH.

The conversion of phosphorus oxychloride to bisphosphoramidate product **117** was observed between pH 9.2 and 12.7 (Scheme 4.3).

Scheme 4.3

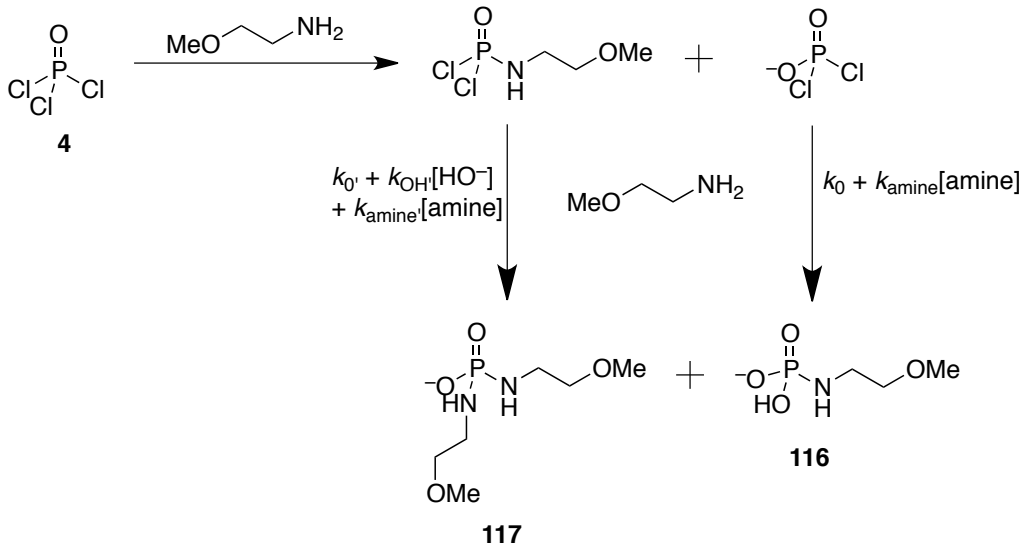

The percentage conversion to bisphosphoramidate **117** initially increases from 2 to 6 % between pH 9.2 to 10.2, corresponding to an increase in free amine concentration, however decreases upon a further increase in reaction pH.

This series of phosphorylation experiments, with each experiment at a different pH, were repeated using oxyphosphodichloridate ion as the phosphorylating agent. From kinetic investigations of aminolysis (Chapter 3), k_N = 0.88 $M^{-1}s^{-1}$ for the reaction of oxyphosphodichloridate ion with 2-methoxyethylamine. Therefore, for the phosphorylation of 2-methoxyethylamine at a concentration of 0.1 M, k_N[amine] is expected to contribute ~0.088 s^{-1} to k_{obs}. The conversion of oxyphosphodichloridate ions to phosphoramidate product **116** may then be predicted from Equation 4.1.

Phosphorylation of 2-methoxyethylamine **115** with oxyphosphodichloridate ion **89** was performed at pHs between 8.2 to 12.7. Under these conditions, hydroxide-catalysed hydrolysis of oxyphosphodichloridate ion is not observed. Thus, Equation 4.1 may be simplified to Equation 4.2.

$$\% \text{ conversion} = \frac{k_N[\text{amine}]}{(k_N[\text{amine}] + k_0)} \qquad \textbf{Equation 4.2}$$

A 94% conversion of oxyphosphodichloridate ion to phosphoramidate product was expected from the application of kinetic data (k_N = 0.88 $M^{-1}s^{-1}$, [amine] ~ 0.1 M and k_0 = 5.5 × $10^{-3}s^{-1}$) to Equation 4.2.

The percentage conversions obtained for each reaction are presented in Figure 4.2.

Figure 4.2 **Percentage conversion of phosphorylation products *vs* pH by ^{31}P NMR spectroscopy for the reaction of oxyphosphodichloridate ion with 2-methoxyethylamine in aqueous solution.**

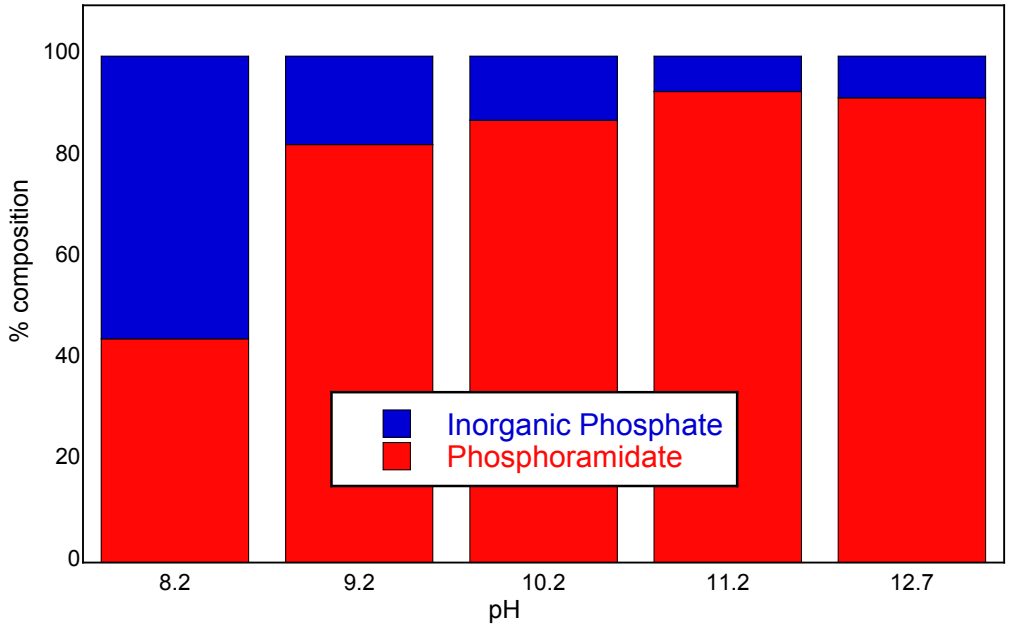

A similar trend in the conversion of phosphorylating agent to phosphoramidate is observed with both phosphorus oxychloride and oxyphosphodichloridate ion. However, a higher conversion of oxyphosphodichloridate ion *vs* phosphorus oxychloride to phosphoramidate was observed at each pH studied.

At the optimal reaction pH (11.2) a 93 % conversion of $KOPOCl_2$ to phosphoramidate was observed with only phosphate (7 %) formed as a by-product. This result is in agreement with the conversion percentage (94 %) calculated using kinetic data obtained in Chapter 3. The conversion levels of oxyphosphodichloridate **89** to phosphoramidate **116** are similar at pHs 11.2 and 12.7 (93 vs 92%), which suggests that the contribution of hydrolysis to the overall reaction is effectively constant within this pH region. This result is in full agreement with the pH-k_{obs} profile for the

hydrolysis of $KOPOCl_2$, which indicates that hydroxide-catalysed hydrolysis of oxyphosphodichloridate to give inorganic phosphate should only become significant at pHs above 13. In addition, the use of oxyphosphodichloridate ion as phosphorylating agent may avoid the formation of any bisphosphoramidate product **117** as there is only one potential chance of reaction of 2-methoxyethylamine with $KOPOCl_2$, compared with two potential chances of reaction with $POCl_3$.

The results presented in Figures 4.1 and 4.2 indicate that the oxyphosphodichloridate ion is a more selective mono-phosphorylating agent than phosphorus oxychloride for the phosphorylation of 2-methoxyethylamine in aqueous solution from pH 8.2 to 12.7. Higher conversions of phosphorylating agent to phosphoramidate product are observed with $KOPOCl_2$ than with phosphorus oxychloride (93 *vs* 83 % conversion at optimal pHs) and fewer by-products are formed, leading to simpler chromatography procedures, if required.

Based on these preliminary results, we expect the phosphorylation of amino nucleosides, such as 5'-amino-5'-deoxyguanosine, to yield higher conversions of phosphoramidate product when oxyphosphodichloridate ion is utilised as the phosphorylating agent rather than phosphorus oxychloride.

With these positive results in hand, we followed the thiophosphorylation of 2-methoxyethylamine using thiophosphoryl chloride and thiophosphodichloridate ion as thiophosphorylating agents and present our results and conclusions in Section 4.22.

4.2.2 Thiophosphorylation of 2-methoxyethylamine

The pH-stat method described in Section 4.2 was applied to the thiophosphorylation of 2-methoxyethylamine in aqueous solution using either thiophosphoryl chloride **13** or thiophosphodichloridate ion **95** as the thiophosphorylating agent (Scheme 4.4).

Scheme 4.4 **Thiophosphorylation of 2-methoxyethylamine in aqueous solution using thiophosphoryl chloride or thiophosphodichloridate ion. Reaction pH was maintained by a pH-stat.**

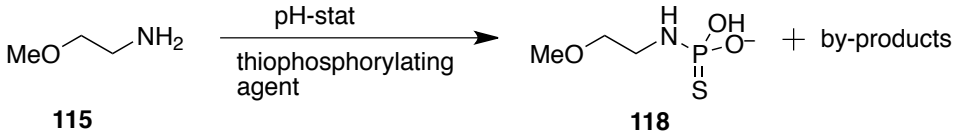

115 **118**

The conversions of thiophosphoryl chloride to thiophosphoramidate **118** and by-products in aqueous amine solution of pH 8.2 to 12.7 are presented in Figure 4.3.

Figure 4.3 **Percentage conversion of phosphorylating agent *vs* pH by ^{31}P NMR spectroscopy for the reaction of thiophosphoryl chloride with 2-methoxyethylamine in aqueous solution.**

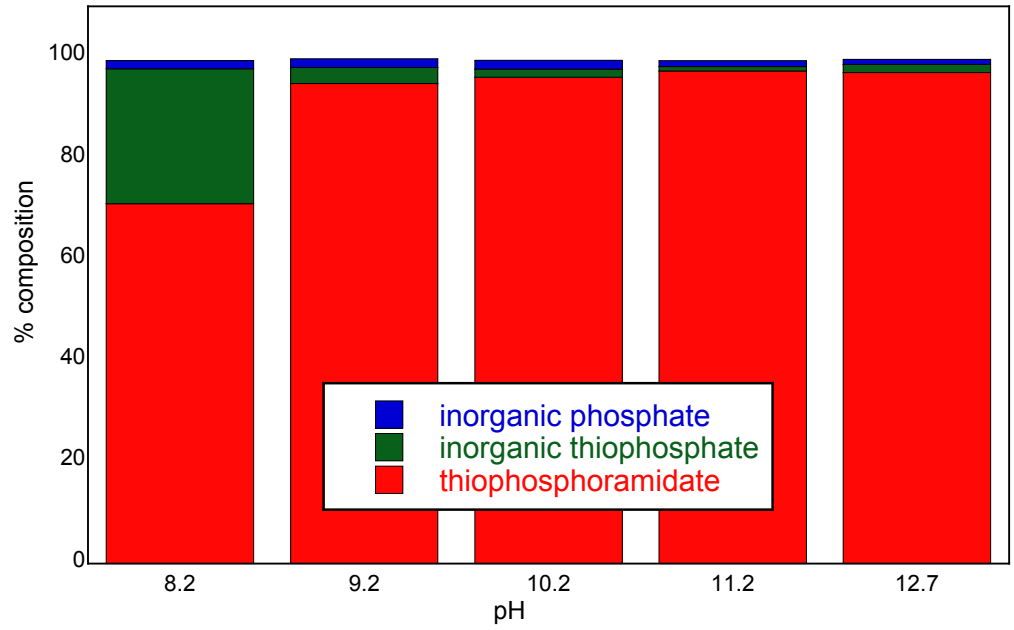

The conversion of thiophosphoryl chloride **13** to thiophosphoramidate **118** was shown to increase significantly (71 to 95 %) between pH 8.2 to 9.2 as a consequence of the increase in amine concentration (~4 to 30 mM) present in solution. The optimal pH for conversion was between pH 11.2 and 12.7, where 97 % phosphoramidate was formed with inorganic phosphate and thiophosphate by-products (~3%). The conversion of thiophosphoryl chloride to bisthiophosphoramidate was not observed in these studies.

These phosphorylation experiments were repeated using thiophosphodichloridate ion as the phosphorylating agent. From kinetic investigations of aminolysis (Chapter 3), k_N

= 0.33 $M^{-1}s^{-1}$ for the reaction of thiophosphodichloridate ion with 2-methoxyethylamine. Thiophosphorylation of 2-methoxyethylamine with thiophosphodichloridate ion was performed at pHs between 8.2 to 12.7. Under these conditions, hydroxide-catalysed hydrolysis of thiophosphodichloridate ion is not observed. A 91% conversion of thiophosphodichloridate ion to thiophosphoramidate product is expected from the application of kinetic data (k_N = 0.33 $M^{-1}s^{-1}$, [amine] = 0.1 M and $k_0 = 3.3\times 10^{-3}s^{-1}$) to Equation 4.2. The percentage conversions obtained for each reaction are presented in Figure 4.4.

Figure 4.4 **Percentage conversion of phosphorylation products *vs* pH by ^{31}P NMR spectroscopy for the reaction of thiophosphodichloridate ion with 2-methoxyethylamine in aqueous solution.**

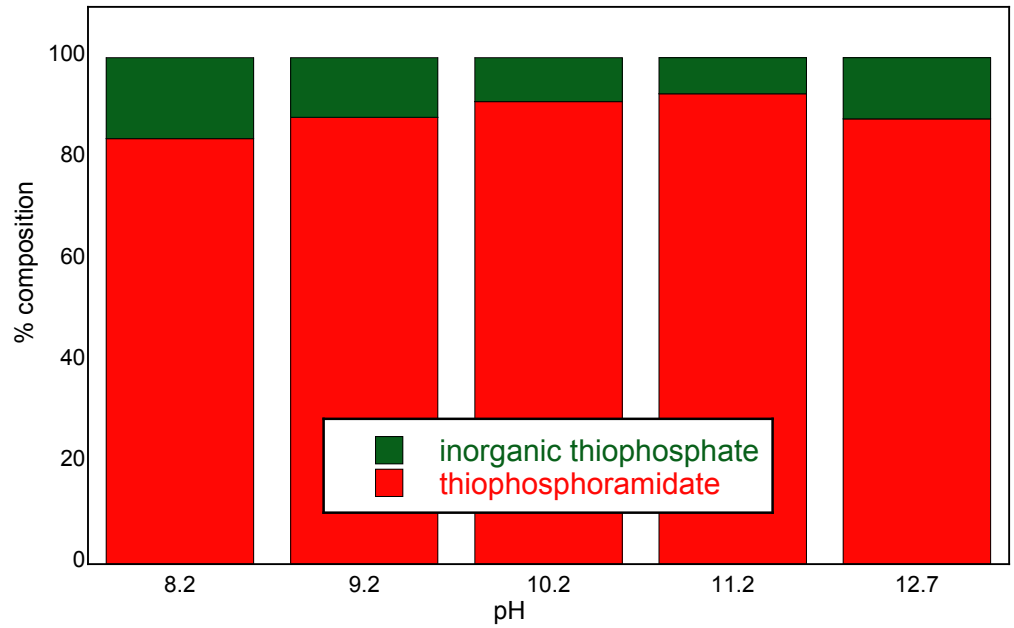

A similar trend in the conversion of phosphorylating agent to phosphoramidate **118** was observed with both thiophosphoryl chloride and thiophosphodichloridate ion. However, a lower conversion of thiophosphodichloridate ion *vs* thiophosphoryl chloride to thiophosphoramidate was observed between pH 9.2 and 12.7.

At the optimal reaction pH (11.2), a 93 % conversion of $KOPSCl_2$ to thiophosphoramidate was observed with inorganic thiophosphate (7 %) formed as the only by-product. This result is in agreement with the conversion percentage (90%) calculated using kinetic data obtained in Chapter 3.

The results presented in Figures 4.3 and 4.4 indicate that thiophosphoryl chloride is a better thiophosphorylating agent than thiophosphodichloridate ion for the thiophosphorylation of 2-methoxyethylamine under the reaction conditions from pH 8.2 to 12.7. Differences in the conversions of thiophosphorylating agent to thiophosphoramidate product for $PSCl_3$ *vs* $KOPSCl_2$ are likely due to the fact there are two potential chances for thiophosphorylation of 2-methoxyethylamine, whereas $KOPSCl_2$ has only one chance of reaction with 2-methoxyethylamine. Therefore, if $PSCl_3$ reacts with a molecule of water to generate $KOPOCl_2$, it is presented with another opportunity for reaction with 2-methoxyethylamine.

Another potential explanation for the differences in observed conversion levels relates to the solubility of $PSCl_3$ *vs* $KOPSCl_2$ in aqueous solution. $KOPSCl_2$ is fully soluble in aqueous solution and thiophosphorylation of 2-methoxyethylamine is therefore expected to occur under aqueous conditions. On the other hand, stopped-flow studies in Chapter 2 have demonstrated that $PSCl_3$ is insoluble in aqueous solution, where the addition of $PSCl_3$ in anhydrous solvent leads to a mixed phase system. Upon addition of $PSCl_3$ to each reaction solution, 2-methoxyethylamine may partition from the aqueous phase towards the organic phase and subsequently undergo thiophosphorylation to give the resulting thiophosphoramidate. This in turn may minimise the conversion of $PSCl_3$ to inorganic thiophosphate, thus leading to higher than expected conversion levels.

4.3 Thiophosphorylation of 5'-amino-5'-deoxyguanosine

Following the study of the (thio)phosphorylation of 2-methoxyethylamine in aqueous solution, the aqueous based pH-stat method was adapted toward the thiophosphorylation of 5'-amino-5'-deoxyguanosine.

5'-amino-5'-deoxyguanosine **41** was synthesised from guanosine **119** according to the literature procedure developed by Dean (Scheme 4.5).[60]

Scheme 4.5 Dean's literature method towards the synthesis of 5'-amino-5'-deoxyguanosine.[60]

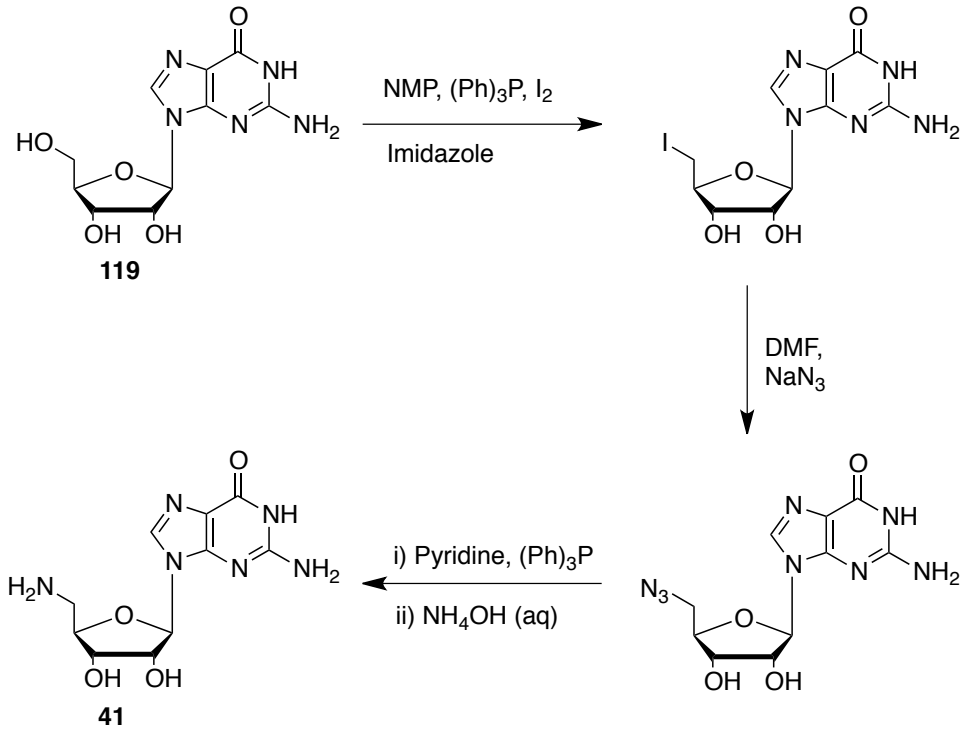

According to Scheme 4.5, 5'-amino-5'-deoxyguanosine **41** was prepared over three steps in a yield of 39% and was purified by recrystalisation in water.[60]

The alkylation of thiophosphorylated 5'-amino-5'-deoxyguanosine may give rise to potential phosphate ester mimics, and therefore the pH-stat method described in Section 4.2 was applied to the thiophosphorylation of 5'-amino-5'-deoxyguanosine in aqueous solution using either thiophosphoryl chloride or thiophosphodichloridate ion as the phosphorylating agent (Scheme 4.6).

Scheme 4.6 **Thiophosphorylation of 5'-amino-5'-deoxyguanosine in aqueous solution using thiophosphoryl chloride or thiophosphodichloridate ion. Reaction pH was maintained by a pH-stat instrument.**

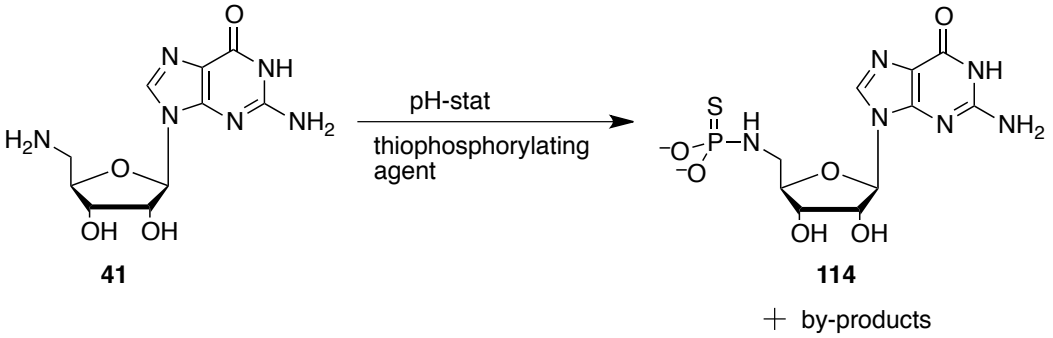

The conversions of thiophosphoryl chloride to thiophosphoramidate **114** and by-products in aqueous amine solution of pH 11 to 12.5 are presented in Figure 4.5.

Figure 4.5 **Percentage conversion of phosphorylation products vs pH by A) ^{31}P and B) ^{1}H NMR spectroscopy for the reaction of thiophosphoryl chloride with 5'-amino-5'-deoxyguanosine in aqueous solution.**

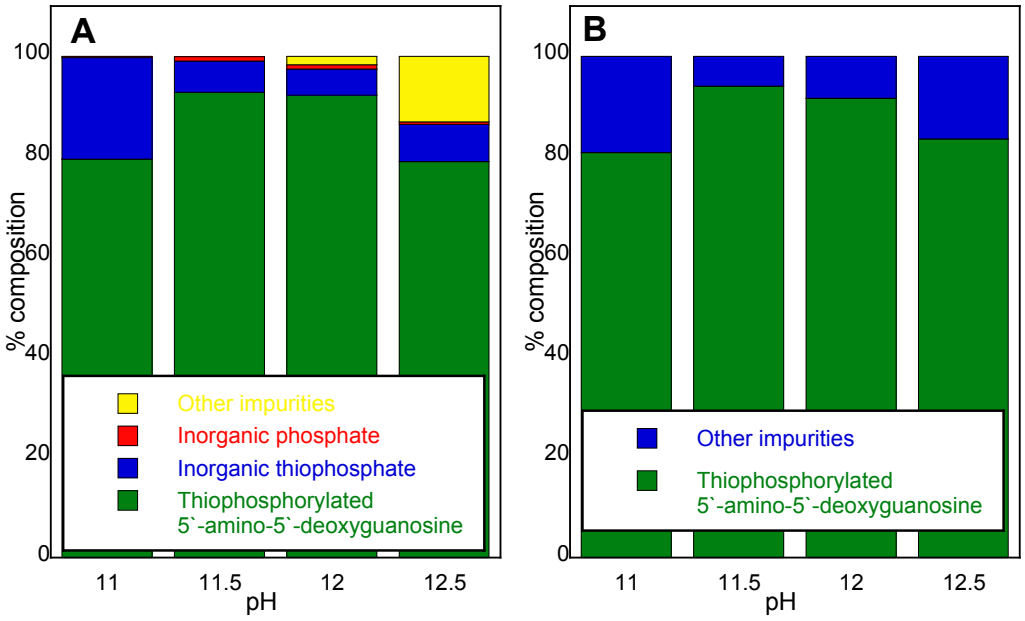

The conversion of thiophosphoryl chloride to thiophosphoramidate 114 was shown to increase (79 to 93 %) between pH 11 to 11.5. The optimal pH for conversion was pH 11.5, where 93 % phosphoramidate was formed with inorganic thiophosphate (6%) and inorganic phosphate (1%) by-products. Upon addition of thiophosphoryl chloride (0.4 M in dry MeCN) to a stirred aqueous solution of 5'-amino-5'-deoxyguanosine 41,

a white crust formed on surface of the reaction solution. This was likely due to the protonation of 5'-amino-5'-deoxyguanosine by the acid generated upon the hydrolysis of $PSCl_3$ to $KOPSCl_2$. The protonation of 5'-amino-5'-deoxyguanosine renders it insoluble in aqueous solution and so it formed a precipitate at the surface of the reaction solution. This effect was minimized, but not prevented, through rapid stirring of the reaction mixture and dropwise addition of thiophosphoryl chloride.

The conversions of thiophosphodichloridate ion to thiophosphoramidate **114** and by-products in aqueous amine solution of pH 11 to 12.5 are presented in Figure 4.6

Figure 4.6 **Percentage conversion of phosphorylation products *vs* pH by A) ^{31}P and B) ^{1}H NMR spectroscopy for the reaction of thiophosphodichloridate ion with 5'-amino-5'-deoxyguanosine in aqueous solution.**

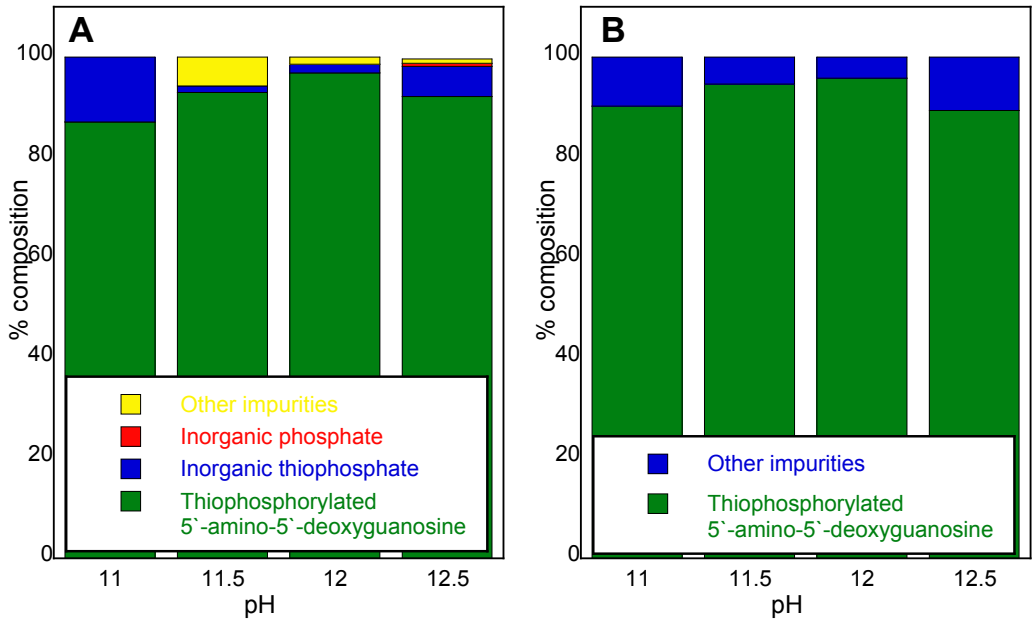

The conversion of thiophosphodichloridate ion to thiophosphoramidate **114** was shown to increase (87 to 97 %) from pH 11 to 12. The optimal pH for conversion was pH 12, where 97 % phosphoramidate was formed with inorganic thiophosphate (1%) and additional by-products (2%).

From the thiophosphorylation studies of 2-methoxethylamine, we expected thiophosphoryl chloride to be a more effective thiophosphorylating agent towards 5'-amino-5'-deoxyguanosine than thiophosphodichloridate ion. However, the results

presented in Figures 4.3 and 4.4 suggest that thiophosphodichloridate ion is in fact the more effective thiophosphorylating agent in aqueous solution from pH 11 to 12.5.

In contrast with 2-methoxyethylamine, the insolubility of 5'-amino-5'-deoxyguanosine in organic solvents prevents phase transfer from the aqueous phase into the organic phase. Reaction of 5'-amino-5'-deoxyguanosine with $PSCl_3$ must therefore occur within the aqueous phase, which may in turn lead to lower than expected conversion levels to thiophosphoramidate, based on data obtained for the reaction of $PSCl_3$ with 2-methoxyethylamine.

Lower than expected conversions of $PSCl_3$ to thiophosphoramidate product may also be due to the precipitation of 5'-amino-5'-deoxyguanosine upon the addition of thiophosphorylating agent. In contrast, no precipitation was observed upon the addition of thiophosphodichloridate ion to aqueous solutions of **41** and conversions from $KOPSCl_2$ to thiophosphoramidate product should not be affected.

The error involved in the integration of ^{31}P signals due to thiophosphoramidate product and by-products may also contribute to differences in the determined percentages of conversion of phosphorylating agent to phosphoramidate product. (Thio) phosphorylation experiments of commercially available 2-methoxyethylamine were undertaken on larger scales than for the (thio) phosphorylation of 5'-amino-5'-deoxyguanosine (2×10^{-3} *vs* 5×10^{-4} mol per reaction). This enabled more concentrated ^{31}P NMR samples to be analysed, which in turn reduced the signal to noise ratio. Owing to the reduced amount of thiophosphorylated 5'-amino-5'-deoxyguanosine product mixture available for study by ^{31}P NMR spectroscopy, a larger signal to noise ratio was observed.

Following the study and synthesis of thiophosphorylated 5'-amino-5'-deoxyguanosine from reaction of 5'-amino-5'-deoxyguanosine with $PSCl_3$ and $KOPSCl_2$, we studied its reaction with the alkylating agents bromoethanol, benzyl chloride and methyl iodide in aqueous solution of varying pH. The results of these alkylation studies are presented and discussed in Section 4.3.

4.3 Alkylation of *N*-linked 5'-amino-5'-deoxyguanosine thiophosphoramidate

As part of an overall research group project toward the synthesis of NMP and NDP sugar mimics, Trmčić developed a one-pot synthesis for the *S*-alkylation of thiophosphorylated 5'-amino-5'-deoxyguanosine **114** using bromoethanol and methyl iodide alkylating agents (Scheme 4.7).

Scheme 4.7 Trmčić's one-pot thiophosphorylation of 5'-amino-5'-deoxyguanosine and alkylation with benzyl chloride and methyl iodide.

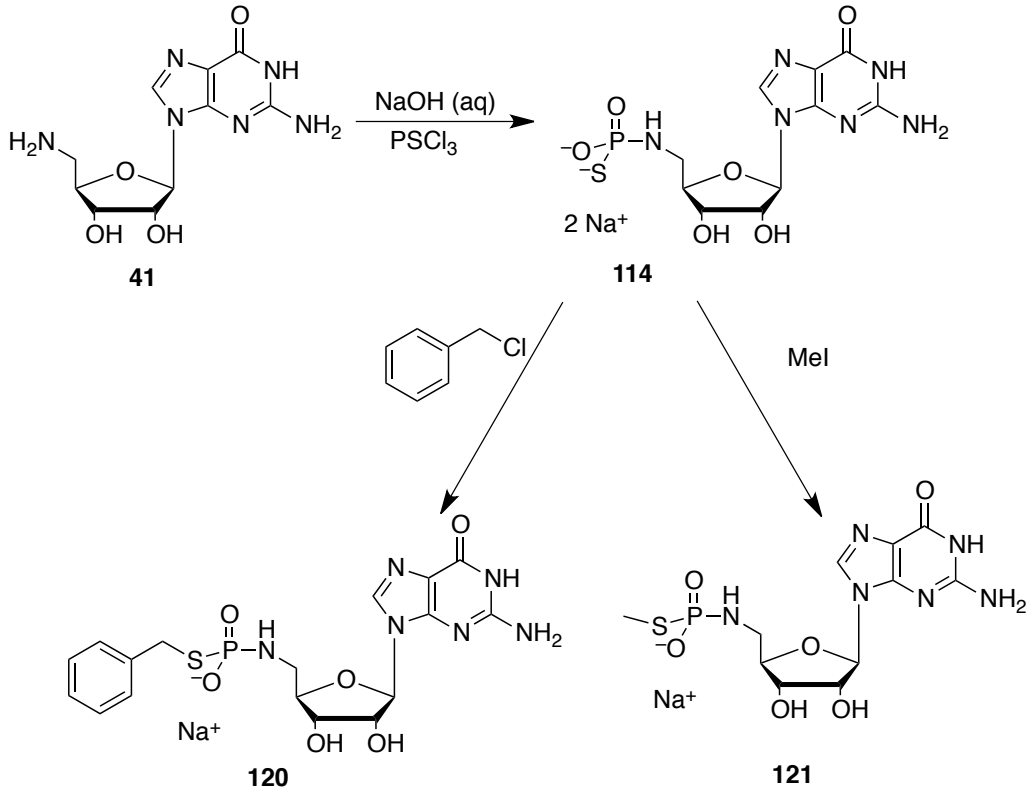

As shown in Scheme 4.7, benzyl chloride and methyl iodide alkylating agents were simply added with one equivalent of hydroxide to aqueous solutions containing the reaction products from the thiophosphorylation of 5'-amino-5'-deoxyguanosine. Alkylated thiophosphoramidates **120** and **121** were subsequently formed, respectively. The reaction pH was not monitored or maintained during alkylation.

Following the optimisation of reaction conditions for the thiophosphorylation of 5'-amino-5'-deoxyguanosine, we attempted to determine the importance of reaction pH

for the alkylation of 5'-amino-5'-deoxyguanosine thiophosphoramidate with simple alkylating agents using pH-stating instrumentation (Scheme 4.8).

Scheme 4.8 Aqueous method of *S*-alkylation of thiophosphorylated 5'-amino-5'-deoxyguanosine at fixed pH using a pH-stat.

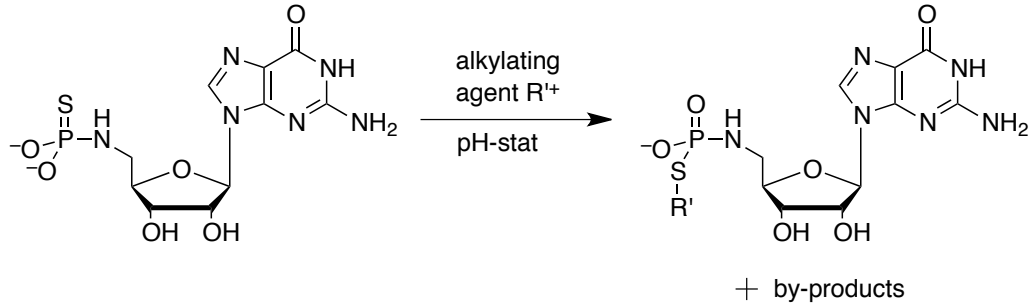

Thiophosphorylated 5'-amino-5'-deoxyguanosine was made up in water and potassium hydroxide solution at a concentration of 20 mM at the pHs 8-12. The reaction pH for each alkylation was maintained using a pH-stat instrument. An excess of alkylating agent was added to each reaction and was stirred at 25 °C for the reaction time employed by Trmčić. Reactions were shown to be complete by ^{31}P NMR spectroscopy. Following alkylation, excess alkylating agent was extracted from the reaction solution, acetonitrile was removed in *vacuo* and the aqueous solution lyophilized until dry. The resulting white solids were either re-dissolved in D_2O and immediately analysed by ^{31}P NMR spectroscopy or stored at –18 °C for analysis at a later date.

The following sections present the results for the alkylation of thiophosphorylated 5'-amino-5'-deoxyguanosine with benzyl chloride, methyl iodide and bromoethanol alkylating agents. Observed trends are discussed and conversions of alkylated thiophosphoramidates are compared to those reported by Trmčić.

4.3.1 Benzyl chloride

Thiophosphorylated 5'-amino-5'-deoxyguanosine was *S*-alkylated with benzyl chloride in aqueous solution of varying pH according to Scheme 4.9.

Scheme 4.9 ***S*-Alkylation of thiophosphorylated 5'-amino-5'-deoxyguanosine with benzyl chloride in aqueous solution. Reaction pH was maintained through use of a pH stat instrument.**

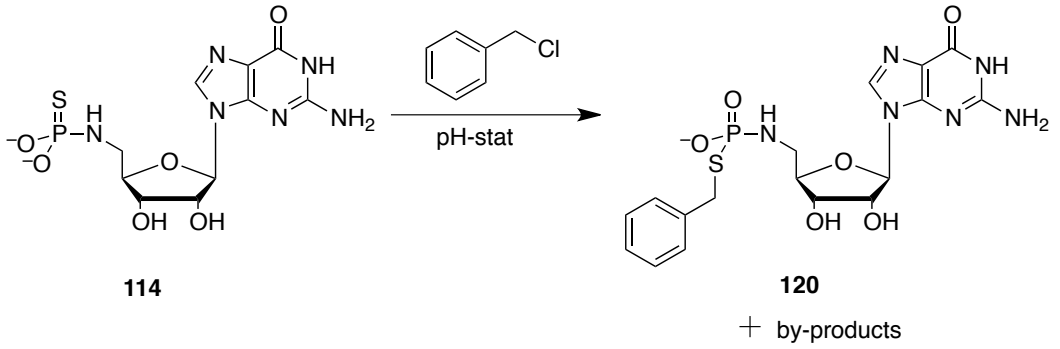

The resulting percentage conversions of benzylalkylated thiophosphorylated 5'-amino-5'-deoxyguanosine **120** from pH 8 to 12 were determined by ^{31}P NMR spectroscopy and are shown in Figure 4.7.

Figure 4.7 **Percentage conversion of benzylalkylated thiophosphorylated 5'-amino-5'-deoxyguanosine *vs* pH by A) ^{31}P and B) ^{1}H NMR spectroscopy in aqueous solution.**

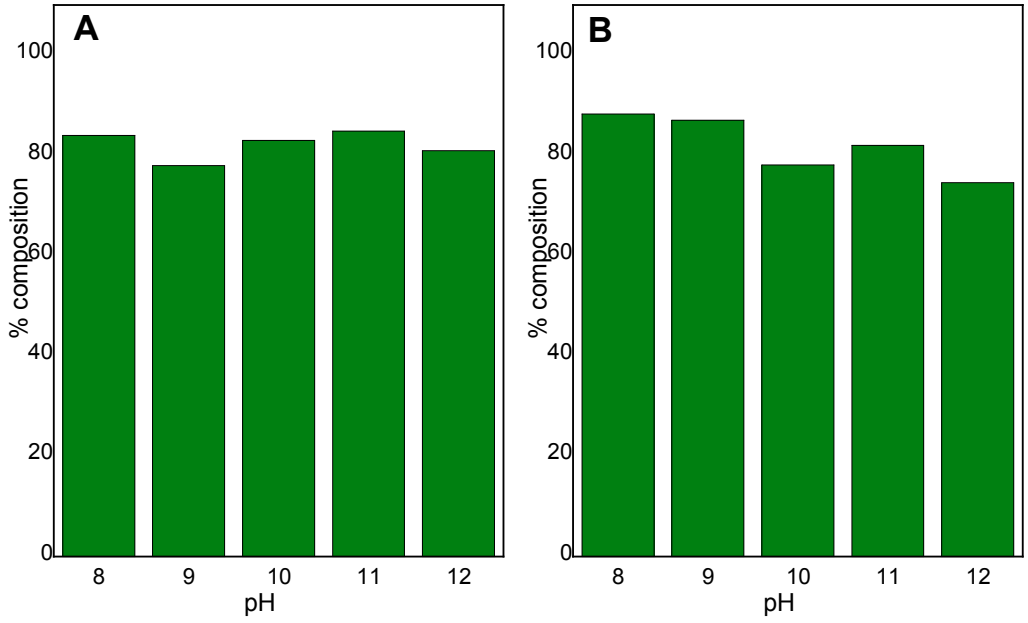

Figure 4.7 shows there is no real dependence for the alkylation of thiophosphorylated 5'-amino-5'-deoxyguanosine **114** with benzyl chloride on pH between pH 8 and 12. In these studies, the average conversion of 5'-amino-5'-deoxyguanosine to benzylalkylated thiophosphorylated 5'-amino-5'-deoxyguanosine **120** observed by ^{31}P

NMR spectroscopy was 84%. By-products observed by ^{31}P NMR spectroscopy following benzylation were inorganic phosphate and other phosphorus-containing species that were not identified. In comparison, Trmčić observed a 78% conversion for alkylation with benzyl chloride *via* the one-pot method. This shows a 6% increase in the conversion of 5'-amino-5'-deoxyguanosine to benzylalkylated thiophosphorylated 5'-deoxy-5'-aminoguanosine **120**.

4.3.2 Methyl iodide

Thiophosphorylated 5'-amino-5'-deoxyguanosine was *S*-alkylated with methyl iodide in aqueous solution of varying pH according to Scheme 4.10.

Scheme 4.10 ***S*-Alkylation of thiophosphorylated 5'-amino-5'-deoxyguanosine with methyl iodide in aqueous solution. Reaction pH was maintained through use of a pH stat instrument.**

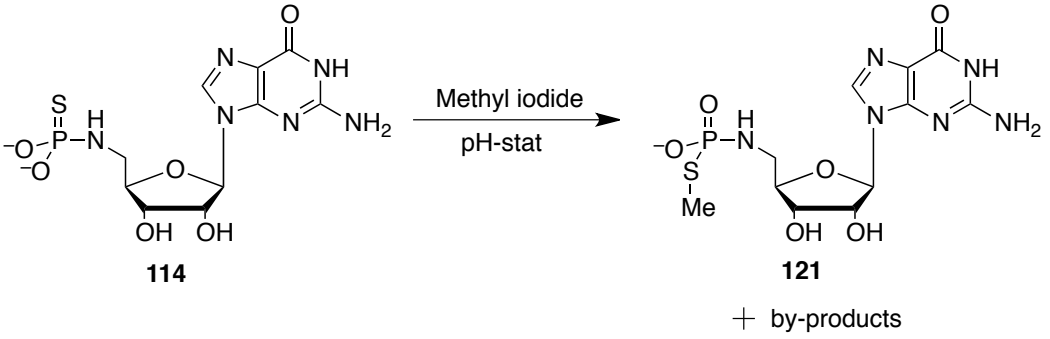

The resulting percentage conversions of methylalkylated thiophosphorylated 5'-amino-5'-deoxyguanosine **121** from pH 8 to 12 were determined by ^{31}P NMR spectroscopy and are shown in Figure 4.8.

Figure 4.8 **Percentage conversion of methylalkylated thiophosphorylated 5'-amino-5'-deoxyguanosine *vs* pH by A) ^{31}P and B) ^{1}H NMR spectroscopy in aqueous solution.**

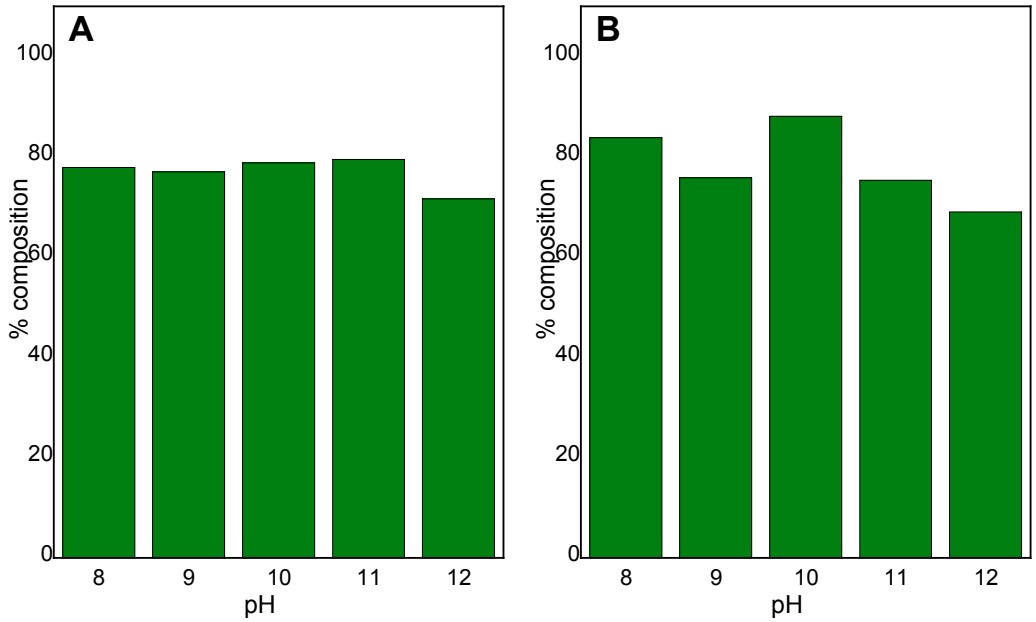

Figure 4.8 shows there is no real dependence for the methylation of thiophosphorylated 5'-amino-5'-deoxyguanosine **114** with methyl iodide on pH between pH 8 and 12. In these studies, the average conversion of 5'-amino-5'-deoxyguanosine to methylated thiophosphorylated 5'-amino-5'-deoxyguanosine **121** observed by ^{31}P NMR spectroscopy was 78%. By-products observed by ^{31}P NMR spectroscopy following methylation were inorganic phosphate and other phosphorus-containing species that were not identified. In comparison, Trmčić observed a 74 % conversion for alkylation with methyl iodide *via* the one-pot method. This shows a 4% increase in the conversion of 5'-amino-5'-deoxyguanosine to methylalkylated thiophosphorylated 5'-amino-5'-deoxyguanosine **121**.

4.3.3 Bromoethanol

Thiophosphorylated 5'-amino-5'-deoxyguanosine was *S*-alkylated with bromoethanol in aqueous solution of varying pH according to Scheme 4.11.

Scheme 4.11 ***S*-Alkylation of thiophosphorylated 5'-amino-5'-deoxyguanosine with bromoethanol in aqueous solution. Reaction pH was maintained through use of a pH stat instrument.**

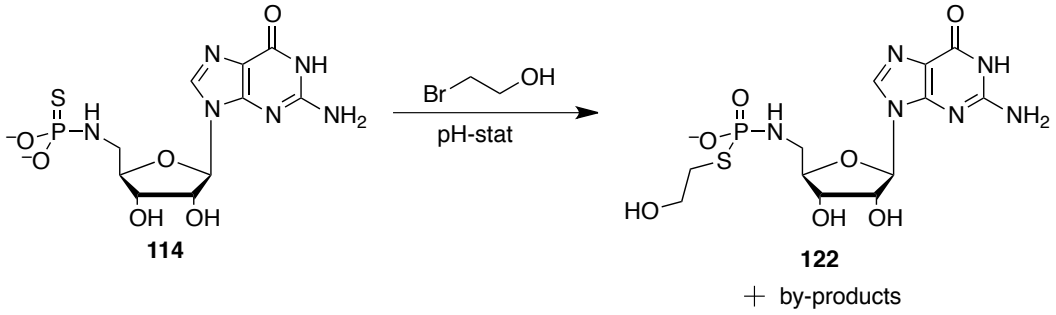

The resulting percentage conversions of ethanolalkylated thiophosphorylated 5'-amino-5'-deoxyguanosine **122** from pH 9 to 12 were determined by ^{31}P NMR spectroscopy and are shown in Figure 4.9.

Figure 4.9 **Percentage conversion of ethanolalkylated thiophosphorylated 5'-amino-5'-deoxyguanosine *vs* pH by A) ^{31}P and B) ^{1}H NMR spectroscopy in aqueous solution.**

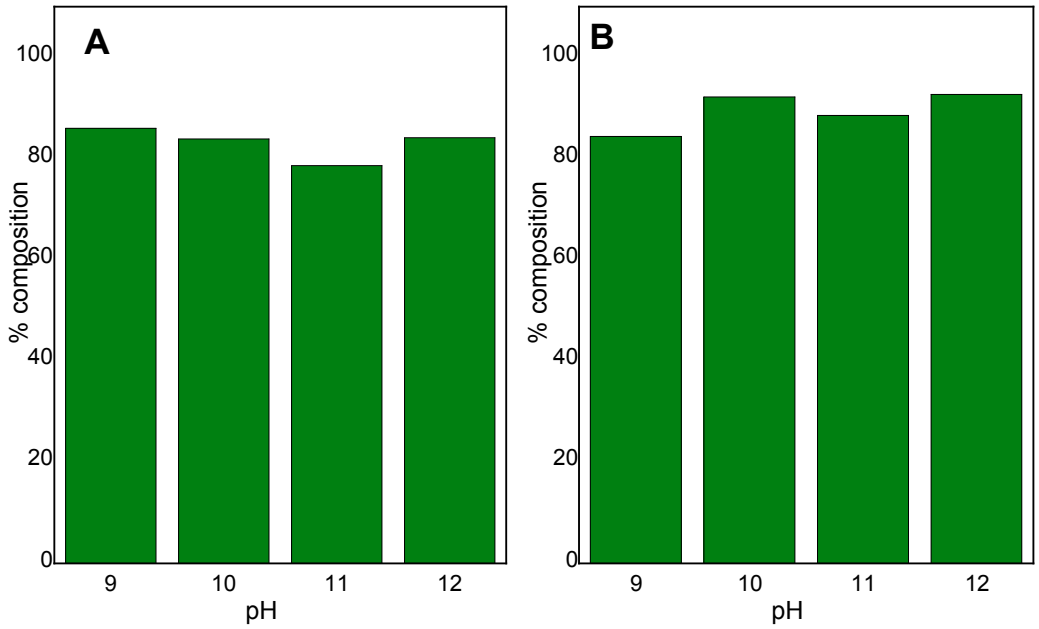

Figure 4.9 suggests there is no real dependence for the alkylation of thiophosphorylated 5'-amino-5'-deoxyguanosine **114** with bromoethanol on pH between pH 9 and 12. In these studies, the average conversion of 5'-amino-5'-deoxyguanosine to alkylated thiophosphorylated 5'-amino-5'-deoxyguanosine **122** observed by ^{31}P NMR spectroscopy was 83%. Inorganic phosphate and other

phosphorus containing by-products that were not identified were also observed by ^{31}P NMR spectroscopy.

4.4 Summary

We have in part applied our kinetic understanding to the (thio)phosphorylation of amines in aqueous solution. As part of these investigations we have determined and compared conversions of oxy and phosphodichloridate ion *vs* $POCl_3$ and $PSCl_3$ to (thio)phosphoramidate product, respectively. We observed greater selectivities toward aminolysis using 2-methoxyethylamine over hydrolysis processes for oxyphosphodichloridate ion vs $POCl_3$ in aqueous reaction mixtures. In contrast, selectivities toward aminolysis using 2-methoxyethylamine over hydrolysis processes in aqueous solution were slightly greater for $PSCl_3$ *vs* thiophosphodichloridate ion.

We then studied the conversion of thiophosphorylating agent to thiophosphoramidate product for reaction with 5'-amino-5'-deoxyguanosine in aqueous solutions of pH 11-12.5. The conversion of thiophosphodichloridate ion to thiophosphorylated 5'-amino-5'-deoxyguanosine was slightly greater than with thiophosphoryl chloride. The optimum reaction pH was determined to be pH=12 for both thiophosphorylating agents, where conversions to thiophosphoramidate product were greater than 90%. These high conversions demonstrate the effectiveness of this aqueous method towards the synthesis of (thio)phosphorylated 5'-amino nucleosides, where near quantitative conversion of (thio)phosphorylating agent to (thio)phosphoramidate is observed.

The alkylation of thiophosphorylated 5'-amino-5'-deoxyguanosine **114** with methyl iodide, benzyl chloride and bromoethanol was studied at high pH to determine the effects of pH on conversion levels of thiophosphoramidate to alkylated product. However, no real trends were observed for the conversion of thiophosphoramidate to alkylated product *vs* pH for any of the alkylating agents studied.

Chapter 5

Proton transfer at carbon in α-naphthylacetate esters

5.0 Foreword

The rate constants for exchange of hydrogen for deuterium at the α-CH_2 positions of naphthalen-1-yl-acetic acid *tert*-butyl ester **123** and 8-(*N*,*N*-dimethylamino-naphthalen-1-yl)-acetic acid *tert*-butyl ester **124** have been determined in potassium deuteroxide solutions in 1:1 D_2O:CD_3CN, in order to quantify the effect of the neighbouring *peri*-dimethylamino substituent on α-deprotonation.

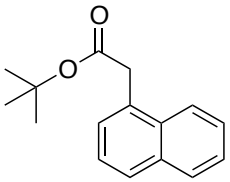

123

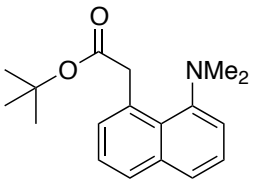

124

5.1 Introduction

Proton transfer is an essential part of enzymatic catalysis. Although typically fast, efficient catalysis is required to ensure that proton transfer does not become rate limiting. This is particularly important when dealing with proton transfer at carbon, or for concerted reactions involving bond formation or cleavage to heavy (i.e. non-hydrogen) atoms.

Small molecule models which contain catalytic functional groups held in close proximity to the substrate reaction centre may be studied as enzyme mimics as part of an investigation into catalysis in enzymes.[61-65] We are interested in the factors that control proton transfer in solution and at enzyme active sites. In this introduction we review literature pertaining to proton transfer in the active site of mandelate racemase and at carbon in two small enzyme mimics.

5.1.1 Proton transfer to and from carbon in mandelate racemase

Mandelate racemase (MR) catalyses the racemization of mandelate ion **125** by enolisation (Scheme 5.1).

Scheme 5.1 Proton transfer to carbon in the active site of mandelate racemase.[6]

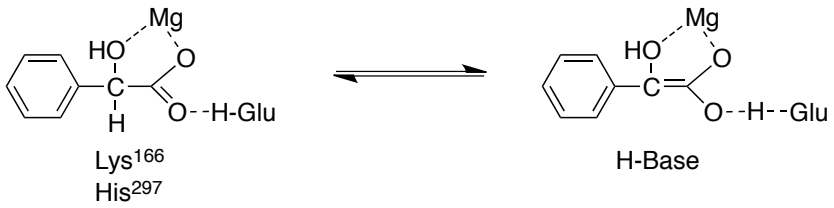

125

As shown in Scheme 5.1, an amine base of lysine-166 (conjugate acid pK_a of *ca* 10) inside the active site of mandelate racemase is able to deprotonate mandelate at the α -benzylic carbon (pK_a ca 22) in solution to give dianion 5.3.[66-68] Proton transfer from the imidazolium ion of His-297 or the amino group of Lys-166 to the benzylic carbon of **125** then results in the enolisation of either mandelate enantiomer. Given that deprotonation of the mandelate anion by a base of lower pK_a than the conjugate base (difference of 12 pK_a units) is thermodynamically unfavourable, proton transfer must

be highly efficient, and this is partially achieved through hydrogen bonding stabilization of the in-flight proton in the transition state.

5.1.2 Models systems for proton transfer at carbon

Proton transfer within the active site of mandelate racemase is postulated to have been developed and optimized through evolution in order to maximize the efficiency of catalysis.[66-68] Through the use of simple synthetic enzyme models, it is possible to alter the geometry and arrangement of neighbouring functional groups, in order to develop efficient proton transfer systems, which may help explain why proton transfer is so efficient in enzymes such as mandelate racemase.

Effective molarity (EM), defined as the ratio of intramolecular first-order and *inter*molecular second order rate constants, provides a means of quantifying the efficiency of intramolecular proton transfer in small model systems. High effective molarities are observed for intramolecular proton transfer in small molecules when the transition state and resulting product are stabilized by a strong intramolecular hydrogen bond[63, 65, 69-71]. To illustrate this principle, two enzyme mimics of high effective molarities will now be discussed.

5.1.2.1 Intramolecular general acid catalysis of enol ether 126

Williams and Kirby studied the hydrolysis of enol ether **126**, involving irreversible proton transfer from the neighbouring carboxy group to give oxocarbenium ion **127** and subsequent acylal product **128** (Scheme 5.2).[71]

Scheme 5.2 Intramolecular catalysis of enol ether protonation

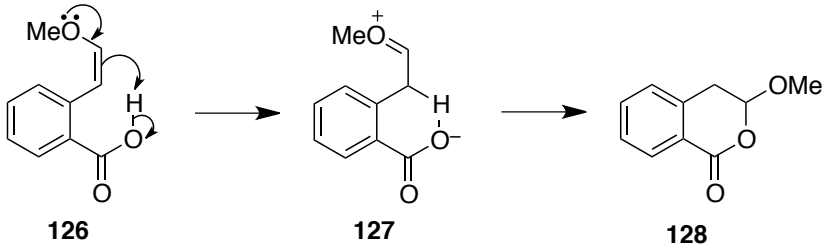

126 **127** **128**

A pH- k_{obs} profile for the hydrolysis of methyl vinyl ether **126** was constructed

from first-order k_{obs} values determined in aqueous buffered solution between pH 0 and 5, at 39 °C and I=1 (KCl) (Figure 5.1).

Figure 5.1 **First-order rate constants for the hydrolysis of methyl vinyl ether 126 as a function of pH in aqueous buffered solution at 39 °C and I=1 (KCl).**[71]

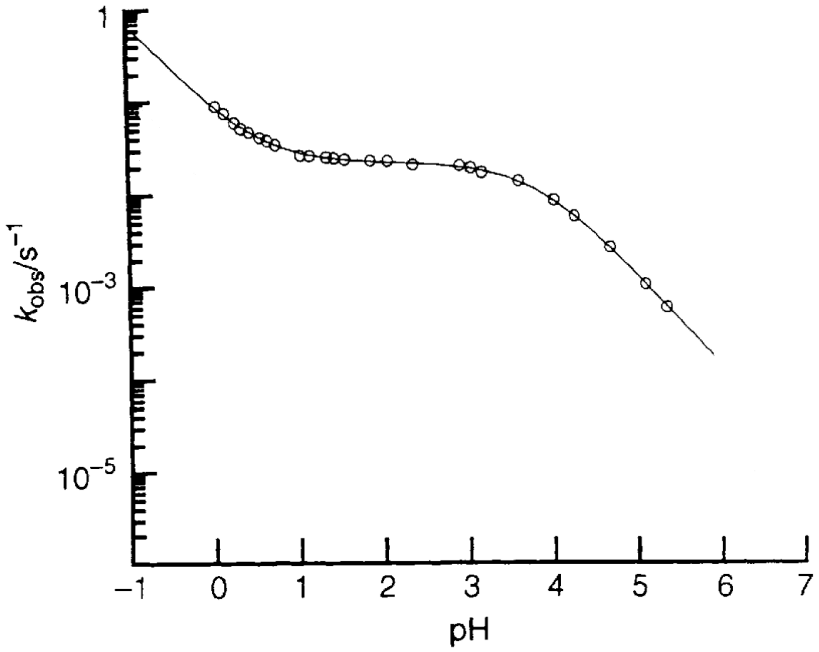

(Reproduced with permission from Royal Society Chemistry)

The pH-k_{obs} profile in Figure 5.1 is constructed from three different pH regions, where k_{obs} depends on the ionisation state of the neighbouring carboxy group (pK_a = 3.80 ± 0.02). At low pH (pH < ~1), the decrease in k_{obs} is due to external acid-catalysed hydrolysis of enol ether **126**. Between pH 1 and 3.5 lies a pH-independent region due to intramolecular general acid-catalysed hydrolysis. At high pH (pH > ~3.5), the carboxy group is mainly in its anionic form, and resulting decreases in k_{obs} are due only to external acid-catalysed hydrolysis.

An effective molarity of 2200 M was determined for intramolecular proton transfer to carbon in the hydrolysis of enol ether **126**.[71] Such a high EM for general acid catalysis was attributed to a stabilising intramolecular hydrogen bond in the transition state for proton transfer.

5.1.2.2 Intramolecular general acid catalysis of enol ether 129

Efficient intramolecular proton transfer was also observed by O'Carroll and Kirby for the hydrolysis of enol ether **129** (Scheme 5.3).[65]

Scheme 5.3 ***Peri*-dimethylammonium catalysis of enol ether protonation.**

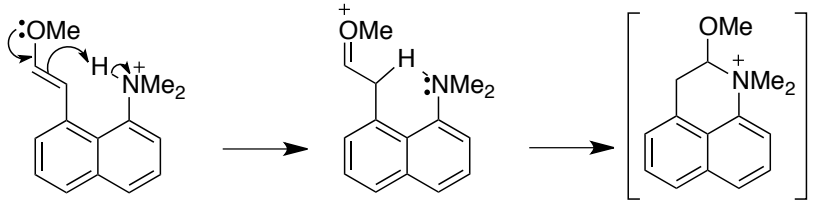

129 **130** **131**

The effective molarity for intramolecular catalysis of the hydrolysis of enol ether **129** by the neighbouring *peri*-dimethylammonium group was determined to be greater than 60000 M. This is the highest EM recorded for intramolecular proton transfer at carbon and was attributed to the formation of a strong intramolecular hydrogen bond in oxocarbocation intermediate **130**.[65]

Proton transfer to carbon from the *peri*-dimethylammonium group in **129** is so efficient that the rate-determining step is not proton transfer to carbon, but instead is the opening of the strong intramolecular hydrogen bond to the oxocarbenium ion intermediate **130**, which is followed by the rapid addition of the *peri*-dimethylamino group to give **131** (Scheme 5.3).[65] Due to the strength of the intramolecular hydrogen bond in intermediate **130**, exchange of hydrogen for deuterium with solvent D_2O is not observed.

5.1.3 Project outline

The structure of 8-(*N*,*N*-dimethylamino-naphthalen-1-yl)-acetic acid *tert*-butyl ester **124** has been designed as a small model to mimic proton transfer at carbon in the active site of mandelate racemase.

The *peri*-dimethylammonium substituent of enol ether **129** has already been shown to be extremely efficient in the catalysis of the reverse proton transfer reaction in enol ether hydrolysis (Scheme 5.2). Ester **124** has a similar geometry and arrangement of functional groups to ether **129** and so proton transfer between the α-CH_2 proton and neighbouring *peri*-dimethylammonium substituent is expected to be extremely efficient, such that **124** should act as an effective enzyme mimic to MR.

The first aim of the project was to synthesise naphthalen-1-yl-acetic acid *tert*-butyl ester **123** and 8-(*N*,*N*-dimethylamino-naphthalen-1-yl)-acetic acid *tert*-butyl ester **124**. Ester **124** differs from ester **123** by the presence of the *peri*-dimethylamino group in the neighbouring position to the methylene-ester substituent on the naphthalene ring.

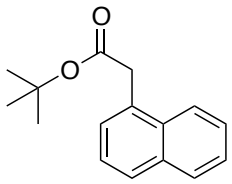

123

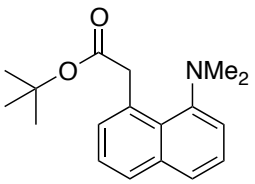

124

The second aim of the project was to study proton transfer at the α-CH_2 positions of naphthalen-1-yl-acetic acid *tert*-butyl ester **123** and 8-(*N*,*N*-dimethylamino-naphthalen-1-yl)-acetic acid *tert*-butyl ester **124**. As part of these studies, we have determined the pK_a of the *peri*-dimethyl ammonium substituent of ester **124** by conventional UV-Vis spectrophotometry. A deuterium exchange method was used to follow the exchange of hydrogen for deuterium at the α-CH_2 positions of α-naphthyl esters **123** and **124** in order to probe the effect of the *peri*-dimethylamino substituent on keto-enol tautomerization. Intramolecular catalysis by the *peri*-dimethyl ammonium substituent of ester **124** has been modelled computationally using DFT calculations.

5.2 Results

5.2.1 Synthesis of Naphthalene Esters

Naphthalen-1-yl-acetic acid *tert*-butyl ester **123** was synthesised in two steps from 1-naphthyl acetic acid **132** (Scheme 5.4).

Scheme 5.4 Synthesis of naphthalen-1-yl-acetic acid *tert*-butyl ester 123

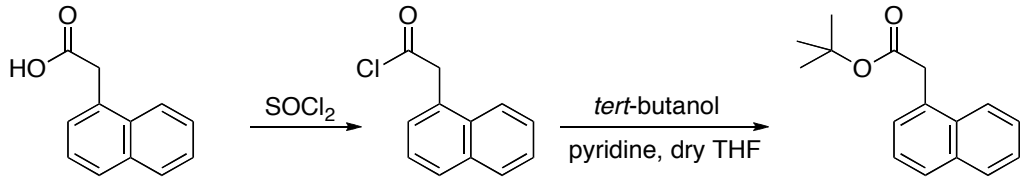

132 **133** **123**

43%

Reaction of 1-naphthyl acetic acid **132** with $SOCl_2$ resulted in the formation of acid chloride **133**. Nucleophilic attack by *tert*-butanol on acid chloride **133** in the presence of pyridine gave ester **123**. Purification by column chromatography using an eluent of (9:1) cyclohexane: diethyl ether afforded **123** as a colourless oil in a yield of 43 %.

8-(*N,N*-dimethylamino-naphthalen-1-yl)-acetic acid *tert*-butyl ester **124** was synthesised in three steps from 1-naphthyl acetic acid **134** (Scheme 5.5).

Scheme 5.5 Synthesis of 8-(*N,N*-dimethylamino-naphthalen-1-yl)-acetic acid *tert*-butyl ester 124.

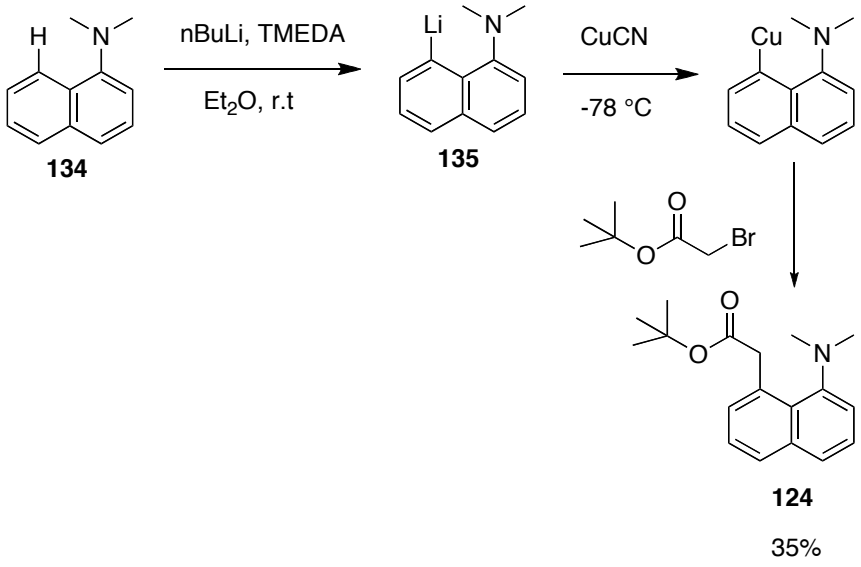

Lithiation of 1-naphthyl acetic acid **134** in the presence of *n*BuLi and *N,N′,N′,N′*-tetramethylethylenediamine resulted in the formation of the lithiated intermediate **135**. The addition of copper(I) cyanide by cannulation under inert conditions resulted in the exchange of lithium for copper(I). *Tert*-butyl bromoacetate was subsequently added to generate crude ester **124**. Purification by column chromatography using an eluent of (9:1) cyclohexane: diethyl ether afforded **124** as a colourless oil in a yield of 35 %.

5.2.2 Determination of the pK_a of the *peri*-dimethylammonium substituent of ester 124

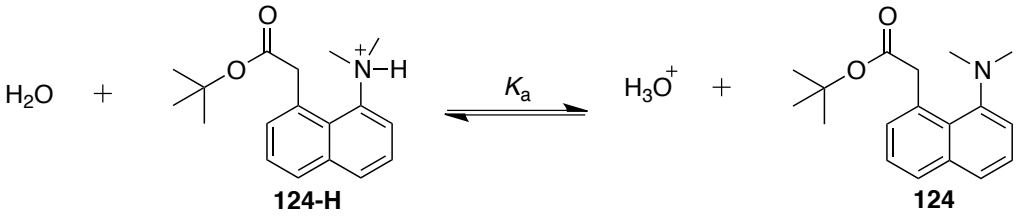

The pK_a of the *peri*-dimethyl ammonium substituent **124-H** was determined by conventional UV-Vis spectrophotometric methods.

UV-Visible spectra of 8-(*N,N*-dimethylamino-naphthalen-1-yl)-acetic acid *tert*-butyl ester (3×10^{-5} M) at varying pH were recorded at 25 ºC. Due to the insolubility of ester

124 in H_2O, it was necessary to perform all UV-Visible experiments in solutions of 1:1 H_2O:CH_3CN. These are shown in Figure 5.2, with scans 1-13 corresponding to the conditions presented in Table 5.1.

Figure 5.2 UV-Visible spectra of ester 2 and 2-H in 1:1 H_2O:CH_3CN solutions of varying pH at 25 °C.

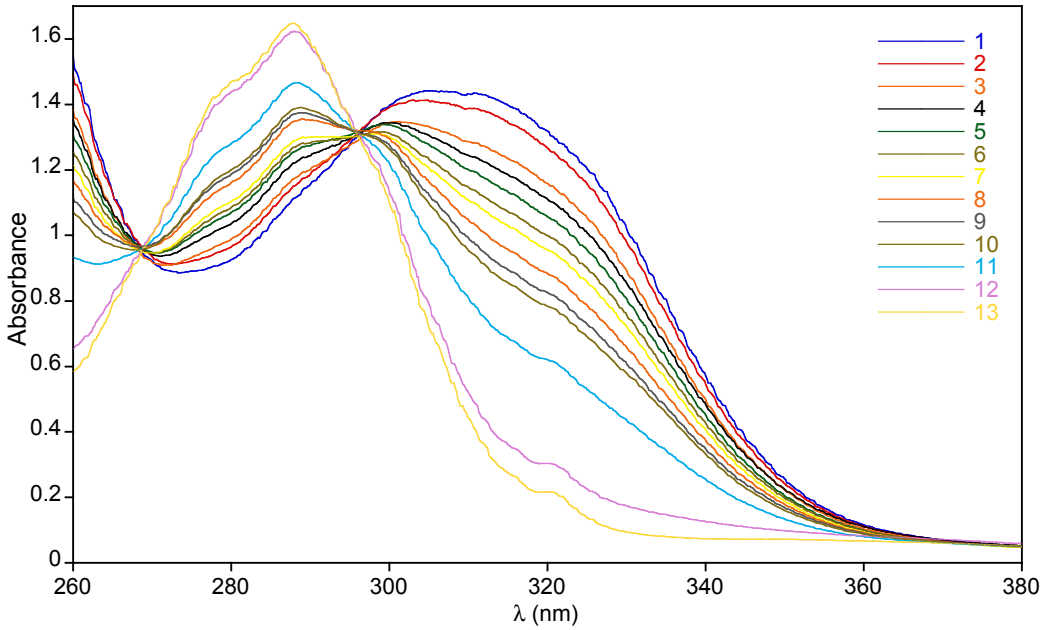

Table 5.1 Absorbance data for solutions of 8-(*N,N*-dimethylamino-naphthalen-1-yl)-acetic acid *tert*-butyl ester[a] 124 and 124-H in 1:1 H_2O:CH_3CN of varying pH at 325 nm and 25 °C, *I*=0.1 (KCl).

Spectrum number	Buffer	pH	A_{obs}[b]
1	0.1 M KOH	13.95	1.207
2	0.045 M H_3PO_4 / 0.005 M KH_2PO_4	2.37	1.151
3	0.01 M HCl	1.89	1.032
4	0.015 M HCl	1.71	1.004
5	0.02 M HCl	1.61	0.952
6	0.025 M HCl	1.51	0.895
7	0.03 M HCl	1.40	0.852
8	0.04 M HCl	1.26	0.790
9	0.05 M HCl	1.18	0.724
10	0.06 M HCl	1.11	0.681
11	0.1 M HCl	0.88	0.524
12	0.5 M HCl	0.18	0.224
13	2 M HCl[c]	0.03	0.136

(a) The concentration of 8-(*N,N*-dimethylamino-naphthalen-1-yl)-acetic acid *tert*-butyl ester was 3×10^{-5} M

(b) A_{obs} is the absorbance at 325 nm for a given mixture of neutral and protonated amine

(c) Measurements taken at an ionic strength greater than 0.1 M.

A comparison of spectra obtained in 0.1 M HCl and 0.1 M KOH solutions showed a distinct red shift upon deprotonation of the *peri*-substituent. In a solution of 2.0 M HCl the observed absorbance maximum at λ = 325 nm represents 100% protonated ester **124-H** (Figure 5.2). In contrast, in a solution of 0.1 M KOH the observed absorbance minimum at λ = 325 nm represents 100% neutral ester **124**. The absorbance due to the protonated species and the neutral species at 325 nm are referred to as A_{max}^{325} and A_{min}^{325} respectively. Between A_{max}^{325} and A_{min}^{325} lies a mixture of protonated and neutral forms of the ester **124-H** and **124** (the amount of each species is dependant on the pH of the solution) giving an absorbance of A_{obs}^{325}.

The observed changes in absorbance of ester **124** with pH at 325 nm were fitted by non-linear least squares to Equation 5.1.

$$A_{obs} = \frac{A_{min}10^{-pH} + K_a A_{max}}{10^{-pH} + K_a}$$ **Equation 5.1**

In Equation 5.1, A_{obs} is the observed absorbance at a given pH, A_{max} is the absorbance of the neutral amino substituent and A_{min} is the absorbance of the fully protonated ammonium ion form at λ = 325 nm.

The observed absorbance, A_{obs}, of each sample (at 325 nm) was plotted againsted the corresponding pH of each solution and is shown in Figure 5.3.

Figure 5.3 **Non-linear least squares fitting to Equation 5.1 of the change in the observed absorbance, A_{obs} (325 nm), of ester 124 with pH in 1:1 H_2O:CH_3CN solutions.**

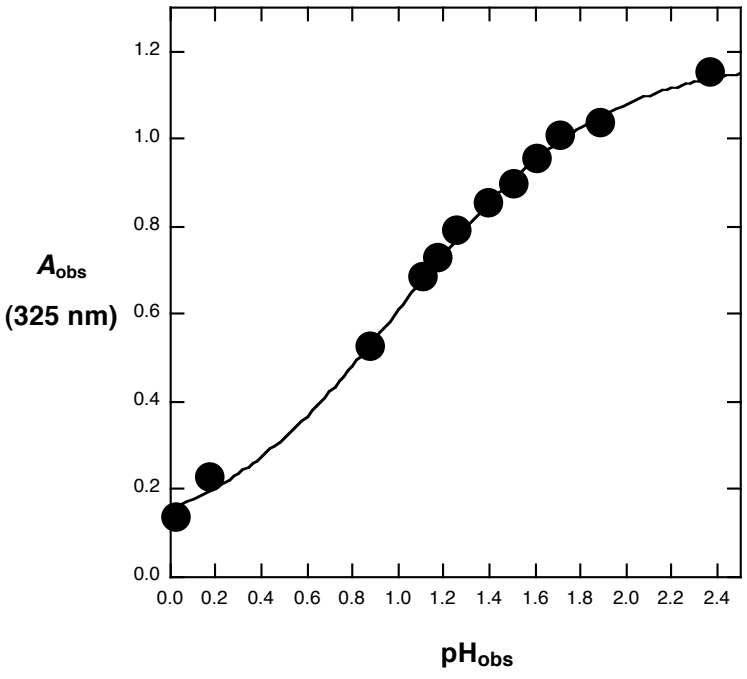

The changes in absorbance with pH at the chosen analytical wavelength, λ = 325 nm, were fitted to Equation 5.1 using a non-linear least squares analysis to give an equilibrium constant K_a = 9.61 × 10^{-2} M (pK_a = 1.02 ± 0.03) for the *peri*-dimethylammonium substituent of naphthalene ester **124**.

5.3.2 Deuterium exchange of naphthalene esters followed by ^{1}H NMR spectroscopy

Rate constants for deuterium exchange of naphthalene esters **123** and **124** were measured in 1:1 D_2O:CD_3CN solutions of varying concentration of potassium deuteroxide using ^{1}H NMR spectroscopy.

The exchange of hydrogen for deuterium of naphthyl esters **123** and **124** was analysed at a range of pD values by 400 MHz and 500 MHz ^{1}H NMR spectroscopy respectively. Due to the insolubility of esters **123** and **124** in D_2O, it was necessary to perform all deuterium exchange experiments in solutions of 1:1 D_2O:CD_3CN. The disappearance of the α-CH_2 in D_2O solution due to deuterium exchange was monitored at 25 °C and *I*=0.1 (KCl). From these data, first and second-order rate constants for deprotonation of substrate by deuterioxide ion to give the corresponding mono-deuterated exchange products were estimated.

The exchange of hydrogen for deuterium at the α-carbon of naphthyl esters **123** and **124** is shown in Scheme 5.6.

Scheme 5.6 Deuterium exchange at α-carbon of naphthalene esters 123 and 124.

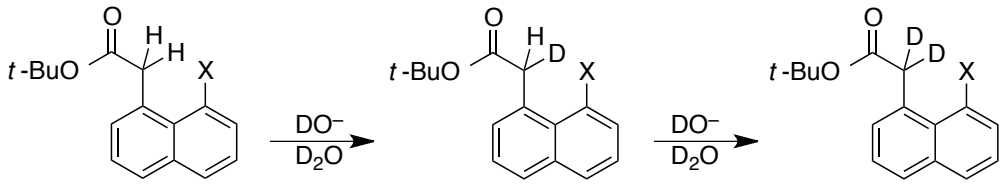

123 X = H
124 X = NMe_2

136 X = H
137 X = NMe_2

138 X = H
139 X = NMe_2

Due to the small concentrations of each naphthyl ester (5 mM) used in exchange experiments, the concentration of DOH formed during exchange was insignificant in comparison to the concentration of solvent D_2O. As a result, deprotonation by deuteroxide must be followed by irreversible conversion to give the mono-deuterated exchange products **136** and **137** upon reprotonation in D_2O. Additional exchange at the α-carbon of **136** and **137** leads to the di-deuterated products **138** and **139**, respectively.

Hydrolysis of naphthyl esters **123** and **124** was not observed throughout the deuterium exchange studies. This is likely to be due to the presence of the bulky *tert*-butyl groups, which hinder and prevent attack of the carbonyl group by D_2O / DO^-. It was therefore possible to follow exchange of H for D for both esters for three half-lives in the absence of any competing side reactions.

The deuterium exchange reactions of ester **123** were analysed using 400 MHz ^{1}H NMR spectroscopy. Each reaction was performed on a large scale (12 mL) and initiated by the addition of KOD (of varying concentration) in D_2O (6 mL) to a solution of substrate and internal standard in acetonitrile (6 mL). Samples were immediately incubated at 25 °C in a water bath and reaction progress was monitored over time by withdrawing aliquots (800 μL) at timed intervals. These aliquots were immediately quenched to pD 9 by addition of >1 M DCl solution. The samples were stored at –20 °C prior to analysis by ^{1}H NMR spectroscopy.

The deuterium exchange experiments of ester **124** were analysed using 500 MHz ^{1}H NMR spectroscopy. Following the addition of deuteroxide to substrate, each sample (0.75 mL) remained in the NMR probe at 25 °C throughout the reaction time course with spectra being taken over varying time periods. Each ^{1}H NMR spectrum was recorded over a period of 24 minutes (64 transients). For reactions monitored directly in the NMR probe, the reaction time *t* was calculated from the time at the midpoint of the analyses.

A typical ^{1}H NMR spectrum showing the peaks due to the α-CH_2 and α –CHD protons, obtained during the exchange reaction of naphthyl ester substrate **123** in 1:1 D_2O:CD_3CN at 25 °C and I=0.1 (KCl), is shown in Figure 5.4.

Figure 5.4 **A typical ^{1}H NMR spectrum, obtained during the exchange reaction of naphthyl ester substrate 123 in 1:1 D_2O:CD_3CN at 25 °C and *I*=0.1 (KCl).**

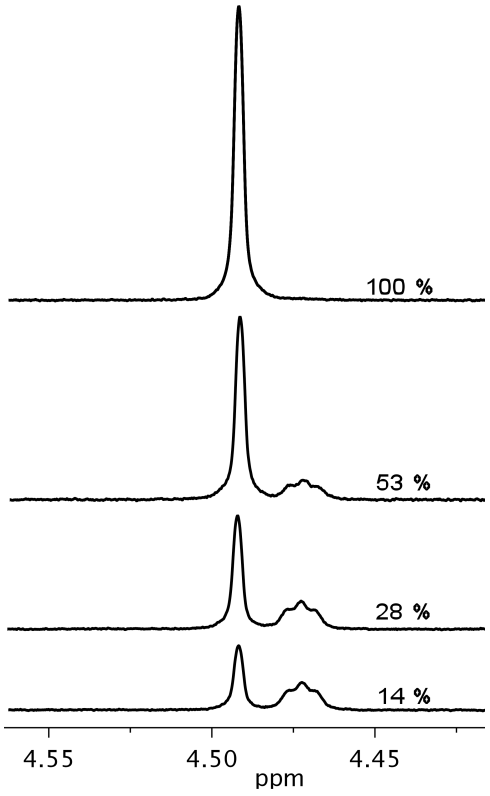

The signals due to the α-CH_2 protons of esters **123** and **124** are visible as broad singlets at 4.49 and 4.71 ppm, respectively. Over time the area of these signals decay to give upfield multiplets at 4.47 and 4.69 ppm, due to the formation of the mono-deuterated products **136** and **137**. The signal due to the twelve methyl hydrogens of the internal standard, tetramethylammonium deuteriosulfate, appears as a broad singlet at 3.60 ppm. Splitting at the top of this broad singlet to give a multiplet is observed in high-resolution spectra due to coupling of ^{15}N to the methyl hydrogens. The hydrogens of the internal standard do not undergo exchange under the reaction conditions used.

The progress of deuterium exchange of naphthalene esters **123** and **124** was monitored by measuring the decrease in the integrated area of the singlet corresponding to the α-CH_2 (4.49 and 4.71 ppm, A_{CH2}), over time relative to the twelve non-exchanging methyl hydrogens of the internal standard at 3.60 ppm (A_{std}). By comparison there was

no detectable change in the areas of the peaks due to all other protons relative to the standard peak with time.

The fraction of substrate remaining, *f*(s), for naphthyl esters **123** and **124** was determined from Equation 5.2.

$$f(\mathrm{s}) = \frac{(A_{\mathrm{CH_2}}/A_{\mathrm{Std}})_{\mathrm{t}}}{(A_{\mathrm{CH_2}}/A_{\mathrm{Std}})_{\mathrm{t}=0}} \qquad \textbf{Equation 5.2}$$

The observed pseudo-first-order rate constants for exchange of the α-CH_2 of **123** and **124** for deuterium were then determined from semi-logarithmic plots of *f*(s) against time (Equation 5.3). Rate constants were obtained for the first three half-lives of each exchange reaction and were examined with 6-13 data points. The resulting plots from Equation 5.3 were linear.

$$\ln f(\mathrm{s}) = -k_{\mathrm{obs}}\mathrm{t} \qquad \textbf{Equation 5.3}$$

The pseudo-first-order rate constant for deuterium exchange is formally the sum of the first-order rate constants for exchange by solvent D_2O, intramolecular *peri*-dimethylamino group, and deuteroxide ion (Equation 5.4).

$$k_{\mathrm{obs}} = k_{\mathrm{D_2O}} + k_{\mathrm{NMe_2}} + k_{\mathrm{DO}}[\mathrm{DO^-}] \qquad \textbf{Equation 5.4}$$

Negligible intercepts were observed for plots of k_{obs} against potassium deuterioxide concentration (Figures 5.7 and 5.10). On this basis, the k_{D_2O} and k_{NMe_2} terms may be removed and, thus, the experimentally observed rate constant (k_{obs}, s^{-1}) determined in this work may therefore be represented by Equation 5.5.

$$k_{\mathrm{obs}} = k_{\mathrm{DO}}[\mathrm{DO^-}] \qquad \textbf{Equation 5.5}$$

The second-order rate constants for the deuterium exchange of naphthalene esters **123** and **124**, k_{DO}–($M^{-1}s^{-1}$), were determined from the gradients of the plots of k_{obs} (s^{-1}) against concentration of deuteroxide (M).

5.3.2.1 H/D exchange of naphthalen-1-yl-acetic acid *tert*-butyl ester 123

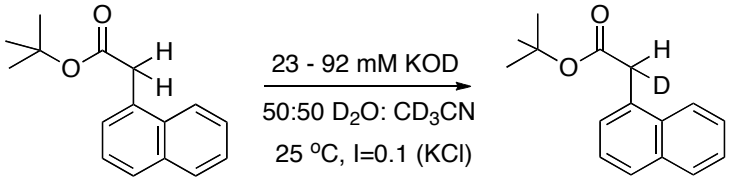

123 **136**

Rate constants for deuterium exchange of naphthalen-1-yl-acetic acid *tert*-butyl ester **123** in 1:1 D_2O:CD_3CN solutions of varying concentrations of potassium deuteroxide at 25 °C were monitored by 400 MHz ^{1}H NMR spectroscopy. In the case of the exchange reactions of naphthalen-1-yl-acetic acid *tert*-butyl ester **123**, all of the tabulated reaction data is presented in Appendix C.

Figure 5.5 shows representative ^{1}H NMR spectra illustrating the deuterium exchange of naphthalen-1-yl-acetic acid *tert*-butyl ester **123** (5 mM, 0.083 M KOD), obtained during the exchange for deuterium of the α-CH_2 in 1:1 D_2O:CD_3CN at 25 °C and I=0.1 (KCl). Deuterium exchange results in the disappearance of the singlet peak corresponding to the α-CH_2 at 4.49 ppm (B) to form the α-CHD multiplet at 4.47 ppm (C) due to mono-deuterated exchange product **136**. The disappearance of the singlet (B) is measured relative to the internal standard peak (D). As the reaction proceeds, the singlet (B) decreases in intensity, and the intensity of the upfield multiplet (C) initially increases. Deuterium exchange of **136** to form the di-deuterated exchanged product **138** results in a decrease in the intensity of multiplet (C). The peaks due to the aromatic protons appear as a multiplet at 7.85-8.50 ppm (A). The peak due to the $C(CH_3)_3$ protons appears as a singlet at 1.87 ppm (E). No additional signals due to other products (e.g. hydrolysis) were identified during the timescale for complete deuterium exchange of naphthalen-1-yl-acetic acid *tert*-butyl ester **123**. In the reaction timeframe there is no change in the total integrated area for the signals due to all other protons relative to the constant peak area of the broad triplet at 3.60 ppm (D) due to the internal standard, indicating that exchange of hydrogen for deuterium is not occurring at any position other than at α-CH_2 under the experimental conditions used.

Figure 5.5 **Representative ^{1}H NMR spectra at 400 MHz of the deuterium exchange of naphthalen-1-yl-acetic acid *tert*-butyl ester 123 (5 mM, 0.083 M KOD), obtained during exchange of the α-CH_2 for deuterium in 1:1 D_2O:CD_3CN at 25 ºC and *I*=0.1 (KCl). The time elapsed is indicated above each spectrum in seconds.**

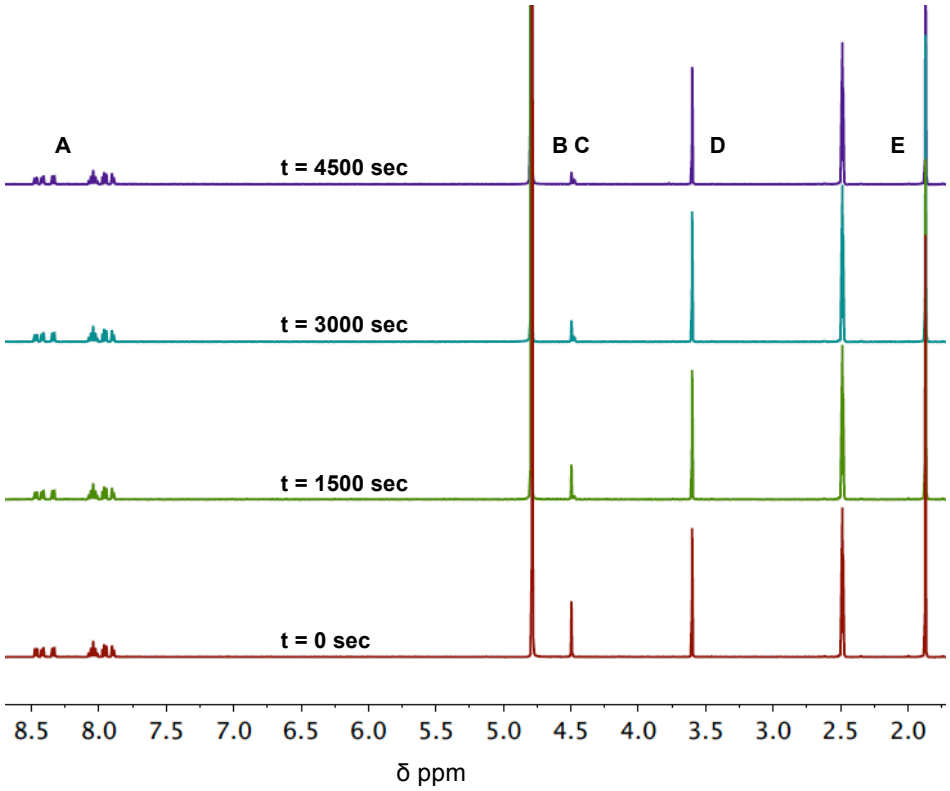

Semi-logarithmic analysis of the fraction of un-reacted ester **123** over time by application of Equations 5.2 and 5.3 yielded first-order rate constants k_{obs} (s^{-1}) at six different concentrations of KOD. The results of these studies are summarised in Figure 5.6 and Table A.9 (Appendix C).

Figure 5.6 **Semi-logarithmic plot of the fraction of remaining α-CH_2 hydrogen against time for the deuterium exchange of naphthalen-1-yl-acetic acid *tert*-butyl ester at 0.023 M (■), 0.046 M (●), 0.060 M (♦), 0.070 M (▼), 0.083 M (▲), and 0.092 M (◢) KOD in 1:1 D_2O:CD_3CN at 25 ºC, *I*=0.1 (KCl).**

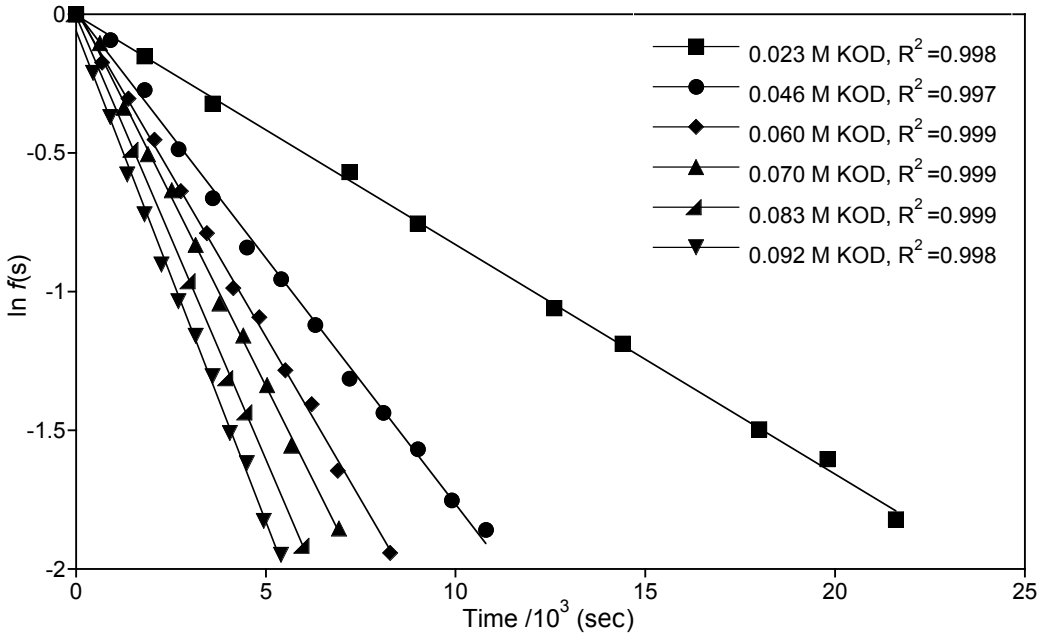

The combined reaction data of naphthalen-1-yl-acetic acid *tert*-butyl ester **123** in deuteroxide solution are shown in Figure 5.7.

Figure 5.7 **Plot of k_{obs} (s^{-1}) against [KOD] (M) for the deuterium exchange reaction of naphthalen-1-yl-acetic acid *tert*-butyl ester 123 in 1:1 D_2O:CD_3CN at 25 °C, *I*=0.1 (KCl).**

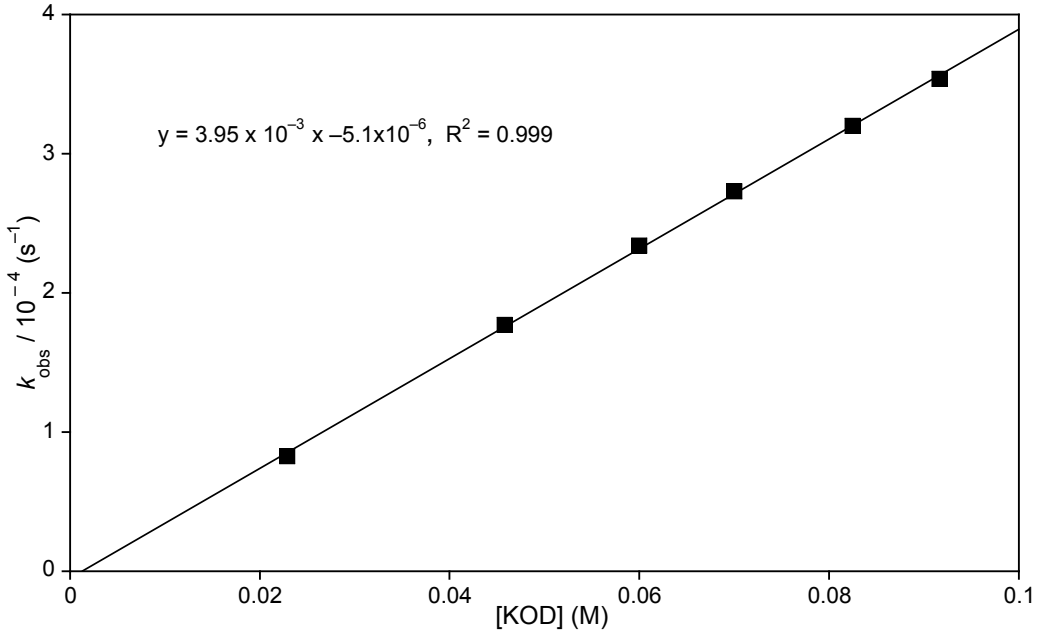

The second-order rate constant k_{DO} for the deuterium exchange of naphthalen-1-yl-acetic acid *tert*-butyl ester **123** was determined from the slope in Figure 5.7 as k_{DO} = 3.95×10^{-3} $M^{-1}s^{-1}$.

5.3.2.2 H/D exchange of 8-(*N*,*N*-dimethylamino-naphthalen-1-yl)-acetic acid *tert*-butyl ester 124

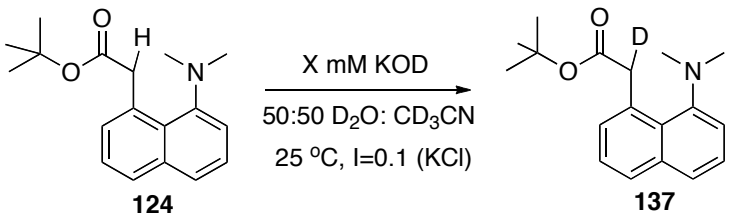

124 **137**

Deuterium exchange of 8-(*N*,*N*-dimethylamino-naphthalen-1-yl)-acetic acid *tert*-butyl ester **124** in 1:1 D_2O:CD_3CN of varying concentrations of potassium deuteroxide at 25 °C was monitored by 500 MHz ^1H NMR spectroscopy.

Figure 5.8 shows representative ^{1}H NMR spectra illustrating the deuterium exchange of 8-(*N*,*N*-dimethylamino-naphthalen-1-yl)-acetic acid *tert*-butyl ester **124** (5 mM, 0.070 M KOD), obtained during the exchange for deuterium of the α-CH_2 in 1:1 D_2O:CD_3CN at 25 °C and I=0.1 (KCl). Deuterium exchange results in the disappearance of the singlet peak corresponding to the α-CH_2 at 4.71 ppm (B) to form the α-CHD multiplet at 4.69 ppm (C) due to mono-deuterated exchange product **137**. The disappearance of the singlet (B) is measured relative to the internal standard peak (D). As the reaction proceeds, the singlet (B) decreases in intensity, and the intensity of the upfield multiplet (C) initially increases. Deuterium exchange of **137** to form the di-deuterated exchanged product **139** results in a decrease in the intensity of multiplet (C). The peaks due to the aromatic protons appear as a multiplet at 7.72-8.33 ppm (A). The signals due to the $N(CH_3)_2$ protons appear as a singlet at 3.10 ppm (E). The peak due to the $C(CH_3)_3$ protons appear as a singlet at 1.85 ppm (F). No additional signals due to other products (e.g. hydrolysis) were identified during the timescale for complete deuterium exchange of 8-(*N*,*N*-dimethylamino-naphthalen-1-yl)-acetic acid *tert*-butyl ester **124**. In the reaction timeframe there is no change in the total integrated area for the signals due to all other protons relative to the constant peak area of the broad triplet at 3.60 ppm (D) due to the internal standard, indicating that exchange of hydrogen for deuterium is not occurring at any position other than at α-CH_2 under the experimental conditions used.

Figure 5.8 **Representative ^{1}H NMR spectra at 500 MHz of the deuterium exchange of 8-(*N*,*N*-dimethylamino-naphthalen-1-yl)-acetic acid *tert*-butyl ester 124 (5 mM), in 0.070 M KOD solution in 1:1 D_2O:CD_3CN at 25 °C and *I*=0.1 (KCl). The time elapsed is indicated above each spectrum in seconds.**

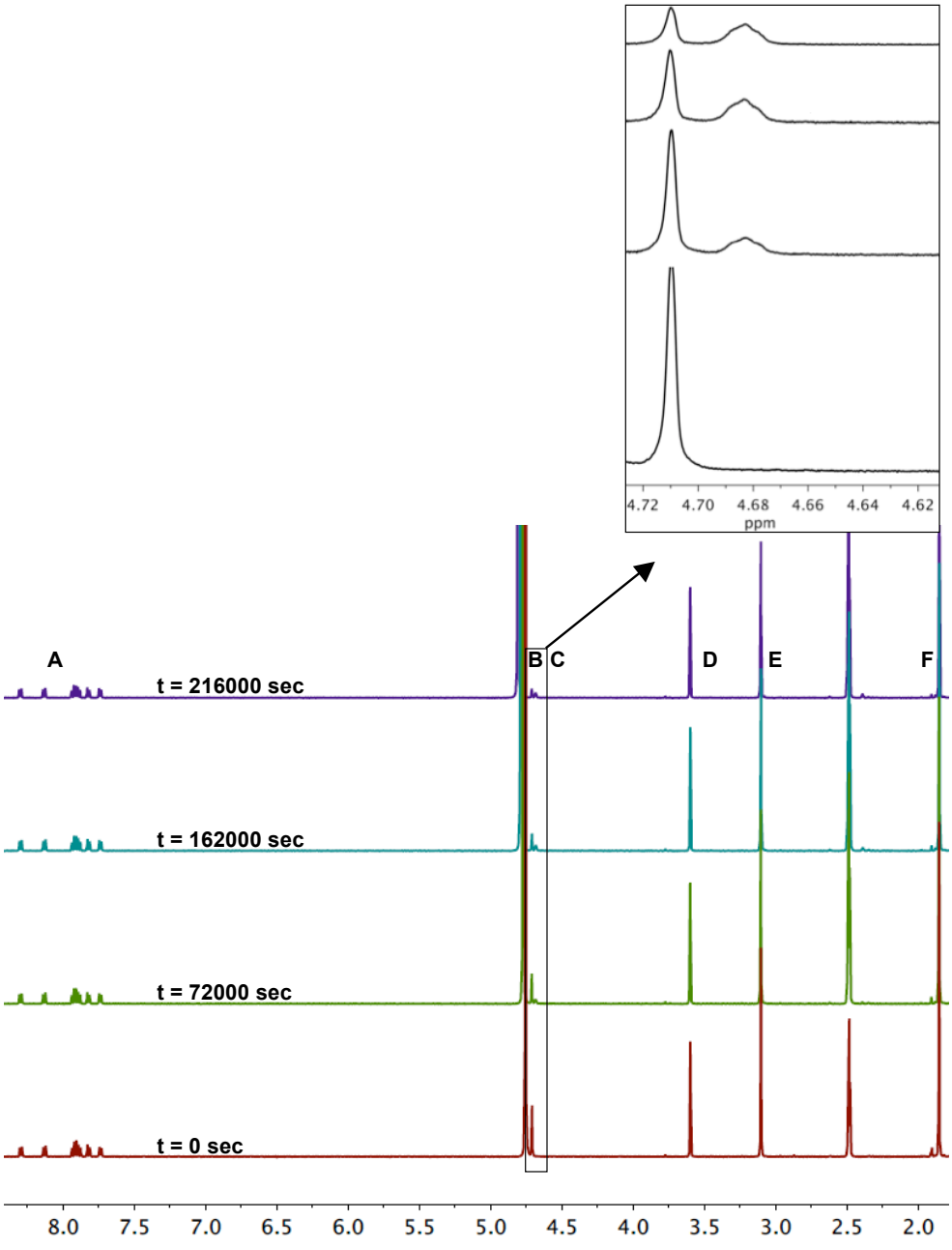

Semi-logarithmic analysis of the fraction of un-reacted ester **124** over time by application of Equations 5.2 and 5.3 yielded first-order rate constants k_{obs} (s^{-1}) at six different concentrations of KOD. The results of these studies are summarised in Figure

5.9 and Table A.10 (Appendix C).

Figure 5.9 **Semi-logarithmic plot of the fraction of remaining α- carbon CH_2 hydrogen against time for the deuterium exchange of 8-(*N*,*N*-dimethylamino-naphthalen-1-yl)-acetic acid *tert*-butyl ester 124 (5mM) at 0.023 M (■), 0.046 M (●), 0.060 M (♦), 0.070 M (▼), 0.083 M (▲), and 0.092 M (◢) KOD in 1:1 D_2O:CD_3CN at 25 ºC, *I*=0.1 (KCl).**

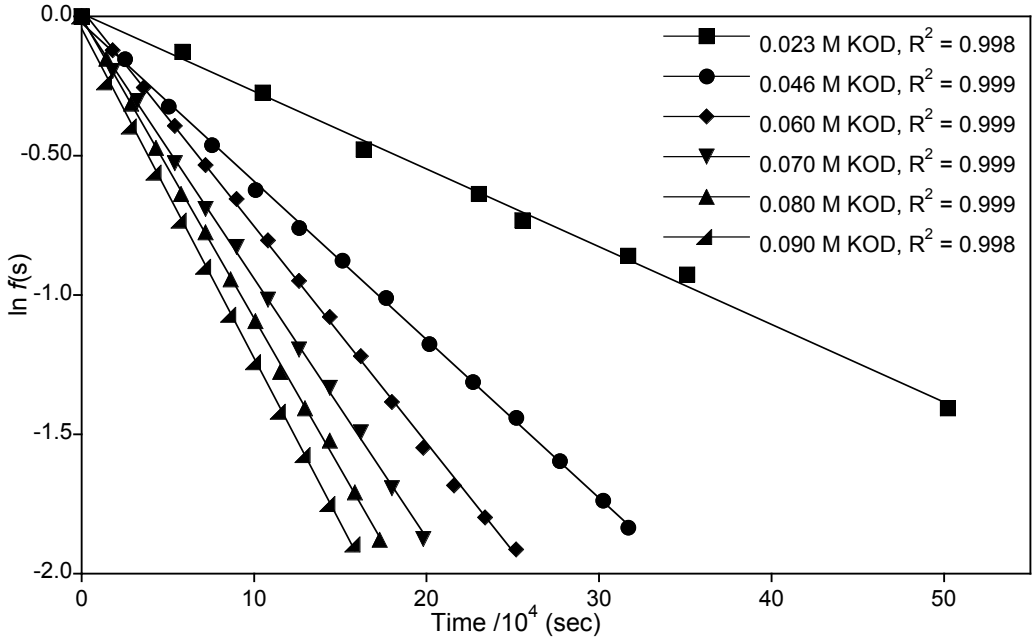

The combined reaction data of 8-(*N*,*N*-dimethylamino-naphthalen-1-yl)-acetic acid *tert*-butyl ester **124** in deuteroxide solution are shown in Figure 5.10.

Figure 5.10 Plot of k_{obs} (s^{-1}) against [DO^-] (M) for the deuterium exchange reaction of 8-(*N*,*N*-dimethylamino-naphthalen-1-yl)-acetic acid *tert*-butyl ester 124 in 1:1 D_2O:CD_3CN at 25 ºC, *I*=0.1 (KCl).

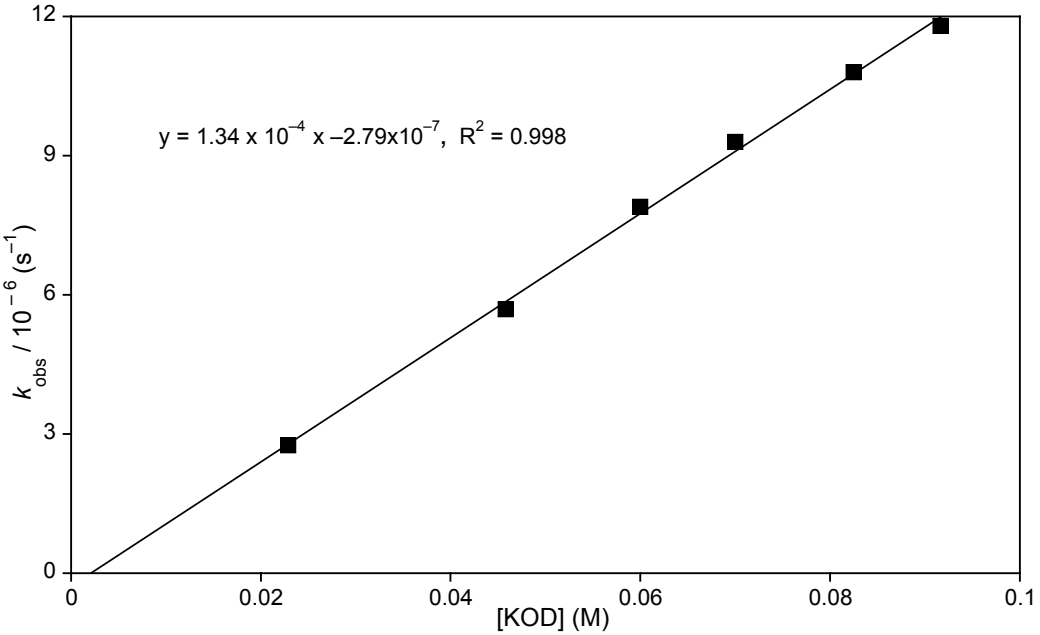

The second-order rate constant k_{DO} for the deuterium exchange of 8-(*N*,*N*-dimethylamino-naphthalen-1-yl)-acetic acid *tert*-butyl ester **124** was determined from the slope in Figure 5.10 to be $k_{DO}= 1.35 \times 10^{-4}$ $M^{-1}s^{-1}$.

5.3.3 Computational studies of deuterium exchange

As part of investigations of proton transfer at carbon, computational modelling of naphthalen-1-yl-acetic acid *tert*-butyl ester and 8-(*N*,*N*-dimethylamino-naphthalen-1-yl)-acetic acid *tert*-butyl ester was undertaken using the Gaussian09 package[72] with the DFT hybrid functional B3LYP method[73, 74] and the 6-31G* basis set.[75, 76]

Computational studies of esters **123** and **124** were performed under 'gas-phase' conditions which are simpler to model than those under 'solution-phase, where complicated factors observed in aqueous acid and base solutions must be considered.

5.3.3.1 pK_a of the *peri*-dimethylammonium substituent on ester 124

The UV-Vis spectra of 8-(*N*,*N*-dimethylamino-naphthalen-1-yl)-acetic acid *tert*-butyl ester (322 nm) and its protonated form (299 nm) were determined computationally and are in close agreement with experimentally determined results 312 and 289 nm in aqueous solution for **124** and **124-H**, respectively) (Figure 5.2). Molecular orbital diagrams were calculated for the lowest energy bands of 8-(*N*,*N*-dimethylamino-naphthalen-1-yl)-acetic acid *tert*-butyl ester and its protonated form 2-H. These are given in Figure 5.11.

Figure 5.11 Computed molecular orbital diagrams for 8-(*N*,*N*-dimethylamino-naphthalen-1-yl)-acetic acid *tert*-butyl ester 124 and its protonated form 124-H

Compound	HOMO	LUMO
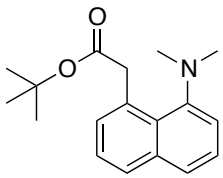 **124**	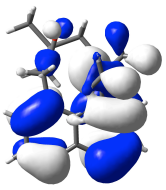	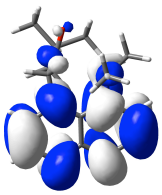
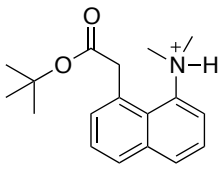 **124-H**	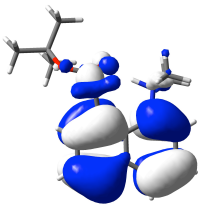	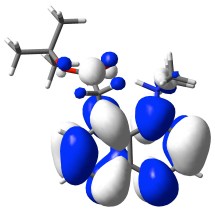

The lowest energy band for 8-(*N*,*N*-dimethylamino-naphthalen-1-yl)-acetic acid *tert*-butyl ester **124** is assigned to the π(NMe_2 + naphthalene) > π* (naphthalene) transition and the lowest energy band for **124-H** is assigned to the π(naphthalene) > π* (naphthalene) transition.

Computed 'gas-phase' acidities and experimental pK_a values for water, 8-(*N*,*N*-dimethylamino-naphthalen-1-yl)-acetic acid *tert*-butyl ester and enol ether **129** are given in Table 5.2.

Table 5.2 Computed 'gas-phase' acidities and experimental pK_a values for water and amines 124 and 129.

Compound	Computed 'gas-phase' acidities (*k*cal mol^{-1})	Experimental pK_a
water	175.8	–1.74
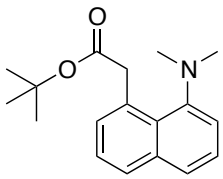 **124**	251.6	1.02
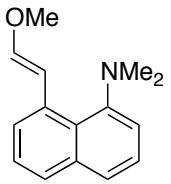 **129**	261.9	4.01

The data in Table 5.2 shows that the trend of computed 'gas-phase' acidities corresponds with the trend in experimentally determined pK_a values.

5.3.3.2 Keto-enol tautomerism of naphthalene esters 123 and 124

The relative energies of keto and enol tautomers of naphthalene esters **123** and **124** have been calculated and are presented in Figure 5.12.

Figure 5.12 Relative energies of keto and enol tautomers of A) 8-(*N*,*N*-dimethylamino-naphthalen-1-yl)-acetic acid *tert*-butyl ester and B) naphthalen-1-yl-acetic acid *tert*-butyl ester.

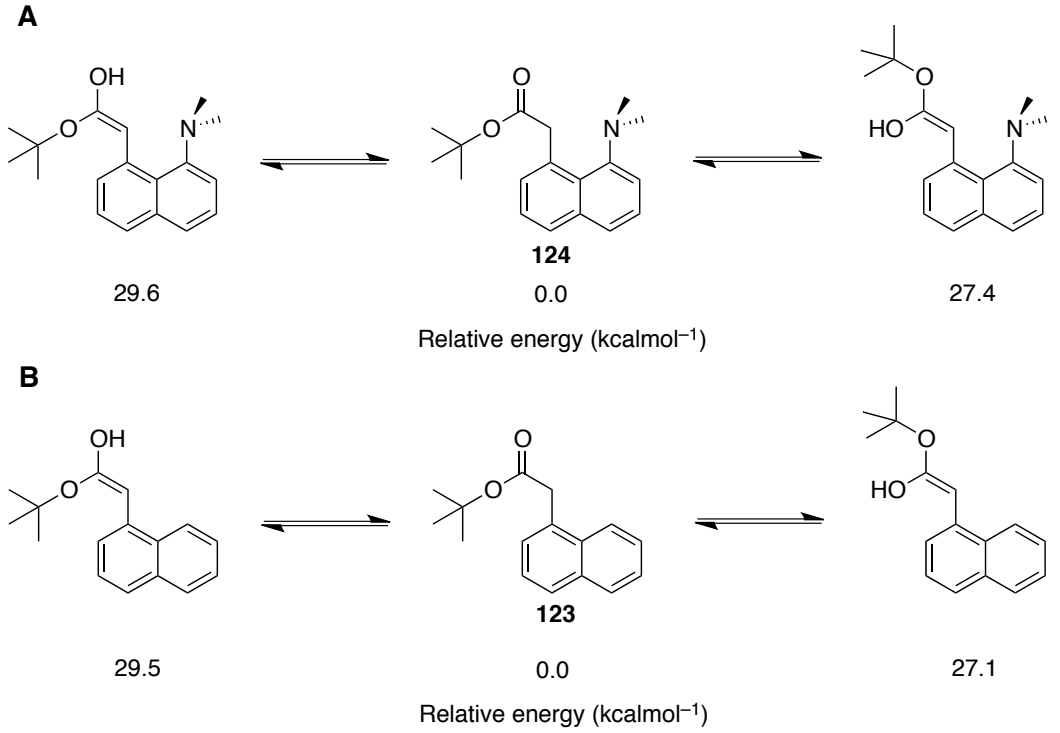

The relative energies for keto-enol tautomerisation (Figure 5.12) are computationally similar for naphthalene esters **123** and **124**. Thus, the *peri*-dimethylamino group of ester **124** appears to have no effect on keto-enol tautomerism. In both cases, the keto form is more stable than the enol form by ~27 kcalmol^{-1}. This observation is consistent with experimental ^{1}H NMR spectroscopic data, where each ester is only observed in its keto form.

5.4 Discussion

5.41 Determination of the pK_a of the *peri*-dimethylammonium substituent

The pK_a of the *peri*-dimethylammonium substituent of naphthalene ester **124** has been determined by UV-Vis spectrophotometry as 1.02 ± 0.03 in 1:1 H_2O:CH_3CN (Section 5.3.2). Given that all deuterium exchange studies were undertaken at high pD (> 12), it is clear that the *peri*-substituent will be present in its neutral form under these conditions. Therefore, any *intramolecular* proton transfer reaction that may occur will be pD-independent.

Table 5.3 reports literature pK_a values for X-substituted *peri*-dimethylamino naphthalene:

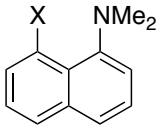

Table 5.3 Literature pK_a values for X-substituted *peri*-dimethylamino naphthalene.

X-$H^+$$NMe_2$	pK_a
H	4.6
NMe_2	12.1
OPO_3^{2-}	9.31
OCH_2OMe	7.75
OMe	7.40
$OP(O)_2OMe^-$	7.01 ± 0.5
$OP(O)(OEt)_2$	4.63
E-CH=CHOMe	4.01 ± 0.08[65]
t-$BuO_2C.CH_2$	1.02 ± 0.03

The data in Table 5.3 indicates that the *peri*-dimethylammonium group of **124** is significantly less basic than would be expected based on the pK_a of the *peri*-dimethylammonium substituent of enol ether **129** (pK_a = 4.01 ± 0.08), which is similar in structure and geometry to ester **124**.[65] The pK_a of the NMe_2 group of ester **124** is

lower than all others in Table 5.3 including dimethylaminonaphthalene (X = H, pK_a = 4.6). The lower pK_a could be due to the relief of steric congestion between the two *peri*-substituents upon loss of a proton.

5.4.2 Deuterium exchange of naphthalene esters 123 and 124

Second order rate constants for deuteroxide-catalysed exchange, k_{DO}, of hydrogen for deuterium at the α-CH_2 position of naphthalene esters **123** and **124** have been determined as 3.95×10^{-3} and 1.38×10^{-4} $M^{-1}s^{-1}$ respectively. A relatively small suppression (28.6 fold) of deuteroxide-catalysed exchange upon addition of the *peri*-dimethylammonium substituent of ester **123** was observed. In order to determine the cause of a 29-fold suppression in the rate of exchange, all potential mechanisms of exchange for esters **123** and **124** will be discussed.

5.4.2.1 Mechanism of exchange of ester 123

A detailed mechanism for deuterioxide ion-catalysed exchange of naphthyl ester **123** is shown in Scheme 5.7.

Scheme 5.7 Pathway for deuterium exchange at the α -carbon of naphthalene ester 123

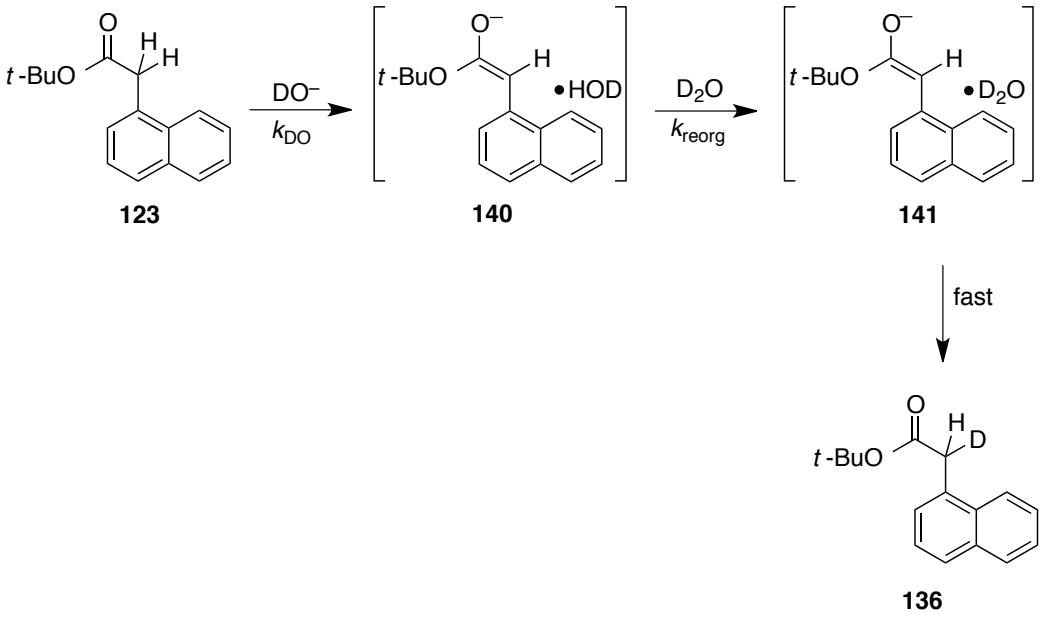

123 **140** **141** **136**

In 1:1 D_2O:CD_3CN solution, the deuterioxide base encounters ester **123** and results in proton abstraction (k_{DO}) to give [enolate.HOD] complex **140**. The large excess of solvent deuterium atoms from D_2O (55 M D in 1:1 D_2O:CD_3CN) ensures that solvent reorganisation of HOD with bulk solvent occurs to give [enolate.D_2O] complex **141**. The intimate solvated pair is then rapidly deuterated to give mono-deuterated exchange product **136**. The rate constant for solvent reorganization, k_{reorg} may be equated to that for the dielectric relaxation of the solvent, $k_{reorg} \approx 10^{11}$ s^{-1}. Exchange of the remaining hydrogen for deuterium at the α-carbon position can occur *via* an identical pathway to give di-deuterated product **138**.

5.4.2.2 Mechanism of exchange of ester 124

Exchange of hydrogen for deuterium at the α-carbon position of naphthyl ester **124** may proceed either *via* an intramolecular (A or B) or intermolecular pathway (C) (Scheme 5.8).

Scheme 5.8 Potential pathways for deuterium exchange at the α-carbon of naphthyl ester 124

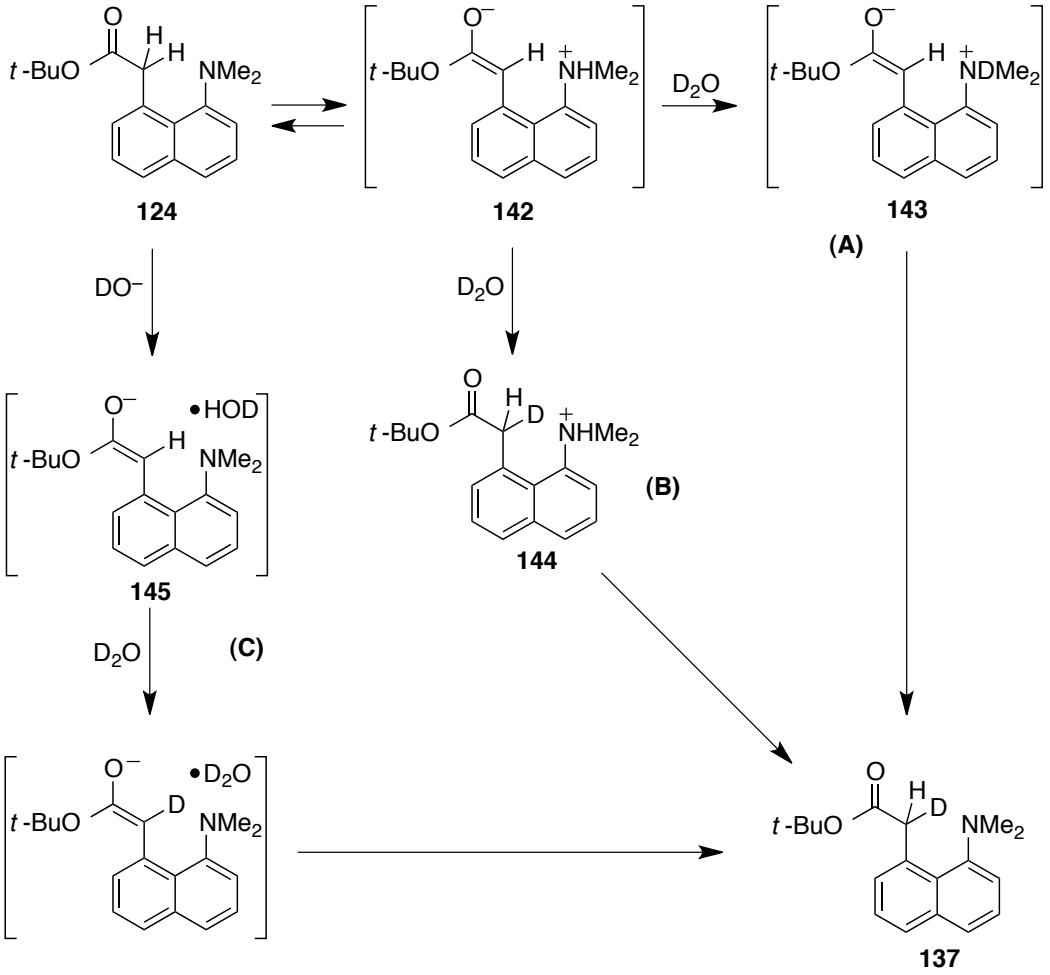

Any intramolecular exchange must involve deprotonation of the α-CH_2 proton by the adjacent *peri*-dimethylamino substituent to generate zwitterionic enolate **142**. Exchange of hydrogen for deuterium could then occur *via* two possible routes. The exchange of hydrogen for deuterium at the *peri*-dimethyl ammonium group of zwitterion **142** may generate zwitterionic enolate **143**, and subsequent intramolecular protonation of the α- carbon by the *peri*-ammonium group would then occur to generate mono-deuterated ester **137** (pathway A). Alternatively, reprotonation of zwitterion enolate **142** in solvent D_2O would give **144**, which in turn would give ester **137** by deprotonation of the adjacent *peri*-dimethyl ammonium group by deuteroxide ion (pathway B).

However, a positive intercept was not observed in the plot of first order rate constants against deuteroxide concentration (Figure 5.10 Section 5.3), indicating there are no intramolecular exchange processes that compete with the intermolecular deprotonation by deuteroxide ion (0.025 – 0.093 M) within the range of pD values studied. It was not possible to follow exchange at lower pD values by ^{1}H NMR spectroscopy due to significantly longer reaction times. For example, the half-life for exchange of hydrogen for deuterium of ester **124** at pD 11.8 (50% FB quinuclidine buffer) was estimated as 23 days at 25 ºC. As a consequence, it was not possible to identify whether any competing intramolecular exchange reactions were in operation at a lower pD.

For intramolecular deuterium exchange to occur, the replacement of hydrogen for deuterium of the ammonium group by solvent D_2O (k_1) and/ or protonation of enolate in D_2O (k_2) must be faster than the reprotonation of enolate **142** to regenerate ester **124** (k_{HNMe2}).

The magnitude of k_{HNMe2+} may be estimated through comparison of known rate constants for the protonation of typical enolates with amine basicity. For example, the protonation of the enolate of ethyl acetate by protonated 3-quinuclidinone (pK_a = 7.5) has been estimated to be diffusion limited.[77, 78] Given that the *peri*-dimethylammonium substituent is 6.5 pK_a units more acidic than 3-quinuclidinone, it is expected that the intermolecular protonation of enolate **142** by an external Brønsted acid of pK_a ~ 1 will be diffusion limited. The intramolecular protonation of enolate **142** by the *peri*-dimethylammonium group, k_{HNMe2+}, is therefore expected to be significantly faster than this given the greater acidity of the *peri*-dimethylammonium group.

The rate constant for proton exchange between protonated quinuclidines (pK_a = 4.62) and water has been determined as < 10^3 s^{-1}.[79] Due to the greater acidity of the *peri*-dimethylammonium group versus the quinuclidinium ion, the rate constant k_{HNMe2+} is expected to be greater than 10^3 s^{-1}. However, even after taking this into account, proton exchange between the *peri*-dimethylammonium substituent and solvent D_2O will be significantly slower than reprotonation of enolate **142** to give starting ester **124** as the *peri*-dimethylammonium ion is significantly more acidic than D_2O as a Brønsted

acid. Therefore, reprotonation of the enolate by the *peri*-dimethylammonium ion would still be expected to be much faster than protonation of enolate by D_2O.

Given that the pK_a value of the *peri*-dimethylammonium group is 15.6 pK_a units lower than that of solvent deuterium oxide (pK_a = 16.6 in 100% water), it seems to be likely that intramolecular deprotonation at the α -CH_2 groups of ester **124** by the *peri*-dimethylamino substituent cannot outcompete intermolecular deprotonation by the significantly more basic deuteroxide ion present at relatively high concentrations (0.025 – 0.092 M). In contrast, intramolecular protonation of enol ether **129** by the peridimethylammonium group (pK_a = 4.01) efficiently outcompetes intermolecular protonation by up to 1 M hydronium ion, H_3O^+ (pK_a = -1.74).

The failure to observe intramolecular general base catalysis of the deuterium exchange reaction of **124** may also be due to a steric barrier to rotation of the *peri*-dimethylammonium group into a position where the deuterium exchange reaction with D_2O can occur. A steric barrier to rotation would therefore further favour intramolecular reprotonation over exchange in the case of enolate **142**. In addition, the hydrogen bond between the carbanion and *peri*-dimethylammonium proton of enolate **142** must be cleaved in order for exchange with solvent D_2O to occur. Although hydrogen bonds to weakly electronegative carbanions are thought to be weak, its presence may still hinder intramolecular deuterium exchange.

Given that deuterium exchange of ester **124** cannot proceed *via* either intramolecular pathway (A or B), exchange must proceed by intermolecular exchange pathway C *via* **145**, analogous to that of ester **123**. Second order rate constants for deuteroxide-catalysed exchange, k_{DO}, of hydrogen for deuterium at the α-CH_2 position of naphthalene esters **123** and **124** have been determined as 3.95×10^{-3} and 1.38×10^{-4} $M^{-1}s^{-1}$ respectively. The observed 29.3-fold suppression of deuterium exchange by the *peri*-dimethylamino substituent can only be attributed to electronic substituent effects and/ or steric repulsions associated with intermolecular deprotonation by deuteroxide ion.

5.4.3 Estimation of the carbon acid pK_a values for naphthyl esters 123 and 124

Carbon acid pK_a values may be estimated for naphthalene esters **123** and **124** using the observed rate constants for deuteroxide-catalysed exchange, k_{DO}. T. Aymes and J. P. Richard estimated the pK_a of ethyl acetate as 25.6 in aqueous solution, from the combination of the second order rate constant for deprotonation by deuteroxide in D_2O (k_{DO} = 1.7 x 10^{-3} $M^{-1}s^{-1}$) with a secondary solvent isotope effect of k_{DO}/k_{HO} = 1.4 (calculated from reactions involving proton transfer from carbon to lyoxide ion).[77] From the combination of k_{DO} values for intermolecular deuteroxide-catalysed exchange of naphthyl esters **123** and **124** with k_{DO}/ k_{HO} = 1.4, second order rate constants of k_{HO} = 2.82 × 10^{-3} $M^{-1}s^{-1}$ and 9.64 ×10^{-5} $M^{-1}s^{-1}$ were estimated for the deprotonation of esters **123** and **124** by hydroxide ion at α-carbon, respectively.

J. P. Richard and co-workers have correlated of k_{HO} parameters for the deprotonation of neutral α-carbonyl acids with corresponding carbon acid pK_a values in water.[78] A linear correlation was observed for a broad range of aldehydes, ketones, esters and amides using Equation 5.6, in which both k_{HO} and pK_a are statistically corrected for the number of acidic protons, p, at the carbon acid.

$$\log(\frac{k_{HO}}{p}) = 6.52 - 0.40\ (pK_a + \log p) \qquad \textbf{Equation 5.6}$$

pK_a values of 23.1 and 26.8 can be estimated for esters **123** and **124** through the application of second order rate constants of k_{HO} = 2.82 × 10^{-3} $M^{-1}s^{-1}$ and 9.64 ×10^{-5} $M^{-1}s^{-1}$, and p = 2 to Equation 5.6. These values are similar in magnitude to the pK_a value of 25.6 determined for ethylacetate in aqueous solution.[77] A pK_a decrease of 2.5 pK_a units is observed from ethyl acetate to ester **123**, which is similar to the pK_a decrease observed in from ethylacetate to α-phenylethyl acetate (pK_a = 22.7) in water.[80] This suggests that the *tert*-butyl functional group and 50% acetonitrile co-solvent has little effect on carbon acidity relative to that of the α-aryl substituent. A pK_a increase of 1.2 pK_a units is observed from ethyl acetate to ester **124**, which suggests that the *peri*-dimethylamino group counteracts the acidifying α-naphthyl substituent effect resulting in an overall increase in basicity relative to ethyl acetate.

5.4 Summary

Intramolecular general base catalysis by the (weakly basic) neighbouring group was not detected. Negligible intercepts were observed for plots of k_{obs} against potassium deuterioxide concentration (Figures 5.5 and 5.8). Second-order rate constants, k_{DO}, for the deuterium exchange reactions of esters **123** and **124** have been determined as 3.95×10^{-3} $M^{-1}s^{-1}$ and 1.35×10^{-4} $M^{-1}s^{-1}$, respectively. The unexpected 29-fold decrease in the k_{DO} value upon the introduction of a *peri*-dimethylamino group is attributed to an unfavourable steric and/or electronic substituent effect on intermolecular deprotonation by deuteroxide ion. From the experimental k_{DO} values, carbon acid pK_a values of 23.1 and 26.8 have been calculated for esters **123** and **124**.

From the study of two small proton transfer enzyme mimics (**126** and **129**),[65, 71] the positioning of functional groups in ester **124** was predicted to be optimal for efficient intramolecular proton transfer. Unfortunately, it is not possible to quantify any intramolecular effect because intramolecular reprotonation of enolate **142** is faster than the intermolecular exchange reaction. Thus, an effective molarity for catalysis cannot be determined. Enzymes such as mandelate racemase are able to alter the geometry of their active site to ensure intramolecular processes occur in preference to reverse reactions. Therefore, these observations highlight a limitation of simple synthetic enzyme models that cannot easily mimic the inherent ability of proteins to effect subtle conformational adjustments as part of catalysis.

Chapter 6
Summary and future work

As part of an on-going programme to develop aqueous methods of aminophosphorylation, the work in this thesis has investigated the reactivities of phosphorus (V) chlorides towards water and amines in aqueous solution.

pH-k_{obs} profiles have been determined for the hydrolyses of phosphodichloridate and thiophosphodichloridate ions in aqueous solutions by conventional UV-Vis spectrophotometry. For the hydrolysis of oxyphosphodichloridate ion **1**, a plateau in reactivity was observed up to pH **~** 12 with $k_0 = 5.7 \times 10^{-3}$ s^{-1}. At higher pH values, the observed rates of hydrolysis increased with hydroxide ion concentration, giving a second-order rate constant $k_{OH} = 5.6 \times 10^{-2}$ M^{-1} s^{-1}. The hydrolysis of thiophosphodichloridate ion **2** in aqueous solution showed essentially constant reactivity across the pH range from **~** 2 to **~** 13, with $k_0 = 3.6 \times 10^{-3}$ s^{-1}. This demonstrates that thiophosphodichloridate ions **2** do not show significant reactivity toward hydroxide ions over and above reactivity with water, in aqueous solution where $[HO^-] <$ **~** 0.2 M.

The observed "thio-effect" on the k_0 values for the attack of water as the nucleophile on oxy and thiophosphodichloridate ions **89** and **95** species was determined as a 1.6-fold reduction on substituting oxygen with sulfur. This suggests that nucleophilic attack by water on **89** and **95** proceeds *via* an $S_N2(P)$-like mechanism, as suggested by Hudson and Moss.[37] In contrast, a larger "thio-effect" (~31 fold) was determined for the k_{OH} values for the attack of hydroxide ions on **89** and **95** upon substitution of oxygen for sulfur. This may be attributed to differing amounts of negative charge stabilization by oxygen and sulfur in the transition state for hydroxide-catalysed hydrolysis, where sulfur is less able to accommodate a build up of negative charge compared to the more electronegative oxygen substituent.

Preliminary efforts have been made towards the determination of pseudo first-order rate constants for the hydrolysis of phosphorus oxychloride and thiophosphoryl chloride in aqueous solution by stopped-flow UV-Vis spectrophotometry, however, these studies were hindered by potential mass transfer processes. Future work may involve the study of the solubility of $POCl_3$ in water to assess whether a mixing or mass transfer effect is in operation. The application of an alternative analytical method,

for example by stopped-flow ion conductiometry, could also be explored.

Following the study of the hydrolyses of oxy and thiophosphodichloridate ions in aqueous solution, investigations were made into the aminolyses of the dichloridate ions to provide an insight into the reactivity of these phosphorylating agents towards amines. Second order rate constants were determined by UV-Vis spectrophotometry for the reaction of oxy and thiophosphodichloridate ions with the following types of amine in aqueous solution (25 °C and I=1 (KCl)): anilines, primary alkyl amines, secondary alkyl amines and hypernucleophilic amines. Due to the short reaction times associated with (thio)phosphorylation of hypernucleophilic amines, it was only possible to determine k_N rate constants for methoxylamine and hydroxylamine. Future work may involve the study of reactions between (thio)phosphodichloridate ions and hypernucleophilic amines of high pK_a (>6.1), for example hydrazine, by methods such as stopped-flow UV-Vis spectrophotometry.

Brønsted plots were constructed from the determined log (k_N) values and measured amine pK_a values for both phosphorylating agents. Similar β_{nuc} values were determined for the (thio)phosphorylation of each class of amine, which suggests that identical mechanisms are in operation for the aminolysis of oxy and thiophosphodichloridate ions. The constructed Brønsted plots (Figure 3.5) may be used to estimate k_N values for amines that have not been kinetically studied. These rate constants may in turn be used to predict conversions (%) of (thio)phosphodichloridate ions to (thio)phosphoramidate products in aqueous amine solution by application of kinetic data to Equation 3.3.

We have in part applied our kinetic understanding to the (thio)phosphorylation of amines in aqueous solution. As part of these investigations we determined and compared conversions of oxy and phosphodichloridate ions *vs* $POCl_3$ and $PSCl_3$ to phosphoramidate and thiophosphoramidate products in aqueous solution of varying pH, respectively. We observed greater selectivities toward aminolysis over hydrolysis processes upon addition of oxyphosphodichloridate ion *vs* $POCl_3$ to aqueous solutions containing 2-methoxyethylamine. Although similar, selectivities toward aminolysis over hydrolysis processes were slightly greater for the addition of $PSCl_3$ *vs* thiophosphodichloridate ion to aqueous solutions containing 2-methoxyethylamine. For these experiments we observed the optimum reaction pH was pH=11.2, where the

conversion of (thio)phosphorylating agent to inorganic (thio)phosphate was minimized.

We then studied the conversion of thiophosphorylating agent to thiophosphoramidate product for reaction with 5'-deoxy-5'-aminoguanosine in aqueous solutions of pH 11-12.5. The conversion of thiophosphodichloridate ion to thiophosphorylated 5'-deoxy-5'-aminoguanosine was slightly greater than with thiophosphoryl chloride. The optimum reaction pH was determined to be pH=12 for both thiophosphorylating agents, where conversions to thiophosphoramidate product were greater than 95 %. These high conversions demonstrate the effectiveness of this aqueous method towards the synthesis of (thio)phosphorylated 5'-amino nucleosides, where near quantitative conversion of (thio)phosphorylating agent to (thio)phosphoramidate is observed. Future work may involve the comparative study of the phosphorylation of 5'-deoxy-5'-aminoguanosine in aqueous solution of varying pH using oxyphosphodichloridate ions *vs* phosphorus oxychloride.

Following the synthesis of thiophosphorylated 5'-amino-5'-deoxyguanosine, we have studied its reactions with methyl iodide, benzyl chloride and bromoethanol alkylating agents in aqueous solution of pH 9-12 to determine the effects, if any, of pH on conversion levels of thiophosphoramidate to alkylated product. However, no simple trends were observed in these studies.

The use of solid forms of the potassium salts of oxy and thiophosphodichloridates **89** and **95** as (thio)phosphorylating agents in aqueous solution has not been studied to date. Potassium salts of both oxy and thiophosphodichloridate ions are known to show increased stabilities over the acetonitrile solutions that we have employed in our kinetic studies and the acetone solutions employed by others.[49] Future study would determine the effectiveness of solid phosphodichloridates **89** and **95** as (thio)phosphorylating agents. If the results were promising, these salts may then be developed as effective synthetic reagents that could be used “off the shelf”, even after prolonged storage.

The kinetic methods presented in this thesis may also be applied to the development of effective synthetic methods towards bis(thio)phosphoramidates from addition of

amino(thio)phosphodichloridate species to aqueous amine solutions (Scheme 6.1).

Scheme 6.1

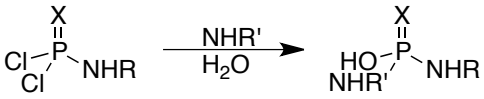

89 X=O/S **28 X=O/S**

Amino(thio)phosphodichloridates may be prepared upon the addition of one equivalent of amine to phosphorus oxychloride or thiophosphoryl chloride under anhydrous conditions, allowing for the synthesis of a large array of different (thio)phosphorylating agents. The kinetic study of the hydrolysis of these species in aqueous solution should allow for the determination of k_w and k_{OH} rate constants for the hydrolysis of **89** to **90** and potentially for hydrolysis to (thio)phosphoramidate **28** (Scheme 6.2).

Scheme 6.2

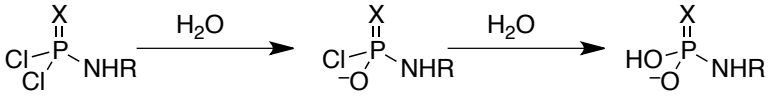

89 **90** **28**

With the k_w and k_{OH} rate constants in hand for the hydrolyses of an array of different amino(thio)phosphodichloridate species, optimum reaction conditions for the (thio)phosphorylation of amines could be determined. In addition, the determined rate constants may be compared with those reported for the hydrolysis of oxy and thiophosphodichloridate ions to fully quantify the effect of the amino substituent on reactivity.

The addition of amino(thio)phosphodichloridates to aqueous amine solutions would lead to the formation of bis(thio)phosphoramidates **28** where the amino substituents may differ from one another. Given that high conversions of (thio)phosphodichloridate ions to (thio)phosphoramidate products were obtained for the (thio)phosphorylation of amines in aqueous solution (Chapter 4), it would be expected that bis(thio)phosphoramidates may also be formed in high conversions. This in turn would allow for the development of an effective aqueous method towards the generation of a

large array of bis(thio)phosphoramidate products, which should require little or no purification.

In Chapter 5, the rate constants for exchange of hydrogen for deuterium at the α-CH_2 positions of naphthalen-1-yl-acetic acid *tert*-butyl ester **123** and 8-(*N*,*N*-dimethylamino-naphthalen-1-yl)-acetic acid *tert*-butyl ester **124** were determined in potassium deuteroxide solutions in 1:1 D_2O:CD_3CN, in order to quantify the effect of the neighbouring *peri*-dimethylamino substituent on α-deprotonation. Intramolecular general base catalysis by the (weakly basic) neighbouring group was not detected. Second-order rate constants, k_{DO}, for the deuterium exchange reactions of esters **123** and **124** have been determined as 3.95×10^{-3} M^{-1} s^{-1} and 1.35×10^{-4} M^{-1} s^{-1}, respectively. The unexpected 29-fold decrease in the k_{DO} value upon the introduction of a *peri*-dimethylamino group is attributed to an unfavourable steric and/or electronic substituent effect on intermolecular deprotonation by deuteroxide ion.

Chapter 7
Experimental

7.0 Foreword

This chapter is divided into five subsections. Section 7.1 describes the general instrumentation and materials utilised. Section 7.2 describes the synthesis of compounds required for kinetic study. Section 7.3 describes the preparation of solutions and kinetic methods used in following the hydrolyses and aminolyses of phosphodichloridate and thiophosphodichloridate ions (Chapters 2-3). Section 7.4 describes the experimental methods involved in the optimisation of aqueous methods of (thio)phosphorylation and alkylation (Chapter 4). Finally, the kinetic methods used in the study of proton transfer at carbon in α-naphthylacetate esters (Chapter 5) are presented in Section 7.5.

7.1 General instrumentation and materials used

NMR samples were prepared in chloroform-d_1, deuterium oxide-d_2, acetonitrile-d_3 and dimethyl sulfoxide-d_6 (DMSO). ^{1}H NMR spectra at 400 and 500 MHz, ^{31}P NMR spectra at 162 MHz and ^{13}C NMR spectra at 100 and 125 MHz were recorded on Bruker Ultrashield 400, Varian Mercury 400 and Varian Inova 500 spectrometers in Durham University. NMR data is presented as follows: chemical shift, integration, multiplicity (br = broad, s = singlet, d = doublet, t = triplet, q = quartet, sep = septet, m = multiplet), coupling constants in Hertz (Hz), and assignment.

All UV-Vis measurements were carried out on Cary-100 and Cary-50 UV-VIS spectrophotometers using 3 mL quartz cuvettes at a temperature of 25 ± 0.1 °C. Stopped-flow spectrophotometry was performed on an Applied Photophysics SX-17MV instrument. Elemental analyses were obtained from the Microanalytical Unit, Chemistry Department, Durham University. Thin Layer Chromatography was carried out using silica-backed Merck Kieselgel 60 F254 plates. Column chromatography was carried out using silica gel.

The pH values (±0.03) of buffered solutions were determined at 25 ºC using a MeterLab^{TM} PHM 290 combination electrode, that was standardised for measurement between pH 4-7 or pH 7-12.46 depending on the pH of the buffer solution. For higher pH measurements, the electrode was calibrated at pH 12.46 using a saturated solution of calcium hydroxide at 25 °C.[81] The pH-stat instrument utilised in this work was a Radiometer TIM-856 instrument.

All reactions involving air or moisture sensitive reagents were performed under an argon atmosphere using oven-dried glassware. Solvents were dried prior to use using an Innovative Technology Inc. solvent purification system and stored over molecular sieves. Lyophilisation was carried out on a Jouan high vacuum system. Solvents were removed *in vacuo* using a Büchi Rotavapor R 110.

Deuterium oxide (99.9% D) was purchased from Apollo Scientific Ltd. Acetonitrile-d_3 (99.8 % D) was purchased from Goss Scientific. Deuterium chloride (35% wt, 99.5 % D), potassium deuteroxide (40% wt, 98+% D), dimethyl

sulfoxide-d_6 (99.8 % D) deuterated chloroform (99.8% D) were purchased from Sigma Aldrich. Phosphorus oxychloride and thiophosphoryl chloride were distilled under a stream of nitrogen prior to use. 1-naphthylacetic acid (>90%), and *N*,*N*-dimethyl-1-naphthylamine (99%) 1-naphthylacetic acid and *N*,*N*-dimethyl-1-naphthylamine were recrystallized from ethanol prior to use. Molecular sieves were dried at 60 °C in the Büchi B-585 glass oven under vacuum with phosphorus pentoxide as drying agent. Pyridine was refluxed over calcium hydride in a still for at least 3 h before being extracted for use. All other chemicals were reagent grade and were used without further purification.

7.2 Synthesis of compounds for kinetic study

7.2.1 Synthesis of oxy and thiophosphodichloridate ions

7.2.1.1 Potassium phosphodichloridate

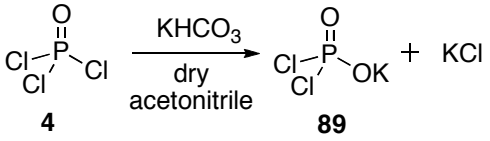

4 **89**

A solution of phosphorus oxychloride **4** (1.275 g, 8.33×10^{-3} mol) in anhydrous acetonitrile (25 mL) was added to a flask containing oven-dried potassium hydrogen carbonate (1.675 g, 0.0167 mol). The mixture was stirred vigorously under argon for 10 min, and the KCl precipitate that formed was removed by filtration to give potassium phosphodichloridate **89** as a 0.33 M solution in dry MeCN (^{31}P NMR: −8.0 ppm, 100%). Stock solutions were prepared regularly and stored in sealable screw top vials that were placed in polythene bags containing anhydrous calcium chloride. Under these conditions, stock solutions showed ~5% hydrolysis of the dichloridate **89** to inorganic phosphate **28** over the course of a week.

7.2.1.2 Potassium thiophosphodichloridate

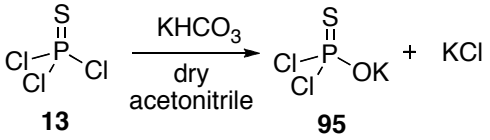

13 **95**

A solution of thiophosphoryl chloride **13** (1.410 g, 8.33×10^{-3} mol) in anhydrous acetonitrile (25 mL) was added to a flask containing oven-dried potassium hydrogen carbonate (1.675 g, 0.0167 mol). The mixture was stirred vigorously under argon for 12 h, and the KCl precipitate that formed was removed by filtration to give potassium thiophosphodichloridate **95** as a 0.33 M solution in dry MeCN (^{31}P NMR: 39.8 ppm, 100%). Stock solutions were stored in sealable screw top vials that were placed in polythene bags containing anhydrous calcium chloride. Under these conditions, **95** showed no apparent decomposition over one month.

7.2.2 Synthesis of 5'-amino-5'-deoxyguanosine

7.2.2.1 5'-Iodo-5'-deoxyguanosine[82]

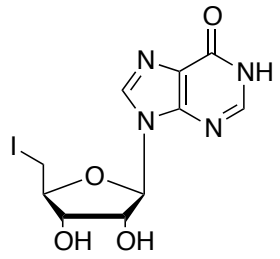

Following a literature procedure reported by Can *et al.,* iodine (6.67 g, 26 mmol) was added over a period of 5 minutes to a stirred mixture of guanosine (2.5 g, 8.83 mmol), triphenylphosphine (7.3 g, 27.8 mmol), imidazole (3.75 g, 55 mmol) and *N*-methyl pyrrolidinone (34 mL, dried over activated molecular sieves) in a 500 mL round-bottomed flask. Following the addition of iodine, the suspension dissolved and gave a yellow solution. The flask was then covered by foil to prevent exposure of the reaction solution to light and was fitted with a calcium chloride drying tube. After stirring at room temperature for 3 h, DCM (335 mL) and water (100 mL) were added to the solution, resulting in the precipitation of a white solid. The mixture was refrigerated for 48 h prior to collection of the white solid on a Büchner funnel. The crude solid was oven dried, ground in a pestle and mortar and then refluxed in DCM (100 mL) for 1 h and then in water (100 mL) for 0.5 h. The solid was collected *via* Büchner funnel and dried overnight at 95 °C to give 5'-iodo-5'-deoxyguanosine as a white powder (1.70 g, 49 %). mp= 195-200 °C (dec); δ_H(400 MHz; DMSO-d_6) 3.50-3.52 (1 H, *ABX* system, J_{AB} 10.5 and J_{AX} 6.5, 5'-CH_AH_B), 3.62 (1 H, *ABX* system, J_{AB} 10.5 and J_{BX} 6.0, 5'-CH_AH_B), 3.95-4.07 (1 H, m, 4'-CH_x), 4.10-4.20 (1 H, m, 3'-*H*) 4.68 (1 H, q, *J* 5.5, 2'-*H*), 5.47 (1 H, d, *J* 4.5, 3'-O*H*), 5.63 (1 H, d, *J* 5.5, 2'-O*H*), 5.79 (1 H, d, *J* 6.0, 1'-*H*), 6.57 (2 H, s, NH_2), 8.00 (1 H, s, 8-*H*) and 10.74 (1 H, s, N*H*); δ_C(101 MHz; DMSO-d_6) 7.9 (5'-CH_2I), 72.7 (3'-*C*), 73.1 (2'-*C*), 83.7 (4'-*C*), 86.5 (1'-*C*), 116.7 (5-*C*), 135.8 (8-*C*), 151.4 (4-*C*), 153.5 (2-*C*) and 156.7 (6-*C*).

7.2.2.2 5'-Azido-5'-deoxyguanosine[60]

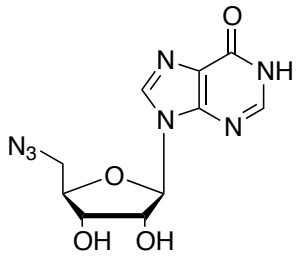

Sodium azide (1.15 g, 7.6 mol) was added to a 100 mL round bottom flask containing a stirred mixture of 5'-iodo-5'-deoxyguanosine (3.00 g, 7.63 mmol) in anhydrous DMF (24 mL, dried over molecular sieves). The resulting mixture was heated at 80 °C for 20 h and subsequently cooled to room temperature. The solvent was removed in *vacuo* to give a beige coloured solid, which was then stirred in a solution of water (50 mL) to remove any remaining sodium azide. The solid was collected *via* Büchner funnel and washed with water (2 x 20 mL), cold ethanol (15 mL) and finally diethyl ether (10 mL). The resulting solid was dried in a vacuum desiccator to give 5'-azido-5'-deoxyguanosine (1.271 g, 54%) as a white powder. mp=197-205° C (dec.); δ_H(400 MHz; DMSO-d_6) 3.52 (1 H, *ABX* system, J_{AB} 13.2 and J_{AX} 3.2, 5'-CH_AH_B), 3.66 (1 H, *ABX* system, J_{AB} 13.2 and J_{BX} 7.2, 5'-CH_AH_B), 3.95–4.02 (1 H, m, 4'-CH_x), 4.04–4.00 (1 H, m, 3'-*H*), 4.59 (1 H, t, *J* 5.2, 2'-*H*), 5.40 (1 H, br s, 3'-O*H*), 5.55 (1 H, br s, 2'-O*H*), 5.70 (1 H, d, *J* 5.6, 1'-*H*), 6.52 (2 H, s, NH_2), 7.89 (1 H, s, 8-*H*);, δ_C(101 MHz; DMSO-d_6) 51.8 (5'-*C*H_2N_3), 70.9 (3'-*C*), 72.6 (2'-*C*), 82.8 (4'-*C*), 86.8 (1'-*C*), 116.8 (5-*C*), 135.8 (8-*C*), 151.3 (4-*C*), 153.7 (2-*C*) and 157.0 (6-*C*).

7.2.2.3 5'-Amino-5'-deoxyguanosine[60]

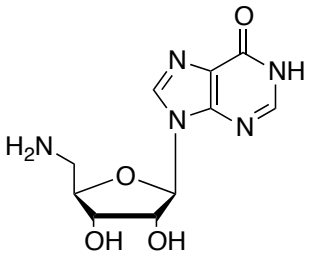

Triphenylphosphine (3.38 g, 12.9 mmol) was added to a 250 mL flask containing 5'-azido-5'-deoxyguanosine and anhydrous pyridine (32.0 mL) under dry conditions at 0 °C. The resulting mixture was stirred at room temperature for 3 h, cooled to 0 °C and ammonium hydroxide solution (10 mL 0.88 ammonia : 35 mL water) was added.

After stirring for an additional 18 h, solvents were removed in *vacuo* and the resulting solid was stirred in ethyl acetate (200 mL) for 20 min. The crude solid was collected *via* Büchner funnel and washed with ethyl acetate (25 mL) and ethyl acetate : methanol (25 mL, 1 : 1). Finally, recrystallization in water gave 5'-amino-5'-deoxyguanosine (2.09 g, 58%) as a white solid. mp= 215-217 °C (dec.); (lit.,[60] 219-220 °C (from water) and lit.,[83] 221 °C); δ_H(400 MHz; DMSO-d_6) 2.75 (1 H, *ABX* system, J_{AB} 13.2 and J_{AX} 5.2, 5'-CH_AH_B), 2.77 (1 H, *ABX* system, J_{AB} 13.2 and J_{BX} 4.4, 5'-CH_AH_B), 3.77–3.83 (1 H, m, 4'-CH_x), 4.09 (1 H, t, *J* 4.8, 3'-*H*), 4.46 (1 H, t, *J* 5.6, 2'-*H*), 5.67 (1 H, d, *J* 6.0, 1'-*H*), 6.56 (2 H, s, NH_2) and 7.99 (1 H, s, 8-*H*); δ_C(101 MHz; DMSO-d_6) 43.5 (5'-*C*H_2NH_2), 70.7 (3'-*C*), 73.2 (2'-*C*), 85.5 (4'-*C*), 86.4 (1'-*C*), 116.8 (5-*C*), 135.8 (8-*C*), 151.4 (4-*C*), 153.9 (2-*C*) and 157.2 (6-*C*).

7.2.3 Synthesis of Naphthalene esters.

7.2.3.1 Naphthalen-1-yl-acetic acid *tert*-butyl ester

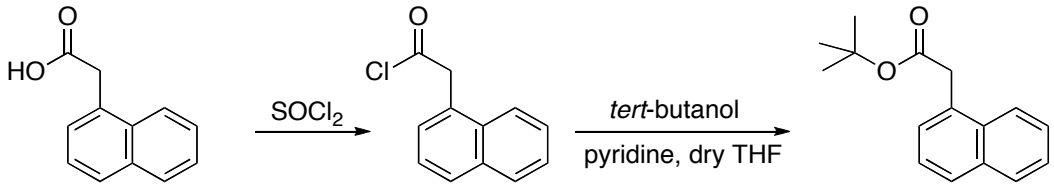

132 **133** **123**

43%

Thionyl chloride (3.00 mL, 41.1 mmol) was added under argon to 1-naphthylacetic acid **132** (4.50 g, 24.1 mmol, recrystallised from ethanol). The resulting solution was stirred for 24 h at room temperature. Excess thionyl chloride was then removed *in vacuo* to give the acid chloride **133** as a brown liquid (4.90 g, 23.9 mmol) which was used without further purification. ^{1}H NMR $\boldsymbol{\delta_H}$ (400 MHz; $CDCl_3$): 7.99-7.21 (m, 7H, aromatic H), 4.62 (s, 2H, CH_2). *Tert*-butanol (1.15 g, 15.4 mmol) and pyridine (8.46 g, 115.4 mmol) were added to a stirred solution of the acid chloride **133** (2.50 g, 11.5 mmol) in anhydrous THF (50 mL). The resulting solution was stirred under argon for 24 h at room temperature. Pentane (150 mL) was added to the mixture, and the solution was filtered to remove the pyridinium chloride salt. The filtrate was washed with saturated sodium

chloride solution (2 × 50 mL), saturated sodium bicarbonate solution (2 × 50 mL), and deionised water (2 × 50 mL). The solution was then dried over magnesium sulfate, the solvent was removed in *vacuo*, and subsequent purification by preparative TLC (cyclohexane : diethylether = 9:1) gave ester **123 (**1.20 g, 4.9 mmol, 43%) as a colourless oil (found: C, 79.42; H, 7.47. Calc. for $C_{16}H_{18}O_2$: C, 79.31; H, 7.49%); R_f (cyclohexane:diethylether = 9:1) = 0.80; $\boldsymbol{\nu}_{\mathbf{max}}$ (neat)/cm^{-1} 1726 and 1135; $\boldsymbol{\delta}_{\mathbf{H}}$ (700 MHz; $CDCl_3$) 7.99 (d, 1H, *J* 8.5, aromatic-H), 7.85 (d, 1H, *J* 8.1, aromatic-H), 7.77 (d, 1H, *J* 11.5, aromatic-H), 7.49 (m, 2H, aromatic-H), 7.40 (m, 2H, aromatic-H), 3.97 (s, 2H, ArCH_2CO), 1.42 (s, 9H, C(CH_3)$_3$); $\boldsymbol{\delta}_C$ (175 MHz; $CDCl_3$) 171.2, 133.8, 132.2, 131.3, 128.7, 128.6, 127.8, 126.1, 125.5, 125.4, 123.9, 81.2, 40.5, and 28.9; *m/z* (ESI$^+$) 265.1 (100); HRMS (ESI$^+$) $C_{16}H_{18}O_2Na$ requires 265.1204, found 265.1207 (+1.1 ppm).

7.2.3.2 8-(*N*,*N*-dimethylamino-naphthalen-1-yl)-acetic acid *tert*-butyl ester

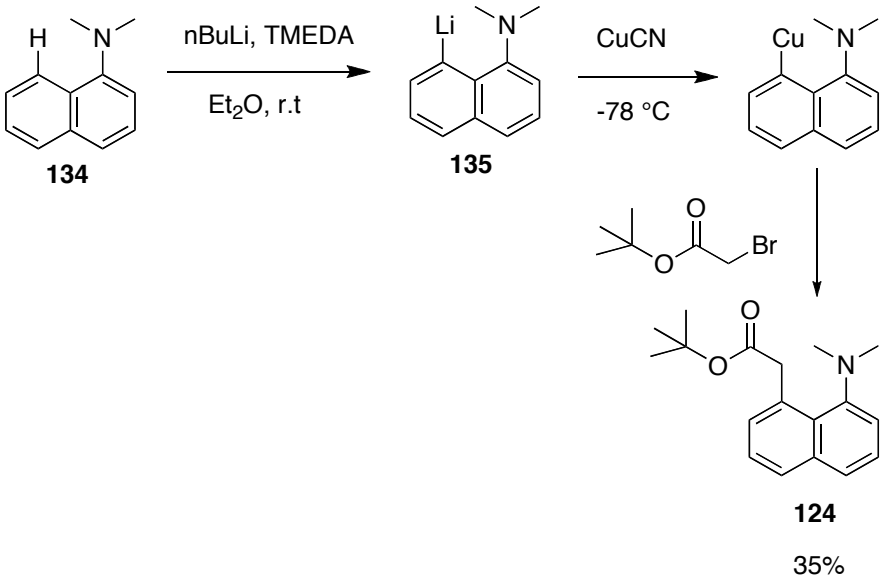

134 **135** **124**

35%

n-Butyllithium (*ca*. 1.6 M, 10.5 mL in hexane, 16.8 mmol) was added to a stirred solution of *N*,*N*-dimethyl-1-naphthylamine **134** (2.0 mL, 11.2 mmol) in anhydrous diethylether (18.0 mL) under an argon atmosphere. *N*,*N*′,*N*′,*N*′-tetramethylethylenediamine (1.94 g, 16.8 mmol) was added to the solution after 15 min of stirring, and the solution was stirred for an additional 14 h. The reaction mixture was then cooled to –78 °C, and a suspension of copper (I) cyanide (1.00 g,

11.2 mmol) in anhydrous diethylether (15 mL) was added. Following the addition of CuCN, the reaction flask was covered in aluminium foil in order to exclude light, and the mixture was stirred for 1 h at room temperature. The reaction mixture was then cooled to –78 °C, and *tert*-butyl bromoacetate (2.18 g, 11.2 mmol) was added. The flask contents were allowed to warm to room temperature and stirred for 1 h. Methanol (150 mL) and diethylether (100 mL) were then added to the reaction flask. The resulting mixture was washed with water (4 × 100 mL) and dried over magnesium sulfate. The crude mixture was concentrated *in vacuo* and purified by column chromatography (cyclohexane to 9:1 cyclohexane:diethylether) to give ester **124** as a colourless oil (1.12 g, 3.91 mmol, 35%). R_f (cyclohexane : diethylether = 9:1) = 0.38; $\boldsymbol{\delta_H}$ (700 MHz; $CDCl_3$) 7.75 (d, 1H, *J* 7.2, aromatic-H), 7.59 (d, 1H, *J* 7.2, aromatic-H), 7.40-7.36 (m, 2H, aromatic-H), 7.27 (d, 1H, *J* 6.3, aromatic-H), 7.23 (d, 1H, *J* 6.3, aromatic-H), 4.34 (s, 2H, ArCH_2CO), 2.73 (s, 6H, N(CH_3)$_2$) 1.42 (s, 9H, C(CH_3)$_3$). $\boldsymbol{\delta_C}$ (175 MHz; $CDCl_3$) 172.0, 152.4, 136.6, 131.5, 131.1, 129.2, 129.0, 125.8, 125.7, 125.5, 117.9, 80.2, 46.6, 44.2, and 28.7; ***m/z*** (ESI^+) 308.2 (100); HRMS (ESI^+) $C_{16}H_{23}NO_2Na$ requires 308.1626, found 308.1613 (–4.2 ppm).

7.3 Hydrolyses and aminolyses of phosphodichloridate and thiophosphodichloridate ions

7.3.1 Fitting of Kinetic Data

All pseudo-first order reaction data (absorbance versus time) obtained for the hydrolyses and aminolyses of phosphodichloridate and thiophosphodichloridate ions were fitted using KaleidaGraph™ according to Equation 7.1.

$$A_{obs} = A_{inf} + (A_0 - A_{inf})e^{-kt}. \qquad \textbf{Equation 7.1}$$

All pseudo-first order plots of absorbance against time had correlation coefficients (R^2) of 0.99-0.9999. In order to reduce the error in observed rate constants, data were only fitted for the first three half-lives of the reaction (corresponding to 87.5% reaction).

7.3.2 Hydrolyses of (thio)phosphorus (V) chlorides

7.3.2.1 ^{31}P NMR Spectroscopy Experiments

Solutions for Initial ^{31}P NMR Spectroscopy Studies.

A similar method was employed in the synthesis of solutions of $KOPOCl_2$ **89** and $KOPSCl_2$ **95** for the initial ^{31}P NMR spectroscopy studies, using a reduced volume of MeCN to give a higher stock solution concentration.

^{31}P NMR kinetic experiments

A solution of potassium carbonate buffer in D_2O (1 mL, pH 10.62, 90 : 10 CO_3^{2-} : HCO_3^-) was locked and shimmed in the NMR spectrometer. A solution of potassium phosphodichloridate **89** or potassium thiophosphodichloridate **95** (100 μL of a 0.66 M solution in dry MeCN) was then added to the NMR sample *via* a Hamilton syringe. The tube was inverted repeatedly to ensure mixing, and spectra were then recorded using ^{31}P NMR spectroscopy at one-minute intervals until the phosphodichloridate **89** or thiophosphodichloridate **95** had been converted into inorganic phosphate **28** or inorganic thiophosphate **98** respectively. The ^{31}P chemical shifts of the signals due to inorganic (thio)phosphate were verified by comparison with spectra of authentic

standards. No additional signals were observed for the hydrolysis of potassium phosphodichloridate **89** or potassium thiophosphodichloridate **95**.

7.3.2.2 UV-Vis Kinetic Experiments

Preparation of Solutions
Stock solutions of potassium hydroxide and hydrogen chloride were prepared by dilution and titration of the commercial concentrated solutions.

Phosphate buffers (H_3PO_4/KH_2PO_4, 0.1 mol dm^{-3}) were used in conjunction with 2-aminobenzoic acid as indicator. The phosphate buffers were prepared from stock solutions of phosphoric acid, monopotassium dihydrogen phosphate, 2-aminobenzoic acid (0.15 mmol dm^{-3}) and potassium chloride (2 mol dm^{-3}). These were made up in deionised water to give buffer solutions of various acid/ base ratios and I=1 (KCl). These buffers covered a pH range of 1.99 to 2.86.

Formate buffers (HCO_2H/HCO_2K, 0.1 mol dm^{-3}) were used in conjunction with 2,4-dinitrophenol as indicator. The formate buffers were prepared from stock solutions of formic acid, potassium formate, 2,4-dinitrophenol (0.15 mmol dm^{-3}) and potassium chloride (2 mol dm^{-3}). These were made up in deionised water to give buffer solutions of various acid/base ratios and I=1 (KCl). These buffers covered a pH range of 3.53 to 4.53.

Phosphate buffers (KH_2PO_4/K_2HPO_4, 0.1 mol dm^{-3}) were used in conjunction with 4-nitrophenol as indicator. The phosphate buffers were prepared from stock solutions of monopotassium dihydrogen phosphate and dipotassium monohydrogen phosphate, 4-nitrophenol (0.15 mmol dm^{-3}) and potassium chloride (2 mol dm^{-3}). These were made up in deionised water to give buffer solutions of various acid/base ratios and I=1 (KCl). These buffers covered a pH range of 6.49 to 7.50.

Carbonate buffers ($KHCO_3/K_2CO_3$, 0.1 mol dm^{-3}) were used in conjunction with 2,5-dimethylphenol as indicator. The carbonate buffers were prepared from stock solutions of potassium hydrogen carbonate, potassium carbonate, 2,5-dimethylphenol (0.15 mmol dm^{-3}) and potassium chloride (2 mol dm^{-3}). These were made up in

deionised water to give buffer solutions of various acid/base ratios and I=1 (KCl). These buffers covered a pH range of 9.70 to 10.63.

Potassium hydroxide solutions of varying concentration were used in conjunction with 1,3,5-trinitrobenzene as indicator. The potassium hydroxide solutions were prepared from stock solutions of potassium hydroxide, 1,3,5-trinitrobenzene (0.15-0.30 mmol dm^{-3}) and potassium chloride (2 mol dm^{-3}). These were made up in deionised water to give solutions containing a range of concentrations of hydroxide ions of I=1 (KCl). These solutions covered a pH range of 11.88 to 13.23.

UV-Vis kinetic method

Reaction solutions were transferred to a cuvette (3 mL) *via* a volumetric glass pipette. Each sample was allowed to equilibrate at 25 ± 0.1 ºC in the Peltier thermostated cell holder for 15 minutes prior to the addition of either potassium phosphodichloridate **89** or potassium phosphothiodichloridate **95** as a solution in anhydrous MeCN (0.33 M) *via* Hamilton syringe. The change in absorbance of the indicator was followed until a constant A_{inf} value was observed to within 5% of their predicted values, and these absorbance-time data were fitted using Equation 7.1 to obtain rate constants. Typically for hydrolysis, a decrease in aborbance of ~0.1 was observed for each reaction. A decrease in pH of ~0.2 was measured for the hydrolysis of $KOPOCl_2$ / $KOPSCl_2$ in solutions of potassium hydroxide (pH 11.88 – 13.23) which led to an absorbance change of ~0.1. For these reactions the observed pseudo first-order rate constant, k_{obs}, was determined from kinetic data for the first 25% of the reaction, corresponding to a pH decrease of ~0.05. Fitting over a greater proportion of the time course, however, gave very similar observed rate constants

7.3.2.3 UV-Vis Stopped-flow Spectrophotometric Kinetic Experiments

Stopped-flow spectrophotometry was used as part of investigations into the attempted determination of rates of hydrolysis of phosphorus oxychloride and thiophosphoryl chloride in aqueous solution. This was achieved using two syringes (2.5 mL and 0.25 mL) in a 10:1 mixing arrangement. The 2.5 mL syringe contained aqueous buffer (50 mM) at I=1 (KCl) and the 0.25 mL syringe contained (thio)phosphorylating agent is

anhydrous acetonitrile solution. The lines were flushed thoroughly with these solutions before data was acquired. These reactions were monitored at a single analytical wavelength.

7.3.3 Aminolyses of phosphodichloridate and thiophosphodichloridate ions

7.3.3.1 Amine pK_a determination

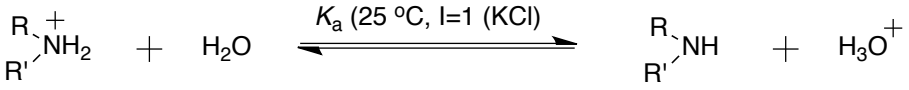

Amine pK_a values were determined in aqueous solution by pH-titration using a pH-stat instrument (Radiometer TIM-856 instrument). Potassium hydroxide solution (0.05-0.1 M) was mde up at I=1 (KCl) using concentrated samples and was added to the automatic burette contained within the pH-stat instrument. Each amine was made up in its protonated form at a concentration of 0.05-0.01 M (depending on its solubility) in aqueous solution. The ionic strength was maintained at I=1 using potassium chloride. 20 mL of the given amine solution was titrated *via* glass bulb pipette into the reaction flask which was thermostated at 25 ºC. The mixture was rapidly stirred and the pH probe and burette outlet were submerged in the amine solution. Potassium hydroxide solution was titrated against the given amine solution at a rate of 0.4 mL /min until the end-point was reached. The resulting pH-titration data was manipulated and the reaction pH was plotted against dvolume (KOH)/dpH. The amine pK_a value was then determined from the pH value which corresponded to the maxima of the resulting plot.

7.3.3.2 UV-Vis kinetic experiments

Preparation of Solutions
For amines of pK_a < 6.2, aqueous amine solutions of varying concentration were made up at I=1 (KCl) and contained phosphate buffer (90% FB KH_2PO_4/K_2HPO_4, 0.1 mol dm^{-3}) and 4-nitrophenol (90% FB, 0.15 mmol dm^{-3}). The phosphate buffers were prepared from stock solutions of monopotassium dihydrogen phosphate and dipotassium monohydrogen phosphate, 4-nitrophenol and potassium chloride (2 mol dm^{-3}).

For amines of pK_a > 6.2 aqueous amine solutions of varying concentration were made up at I=1 (KCl) and contained a phenolate indicator of similar pK_a. Solutions of glycine methyl ester (90% FB) were made up with 2,4-dichlorophenol (λ90% FB, 0.50 mmol dm^{-3}) at I=1 (KCl). Solutions of 2-methoxyethylamine (90% FB) were made up with 4-bromophenol (90% FB, 0.80 mmol dm^{-3}) at I=1 (KCl). Solutions of glycine (90% FB) were made up with 3,5-dimethylphenol (90% FB, 0.50 mmol dm^{-3}) at I=1 (KCl). Solutions of γ -Aminobutyric acid (90% FB) were made up with 2,6-dimethylphenol (90% FB, 0.50 mmol dm^{-3}) at I=1 (KCl). Solutions of 1-Acetyl piperazine (90% FB) were made up with 3-nitrophenol (90% FB, 1.00 mmol dm^{-3}) at I=1 (KCl). Solutions of morpholine (90% FB) were made up with 3-nitrophenol (90% FB, 1.00 mmol dm^{-3}) at I=1 (KCl). Solutions of piperazine (90% FB) were made up with 3,5-dimethylphenol (90% FB, 0.60 mmol dm^{-3}) at I=1 (KCl).

UV-Vis kinetic method

Reaction solutions were transferred to a cuvette (3 mL) *via* a volumetric glass pipette. Each sample was allowed to equilibrate at 25 ± 0.1 ºC in the Peltier thermostated cell holder for 15 minutes prior to the addition of either potassium phosphodichloridate **89** or potassium phosphothiodichloridate **95** as a solution in anhydrous MeCN (0.33 M) *via* Hamilton syringe. The change in absorbance of the indicator was followed until a constant A_{inf} value was observed, and these absorbance-time data were fitted using Equation 7.1 to obtain rate constants. Typically for hydrolysis, a decrease in aborbance of ~0.1 was observed for each reaction.

7.3.3.3 ^{31}P NMR Product Analysis Studies

^{31}P NMR product analysis studies were undertaken for each amine studied kinetically by UV-Vis spectrophotometry to determine conversion levels of oxy and thiophosphodichloridate ions to phosphoramidate and thiophosphoramidate products, respectively.

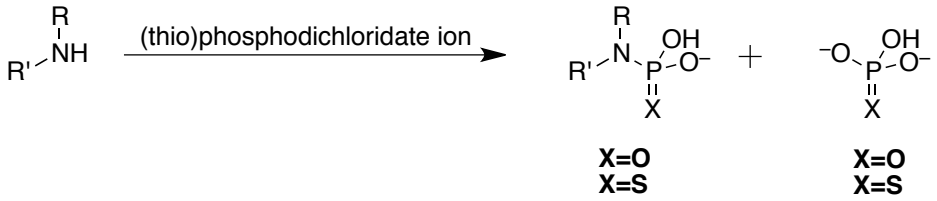

For amines of pK_a < ~9.7, aqueous amine solutions containing 0.5 mol dm^{-3} carbonate buffer (90% FB $KHCO_3/K_2CO_3$) were were prepared at the required amine concentration (stated in Tables 3.6-3.7) in a volumetric flask (1 mL). Either potassium phosphodichloridate **89** or potassium phosphothiodichloridate **95** was immediately added as a solution in anhydrous MeCN (0.33 M) *via* Hamilton syringe. The resulting mixture was inverted and allowed to react. Reaction times were estimated from maniuplation of kinetic data determined for each amine in the UV-Vis spectrophotometry studies.

For amines of pK_a > ~9.7, aqueous solutions of amine (50 mL) were prepared at the required concentration (stated in Tables 3.6-3.7) in a volumetric flask (50 mL). 20 mL of the amine solution was transferred by glass pipette to a thermostated reaction flask and vigorously stirred at 25 °C. A pH-stat instrument was attached to the reaction flask to maintain the reaction pH at pH 12 through addition of 1.0 M potassium hydroxide. Either potassium phosphodichloridate **89** or potassium phosphothiodichloridate **95** was added dropwise as a solution in anhydrous MeCN (0.33 M) *via* Hamilton syringe. The reaction solution was stirred until potassium hydroxide solution was no longer being added by the pH-stat instrument.

After each reaction was complete, the reaction pH was increased to ~pH 12 and the acetonitrile was removed in *vacuo*. The remaining aqueous solution was then lyophilised to give a crude white powder containing (thio)phosphoramidate and (thio)phosphate products. The conversions of oxyphosphodichloridate **89** and thiophosphodichloridate **95** ions to phosphoramidate and thiophosphoramidate products were estimated by ^{31}P NMR spectroscopy, respectively.

7.4 The optimization of (thio)phosphorylation of amines and alkylation of thiophosphoramidates

7.4.1 (Thio)phosphorylation of 2-methoxyethylamine

In order to optimize the phosphorylation and thiophosphorylation of 2-methoxyethylamine, several experiments of varying reaction pH were performed using one equivalent of (thio)phosphorylating agent. Phosphorus oxychloride and potassium oxyphosphodichloridate ion, and thiophosphoryl chloride and potassium thiophosphodichloridate were used to generate 2-methoxyethylamine phosphoramidate **116** and thiophosphoramidate **118**, respectively.

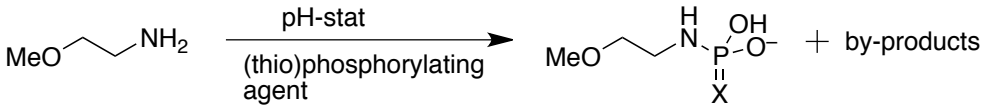

116 X=O
118 X=S

Aqueous solutions (50 mL) of 2-methoxyethylamine (0.376 g, 5.0 mol) were made up at a concentration of 0.1 M in a volumetric flask (50 mL) at the desired pH (see Table 7.1-7.2). 20 mL of the amine solution was transferred by glass pipette to a thermostated reaction flask and vigorously stirred at 25 °C. A pH-stat instrument was attached to the reaction flask to maintain the desired reaction pH through addition of 1.0 M potassium hydroxide. The prepared (thio)phosphorylating agent was made up at a concentration of 0.4 M in dry acetonitrile and added dropwise to the stirred aqueous amine solution. The reaction solution was stirred until potassium hydroxide solution was no longer being added by the pH-stat instrument. After the reaction was complete, the reaction pH was increased to ~pH 12 (if necessary) and the acetonitrile was removed in vacuo. The remaining aqueous solution was then lyophilised to give a crude white powder of 2-methoxyethylamine phosphoroamidate **116** or thiophosphoramidate **118**. The conversions of phosphorylating and thiophosphorylating agent to phosphoramidate and thiophosphoramidate product for reactions undertaken between pH 8.2 to 12.7 were estimated by ^{31}P NMR spectroscopy and are shown in Tables 7.1 and 7.2, respectively.

Table 7.1 Phosphorylation of 2-methoxyethylamine

Reaction pH	Conversion %[a]		
	Phosphoramidate	**Bisphosphoramidate**	**Inorganic phosphate**
i)Phosphorus oxychloride			
8.2	35	0	65
9.2	70	2	28
10.2	72	6	22
11.2	83	3	13
12.7	81	1	18
ii) Potassium oxyphosphodichloridate			
8.2	44	0	56
9.2	83	0	18
10.2	88	0	12
11.2	93	0	7
12.7	92	0	8

[a] Determined by ^{31}P NMR spectroscopy

Table 7.2 Thiophosphorylation of 2-methoxyethylamine

Reaction pH	Conversion %[a]		
	Thiophosphoramidate	**Inorganic thiophosphate**	**Inorganic phosphate**
i)Thiophosphoryl chloride			
8.2	71	27	2
9.2	95	3	2
10.2	96	2	2
11.2	97	1	2
12.7	97	2	1
ii) Potassium thiophosphodichloridate			
8.2	84	16	0
9.2	88	12	0
10.2	92	8	0
11.2	93	7	0
12.7	89	11	0

[a] Determined by ^{31}P NMR spectroscopy

7.4.2 Thiophosphorylation of 5'-amino-5'-deoxyguanosine

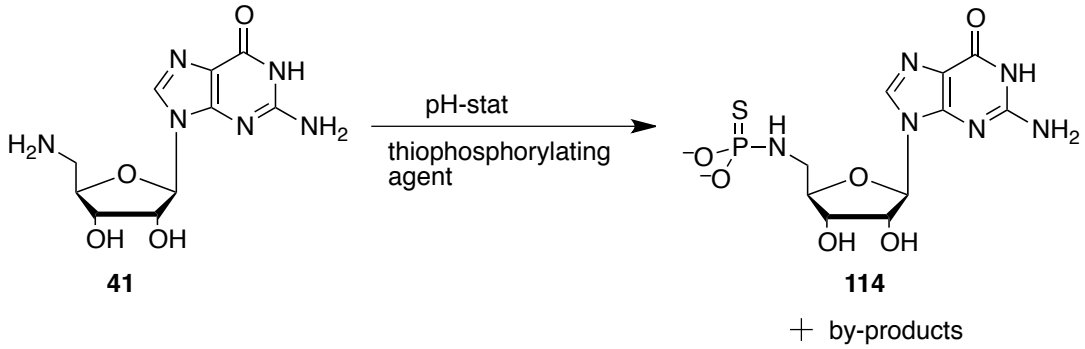

Aqueous solutions (5 mL) of 5'-amino-5'-deoxyguanosine **41** (0.141 g, 0.5 mmol) were made up in the thermostated reaction flask at a concentration of 0.1 M at the desired pH (see Table 7.3), and were vigorously stirred at 25 °C. Thiophosphorylation was undertaken using the method described in Section 7.5.1. The conversion of thiophosphorylating agents to thiophosphoramidate product **114** for reactions undertaken between pH 11 to 12.5 were estimated by ^{31}P and ^{1}H NMR spectroscopies and are shown in Table 7.3.

Table 7.3 Thiophosphorylation of 5'-amino-5'-deoxyguanosine

Reaction pH	Conversion %			
	Thiophosphoramidate	Inorganic thiophosphate[a]	Inorganic phosphate[a]	Unidentified impurities[a]
i) Thiophosphoryl chloride				
11	79[a], 81[b]	20	0	0
11.5	93[a], 94[b]	6	1	0
12	92[a], 92[b]	5	1	2
12.5	79[a], 84[b]	7	1	13
ii) Potassium thiophosphodichloridate				
11	87[a], 90[b]	13	0	0
11.5	93[a], 95[b]	1	0	6
12	97[a], 96[b]	2	0	1
12.5	92[a], 89[b]	6	1	1

[a] Determined by ^{31}P NMR spectroscopy. [b] Determined by ^{1}H NMR spectroscopy.

The other impurities present in the samples were unidentified structures containing phosphate moiety. Crude compound **114**: δ_H(400 MHz; D_2O) 7.73 (1 H, s, 8-*H*), 5.64

(1 H, d, *J* 8.0, 1'-*H*), 4.75 (1 H, t, *J* 7.9 2'-*H*), 4.25-4.30 (1 H, m, 3'-*H*), 4.10–4.14 (1 H, m, 4'-*H*), 2.87–3.03 (2 H, m, 5'-*H*); $\delta_P[^1H]$(283 MHz; D_2O) 43.55 (t, NH*P*S).

7.4.2 Alkylation of 5'-amino-5'-deoxyguanosine thiophosphoramidate

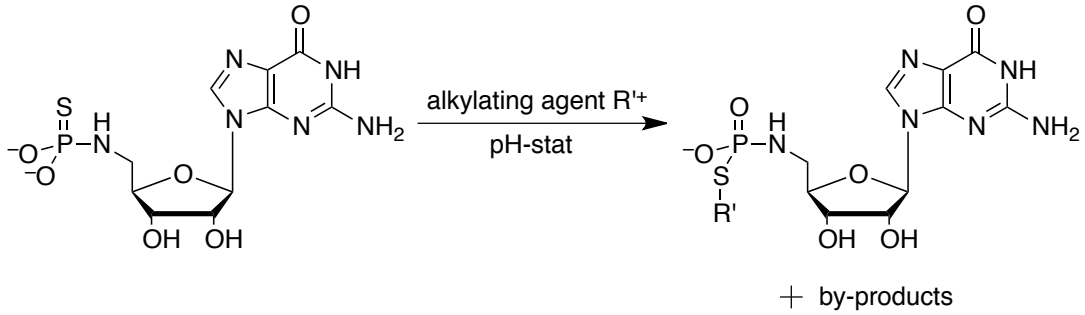

Aqueous solutions (5 mL) of 5'-amino-5'-deoxyguanosine thiophosphoramidate **114** (28.2 mg) were made up in the thermostated reaction flask at a concentration of 20 mM at the desired pH (see Tables 7.4-7.6.), and were vigorously stirred at 25 °C. Methyl iodide (14.3 μL), benzyl chloride (26.5 μL) or bromoethanol (12.4 μL) alkylating agent was then added to the reaction solution *via* Hamilton syringe and stirred for 1 h. The excess of alkylation agent was removed by extraction with diethyl ether (3×10 mL) and the aqueous solution was subsequently lyophilised. The conversions of 5'-amino-5'-deoxyguanosine thiophosphoramidate to alkylated thiophosphoramidate product for reactions undertaken between pH 8 to 12 were estimated by ^{31}P and ^1H NMR spectroscopies and are shown in tables 7.4-7.6. ^{31}P and ^1H Spectroscopic data is presented below.

Table 7.4 ***S*-Alkylation of 5'-amino-5'-deoxyguanosine thiophosphoramidate with methyl iodide in aqueous solution.**

Reaction pH	Purity (%)
8	78[a], 84[b]
9	77[a], 76[b]
10	79[a], 88[b]
11	80[a], 75[b]
12	72[a], 69[b]

[a] Determined by ^{31}P NMR spectroscopy. [b] Determined by ^1H NMR spectroscopy.

δ_H(400 MHz; D_2O) 7.67 (1 H, s, 8-*H*), 5.61 (1 H, d, *J* 8.3, 1'-*H*), 4.90 (1 H, t, *J* 7.4 2'-*H*), 4.23 (1 H, d, *J* 6.0, 3'-*H*), 4.12–4.17 (1 H, m, 4'-*H*), 2.97–3.04 (2 H, m, 5'-*H*), 1.95 (3 H, d, J 12.4, C*H*$_3$S); $\delta_P[^1H]$(283 MHz; D_2O) 24.99 (m, NH*P*S).

Table 7.5 ***S*-Alkylation of 5'-amino-5'-deoxyguanosine thiophosphoramidate with benzyl chloride in aqueous solution.**

Reaction pH	Purity (%)
8	84[a], 88[b]
9	87[a], 87[b]
10	83[a], 78[b]
11	85[a], 82[b]
12	81[a], 75[b]

[a] Determined by ^{31}P NMR spectroscopy. [b] Determined by ^{1}H NMR spectroscopy.

δ_H(400 MHz; D_2O) 7.74 (1 H, s, 8-*H*), 7.21–6.79 (5 H, m, C$_6$*H*$_5$), 5.59 (1 H, d, *J* 8.0, 1'-*H*), 5.02 (1 H, t, *J* 6.8 2'-*H*), 4.23 (1 H, d, *J* 5.8, 3'-*H*), 4.07–4.11 (1 H, m, 4'-*H*), 2.89–2.65 (2 H, m, 5'-*H*); $\delta_P[^1H]$(162 MHz; D_2O) 25.2 (m, NH*P*S).

Table 7.6 ***S*-Alkylation of 5'-amino-5'-deoxyguanosine thiophosphoramidate with bromoethanol in aqueous solution.**

Reaction pH	Purity (%)
9	86[a], 84[b]
10	84[a], 92[b]
11	79[a], 89[b]
12	84[a], 93[b]

[a] Determined by ^{31}P NMR spectroscopy. [b] Determined by ^{1}H NMR spectroscopy.

δ_H(400 MHz; D_2O) 8.02 (1 H, s, 8-*H*), 5.96 (1 H, d, *J* 7.4, 1'-*H*), 5.15 (1 H, t, *J* 6.6 2'-*H*), 4.56 (1 H, d, *J* 4.9, 3'-*H*), 4.43–4.47 (1 H, m, 4'-*H*), 3.82 (2 H, t, *J* 6.2, C*H*$_2$OH) 3.21-3.33 (2 H, m, SC*H*$_2$) 2.89–2.96 (2 H, m, 5'-*H*); $\delta_P[^1H]$(283 MHz; D_2O) 26.5 (m, NH*P*S).

7.5 Proton transfer at carbon in α-naphthylacetate esters

7.5.1 Kinetic methods

Rate constants for exchange for deuterium of the first α-proton of the naphthalene esters studied were determined by monitoring the disappearance of the singlet due to the α-CH_2 group of the substrate by ^{1}H NMR spectroscopy. All reactions were carried out in 1:1 D_2O:CD_3CN at 25 °C and a constant ionic strength of 0.1 maintained with potassium chloride. Generally reaction of substrate was followed for at least three half-lives. For both naphthaene esters, the final substrate and internal standard concentrations in the reaction solutions were 5.0 mM and 2.0 mM respectively. This ensured an approximate 1:2.4 ratio of the singlet arising from the methylene hydrogens (α-CH_2) and the triplet due to the 12 methyl hydrogens of internal standard.

The progress of isotope exchange of naphthalen-1-yl-acetic acid *tert*-butyl ester **123** was followed using a quench-based method. H/D exchange reactions were carried out in 25.0 mL vials which were incubated at 25 ± 0.1 ºC in a thermostated water bath. Reactions were run on a 12 mL scale, and were initiated by addition of 6 mL of substrate stock solution (10 mM in CD_3CN) to a solution of potassium deuteroxide in D_2O (6 mL), containing internal standard, tetramethylammonium deuteriosulfate. Each reaction was monitored over time by withdrawing aliquots (~800 μL) at timed intervals. Each aliquot was quenched to a pD value 3-4 units below that of the reaction mixture by addition of > 1 M DCl solution. The samples were either analysed immediately or placed in a sealed plastic bag containing calcium chloride and stored in the freezer for analysis at a later time.

The progress of isotope exchange of 8-(*N*,*N*-dimethylamino-naphthalen-1-yl)-acetic acid *tert*-butyl ester **124** was followed directly in the probe of the NMR spectrometer. Reactions in a volume of 800 μL were initiated by the addition of 400 μL of a stock solution of **124** (10 mM in CD_3CN) to a solution of potassium deuteroxide in D_2O (400 μL), containing internal standard, tetramethylammonium deuteriosulfate. Samples were run at 25 °C in a Varian Mercury 500 MHz NMR spectrometer, in

which spectra were continuosly obtained until 87.5% of exchange of hydrogen for deuterium at the α–CH_2 had occurred.

^{1}H NMR spectra were acquired with 64 transients. ^{1}H NMR spectral baselines were subject to a first – order drift correction before integration of the peak areas. Substrate and product peak areas were compared with the peak of the internal standard that was set to an arbitrary figure of 1000.

The pH values of buffered solutions were determined at 25 ºC using a MeterLab™ PHM 290 pH-Stat Controller equipped with a radiometer (pH 4 - 7 - 10 @ 25 ºC) combination electrode, that could be standardised between pH 4 - 7 or pH 7 - 10 to encompass the pH of the buffer solution. The pD (± 0.03) was calculated by adding 0.4 to the observed reading of the pH meter. Due to the relatively short shelf-life of the Radiometer combination electrode, it was necessary to replace the electrode once the sensitivity fell below 96%. Although the same model of electrode was always used, values of γ_{DO} were re-determined with each electrode and were found to vary from 0.73-0.77.

The estimated error on the observed pseudo-first-order rate constant for exchange (k_{ex}, s^{-1}) is ± 10 % based on the error of the ^{1}H NMR measurement. Although the measurements of k_{ex} are single determinations, the calculated error in similar carbon acidity measurements and calculations performed by Richard *et al*[78] is ± 10 % for k_{ex} and ± 0.5 units for the pK_a.

7.5.2 Determination of pK_a of the *peri*-dimethylammonium substituent

All UV-Vis spectrophotometry measurements were recorded using a Varian Cary 50 UV-Vis spectrophotometer at 25 ± 0.1 °C in which the same quartz cuvette (1 mL) was used for all absorbance readings.

A stock solution of 8-(*N,N*-dimethylamino-naphthalen-1-yl)-acetic acid *tert*-butyl ester **124** (5.8 mg, 2.03×10^{-5} mmol) was made up in HLPC-grade CH_3CN to give a total concentration of 20.3 mM.

The UV-Vis absorbance (220-600 nm) of ester **124** was determined in solutions of 0.1 M KOH and 0.1 M HCl (1:1 H_2O: CH_3CN) to ensure a suitable change in absorbance was observed between absorbance peaks due to neutral and protonated forms of ester **124** and **124-H** respectively. The absorbance due to ester **124** (325 nm) was shown to decrease at pH < 2.5 and so the change in absorbance was followed in several solutions of hydrochloric acid (1:1 H_2O:MeCN) at an overall ionic strength of I=0.1 (KCl) of varying pH. The hydrochloric acid solutions covered a pH range of 0.03 to 1.89.

For each solution, 1 mL of buffer (of given pH) was added (*via* glass bulb pipette) to the quartz cuvette and allowed to equilibrate at 25 ± 0.1 °C for 10 min. It was subsequently subjected to an accurate (8 minute) spectral scan between 220-600 nm and the absorbance at 325 nm (due to **124**) was then measured for 10 min. 15 μL of stock solution of **124** was then added *via* Hamilton syringe to the hydrochloric acid solution in the cuvette to give an overall ester concentration of 0.3 mM. The solution was mixed and the UV-Vis absorbance scans from 220-600 nm were repeated. The absorbance due to ester **124** at 325 nm was then followed for 10 min to obtain an accurate absorbance measurement and to ensure a constant absorbance value was observed. The background absorbance was subtracted from the absorbance due to substrate to give the true absorbance due to ester **124**. The resulting absorbance spectra are shown in Figure 5.2 and the accurate absorbance values determined for each pH solution were used in the calculation of the pK_a value of the conjugate acid of **124**.

References

(1) Yoshikawa, M.; Kato, T.; Takenish, T. *Bull. Chem. Soc. Jpn.* **1969**, *42,* 3505-3508.
(2) Yoshikawa, M.; Kato, T.; Takenish, T. *Tetrahedron Lett.* **1967**, 5065-5068.
(3) Blackburn, G. M.; Loakes, M. J. G.; Williams, D. M. *Nucleic Acids in Chemistry and Biology*-3rd edition. **2006**, RSC Publishing, Cambridge.
(4) Ludwig, J. *Acta. Biochem. Biophys. Hung*. **1981**, *16*, 131-133.
(5) Ora, M.; Murtola, M.; Aho, S.; M, Oivanen. *Org. Biomol. Chem.* **2004**, *2*, 593-600.
(6) Jastorff, B.; Hettler, H. *Chem. Ber. Recl.* **1969,** *102*, 4119-4127.
(7) Jastorff, B.; Hettler, H. *Tetrahedron Lett.* **1969,** *30*, 2543-2544.
(8) Hampton, A.; Bayer, M.; Gupta, V. S.; Chu, S. Y. *J. Med. Chem.* **1968,** *11*, 1229-1232.
(9) Hampton, A.; Brox, L. W.; Bayer, M. *Biochemistry.* **1969**, *8*, 2303-2311.
(10) Williamson, D.; Cann, M. J.; Hodgson, D. R. W. *Chem. Commun.* **2007**, 5096-5098.
(11) Williamson, D.; Hodgson, D. R. W. *Org. Biomol. Chem.* **2008**, *6*, 1056-1062.
(12) Duncan, R.; Drueckhammer, D. G. *Tetrahedron Lett.* **1993**, *34*, 1733-1736.
(13) Kers, I.; Stawinski, J.; Kraszewski, A. *Tetrahedron Lett.* **1998**, *39*, 1219-1222.
(14) Kers, I.; Stawinski, J.; Kraszewski, A. *Tetrahedron.* **1999**, *55*, 11579-11588.
(15) Ora, M.; Mattila, K.; Lönnberg, T.; Oivanen, M.; Lönnberg, H. *J. Am. Chem. Soc.* **2002**, *124*, 14364-14372.
(16) Das, S. R.; Piccirilli, J. A. *Nat. Chem. Biol.* **2005**, *1*, 45-52.
(17) Das, S. R.; Fong, R.; Piccirilli, J. A. *Curr. Opin. Chem. Biol.* **2005**, *9*, 585-593.
(18) Mara, C.; Dempsey, E.; Bell, A.; Barlow, J. W. *Bioorg. Med. Chem. Lett.* **2011**, *21*, 6180-6183.
(19) Venkatachalam, T. K.; Yu, G.; Samuel, P.; Qazi, S.; Pendergrass, S.; Uckun, F. M. *Eur. J. Med. Chem.* **2004**, *39*, 665-683.
(20) Ruman, T.; Dlugopolska, K.; Jurkiewicz, A.; Rut, D.; Fraczyk, T.; Ciesla, J.; Les, A.; Szewczuk, Z.; Rode, W. *Bioorg. Chem.* **2010**, *38*, 74-80.
(21) Pirrung, M. C.; James, K. D.; Rana, V. S. *J. Org. Chem.* **2000**, *65*, 8448-8453.
(22) Trmčić, M.; Hodgson, D. R. W. *Chem. Commun.* **2011**, *47*, 6156-6158.
(23) Chanley, J. D.; Feageson, E. *J. Am. Chem. Soc.* **1958**, *80*, 2686-2691.
(24) Butcher, W. W.; Westheimer, F. H. *J. Am. Chem. Soc.* **1955**, *77*, 2420-2424.
(25) Benkovic, S. J.; Sampson, E. J. *J. Am. Chem. Soc.* **1971**, *93*, 4009-4016.
(26) King, J. F.; Rathore, R.; Lam, J. Y. L.; Guo, Z. R.; Klassen, D. F. *J. Am. Chem. Soc.* **1992**, *114*, 3028-3033.
(27) Rogne, O. *J. Chem. Soc. B.* **1968**, 1294-1296.
(28) Rogne, O. *J. Chem. Soc. B.* **1970**, 1056-1058.
(29) Rys, P. *Angew. Chem. Int. Edit.* **1977**, *16*, 807-817.
(30) Bourne, J. R. *Org. Process Res. Dev.* **2003,** *7*, 471-508.
(31) Meerwein, H.; Bodendorf, K. *Ber. Dtsch. Chem. Ges.* **1929**, *62*, 1952-1953.
(32) Goubeau, J.; Schulz, P. *Z. Anorg. Allg. Chem.* **1958,** *294*, 224-232.
(33) Askitopoulos, K. I. *Praktika Akad. Athenon.* **1943**, *18*, 146.
(34) Grunze, H. *Z. Anorg. Allg. Chem.* **1962,** *313*, 317-322.
(35) Grunze, H. *Z. Anorg. Allg. Chem.* **1962,** *313*, 323-337.
(36) Koransky, W.; Munch, G.; Grunze, H. *Z. Naturforsch. Pt. B.* **1962**, *17*, 291.
(37) Hudson, R. F.; Moss, G. *J. Chem. Soc.* **1962**, 3599-3604.
(38) Prince, R. H. *T. Faraday. Soc.* **1958**, *54*, 838-848.

(39) Hudson, R. F.; Wardill, J. E. *J. Chem. Soc.* **1950**, 1729-1733.
(40) Hudson, R. F.; Keay, L. *J. Chem. Soc.* **1960**, 1859-1931.
(41) Dostrovsky, I.; Halmann, M. *J. Chem. Soc.* **1953**, 502-507.
(42) Dostrovsky, I.; Halmann, M. *J. Chem. Soc.* **1956**, 1004-1007.
(43) Hudson, R. F.; Loveday, G. *J. Chem. Soc.* **1962**, 1068.
(44) Achmatowicz, M. M.; Thiel, O. R.; Colyer, J. T.; Hu, J.; Elipe, M. V. S.; Tomaskevitch, J.; Tedrow, J. S.; Larsen, R. D. *Org. Process Res. Dev.* **2010**, *14*, 1498-1508.
(45) Winstein, S.; Grunwald, E.; Jones, H. W. *J. Am. Chem. Soc.* **1951**, *73*, 2700-2707.
(46) Brown, D. M.; Hamer, N. K. *J. Chem. Soc.* **1960**, 1155-1161.
(47) Mitchell, R. A. *J. Chem. Soc. Dalton.* **1997**, 1069-1073.
(48) Mitchell, R. A. *FASEB. J.* **2003**, *17*, A563.
(49) Segall, Y.; Quistad, G. B.; Sparks, S. E.; Casida, J. E. *Chem. Res. Toxicol.* **2003,** *16*, 350-356.
(50) Quistad, G. B.; Zhang, N. J.; Sparks, S. E.; Casida, J. E. *Chem. Res. Toxicol.* **2000,** *13*, 652-657.
(51) Martin, M. L.; Halbert, M.; Poignant, S. *J. Chem. Soc. Perkin. Trans. 2.* **1977**, 1243.
(52) Teichmann, H.; Schulz, J. *Phosphorus. Sulfur.* **1990**, *54*, 31-37.
(53) Khalifah, R. G. *J. Biol. Chem.* **1971**, *246*, 2561-2573.
(54) Kresge, A. J. *Acc. Chem. Res.* **1975**, *8*, 354-360.
(55) Meisenheimer, J. *Justus Liebigs. Ann. Chem.* **1902**, *323*, 205-246.
(56) Bernasconi, C. F. *J. Am. Chem. Soc.* **1970**, *92*, 4682-4688.
(57) Herschlag, D.; Piccirilli, J. A.; Cech, T. R. *Biochemistry.* **1991**, *30*, 4844-4854.
(58) Heo, C. K. M.; Bunting, J. W. *J. Chem. Soc. Perkin. Trans. 2.* **1994**, 2279-2290.
(59) Dean, D. K. *Synthetic. Commun.* **2002**, *32*, 1517-1521.
(60) Backstrom, N.; Burton, N. A.; Watt, C. I. F. *J. Phys. Org. Chem.* **2010**, *23*, 711-722.
(61) Kirby, A. J. *Adv. Phys. Org. Chem.* **1980**, *17*, 183-278.
(62) Kirby, A. J. *Acc. Chem. Res.* **1997**, *30*, 290-296
(63) Watt, C. I. F. *J. Phys. Org. Chem.* **2010**, *23*, 561-571.
(64) Kirby, A. J.; Ocarroll, F. *J. Chem. Soc. Perkin. Trans. 2.* **1994**, 649-655.
(65) Babbitt, P. C.; Mrachko, G. T.; Hasson, M. S.; Huisman, G. W.; Kolter, R.; Ringe, D.; Petsko, G. A.; Kenyon, G. L.; Gerlt, J. A. *Science.* **1995**, *267*, 1159-1161.
(66) Gerlt, J. A.; Babbitt, P. C. *Ann. Rev. Biochem.* **2001**, *70*, 209-246.
(67) Glasner, M. E.; Gerlt, J. A.; Babbitt, P. C. *Curr. Opin. Chem. Biol.* **2006**, *10*, 492-497.
(68) Asaad, N.; Davies, J. E.; Hodgson, D. R. W.; Kirby, A. J.; Van Vliet, L.; Ottavi, L. *J. Phys. Org. Chem.* **2005**, *18*, 101-109.
(69) Hodgson, D. R. W.; Kirby, A. J.; Feeder, N. *J. Chem. Soc. Perkin. Trans. 1.* **1999**, 949-954.
(70) Kirby, A. J.; Williams, N. H. *J. Chem. Soc. Perkin. Trans. 2.* **1994**, 643-648.
(71) Frisch, M. J.; Schlegel,G. W. T.; Scuseria, H. B. G. E.; Robb, M. A.; Cheeseman J. R.; Scalmani, G.; Barone, V.; Mennucci, B.; Petersson, G. A.; Nakatsuji, H.; Caricato, M.; Li, X.; Hratchian, H. P.; Izmaylov, A. F.; Bloino, J.; Zheng, G.; Sonnenberg, J. L.; Hada, M.; Ehara, M.; Toyota, K.; Fukuda, R.;

Hasegawa, J.; Ishida, M.; Nakajima, T.; Honda, Y.; Kitao, O.; Nakai, H.; Vreven, T.; Montgomery, J. A.; Peralta, J. E.; Ogliaro, F.; Bearpark, M.; Heyd, J. J.; Brothers, E.; Kudin, K. N.; Staroverov, V. N.; Kobayashi, R.; Normand, J.; Raghavachari, K.; Rendell, A.; Burant, J.C.; Iyengar, S. S.; Tomasi, J.; Cossi, M.; Rega, N.; Millam, J. M.; Klene, M.; Knox, J. E.; Cross, J. B.; Bakken, V.; Adamo, C.; Jaramillo, J.; Gomperts, R.; Stratmann, R. E.; Yazyev, O.; Austin, A. J.; Cammi, R.; Pomelli, C.; Ochterski, J. W.; Martin, R. L.; Morokuma, K.; Zakrzewski, V, G.; Voth, G. A.; Salvador, P.; Dannenberg, J. J.; Dapprich, S.; Daniels, A. D.; Farkas, O.; Foresman, J. B.; Ortiz, J. V.; Cioslowski, J. *Gaussian Inc,* **2009**.

(72) Lee, C.; Yang, W.; Parr, R. G. *Phys. Rev. B.* **1988**, *37*, 785-789.

(73) Becke, A. D. *J. Chem. Phys.* **1993**, *98*, 5648-5652.

(74) Petersson, G. A.; Bennett, A.; Tensfeldt, T. G.; Al-Laham, M. A.; Shirley, W. A.; Mantzaris, J. *J. Chem. Phys.* **1988**, *89*, 2193-2218.

(75) Petersson, G. A.; Al-Laham, M. A. *J. Chem. Phys.* **1991**, *94*, 6081-6090.

(76) Berg, U.; Jencks, W. P. *J. Am. Chem. Soc.* **1991**, *113*, 6997-7002.

(77) Amyes, T. L.; Richard, J. P. *J. Am. Chem. Soc.* **1996**, *118*, 3129-3141.

(78) Richard, J. P.; Williams, G.; O'Donoghue, A. C.; Amyes, T. L. *J. Am. Chem. Soc.* **2002,** *124*, 2957-2968.

(79) Berg, U.; Jencks, W. P. *J. Am. Chem. Soc.* **1991**, *113*, 6997-2002.

(80) Bordwell, F. G.; Fried, H. E. *J. Org. Chem.* **1981,** *46*, 4327-4331.

(81) R. G. Bates. *J. Res. Natl. Bur. Stand.* **1956**, 56, 305-312.

(82) McGee, D. P. C.; Martin, J. C. *Can. J. Chem.* **1986,** *64,* 1885-1889.

(83) Schattka, K.; Jastorff, B. *Chem. Ber.-Rec.* **1972,** *105*, 3824-3832.

Appendices

Appendix A

Figure A.1 **Plot of the observed rate constants, k_{obs}, against concentrations of formate buffer (90% FB) for the hydrolyses of $KOPOCl_2$ (■) and $KOPSCl_2$ (•) in aqueous solution.**

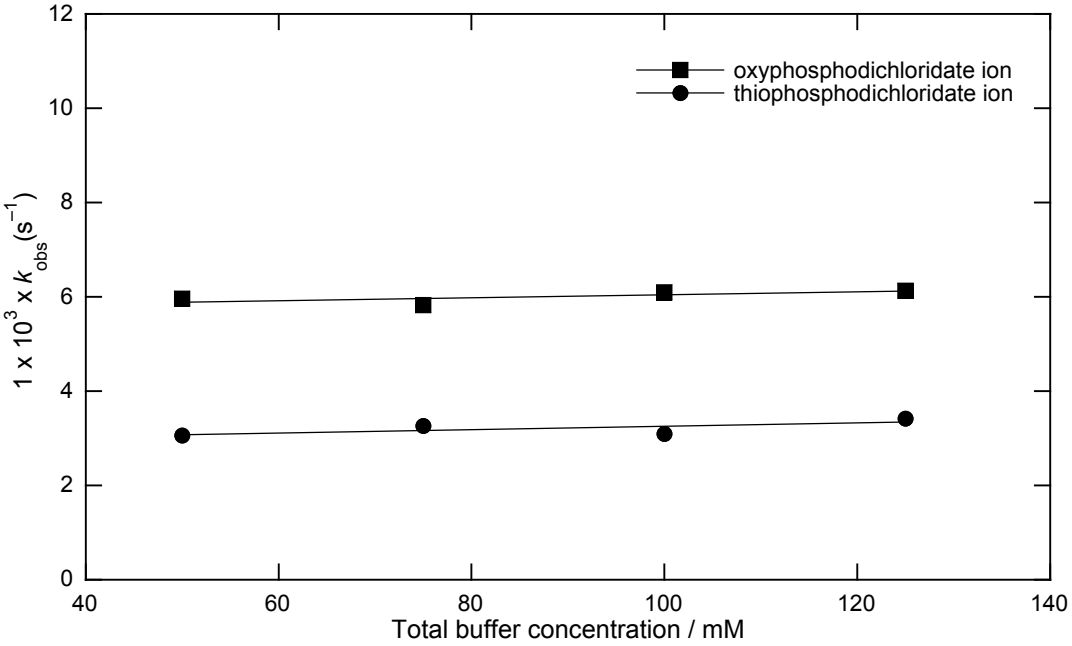

Figure A.2 **Plot of the observed rate constants, k_{obs}, against concentrations of carbonate buffer (90% FB) for the hydrolyses of $KOPOCl_2$ (■) and $KOPSCl_2$ (•) in aqueous solution.**

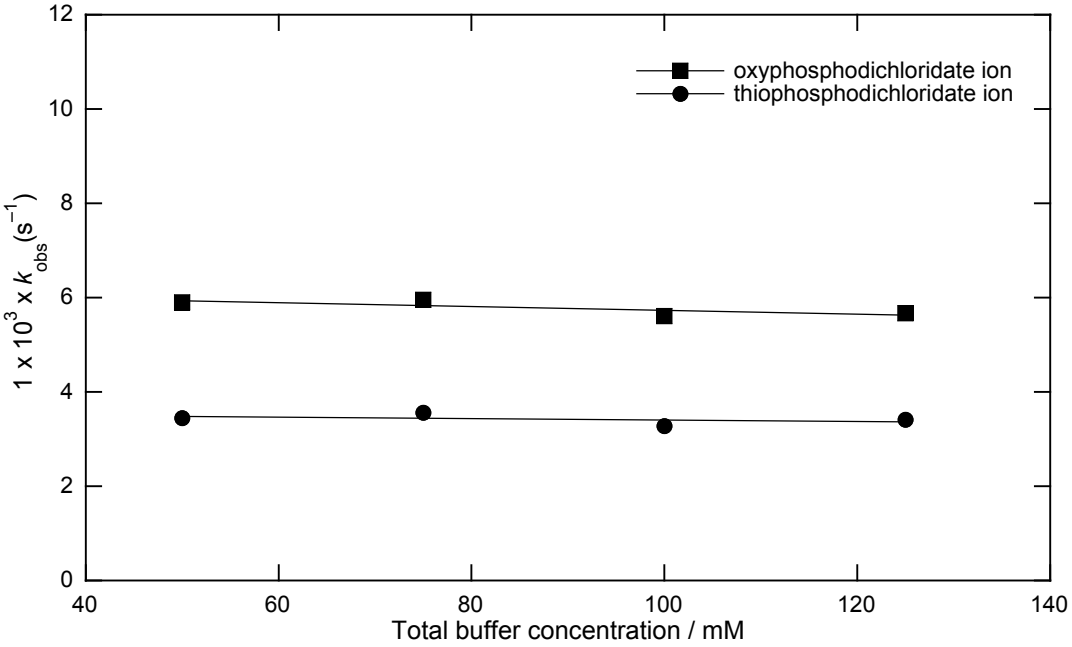

Appendix B

Table A.1 Pseudo first order rate constants (s^{-1}) and determined second order rate constants ($M^{-1}s^{-1}$) for parallel hydrolysis and aminolysis of $KOPOCl_2$ in aqueous solution for five substituted anilines of varying concentration, at 25 °C and *I*=1 (KCl).

Substituted aniline	[Amine] (M)	pH	[$KOPOCl_2$] $\times 10^3$ (M)	$10^3 \times k_{obs}$ (s^{-1})	k_N ($M^{-1}s^{-1}$)
Aniline	0.025	7.52	1.10	6.19	0.027
	0.050	7.53	1.10	7.16	
	0.10	7.53	1.10	8.42	
	0.125	7.55	1.10	9.05	
	0.15	7.55	1.10	10.03	
	0.20	7.54	1.10	11.20	
3-Aminoaniline	0.050	7.50	1.10	7.18	0.039
	0.075	7.52	1.10	8.51	
	0.10	7.53	1.10	9.54	
	0.15	7.53	1.10	12.73[a]	
4-Fluoroaniline	0.05	7.52	1.10	8.28	0.047
	0.075	7.51	1.10	9.16	
	0.10	7.54	1.10	10.37	
	0.15	7.55	1.10	12.88	
4-Ethoxyaniline	0.03	7.49	1.10	7.88	0.073
	0.05	7.51	1.10	9.28	
	0.06	7.54	1.10	10.09	
	0.07	7.53	1.10	10.92	
	0.08	7.55	1.10	11.62	
4-Aminophenol	0.01	7.52	1.10	6.59	0.095
	0.02	7.53	1.10	7.85	
	0.03	7.52	1.10	8.79	
	0.05	7.54	1.10	10.44	

[a]Data point omitted from plot of k_{obs} *vs* [amine]

Table A.2 Observed pseudo first order rate constants for the parallel hydrolysis and aminolysis of $KOPOCl_2$ and derived second order rate constants in aqueous solutions of in aqueous solutions of primary amines at 25 °C and *I*=1 (KCl).

Primary amine	[Amine] (M)	pH	$[KOPOCl_2] \times 10^3$ (M)	$10^3 \times k_{obs}$ (s^{-1})	k_N ($M^{-1}s^{-1}$)
2,2,2-Trifluoroethylamine	0.050	7.53	1.10	11.50	0.116
	0.075	7.53	1.10	14.06	
	0.100	7.54	1.10	17.66	
	0.150	7.55	1.10	23.07	
Glycine methyl ester	0.018	8.59	0.67	12.02	0.362
	0.054	8.61	2.00	24.69	
	0.072	8.62	2.78	31.08	
	0.090	8.65	3.33	46.21	
	0.135	8.69	4.66	51.57	
2-Methoxyethylamine	0.018	10.36	0.78	20.14	0.883
	0.036	10.43	1.55	38.54	
	0.054	10.52	2.33	52.63	
Glycine	0.009	10.58	0.39	14.23	1.157
	0.018	10.61	0.78	26.32	
	0.027	10.65	1.17	35.68	
	0.036	10.68	1.55	47.17	
γ-Aminobutyric acid	0.009	11.36	0.39	20.79	1.810
	0.018	11.39	0.78	36.18	
	0.027	11.44	1.17	49.47	
	0.036	11.47	1.55	72.91	

Table A.3 Observed pseudo first order rate constants for the parallel hydrolysis and aminolysis of $KOPOCl_2$ and derived second order rate constants in aqueous solutions of in aqueous solutions of secondary amines at 25 °C and *I*=1 (KCl).

Secondary amine	[Amine] (M)	pH	[$KOPOCl_2$] $\times 10^3$ (M)	$10^3 \times k_{obs}$ (s^{-1})	k_N ($M^{-1}s^{-1}$)
1-Methyl piperazine	0.020	7.52	1.10	9.77	0.199
	0.030	7.50	1.10	11.45	
	0.040	7.51	1.10	13.92	
	0.050	7.53	1.10	15.67	
Piperazine.HCl	0.020	7.50	1.10	25.20	1.002
	0.030	7.50	1.10	35.45	
	0.040	7.53	1.10	47.32	
	0.060	7.51	1.10	65.19	
1-Acetyl piperazine	0.018	9.15	0.77	31.54	1.496
	0.027	9.18	1.17	46.84	
	0.036	9.21	1.55	61.55	
	0.045	9.20	1.94	71.60	
Morpholine	0.009	9.25	0.44	23.69	2.249
	0.018	9.30	0.89	40.39	
	0.027	9.36	1.33	63.84	
	0.036	9.49	1.78	86.94	
Piperazine	0.009	10.83	0.44	41.07	4.634
	0.014	10.84	0.66	68.40	
	0.018	10.86	0.89	85.78	
	0.023	10.89	1.10	112.01	

Table A.4 **Observed pseudo first order rate constants for the parallel hydrolysis and aminolysis of $KOPOCl_2$ and derived second order rate constants in aqueous solutions of in aqueous solutions of hydroxylamine and methoxylamine at 25 °C and *I*=1 (KCl).**

Hypernucleophilic amine	[Amine] (M)	pH	[$KOPOCl_2$] $\times 10^3$ (M)	$10^3 \times k_{obs}$ (s^{-1})	k_N ($M^{-1}s^{-1}$)
Methoxylamine	0.050	7.53	1.10	13.40	0.132
	0.100	7.52	1.10	19.33	
	0.150	7.53	1.10	25.39	
	0.200	7.54	1.10	32.80	
Hydroxylamine	0.005	7.49	1.10	13.46	1.432
	0.010	7.50	1.10	20.53	
	0.015	7.51	1.10	27.53	
	0.020	7.50	1.10	35.19	
	0.025	7.51	1.10	41.88	

Table A.5 **Observed pseudo first order rate constants for the parallel hydrolysis and aminolysis of $KOPSCl_2$ and derived second order rate constants in aqueous solutions of in aqueous solutions of substituted anilines at 25 °C and *I*=1 (KCl).**

Substituted aniline	[Amine] (M)	pH	[$KOPSCl_2$] $\times 10^3$ (M)	$10^3 \times k_{obs}$ (s^{-1})	k_N ($M^{-1}s^{-1}$)
Aniline	0.025	7.52	1.10	4.19	0.016
	0.050	7.53	1.10	4.45	
	0.100	7.53	1.10	5.17	
	0.150	7.55	1.10	6.03	
	0.200	7.54	1.10	7.00	
4-Fluoroaniline	0.050	7.52	1.10	4.91	0.027
	0.100	7.54	1.10	6.46	
	0.150	7.55	1.10	8.15	
	0.200	7.55	1.10	8.81	
3-Aminoaniline	0.025	7.49	1.10	4.46	0.030
	0.050	7.52	1.10	5.17	
	0.075	7.52	1.10	6.02	
	0.100	7.53	1.10	6.64	
4-Ethoxyaniline	0.010	7.50	1.10	3.79	0.044
	0.030	7.49	1.10	4.49	
	0.050	7.51	1.10	5.49	
	0.060	7.54	1.10	6.00	
	0.080	7.55	1.10	7.03	
4-Aminophenol	0.020	7.53	1.10	4.50	0.055
	0.030	7.52	1.10	5.05	
	0.040	7.55	1.10	5.70	
	0.050	7.54	1.10	6.39	

Table A.6 Observed pseudo first order rate constants for the parallel hydrolysis and aminolysis of $KOPSCl_2$ and derived second order rate constants in aqueous solutions of in aqueous solutions of primary amines at 25 °C and *I*=1 (KCl).

Primary amine	[Amine] (M)	pH	[$KOPSCl_2$] × 10^3 (M)	$10^3 \times k_{obs}$ (s^{-1})	k_N ($M^{-1}s^{-1}$)
2,2,2-Trifluoroethylamine	0.025	7.51	1.10	4.51	0.042
	0.050	7.53	1.10	5.67	
	0.075	7.53	1.10	6.87	
	0.100	7.54	1.10	7.65	
	0.150	7.55	1.10	9.81	
Glycine methyl ester	0.018	8.59	0.67	5.63	0.156
	0.054	8.61	2.00	11.60	
	0.090	8.65	3.33	18.30	
	0.135	8.69	4.66	24.63	
2-Methoxyethylamine	0.018	10.36	0.78	8.58	0.327
	0.036	10.43	1.55	15.11	
	0.054	10.52	2.33	20.92	
	0.072	10.53	3.11	26.88	
Glycine	0.018	10.61	0.78	10.86	0.400
	0.036	10.68	1.55	19.34	
	0.054	10.76	2.33	25.19	
	0.072	10.79	3.11	32.90	
γ-Aminobutyric acid	0.009	11.36	0.39	7.93	0.680
	0.018	11.39	0.78	13.28	
	0.027	11.44	1.17	20.62	
	0.036	11.47	1.55	24.25	

Table A.7 Observed pseudo first order rate constants for the parallel hydrolysis and aminolysis of $KOPSCl_2$ and derived second order rate constants in aqueous solutions of in aqueous solutions of secondary amines at 25 °C and *I*=1 (KCl).

Secondary amine	[Amine] (M)	pH	$[KOPSCl_2] \times 10^3$ (M)	$10^3 \times k_{obs}$ (s^{-1})	k_N ($M^{-1}s^{-1}$)
1-Methyl piperazine	0.020	7.52	1.10	4.65	0.076
	0.030	7.50	1.10	5.80	
	0.040	7.51	1.10	6.70	
	0.050	7.53	1.10	7.23	
Piperazine.HCl	0.020	7.50	1.10	10.77	0.348
	0.030	7.50	1.10	14.21	
	0.040	7.53	1.10	17.66	
	0.060	7.51	1.10	24.50	
1-Acetyl piperazine	0.009	9.00	0.39	7.73	0.654
	0.018	9.15	0.77	14.55	
	0.027	9.18	1.17	20.87	
	0.045	9.20	1.94	32.35	
Morpholine	0.009	9.25	0.44	8.66	0.686
	0.018	9.30	0.89	13.53	
	0.027	9.36	1.33	20.55	
	0.036	9.49	1.78	28.54	
Piperazine	0.009	10.83	0.44	15.29	1.310
	0.018	10.86	0.89	22.71	
	0.027	10.92	1.33	37.65	
	0.036	10.95	1.78	49.63	
	0.045	10.99	2.22	62.53	

Table A.8 Observed pseudo first order rate constants for the parallel hydrolysis and aminolysis of $KOPSCl_2$ and derived second order rate constants in aqueous solutions of in aqueous solutions of hydroxylamine and methoxylamine at 25 °C and *I*=1 (KCl).

Hypernucleophilic amine	[Amine] (M)	pH	$[KOPSCl_2] \times 10^3$ (M)	$10^3 \times k_{obs}$ (s^{-1})	k_N ($M^{-1}s^{-1}$)
Methoxylamine	0.050	7.53	1.10	7.99	0.102
	0.100	7.52	1.10	13.39	
	0.150	7.53	1.10	18.17	
	0.200	7.54	1.10	24.01	
Hydroxylamine	0.010	7.50	1.10	21.10	1.572
	0.020	7.50	1.10	36.63	
	0.030	7.52	1.10	51.04	
	0.040	7.51	1.10	70.02	
	0.050	7.52	1.10	80.61	

Appendix C

Table A.9 Pseudo first-order rate constants for the deuterium exchange of naphthalen-1-yl-acetic acid *tert*-butyl ester 123 (5 mM) at 25 ºC in KOD solution of 1:1 D_2O:CD_3CN, I=0.1 (KCl).

[KOD] (M)	Time (s)	f(s)[a]	Ln f(s)[a]	k_{obs}[b] (s^{-1})
0.023	0	1.000	0.000	8.277×10^{-5}
	1800	0.860	–0.151	
	3600	0.725	–0.322	
	7200	0.566	–0.568	
	9000	0.470	–0.755	
	12600	0.347	–1.059	
	14400	0.305	–1.188	
	18000	0.224	–1.497	
	19800	0.201	–1.604	
	21600	0.162	–1.821	
0.046	0	1.000	0.000	1.774×10^{-4}
	900	0.912	–0.092	
	1800	0.762	–0.272	
	2700	0.615	–0.486	
	3600	0.516	–0.662	
	4500	0.432	–0.840	
	5400	0.385	–0.954	
	6300	0.326	–1.120	
	7200	0.269	–1.313	
	8100	0.238	–1.436	
	9000	0.208	–1.568	
	9900	0.174	–1.751	
	10800	0.156	–1.859	
0.060	0	1.000	0.000	2.346×10^{-4}
	690	0.841	–0.173	
	1380	0.738	–0.304	
	2070	0.636	–0.452	
	2760	0.528	–0.638	
	3450	0.454	–0.789	
	4140	0.372	–0.988	
	4830	0.336	–1.092	
	5520	0.277	–1.284	
	6210	0.245	–1.406	
	6900	0.193	–1.646	
	8280	0.143	–1.942	
	0	1.000	0.000	
	630	0.902	–0.104	
	1260	0.714	–0.337	

	1890	0.604	–0.504	
	2520	0.530	–0.635	
0.070	3150	0.435	–0.832	2.728×10^{-4}
	3780	0.352	–1.043	
	4410	0.314	–1.158	
	5040	0.263	–1.337	
	5670	0.211	–1.555	
	6930	0.157	–1.853	
	0	1.000	0.000	
	1500	0.613	–0.489	
0.083	3000	0.382	–0.963	3.198×10^{-4}
	4000	0.269	–1.312	
	4500	0.238	–1.435	
	6000	0.147	–1.916	
	0	1.000	0.000	
	450	0.810	–0.211	
	900	0.690	–0.371	
	1350	0.561	–0.577	
	1800	0.486	–0.721	
	2250	0.405	–0.903	
0.092	2700	0.355	–1.035	3.539×10^{-4}
	3150	0.314	–1.159	
	3600	0.271	–1.305	
	4050	0.221	–1.510	
	4500	0.198	–1.618	
	4950	0.161	–1.826	
	5400	0.142	–1.949	

(a) The fraction of substrate remaining, $f(s)$, was calculated from Equations 5.2 and 5.3 (b) Pseudo first-order rate constants ($k_{obs,}\ s^{-1}$) were obtained as the slopes of the plots of $\ln f(s)$ against time.

Table A.10 **First-order rate constants for deuterium exchange of 8-(*N*,*N*-dimethylamino-naphthalen-1-yl)-acetic acid *tert*-butyl ester 124 (5 mM) at 25 ºC in KOD solution of 1:1 D_2O:CD_3CN, *I*=0.1 (KCl).**

[KOD] (M)	Time (s)	*f*(s)[a]	Ln *f*(s)[a]	k_{obs}[b] (s^{-1})
	0	1	0	
	58500	0.881	–0.126	
	105000	0.761	–0.274	
	163500	0.621	–0.477	
0.023	230400	0.529	–0.637	2.759×10^{-6}
	255600	0.481	–0.732	
	316800	0.423	–0.860	
	351000	0.396	–0.926	
	502200	0.250	–1.39	
	0	1	0.000	
	25200	0.858	–0.153	
	50400	0.724	–0.324	
	75600	0.630	–0.462	
	100800	0.537	–0.622	
	126000	0.469	–0.758	
0.046	151200	0.417	–0.875	5.685×10^{-6}
	176400	0.364	–1.009	
	201600	0.309	–1.118	
	226800	0.269	–1.312	
	252000	0.237	–1.440	
	277200	0.203	–1.600	
	316800	0.160	–1.834	
	0	1.000	0.000	
	18000	0.886	–0.121	
	36000	0.774	–0.256	
	54000	0.676	–0.392	
	72000	0.586	–0.534	
	90000	0.519	–0.656	
0.060	108000	0.448	–0.804	7.900×10^{-6}
	126000	0.387	–0.949	
	144000	0.340	–1.078	
	162000	0.295	–1.220	
	180000	0.251	–1.384	
	216000	0.186	–1.683	
	252000	0.148	–1.913	
	0	1.000	0.000	
	18000	0.822	–0.196	
	32400	0.738	–0.304	
	54000	0.591	–0.526	
	72000	0.501	–0.692	

	90000	0.437	–0.827	
0.070	108000	0.362	–1.017	9.298×10^{-6}
	126000	0.303	–1.196	
	144000	0.264	–1.333	
	162000	0.225	–1.492	
	180000	0.184	–1.693	
	216000	0.153	–1.875	
	234000	0.139	–1.973	
	0	1.00	0.000	
	14400	0.859	–0.152	
	28800	0.731	–0.313	
	43200	0.624	–0.471	
	57600	0.529	–0.637	
	72000	0.461	–0.774	
0.080	86400	0.389	–0.943	1.079×10^{-5}
	100800	0.335	–1.094	
	115200	0.279	–1.275	
	129600	0.245	–1.406	
	144000	0.218	–1.522	
	158400	0.181	–1.708	
	172800	0.153	–1.878	
	0	1.00	0	
	14400	0.790	–0.236	
	28800	0.674	–0.394	
	43200	0.571	–0.561	
	57600	0.481	–0.733	
	72000	0.407	–0.899	
0.090	86400	0.343	–1.071	1.183×10^{-5}
	100800	0.289	–1.241	
	115200	0.242	–1.419	
	129600	0.207	–1.574	
	144000	0.174	–1.750	
	158400	0.150	–1.895	
	172800	0.124	–2.088	

(a) The fraction of substrate remaining, $f(s)$, was calculated from Equations 5.2 and 5.3 (b) Pseudo first-order rate constants ($k_{obs,}\ s^{-1}$) were obtained as the slopes of the plots of $\ln f(s)$ against time.